

NMR Spectroscopy of the Tau-Microtubule Interaction

Dissertation

for the award of the degree

“Doctor rerum naturalium”

of the Georg-August-Universität Göttingen

Submitted by

Harindranath Kadavath

from Malappuram, Kerala, India

Göttingen 2013

Thesis Committee

Prof. Dr. Markus Zweckstetter, Department of NMR based Structural Biology, Max Planck Institute for Biophysical Chemistry

Prof. Dr. Marina Bennati, Electron Spin Resonance Spectroscopy, Max Planck Institute for Biophysical Chemistry

Dr. Vladimir Pena, Macromolecular Crystallography, Max Planck Institute for Biophysical Chemistry

Members of the Examination Board

Referee: Prof. Dr. Markus Zweckstetter, Department of NMR based Structural Biology, Max Planck Institute for Biophysical Chemistry

2nd Referee: Prof. Dr. Marina Bennati, Electron Spin Resonance Spectroscopy, Max Planck Institute for Biophysical Chemistry

Further members of the Examination Board

Dr. Vladimir Pena, Macromolecular Crystallography, Max Planck Institute for Biophysical Chemistry

Prof. Dr. Henning Urlaub, Bioanalytical Mass Spectrometry, Max Planck Institute for Biophysical Chemistry

Prof. Dr. Kai Tittmann, Bioanalytics, Georg-August-University, Göttingen

Dr. Adam Lange, Department of NMR based Structural Biology, Max Planck Institute for Biophysical Chemistry

Date of oral examination: **15th January 2014**

Affidavit

I hereby declare that this thesis has been written independently and with no other sources and aids than quoted.

.....

Harindranath Kadavath

Dedicated to my Parents and Brothers

Acknowledgement

This thesis was performed in the department of NMR-based Structural Biology, Max Planck Institute for Biophysical Chemistry, Göttingen, under the supervision of Prof. Dr. Markus Zweckstetter.

I would like to express my sincere gratitude to my supervisor Prof. Dr. Markus Zweckstetter for the project design and the continuous support, advice, encouragement and stimulating scientific input throughout my thesis.

I am deeply grateful to the director of the department, Prof. Dr. Christian Griesinger, for providing excellent research facilities, teaching, providing useful suggestions and friendly environment in the department.

I owe my gratitude to Prof. Dr. Marina Bennati and Dr. Vladimir Pena for the membership in my thesis committee and for useful discussions.

I am deeply grateful for all the tubulin and Tau samples that were purified or produced in the lab of Prof. Dr. Eckhard Mandelkow. The high quality samples allowed to record excellent spectra. I thank Dr. Jacek Biernat, Subash, Satish and Katharina for their nice 'Tau' collaboration and discussion.

I deeply thank Kerstin Overkamp for her immense effort in the synthesis of Tau peptides and for being a good friend.

I am sincerely grateful to Dr. Stefan Bibow, my predecessor in the Tau project for providing helpful support in the early stage of the project and for the useful suggestions.

I am deeply thankful to Dr. Suresh Kumar Vasa for his constant support and encouragement.

I deeply thank Dr. Nasrollah Rezaei-Ghaleh, Dr. Oroz Javier and Dr. Martin Schwalbe for reading my thesis and suggestions. I thank Jean-Philippe for his valuable suggestions, reading the drafts and for the deep friendship during my MPI life.

I thank Romina Hofele and Prof. Dr. Henning Urlaub for their contribution in chemical cross linking and mass spectrometric experiments and discussions.

I thank Lukasz and Mariusz for their help in structure calculation and many useful tips in structural biology.

I had many fruitful discussions with Davood, Luigi and David. Their valuable tips and ideas helped me a lot to achieve my goal. Thank you all for your support.

I extend my sincere gratitude to Dr. Dirk Bockelmann and Heinz-Jürgen Arwe for a very stable system administration and trouble-shooting with programs.

I thank Petra Breiner for the administrative and personal help. I also thank Sigrid Silberer for her support in the beginning of my MPI life.

I thank Nilamoni, Supriya and Suresh for the time and effort they spent reading this manuscript and for their exceeding personal support and friendship. I thank Yogesh, Arun, Rohit, Pradeep, Suresh, Nilamoni, and Supriya for the regular and enjoyable evenings and weekends.

I am much obliged to my current and former group members: Stefan, Xeujun, Guowei, Sheng Qi, Francesca, Piotr, Saskia, Aldo, Luis, Elias, Frederik, Yunior, Rakhi, Michal, Min Kyu, Hai Young, Lukasz Skora and Raghav. Thank you all for the support to work in a group.

I am thankful to all current and former members of this department; Jens, Donghan, Edward, Adam, Antoine, Birgit, Nina, Pablo, Mike, Mitch, Manuel, Florian, Philipp, Sebastian, Han, Benni, Eibe, Sebastian, Hannes, Sibelle, Leo, Vinesh, Ashuthosh. I would like to thank all my colleagues in the department of NMR based structural biology for a nice and friendly atmosphere making it an enjoyable place to work and to discuss.

My sincere gratitude to Dr.Prinson Samuel, Dr.Binu Ramachandran, Dr.Sarish Sankar, Dr. Shajahan Thamarakunnathu, Dr.Vinod Chandran and Dr.Deepak Nand for being my lovely brothers and for their constant support.

I thank Shajahan, Prinson, Binu, Shanty, Remya, Neethu and Femina for the homely environment in Göttingen. I can't exclude dearest Diyamol and Ishan for their childish expressions that bring happiness all the time.

I deeply thank all my teachers and supervisors during my school, college and university education whose care and blessings brought me upto here.

I am blessed with Anisha's support and constant encouragement, which helped me to achieve a lot till now.

Finally, I would like to thank my lovely family members; my Father, Mother, Sreenath and Gokul for supporting and encouraging me all the time throughout my life.

Abstract

Tau is an intrinsically disordered, microtubule associated protein and is responsible for the promotion of microtubule (MT) formation and stabilization. The human Tau protein has six different isoforms, which are expressed in neurons of the central nervous system. A precise understanding of the molecular mechanism involved in the Tau-MT interaction is highly relevant to the study of neurodegenerative states as irregularities in the function of these proteins may lead to neuronal loss and cell death. For instance, the hyperphosphorylation of Tau leads to the depolymerization of MTs and formation of neurofibrillary tangles of Tau which is one of the hallmarks in neurodegenerative diseases.

Although the function of Tau and MTs had been studied previously, it was still unclear how Tau binds to microtubules and high resolution information allowing the structural characterization of microtubule-bound Tau was missing. The aim of the thesis was to perform an in-depth study of the Tau-MT interaction and to determine the MT-bound conformation of the Tau protein. Furthermore, the identification of the binding sites of Tau on MTs will provide a three-dimensional view of the MT-bound Tau structure.

Among the available techniques to derive structural information, NMR is the only method that allows structural description in near-physiological conditions and at atomic resolution. A divide-and-conquer approach in combination with exchange-transferred NMR methods were employed to overcome the size limitations in NMR and to establish the three-dimensional structure of MT-bound Tau.

This thesis covers the detailed NMR characterization of different Tau isoforms, mutants and shorter Tau constructs, thereby identifying the potential binding hot spots of Tau involved in MT interaction. This allowed the structure determination of highly independent and dynamic binding domains of MT-bound Tau using a ‘divide and conquer’ strategy and tr-NOE method. Sufficient experimental evidences obtained using NMR and other biophysical methods proved that the shorter Tau fragments used for structure determination can function similar to the full-length Tau protein. The influence of site-specific mutations and phosphorylation of Tau and Tau fragments is correlated

with the structure that we identified. The obtained three-dimensional structure thus provides insights into the structure-function relationship of MT-bound Tau. Competition experiments using Tau fragments and MT targeting drugs in combination with tr-NOE, STD and Inpharma experiments revealed that the Tau binding domains compete against each other for binding to a single binding site on tubulin near the binding site of vinblastine. The results are supported by chemical cross linking coupled with mass spectrometry. Together with this information, it is possible to suggest a three-dimensional model of microtubule-bound Tau which is relevant to neurodegenerative diseases.

Table of Contents

AFFIDAVIT	III
ACKNOWLEDGEMENT	VII
ABSTRACT.....	IX
ABBREVIATIONS	XVII
1 INTRODUCTION	1
1.1 NEURODEGENERATIVE DISEASES	1
1.1.1 <i>Alzheimer disease</i>	2
1.1.2 <i>Tau and Alzheimer disease</i>	2
1.2 TAU PROTEIN	4
1.2.1 <i>Tau: A neuronal microtubule associated protein</i>	4
1.2.2 <i>Tau: An intrinsically disordered protein</i>	5
1.2.3 <i>Tau structure, function and regulation</i>	6
1.2.4 <i>Structure of Tau in solution</i>	7
1.2.5 <i>Multiple functions of Tau</i>	9
1.2.6 <i>Physiological and pathological roles of Tau</i>	9
1.3 MICROTUBULES.....	11
1.3.1 <i>MT structure and function</i>	11
1.3.2 <i>Microtubule assembly and dynamics</i>	12
1.3.3 <i>Dynamic instability of MTs</i>	14
1.3.4 <i>MT dynamics and neuronal cells</i>	15
1.3.5 <i>Stabilization by MAPs</i>	15
1.3.6 <i>Microtubule binding drugs</i>	16
1.4 TAU-MT INTERACTION	18
1.4.1 <i>Phosphorylation as a mean to regulate Tau-MT interaction</i>	19
1.5 STRUCTURE OF MT-BOUND TAU	22
1.6 BINDING SITE OF TAU ON MICROTUBULES	23
1.7 PROTEIN NMR SPECTROSCOPY	24
1.7.1 <i>Relevance of structure determination using NMR</i>	24
1.7.2 <i>Application of NMR to structure determination of biomacromolecules</i>	25
1.7.3 <i>Protein-ligand interactions by NMR spectroscopy</i>	25
1.8 AIM OF THE STUDY	27

2 MATERIALS AND METHODS	29
2.1 CHEMICAL COMPOUNDS.....	29
2.2 PROTEIN PREPARATION AND PURIFICATION	29
2.2.1 <i>Tau constructs used in this study</i>	29
2.2.2 <i>Protein expression in E.coli</i>	30
2.2.3 <i>Protein expression in E.coli with isotope labeling</i>	30
2.2.4 <i>Standard 5 x M9 Minimal Media salts without nitrogen source</i>	31
2.2.5 <i>Preparation of 500mL M9 minimal medium</i>	31
2.2.6 <i>Adaptation of E.coli bacteria for growing in D₂O/minimal medium (M9) labeled with ¹⁵N NH₄Cl</i> 31	
2.3 MICROTUBULE ASSEMBLY	32
2.4 SYNTHETIC PEPTIDES.....	32
2.5 NMR SPECTROSCOPY.....	34
2.5.1 <i>Interaction studies</i>	34
2.5.2 <i>2-D NMR experiments</i>	34
2.5.2.1 Heteronuclear Single Quantum Coherence (HSQC)	34
2.5.2.2 TROSY and CRINEPT-HMQC-TROSY	36
2.6 STRUCTURE DETERMINATION OF MT-BOUND TAU PEPTIDES.....	37
2.6.1 <i>NMR structure determination of peptides</i>	37
2.6.1.1 Assignment procedure	37
2.6.1.2 Transferred-NOE (tr-NOE)	39
2.6.1.3 Introduction to INPHARMA	41
2.6.2 <i>Structure calculation</i>	43
2.6.3 <i>Saturation Transfer Difference (STD)</i>	43
2.6.3.1 Experimental set up.....	45
2.6.4 <i>1D HRMAS experiment</i>	45
2.6.5 <i>Turbidity assays</i>	45
2.6.6 <i>Electron Microscopy</i>	46
2.6.7 <i>Chemical cross-linking and Mass spectrometry</i>	46
2.6.7.1 Tau-Tubulin cross-linking.....	46
2.6.7.2 Nano-liquid chromatography separation and MS analysis.....	47
2.6.7.3 Identification of cross-linked peptides.....	48
3 RESULTS.....	49
3.1 INTERACTION OF TAU AND TAU FRAGMENTS WITH TUBULIN AND MICROTUBULE	49
3.2 IDENTIFICATION OF THE BINDING HOT SPOTS OF THE TAU-MT INTERACTION	49
3.2.1 <i>Interaction of hTau40 with MT</i>	49

3.2.2	<i>Isoform specific binding of Tau to MTs</i>	52
3.2.3	<i>Effect of overloading of MTs</i>	54
3.2.4	<i>Influence of ionic strength on Tau-MT binding</i>	55
3.2.5	<i>Interaction of hTau40 with tubulin</i>	56
3.2.6	<i>Characterization of MTs using NMR</i>	57
3.3	INFLUENCE OF MUTATION AND PHOSPHORYLATION	58
3.3.1	<i>Effect of mutation (Y310N) of Tau on MT binding</i>	58
3.3.2	<i>Effect of pseudophosphorylation of Tau on MT binding</i>	59
3.4	INTERACTION OF TAU FRAGMENTS WITH TUBULIN/MT	60
3.4.1	<i>Interaction of K18 with tubulin</i>	60
3.4.2	<i>Characterization of interaction of TauF4 with Tubulin/MT</i>	61
3.4.2.1	Effect of ionic strength on binding of F4 with tubulin/MTs	62
3.4.2.2	MT assembly properties of F4 and hTau40	64
3.4.3	<i>Information from the bound state</i>	65
3.4.3.1	CRINEPT-HMQC of ^2H - ^{15}N F4 bound to tubulin	65
3.4.3.2	CRINEPT-HMQC of ^2H - ^{15}N F4 bound to MTs	65
3.5	STRUCTURE DETERMINATION OF THE MT-BOUND TAU	66
3.5.1	<i>Selection of Tau peptides</i>	67
3.5.2	<i>Assignment of the peptides</i>	68
3.5.3	<i>Assignment of TR3</i>	68
3.5.4	<i>Tau peptides bind effectively to tubulin/MT: STD NMR</i>	69
3.6	STRUCTURE OF MT-BOUND TAU PEPTIDES	70
3.6.1	<i>Structure of MT-bound TR3</i>	71
3.6.1.1	Tr-NOESY NMR spectrum of TR3-MT complex	71
3.6.1.2	Tr-NOESY spectrum of TR4 (Tau327-353)	72
3.6.1.3	Structure calculation	72
3.6.2	<i>Structure of MT-bound TR2</i>	75
3.6.3	<i>Structure of MT-bound TR1</i>	77
3.6.4	<i>Structure of MT-bound TP2</i>	79
3.6.5	<i>Structure of MT-bound TP1</i>	81
3.6.6	<i>Structure of MT-bound TR'</i>	83
3.6.7	<i>Structure of MT-bound TR23</i>	85
3.7	PROPERTIES OF TAU PEPTIDES	87
3.7.1	<i>Competition between Tau and Tau peptides for MT binding</i>	87
3.7.1.1	Competition between TP2 and hTau40 for MT binding	88
3.7.1.2	Competition between TR3 and hTau40 for MT binding	88
3.7.1.3	N-terminal TN1 peptide does not compete for MT binding	89

3.7.2	<i>Effect of phosphorylation and mutations in MT-binding</i>	90
3.7.2.1	Effect of phosphorylation (T231 phosphorylation)	90
3.7.2.2	Effect of genetic mutation on MT binding	91
3.7.3	<i>MT assembly properties of Tau peptides</i>	93
3.7.3.1	MT assembly of Tau peptides	93
3.7.3.2	Effect of phosphorylation in MT assembly	95
3.7.4	<i>Independent binding of Tau fragments to the same binding site</i>	96
3.7.4.1	Inter peptide competition for MT binding	96
3.7.4.2	Intra peptide competition: INPHARMA NOEs	97
3.8	IDENTIFICATION OF BINDING SITE OF TAU ON TUBULIN/MT	99
3.8.1	<i>Interaction of Tau with C-terminal peptides of tubulin</i>	99
3.8.2	<i>Competition of Tau with MT drugs for binding</i>	100
3.8.2.1	Competition experiment with Vinblastine and hTau40	101
3.8.2.2	Competition experiment with Thalidomide and hTau40	102
3.8.2.3	Competition experiment with Baccatin and hTau40	103
3.8.2.4	Competition experiment with Colchicine and hTau40	103
3.8.2.5	Competition experiment with Taxol and hTau40 for MT binding	103
3.8.2.6	Vinblastine compete with hTau40 to bind to tubulin	105
3.8.3	<i>Competition experiments using STD NMR spectroscopy</i>	106
3.8.3.1	Competition between Tau peptides and MT drugs: binding to tubulin	106
3.8.3.2	Competition between Tau peptides and MT drugs: binding to MTs	110
3.8.3.3	Influence of stathmin like peptide I19L	111
3.9	MASS SPECTROMETRY	113
3.9.1	<i>Cross linking TauF4/hTau40 to tubulin</i>	114
3.9.2	<i>Mass spectrometric analysis of cross linked F4 and tubulin</i>	115
4	DISCUSSION	118
4.1	TOWARDS THE STRUCTURE OF MT-BOUND TAU	118
4.2	INTERACTION OF TAU WITH MICROTUBULES	118
4.2.1	<i>Tau-MT interaction studies revealed the highly localized binding hot spots of Tau</i>	120
4.2.1.1	Similar binding mode is present in both 3R and 4R Tau isoforms	120
4.2.1.2	Tau:MT interaction is monophasic	121
4.2.1.3	Tau interacts with tubulin and MTs in the similar manner	122
4.2.1.4	Tau-MT interaction is mediated by both charged and hydrophobic residues	122
4.2.1.5	Site specific mutation and pseudophosphorylation lead to local alteration in MT binding	123
4.2.1.6	Confirmation of the binding hot spots using Tau constructs	124
4.3	INSIGHTS INTO THE STRUCTURE OF MT-BOUND TAU	126
4.3.1	<i>Characteristic structural features of the MT-bound Tau peptides</i>	127
4.4	TAU PEPTIDES RESEMBLE FULL-LENGTH TAU IN THEIR FUNCTION	130

4.4.1	<i>Tau peptides compete with hTau40 for MT binding</i>	130
4.4.2	<i>Linear motifs in Tau cooperate in tubulin binding and polymerization</i>	131
4.4.2.1	Influence of T231 phosphorylation on TP2 in MT assembly	132
4.4.3	<i>Phosphorylation and mutation of specific residues reduces MT binding</i>	132
4.4.3.1	Influence of T231 phosphorylation on TP2 reduced its MT affinity	132
4.4.3.2	P301S mutation in TR3 disrupts MT binding	133
4.4.4	<i>Independent Tau domains target the same binding site on MT</i>	135
4.5	VARIETY OF COMPETITION EXPERIMENTS REVEALED THE BINDING SITE OF TAU ON MTs	136
4.5.1	<i>NMR approaches identified the potential binding site</i>	137
4.5.1.1	Tau-MT interaction involves interaction with C-terminal domain of tubulin	137
4.5.1.2	MT targeting drug Vinblastine and hTau40 compete for binding	138
4.5.1.3	STD NMR method revealed the potential binding site of Tau on MTs	138
4.5.1.4	I19L peptide from the N-terminal stathmin like domain compete with Tau peptides	139
4.5.2	<i>Chemical cross-linking and Mass spectrometry validated the binding site</i>	140
4.5.3	<i>Tau binds to α-tubulin at the inter-dimer interface</i>	141
REFERENCES		144
APPENDIX		161
CURRICULUM VITAE		162

Abbreviations

AD	Alzheimers disease
CNS	Central nervous system
IDP	Intrinsically Disordered Proteins
MT	Microtubule
MTBR	Microtubule binding Repeats
MAP	Microtubule associated proteins
GTP	Guanosine triphosphate
GDP	Guanosine diphosphate
NMR	Nuclear magnetic resonance
NOE	Nuclear Overhauser Effect
NOESY	Nuclear Overhauser Effect spectroscopy
Tr-NOESY	Transferred Nuclear Overhauser Effect spectroscopy
COSY	Correlation spectroscopy
TOCSY	Total correlation spectroscopy
HSQC	Heteronuclear single quantum coherence spectroscopy
HMQC	Heteronuclear multiple quantum coherence spectroscopy
TROSY	Transverse relaxation optimized spectroscopy
CRINEPT	Cross correlated relaxation enhanced polarization transfer
STD	Saturation transfer difference
INPHARMA	Interligand NOEs for pharmacophore mapping
HRMAS	High resolution magic angle spinning

1 Introduction

1.1 Neurodegenerative diseases

The native conformation of a protein is essential for its normal function. The loss of structural identity of individual proteins leads to protein aggregation and thereby several diseases commonly known as protein misfolding diseases. Neurodegenerative diseases, the progressive loss of structure or function of neurons including neuronal death are a class of protein misfolding diseases where the protein aggregation occurs in the brain. These include neuronal pathologic forms in which a progressive loss of either structure or function of neurons is observed. This leads to the neuronal death and associated diseases. Many neurodegenerative diseases are caused by genetic mutations of related proteins. Some of the widely discussed proteins in neurodegenerative diseases include alpha Synuclein (in Parkinson disease), amyloid beta peptide and Tau (in Alzheimer disease), prion protein (in Prion disease) and huntingtin (in Huntington's disease) and so on.

The neurodegenerative diseases related to Tau protein are also known as Tauopathies where predominantly the aggregates of Tau occur. Tauopathies are group of disorders that includes Alzheimer disease (AD), supranuclear palsy, corticobasal degeneration, Pick's disease and frontotemporal dementia and parkinsonism linked to chromosome 17 (FTDP-17). The mechanisms of the formation of aggregates from soluble Tau have been studied in great detail, particularly in AD and FTDP-17 (Esmaeliazad, Mccarty et al. 1994, Lee, Goedert et al. 2001). Dementia is one of the widely discussed and common disorders in elder people as a result of aging. It has become extensive health problem among ageing population (Fratiglioni, De Ronchi et al. 1999).

1.1.1 Alzheimer disease

In 1907 Dr. Alois Alzheimer, a German psychiatrist, described the presence of plaques and tangles in the brain of a demented patient, which were found to be the pathological hallmarks. This class of neurodegenerative disease was later named as Alzheimer disease (AD) (Alzheimer 1907). More than half of the dementia affected people suffer from Alzheimer disease (Fratiglioni, De Ronchi et al. 1999). The previous research in AD highlights the presence of extracellular deposits of amyloid β as plaques and intracellular neurofibrillary tangles (NFTs) of Tau as the hallmarks in AD (Grundke-Iqbal, Iqbal et al. 1989) (Figure 1).

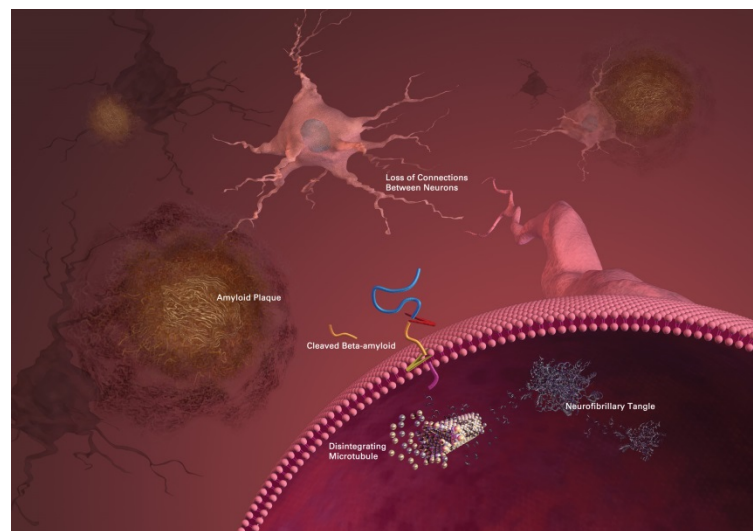


Figure 1: Pictorial representation of the abnormal cellular deposits found in Alzheimer disease. AD is characterized by the presence of two abnormal structures in the brain, (i) extracellular amyloid plaques and (ii) intracellular neurofibrillary tangles (NFTs). The amyloid plaques are composed of the insoluble aggregates of $A\beta$, a small proteolytic fragment from the amyloid precursor protein (APP). NFTs are composed of the insoluble aggregates of Tau in the form of paired helical filaments (PHFs) or fibers. (Image courtesy of the National Institute of Health)

1.1.2 Tau and Alzheimer disease

It has been established that Tau is necessary for the neuronal development and maintenance of the nervous system. Abnormal Tau behavior results in many neurodegenerative diseases, including AD and several other dementias (Spillantini, Tolnay et al. 1999, Spillantini, Van Swieten et al. 2000, Goedert and Spillantini 2006, Ballatore, Lee et al. 2007).

From the neuropathological point of view AD is characterized by the presence of two abnormal structures in the brain. The amyloid plaques are composed of the insoluble aggregates of A β , a small proteolytic fragment from the amyloid precursor protein (APP). NFTs are composed of the insoluble aggregates of Tau in the form of paired helical filaments (PHFs) or fibers (Grundke-Iqbal, Iqbal et al. 1986, Grundke-Iqbal and Iqbal 1989, Grundke-Iqbal, Iqbal et al. 1989). There are many other neurodegenerative diseases which are caused by the insoluble Tau NFTs named as “Tauopathies” (Hutton, Lendon et al. 1998, Spillantini, Murrell et al. 1998) such as FTDP-17, progressive supranuclear palsy (PSP) and corticobasal degeneration (CBD).

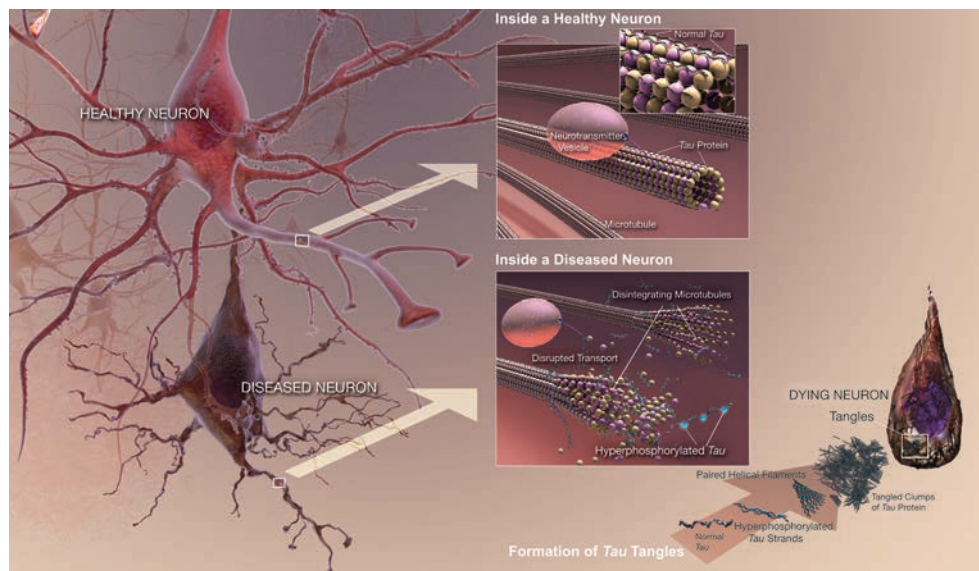


Figure 2: Tau neurofibrillary tangles in healthy and diseased neurons. In a healthy neuron microtubules are stabilized by Tau and thereby support axonal transport of vesicles and organelles. Whereas in a diseased neuron the hyperphosphorylation of Tau leads to microtubule disintegration and disrupt microtubule supported cellular transport. The hyper phosphorylated Tau detaches from microtubules and forms paired helical filaments (NFTs). These NFTs are found to be the intracellular deposits in the form of neurofibrillary tangles which are one of the hallmarks in Alzheimer’s disease. (Image courtesy of the National Institutes of Health)

A number of studies have shown that many neurodegenerative Tauopathies are connected to the hyperphosphorylation and other post translational modifications of Tau that leads to the detachment of Tau from the microtubules and the formation of NFTs of Tau (Wittmann, Wszolek et al. 2001, Noble, Olm et al. 2003). NFTs consist of aggregated straight or paired helical filaments (PHFs) of aberrantly phosphorylated forms of Tau protein (**Figure 2**).

1.2 Tau protein

1.2.1 Tau: A neuronal microtubule associated protein

Tau is an intrinsically disordered, microtubule associated protein and is responsible for the promotion of microtubule (MT) formation and stabilization. Tau protein was initially identified by Weingarten and co-workers in 1975 as a protein belonging to a heat stable family of microtubule-associated proteins that co-purify with tubulin (Gaskin, Cantor et al. 1974, Weingarten, Lockwood et al. 1975). Later on it was realized that Tau restores the microtubule assembly competence of phosphocellulose-purified (PC) tubulin that is essentially devoid of MAPs (Weingarten, Lockwood et al. 1975). Another remarkable finding was that Tau functions stoichiometrically rather than catalytically (Weingarten, Lockwood et al. 1975). In other words it is a characteristic feature of Tau to bind to tubulin and promote microtubule assembly (Weingarten, Lockwood et al. 1975).

The human Tau gene is located on chromosome 17 and it includes 16 exons (Kosik, Joachim et al. 1986, Neve, Harris et al. 1986). Alternative splicing of Tau mRNA from this single Tau gene generates six different Tau isoforms in the central nervous system (CNS) ranging from 352 to 441 amino acids, and several further variants in the peripheral nerve system (Goedert 1996, Andreadis 2005). In fetal neurons only the smallest isoform is expressed and all six isoforms are expressed in adult human brain. These six isoforms possess either three or four 18 amino acid long imperfect repeats, which are separated by shorter inter repeats, depending on the exclusion or inclusion of the exon 10 encoded sequences. These 18 amino acid long repeats were combined with the inter repeats to further simplify them as 31 or 32 amino acid long repeats. It has been shown that these repeats are important for the MT binding and other regulatory activities (Butner and Kirschner 1991, Gustke, Trinczek et al. 1994, Trinczek, Biernat et al. 1995). In addition to these, alternative splicing of exons 2 and 3 leads to the presence of one, two or none 29 amino acid long inserts in the N-terminal region of the protein (Himmler, Drechsel et al. 1989). A diagram of the domain organization of the six Tau isoforms is shown in **Figure 3**.

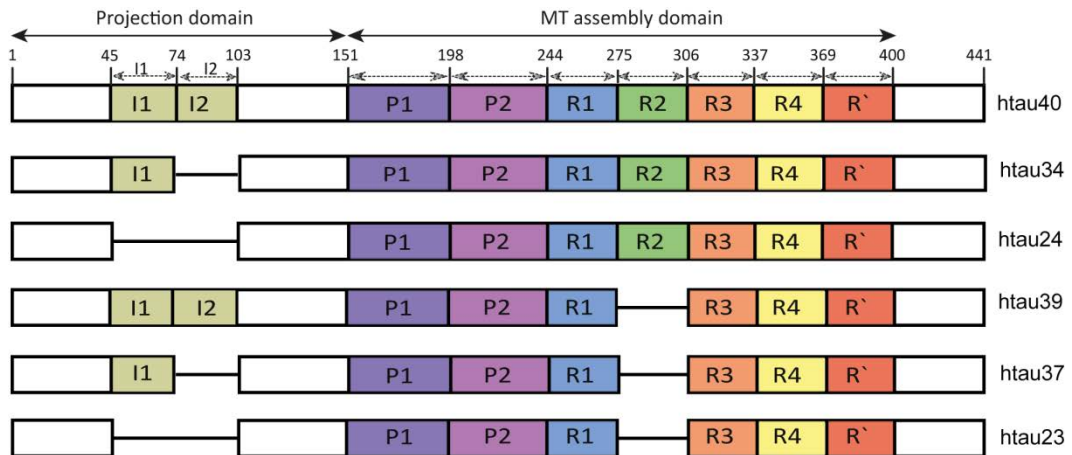


Figure 3: Domain organization of the six different isoforms of Tau in the CNS. Tau isoforms in the CNS are represented with the organization of domains. The N-terminal region of Tau upto the proline rich region is termed as projection domain. Microtubule assembly domain includes three or four repeats (31 residues each, R1-R4), which together with the pseudo repeat R' and proline-rich flanking regions (P1 and P2) constitute the microtubule binding region.

1.2.2 Tau: An intrinsically disordered protein

Proteins that lack a rigid secondary and tertiary structure under physiological conditions are called intrinsically disordered proteins. However, another characteristic feature of IDPs is that they may have certain secondary structure propensities albeit a continuous amino acid stretch of protein is disordered. Although disordered in the isolated state, many of them acquire a well-defined conformation upon interaction with their partners.

Tau is an intrinsically disordered protein. Tau is highly soluble protein with a small number of hydrophobic amino acid residues. The percentage of hydrophobic residues is ~15% in contrast to globular proteins where it is about 30% (von Bergen, Barghorn et al. 2005). The relatively higher number of positively charged residues together with other features like resulting in a pI of 8.3-10.0 depending on the isoform makes it intrinsically disordered protein (Uversky, Gillespie et al. 2000). Tau is one of the largest among the known intrinsically disordered proteins (Dunker, Lawson et al. 2001).

1.2.3 Tau structure, function and regulation

The intricate wiring of the nervous system is established on the basis of terminal neuronal differentiation that is characterized by the formation of specialized cytoplasmic domains such as axons and dendrites. Microtubules have spatially and temporally distinct properties within each subcellular compartment (Ahmad, Pienkowski et al. 1993). Within the body of elongating axonal projections, stable microtubules are organized in a polarized array. The distinctive and specific properties of microtubules in selected neuronal compartments arise in part from the regulated expression and subcellular localization of the structural microtubule associated proteins like Tau, MAP1, and MAP2 (Caceres, Mautino et al. 1992, Gordonweeks 1993, Esmaeliazad, Mccarty et al. 1994).

Tau protein has been best characterized on the basis of their abilities to bind directly to microtubules, promote MT assembly and regulation of MT dynamics (Paglini, Peris et al. 2000, Feinstein and Wilson 2005). Within neuronal cells functions of microtubules are regulated by Tau protein. The Tau functions are regulated by both alternative RNA splicing and phosphorylation (Himmler, Drechsel et al. 1989). The phosphorylation takes place at a number of sites that regulates the binding properties (Hanger, Betts et al. 1998, Gong, Liu et al. 2006). Different Tau isoforms present in CNS are listed in **Table 1**.

The domains of Tau are broadly divided into an acidic N-terminal 'Projection domain' (M1-Y197) and a C-terminal 'assembly domain' (S198- L441) based on limited proteolysis and the involvement of Tau domains in the microtubule binding ability (Gustke, Trinczek et al. 1994). Tau domains are further defined based on the character of the primary sequence. The N-terminal region with amino acids M1-G120 constitutes the acidic domain. This domain includes two insert domains that are alternatively spliced (I1 and I2; E42-A103). The region G120-Q244 is basic in nature and contains many proline residues. Hence it is named as proline rich region with further subdivision into P1 and P2 at Y197. The region T244-K368 is characterized by three or four imperfect repeats (R1-R4) of 31 or 32 residues.

Table 1: List of Tau isoforms present in CNS. Tau isoforms present in CNS listed by name, denotation based on the presence or absence of I and R domains, number of amino acids and the molecular weight (this table is reproduced from Goedert et al., 1989).

Tau isoform	Denotation	Number of amino acids	Molecular weight (Da)
hTau23	0I/3R	352	36750
hTau37	1I/3R	381	39720
hTau39	2I/3R	410	42603
hTau24	0I/4R	383	40007
hTau34	1I/4R	412	42967
hTau40	2I/4R	441	45850

1.2.4 Structure of Tau in solution

It was noticed in the beginning that Tau has an unusual character as a protein with very high resistance to heat and acid treatment without losing its functionality and possess very low secondary structure throughout the sequence (Cleveland, Hwo et al. 1977). Tau behaves as an “intrinsically disordered” protein in solution (Schweers, Schonbrunn-Hanebeck et al. 1994) and it adopts a “paperclip” conformation, whereby the N- and C-terminal domains approach each other and the repeat domain as well (Jeganathan, von Bergen et al. 2006, Jeganathan, Hascher et al. 2008). Several observations suggest that Tau cannot simply be a “random coil” in the strict sense. Small angle x-ray scattering (SAXS) and Forster resonance energy transfer (FRET) were used to obtain further insights into the structure of the Tau protein (Jeganathan, von Bergen et al. 2006, Mylonas, Hascher et al. 2008). Although Tau has been studied for many years, very little structural information is available (Harbison, Bhattacharya et al. 2012).

In fact NMR is the only method that allows the investigation of conformation and dynamics of intrinsically disordered proteins with atomic resolution (Dyson and Wright 2005). Using the divide and conquer strategy different Tau constructs were used for the solution NMR investigations and overcame the NMR size limitation and severe signal overlap. The complete resonance assignment was achieved using state-of-the-art NMR

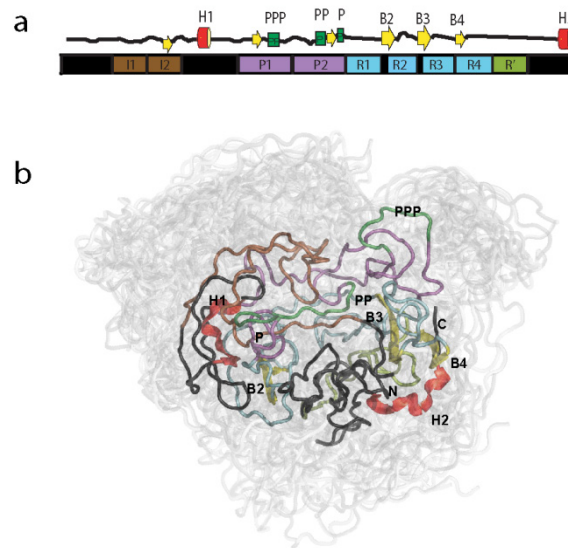


Figure 4: Conformation of monomeric hTau40 in solution. (a) The domain organization diagram of hTau40 with transient secondary structures. Secondary structure propensities are represented as red alpha helix, yellow beta strands and poly proline stretches are coloured green. (b) An ensemble structure of hTau40 calculated from PRE data with the colour coding according to the domain organization diagram. (Figure modified from(Mukrasch, Bibow et al. 2009)).

methods (Mukrasch, Bibow et al. 2009, Narayanan, Dürr et al. 2010). It was revealed that 441-residue Tau is highly dynamic in solution (**Figure 4**) with a distinct domain overlap. The complete resonance assignment was achieved using the advanced NMR character and an intricate network of transient long-range contacts important for pathogenic aggregation. An ensemble description of monomeric Tau in solution was determined in single-residue view provided by the NMR analysis (Mukrasch, Bibow et al. 2009) based on paramagnetic relaxation enhancement (PRE). Tau possess high propensity for the turn conformations in the repeat region within the residue stretches DLKN, DLSN, DLSK and DLFD (Mukrasch, Markwick et al. 2007).

Hyperphosphorylated Tau is found to be the major constituent of paired helical filaments (PHFs) separated from AD brains. It is to be noticed that this conclusion has been drawn based on the creation and characterization of monoclonal antibodies raised against PHFs. These antibodies can be classified into three categories: (1) those which recognize unmodified primary sequences of Tau, (2) those which recognize phosphorylation-dependent epitopes on Tau and (3) those which recognize conformation

dependent epitopes on Tau. Of these antibodies, only the conformation-dependent antibodies appear to be capable of distinguishing normal Tau from PHF-Tau in solution. Phosphorylation of serine and threonine residues in proline-rich sequences induces a conformational change to a type II polyproline helix (Bielska and Zondlo 2006). The N- and C-terminal sections around the core of the Tau filament consists of over 200 amino acids form the fuzzy coat. The dynamic structure of this fuzzy coat was characterized using NMR and the binding of conformation specific antibodies to the Tau protein (Bibow, Mukrasch et al. 2011).

1.2.5 Multiple functions of Tau

Although Tau has been well characterized as a microtubule associated protein (Weingarten, Lockwood et al. 1975, Witman, Cleveland et al. 1976), recent studies have given further insights into its multifunctional properties (Tortosa, Santa-Maria et al. 2009, Morris, Maeda et al. 2011). Tau has many other binding partners such as signaling molecules, cytoskeletal elements and lipids (SurrIDGE and Burns 1994, Fleming, Weisgraber et al. 1996, Fulga, Elson-Schwab et al. 2007, Morris, Maeda et al. 2011). Another class of Tau interacting partners includes heat shock proteins such as Hsp90 chaperones (Tortosa, Santa-Maria et al. 2009). Tau interact with motor proteins such as dynein and kinesin (Ebner, Godemann et al. 1998, Dixit, Ross et al. 2008) increasing the efficiency of axonal transport. Tau regulates the MT stability not only by binding directly to MTs but also through indirect mechanism where it acts as a direct enzyme inhibitor (Perez, Santa-Maria et al. 2009). Albeit the wide range of interacting partners, MTs have got significant attention.

1.2.6 Physiological and pathological roles of Tau

Taken together Tau phosphorylation plays both physiological and pathological roles in the cell. When the phosphorylation state of Tau is appropriately coordinated, it plays critical role in many cellular functions. Tau regulates neurite outgrowth (Biernat and Mandelkow 1999, Biernat, Wu et al. 2002), axonal transport (Tatebayashi, Iqbal et al. 1999, Spittaels, Van den Haute et al. 2000) and microtubule stability and dynamics). However, in pathological conditions in which there is an imbalance in the

phosphorylation of Tau, it causes the Tau filament formation (Abraha, Ghoshal et al. 2000), disrupt microtubule-based molecular transport. Tau hyperphosphorylation and MT destabilization can even cause neuronal loss and increase cell death (Fath, Eidenmuller et al. 2002). All the possible events related to Tau phosphorylation are represented in **Figure 5**.

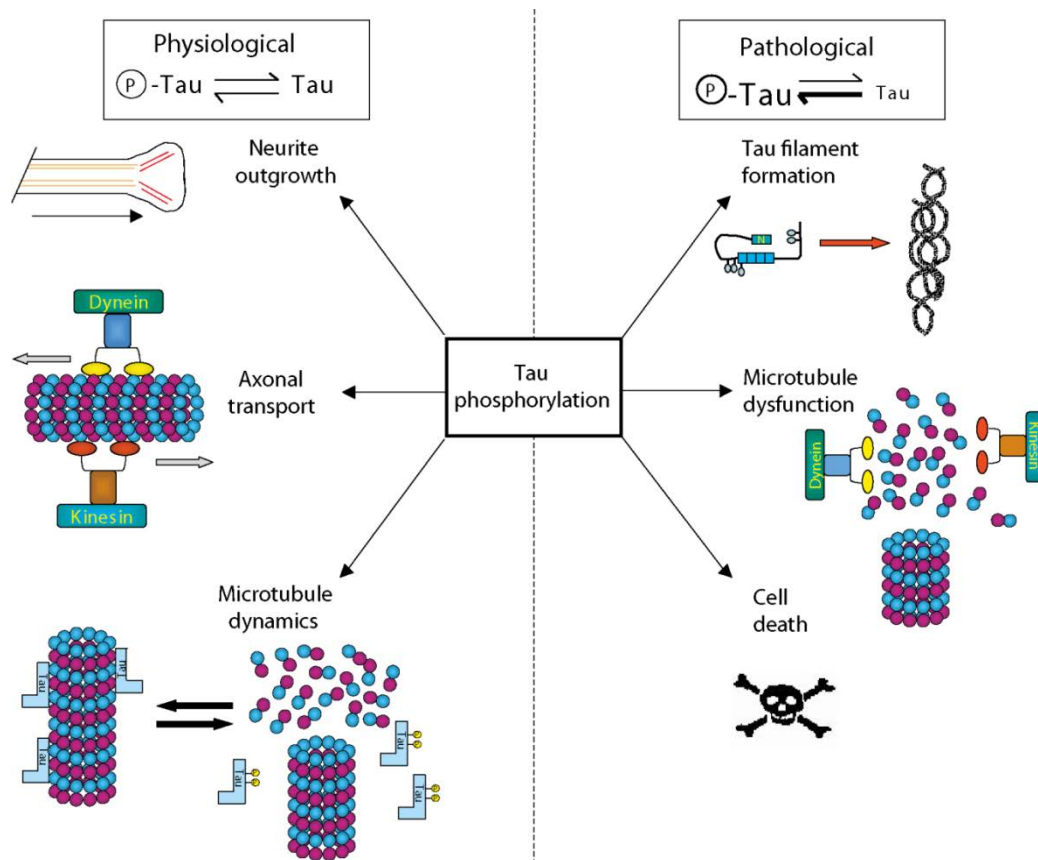


Figure 5: Physiological and pathological roles of Tau. Tau phosphorylation plays both physiological and pathological roles in the cell. When the phosphorylation state of Tau is appropriately coordinated, it regulates neurite outgrowth, axonal transport and microtubule dynamics. However, in pathological conditions upon hyperphosphorylation of Tau, it can cause Tau filament formation, disrupt microtubule binding and increase cause of cell death. (Figure adapted from Johnson et al., 2004 (Johnson and Stoothoff 2004)).

1.3 Microtubules

1.3.1 MT structure and function

Microtubules (MT) constitute one of the three primary elements of the eukaryotic cytoskeleton, which performs a wide range of physiological functions. For example, due to their mechanical strength and stability, microtubules contribute to the maintenance of cell shape and provide a scaffold for intracellular transport. MTs are composed of the internetworked α - β tubulin heterodimers (Weisenberg 1972) - or simply as tubulin. Tubulin assembles into a tubular framework with ~ 13 protofilaments, which together form a tubular and polarized polymer with $\sim 25\text{nm}$ in diameter (**Figure 6**). The typical length of MTs varies from $10\text{-}50\ \mu\text{m}$. Prominent cell functions are regulated with the help of MTs such as cell morphology. In addition, they serve as tracks for the cellular transport of intracellular cargos and organelles via motor proteins like kinesin and dynein. Mitotic cell division is controlled by the formation of spindle MTs (Hirokawa and Takemura 2005, Konzack, Thies et al. 2007). During mitosis, microtubules play an important role to pull apart the aligned chromosomes. During these processes, microtubules are highly dynamic in terms of assembly and disassembly, which is regulated by microtubule-associated proteins (MAPs).

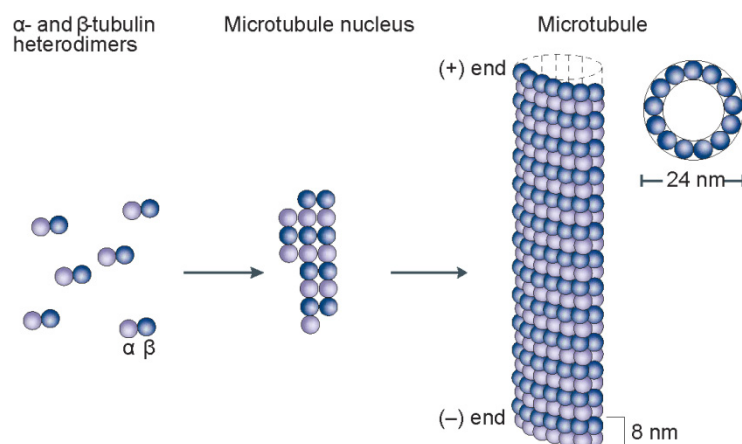


Figure 6: Polymerization of tubulin to form microtubules. α - β tubulin heterodimers assemble in a head to tail fashion to form a microtubule nucleus followed by elongation to form cylindrical microtubules. A typical microtubule is composed of 13 protofilaments with $\sim 24\text{nm}$ diameter. (Figure taken from (**Jordan and Wilson 2004**))

MTs are highly dynamic in nature undergoing continual assembly and disassembly (Desai and Mitchison 1997) and the dynamic nature of MTs is due to the two kinds of mechanisms namely treadmilling (Wilson and Margolis 1978, Margolis and Wilson 1981, Margolis and Wilson 1998, Panda, Miller et al. 1999) and dynamic instability (Kirschner and Mitchison 1986, Vale and Hotani 1988). MT plus ends have been investigated in detail and are found to be kinetically more favorable in terms of their dynamic nature (Kirschner and Mitchison 1986, Goedert, Wischik et al. 1988). In short, the tubulin heterogeneity and differential and distinct binding features of MAPs and function are considered as the primary molecular mechanisms regulating microtubule cellular function (Mandelkow, Lange et al. 1988).

1.3.2 Microtubule assembly and dynamics

In solution, tubulin exists in a dynamic equilibrium between tubulin dimer and polymers; any tubulin present above a defined critical concentration will form polymers (Mitchison and Kirschner 1984, Desai and Mitchison 1997, Hyman and Karsenti 1998). As shown in **Figure 7**, microtubule assembly takes place through two phases, nucleation and elongation. γ tubulin is a third very minor species of tubulin (Oakley and Oakley 1989). *In vivo*, γ tubulin is found solely in microtubule organizing centers (MTOC) (Mitchison and Kirschner 1984, Mcintosh, Roos et al. 1985) and participates in the nucleation of microtubule polymers (Zheng, Wong et al. 1995). In *de novo* tubulin polymerization in the absence of MTOCs, either preformed MTs or MAPs are able to fulfill the nucleation process (Bre and Karsenti 1990). The microtubule polymerization rate is controlled by the binding constant of GTP tubulin to the tubulin ends. However, experiments using GTP analogs indicate that GTP hydrolysis is required only for microtubule depolymerization and not for microtubule assembly (Mandelkow, Mandelkow et al. 1991, Hyman, Salser et al. 1992).

A steady exchange of $\alpha\beta$ heterodimers occurs at the microtubule ends. The microtubules under these conditions are said to be at “steady state” and during which due to the different rates of assembly at the two microtubule ends, there is a net addition of tubulin subunits at the plus ends of the microtubules. Microtubules, therefore, assume two different functional and structural states, alternating between the growing and

shortening phases (Jordan, Walker et al. 1998). Microtubules are significantly more dynamic at the plus end. In comparison to minus ends, plus ends exhibit greater changes in length over time due to higher rates of elongation, higher frequencies of catastrophe and a lower frequency of rescue (Desai and Mitchison 1997). Another factor influencing the level of dynamic behavior is the presence of the structural microtubule associated proteins. The structural MAPs including Tau effectively stabilize microtubule dynamics, primarily by reducing the rate of shortening even at low molar ratios (Panda, Goode et al. 1995, Trinczek, Biernat et al. 1995, Goode, Denis et al. 1997).

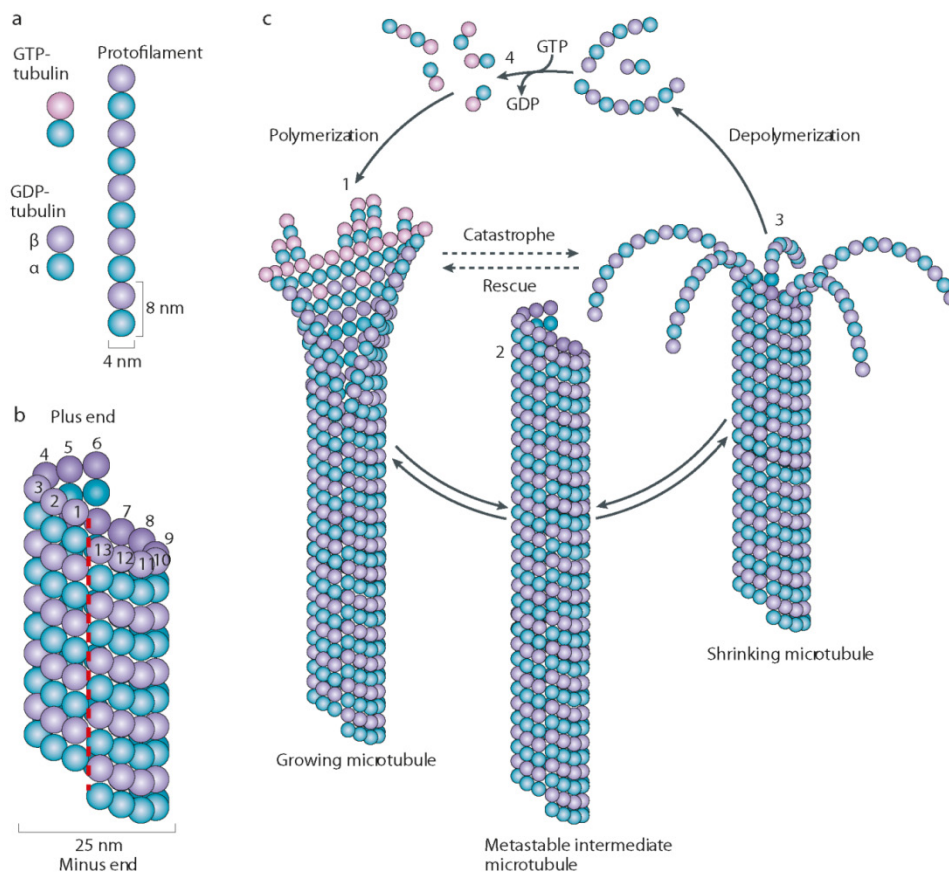


Figure 7: Microtubule structure and dynamic instability. (a-b) Polymerization steps involved in MT assembly. Tubulin α - β dimer assembles in a polar head to tail fashion to form the protofilaments and ~13 protofilaments arrange in parallel to form the microtubules. (c) Diagram showing the different steps involved in MT dynamic instability. The polymerization and depolymerization are driven by the binding, hydrolysis and exchange of a guanine nucleotide on β -tubulin. The process of catastrophe and rescue that happens between the growing and shortening stages of MT assembly are represented through the polymerization-depolymerization cycle (Akhmanova and Steinmetz 2008) (Figure taken from Akhmanova et.al. Nat Rev Mol Cell Biol, 2008).

1.3.3 Dynamic instability of MTs

Under steady state conditions MTs appear to be stable and intact. The stochastic switching of MTs between the polymerized and depolymerized phases is referred to as dynamic instability of MTs (Mitchison and Kirschner 1984). This dynamic instability has significant relevance to coordinate and facilitate the remodeling of the microtubule cytoskeleton to fulfill the various roles of MTs.

Tubulin nucleotide interactions are important in the dynamic instability of MTs. During polymerization, both the α - and β -subunits of the tubulin dimer are bound to a molecule of GTP and the GTP bound to β -tubulin may be hydrolyzed to GDP shortly after assembly resulting in the addition of new dimers (Weisenberg 1972). All these events are represented in the **Figure 7**.

Together with GTP hydrolysis at the tip of the microtubule, a rapid depolymerization and shrinkage begins. This kind of shrinking phase is called 'catastrophe'. GTP-bound tubulin can begin adding to the tip of the microtubule again, protecting the microtubule from shrinking phase and is referred to as 'rescue' (Figure 7).

Thus due to the intrinsic instability of microtubules, they are considered to be in a dynamic equilibrium or steady state (Akhmanova and Steinmetz 2008). This dynamic instability of MTs is influenced by microtubule associated proteins (MAPs) by binding and stabilizing events (Cleveland 1977). The changes in the physicochemical environment such as pH, temperature, ionic strength presence of small molecules, protein partners and drugs can also influence the dynamics of MTs.

MTs are involved in many cellular processes such as cell division, intracellular transport of vesicles and organelles and they also function as the basic element of cytoskeleton architecture. All these functions are regulated by the specific feature, dynamic instability of MTs. Majority of the MT functions are regulated by MAPs.

1.3.4 MT dynamics and neuronal cells

The highly dynamic nature of MTs to undergo continuous assembly and disassembly (Desai and Mitchison 1997) is due to the two kinds of mechanisms treadmilling (Wilson and Margolis 1978, Margolis and Wilson 1981, Margolis and Wilson 1998) and dynamic instability (Kirschner and Mitchison 1986). In neuronal cells significant number of cellular processes like axonal transport, stability etc are controlled by MT dynamics. Irrespective of the intrinsic properties of MTs such as dynamic instability and treadmilling, the highly specific dynamic features and specific functions are to a great extent controlled by Tau and other MAPs (Dehmelt 2003, Feinstein 2005). It has been shown that a proper regulation of neuronal MT dynamics is necessary for the normal functioning of neurons (Baas, Pienkowski et al. 1991) which are modulated by Tau and related MAPs.

1.3.5 Stabilization by MAPs

A series of MAPs have been identified in different cell types with distinct functions such as both stabilizing and destabilizing MTs, guiding MTs towards specific cellular locations, cross-linking microtubules and mediating the interactions of microtubules with other proteins in the cell. MAPs are broadly classified into type I and type II MAPs. Type I MAPs, also called MAP1 family, bind differently to MTs than other MAPs utilizing their charge as the driving force for the interaction (Mandelkow and Mandelkow 1995). Type II MAPs include MAP2, MAP4 and Tau. MAPs can be further classified into MT stabilizing and destabilizing MAPs. Specific examples are Tau and stathmin, which fall under the classification of stabilizing and destabilizing MAPs respectively. It has been found that Tau and stathmin are widely studied MAPs due to their significant roles in many physiological functions and involvement in many neurodegenerative diseases. The stabilizing and destabilizing properties of MAPs and their impact on MT dynamics is represented in **Figure 8**.

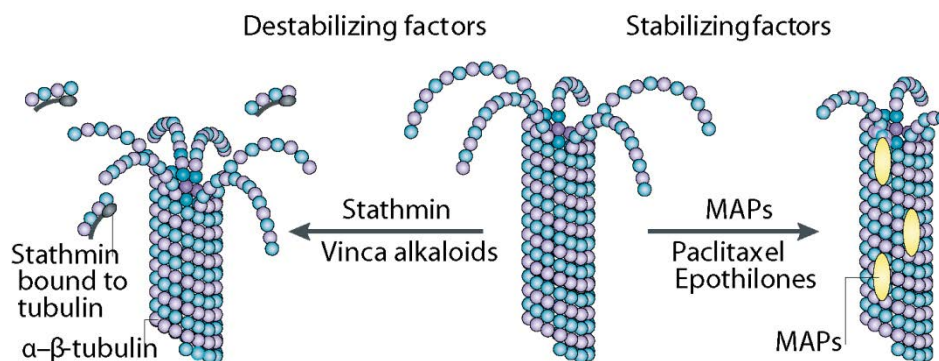


Figure 8: Effects of microtubule associated proteins (MAPs) and tubulin-binding agents on microtubule stability. Microtubule stabilizing proteins like Tau bind and stabilize MTs whereas destabilizing MAPs like stathmin sequester MT assembly. In the same way MT stabilizing drugs like taxol and epothilones stabilize MTs whereas destabilizing drugs promote MT depolymerization. (Figure taken from Kavallaris M, Nat Rev Cancer 2010).

One of the other MAPs that stabilize MTs is Doublecortin that is essential for neuronal migration during human brain development (Moores, Perderiset et al. 2004). Doublecortin stabilizes microtubules and stimulates their polymerization but there is no homology with any other MAPs like Tau. It was also identified by cryo-EM studies that they bind in between the protofilaments and specifically target the 13-protofilament MTs (Moores, Perderiset et al. 2004).

1.3.6 Microtubule binding drugs

A number of naturally occurring and synthetic compounds bind to tubulin or microtubules. Their ability to alter the microtubule dynamics and stability brought them into the category of MT drugs (Cocca, Dorado et al. 2009, Perez 2009, Reiner, de las Pozas et al. 2009). These small molecules are alkaloids, macrolides or peptides which bind to tubulin and play significant roles in MT assembly or disassembly (Jordan and Wilson 2004). Some of the compounds compete for binding and other act synergistically. The interaction of tubulin-binding agents with tubulin/MT and their effects on microtubule dynamics are complex. Like MAPs, these are classified into two main groups based on their effects as microtubule destabilizing agents, which include the clinically important vinca alkaloids (vincristine, vinblastine and vinorelbine), and the

microtubule-stabilizing agents, which include the clinically important taxanes (paclitaxel and docetaxel) and epothilones (Jordan and Wilson 2004).

The binding sites of some of the important MT drugs have been studied in detail and they fall into three regions in the tubulin heterodimers (Wilson and Jordan 2004). The major classification is known as the vinca domain, the colchicine domain and the taxane site. In addition a systematic classification of tubulin drugs lists them on the basis of polymerizing and depolymerizing abilities. The compounds were further classified into four on the basis of the binding sites (Amos 2011). Some of the well studied MT drugs include Paclitaxel (taxol), Baccatin, Epothilone, Thalidomide, Vinblastine, Colchicine etc. These compounds are exploited for a wide range of clinical applications such as in the treatment of cancer, gout etc (Cocca, Dorado et al. 2009, Perez 2009, Perez 2009, Reiner, de las Pozas et al. 2009).

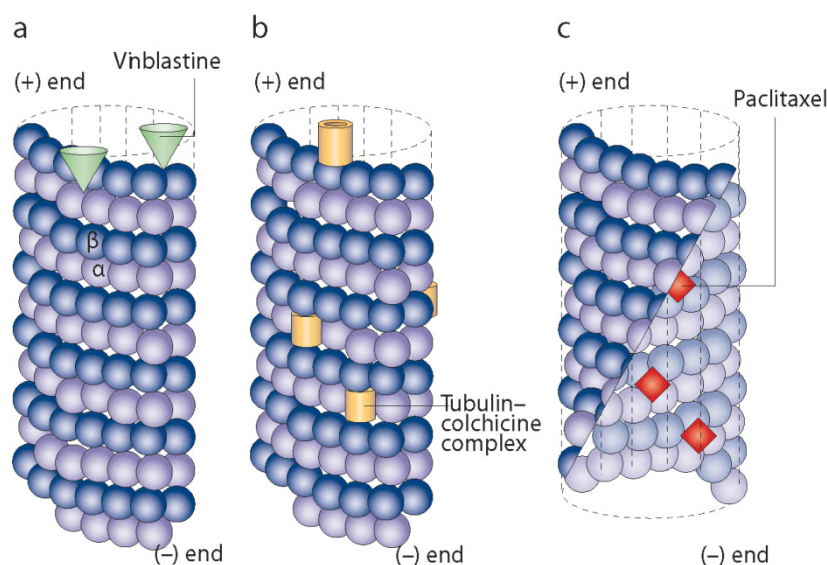


Figure 9: Diverse binding sites of microtubule drugs. Different antimitotic drugs bind at different positions on microtubules. (a) Vinblastine binds at the microtubule plus end on alpha tubulin and binds in between the heterodimer. (b) Colchicine binds in between the dimer and attached to beta tubulin. (c) An interior view of microtubule is shown with taxol binding site. Taxol binds near the M-loop on beta tubulin. (Figure adapted from (Jordan and Wilson 2004))

1.4 Tau-MT interaction

The primary function of Tau is to bind and stabilize microtubules. Tau is also responsible to nucleate and promote MT assembly. It has been established quantitatively that Tau is an important MAP that regulates MT dynamics both *in vitro* and in cells. The effects of Tau upon MT dynamics was examined at high Tau:tubulin ratios (1:30-1:2) and showed that 4R wild type Tau increased the rate and extent of MT growth (Drechsel, Hyman et al. 1992). The recombinant human 4R and 3R Tau isoforms exhibited the similar observations at higher tubulin concentrations under various conditions and it was additionally shown that 4R Tau is a more potent regulator of MTs (Trinczek, Biernat et al. 1995). Later several studies compared the microtubule dynamics regulatory abilities of both 3R and 4R Tau isoforms both *in vitro* and in cells and showed quantitative differences in their properties (Panda, Goode et al. 1995, Panda, Samuel et al. 2003, Bunker, Wilson et al. 2004, Levy, LeBoeuf et al. 2005). It was also demonstrated qualitatively how the Tau:tubulin ratios affect the regulation of MT assembly. That is at lower Tau:tubulin ratios 3R Tau is less active by reducing the MT growth rate whereas 4R Tau exhibit enhancement in MT growth rate. In contrast to this observation, at higher Tau:tubulin ratios both 3R and 4R Tau have increased MT growth rates (Levy, LeBoeuf et al. 2005). Mechanistically, both 3R and 4R Tau bind directly to microtubules, stimulate microtubule polymerization, and regulate microtubule dynamics (Trinczek, Biernat et al. 1995). Both quantitative and qualitative mechanistic differences exist between the two isoform classes and it can be generalized that 4R Tau is more potent than 3-repeat Tau (Goode, Chau et al. 2000).

The capabilities of different 3R and 4R Tau isoforms were compared in different ways and a model for Tau-MT binding was proposed where the first two repeats and the inter repeats form a core MT binding domain (Goode, Chau et al. 2000). This proposed model was supported by many other studies where a number of FTDP-17 and related dementia mutations, which are the basis of neurodegeneration fall in this region. Later on this model was reconsidered and suggested that there is a possibility for this core region that might be composed of different mechanistic capabilities and influenced by other regulatory mechanisms such as phosphorylation (Levy, LeBoeuf et al. 2005).

The regulation of MT dynamic properties of wild type Tau isoforms were compared with their site specific mutated isoforms, especially with the substitution and deletion mutations found in FTDP-17 dementia (Bunker, Kamath et al. 2006, LeBoeuf, Levy et al. 2008). It was demonstrated that significant reduction in the MT binding and regulating properties are associated with specific mutations suggesting that many neurodegenerative diseases are directly correlated to the loss-of-function of Tau in which both amino acid substitutions and altered mRNA splicing in Tau lead to neurodegeneration by diminishing the ability of Tau to properly regulate microtubule dynamics.

The Tau-MT interaction was investigated using NMR spectroscopy using the shorter Tau constructs and full length Tau protein and revealed the MT interacting regions at atomic resolution. It identified the shorter linear motifs of Tau involved in binding which include the domains outside MT binding repeats known as the “Jaws” of the Tau-MT interaction (Mukrasch, von Bergen et al. 2007, Mukrasch, Bibow et al. 2009).

It was suggested that Tau self-assembles by association of the microtubule binding domains of Tau as a result of the abnormal hyperphosphorylation that promotes the self-assembly of Tau into PHFs. This self assembly can occur by neutralizing the inhibitory basic charges of the flanking regions (Alonso, Zaidi et al. 2001). The two hexapeptides, in the repeats R2 and R3 of Tau is found to be important in the formation of PHFs. A recent study using solid state NMR revealed the presence of the rigid core of the fibrils lies in the third repeat with three beta strands (Daebel, Chinnathambi et al. 2012). The surprising and questionable discrepancy has been reported in terms of the Tau-MT interaction that MTs can induce the formation of PHFs (Duan and Goodson 2012).

1.4.1 Phosphorylation as a mean to regulate Tau-MT interaction

Another most important aspect to be investigated is the effects of phosphorylation on the ability of Tau to regulate microtubule dynamics. The effects of in vitro

phosphorylated Tau by cdk5 or MARK upon the regulation of MT dynamics were investigated (Trinczek, Biernat et al. 1995) and it was shown that there is significant reduction in their activity between phosphorylated and non-phosphorylated Tau. The variety of Tau functions of Tau are regulated by its phosphorylation state. The longest isoform of human Tau hTau40 contains 80 Ser or Thr residues and five Tyr residues, and hence 20% of the protein has the tendency to be phosphorylated. There are many phosphorylating agents like kinases and Tau is considered as a “universal phosphate acceptor” (Stoothoff and Johnson 2005).

Phosphorylation at Ser262, Ser214 and T231 result in strong reduction of ability of Tau to bind microtubules (Brandt, Lee et al. 1994, Drewes, Ebner et al. 1997, Ebner, Drewes et al. 1999) and phosphorylation at these sites they are always found in AD (Gustke, Steiner et al. 1992, Mandelkow and Mandelkow 1995, Mandelkow and Mandelkow 1998). It was shown by NMR studies that the phosphorylation of Ser262 causes conformational change and leads to disruption of Tau-MT binding where the experiment was performed by me (Fischer, Mukrasch et al. 2009, Schwalbe, Biernat et al. 2013). Enhanced phosphorylation at several SP/TP motifs and at S214 has been shown in mitotic cells (Illenberger, Drewes et al. 1996). In addition, phosphorylation of Ser214, the major protein kinase-A target site in the proline-rich domain of Tau, decreases the MT-stabilizing and MT-nucleating effects exerted by Tau. This S214 phosphorylation reduces the affinity of Tau from microtubules and thereby, increases the dynamics of MTs. These studies underline the role of Tau and its phosphorylation in the regulation of microtubule dynamics.

On the other hand in Alzheimer’s disease the hyperphosphorylated Tau was found in abnormal fibers, which are one of the histopathological hallmarks of this type of dementia in brain (Buee, Bussiere et al. 2000, Lee, Goedert et al. 2001). The effect of hyperphosphorylation in MT binding and Tau PHF formation is shown in **Figure 10**. The hyperphosphorylation of Tau protein in physiological conditions may not lead to pathologic forms and some unknown factors in the pathological conditions of Alzheimer disease are able to direct hyperphosphorylated protein Tau into abnormal fibers. Tau drug developing strategy to prevent hyperphosphorylation of Tau was studied with selected kinases as drug targets through the three most relevant kinases GSK3 β , CDK5 and ERK2 (Mazanetz and Fischer 2007).

The neuronal MAP Tau is found to be expressed in neuronal cells. The level of Tau expression and molecular complexities are found to be increasing during the developmental stage (Drubin and Kirschner 1986, Caceres and Kosik 1990, Knops, Kosik et al. 1991, Feinstein and Wilson 2005). It is known by previous studies that it is critical to have Tau for promoting the neuronal cell polarity and axonal outgrowth during the developmental stage (Caceres and Kosik 1990, Caceres, Potrebic et al. 1991). It was further shown that Tau is required for neurite outgrowth, the accumulation of microtubule mass and neurite stability (Esmaeliazad, Mccarty et al. 1994). It has also been shown that Tau is able to promote microtubule assembly, stability and bundling (Drubin and Kirschner 1986, Drubin, Kobayashi et al. 1986, Takemura, Okabe et al. 1992). Together with a series of findings related to Tau and neuronal outgrowth it can be generalized as Tau is important in proper neuronal development by regulating microtubule dynamics and axonal stability.

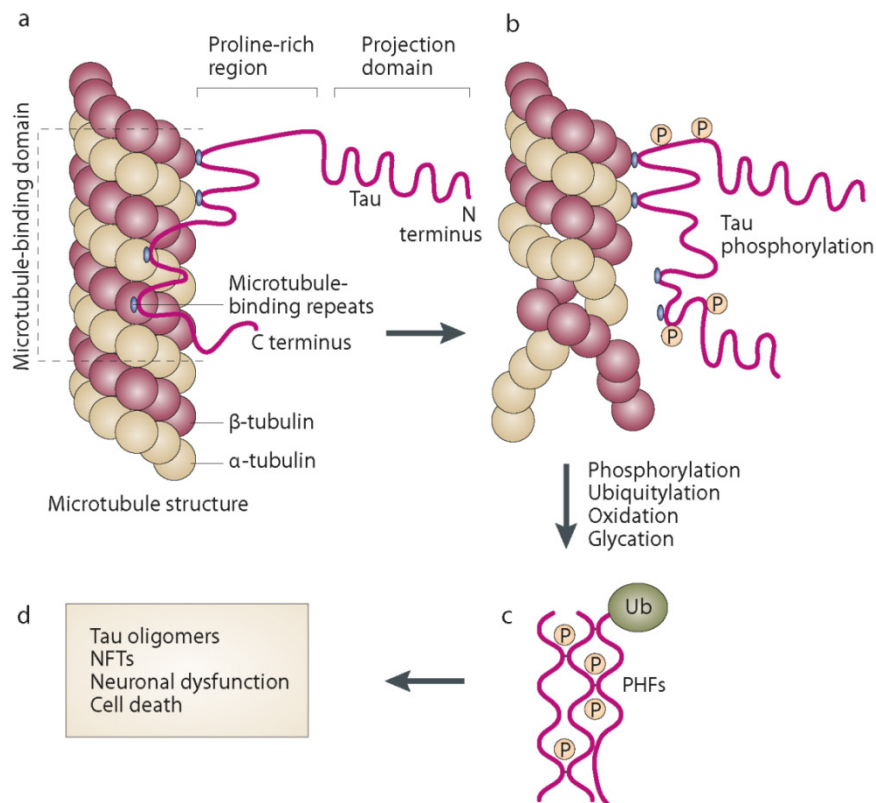


Figure 10: Effect of phosphorylation of Tau on Tau-MT interaction and Tau pathology. Tau stabilizes microtubules using the microtubule binding domains. Phosphorylation in the abnormal rate attenuates Tau binding to microtubules and form paired helical filaments. Proteolytic processing leads to formation of Tau oligomers and aggregates in the form of neurofibrillary tangles (NFTs). (Figure adapted from Mazanetz et al., 2007) .

1.5 Structure of MT-bound Tau

The major function of Tau is to bind and stabilize microtubules. Hence it was expected that the binding of Tau to microtubules induce conformational changes. Several studies based on different biophysical methods such as electron microscopy studies showed that Tau is mainly found on the outer surface of MTs (Hirokawa, Shiomura et al. 1988). Later on several attempts were done to establish a structural view of MT-bound Tau using cryo-EM studies and image reconstruction (Kar, Fan et al. 2003, Santarella, Skiniotis et al. 2004).

It was discussed before that Tau becomes more compact upon binding with microtubules (Butner and Kirschner 1991) where 3 or 4 repeats of Tau were considered as independent tubulin binding domains thereby proposing a model as multiple repeats cross-link the tubulin sub units. Whereas other studies indicated that even in the MT-bound state Tau retains much of its disordered state (Al-Bassam, Ozer et al. 2002, Santarella, Skiniotis et al. 2004). A recent study based on atomic force microscopy showed that at saturating concentrations, Tau forms a ~1nm thick layer around the MTs by binding along the protofilaments and leaving the elasticity of MTs unaffected (Schaap, Hoffmann et al. 2007). Nevertheless, NMR analysis of Tau-microtubule interactions highlighted binding of several linear motifs of amino acid residues in Tau, especially in the repeat domains and the flanking regions to microtubules. The residues ²⁷⁵VQIINKKLDLS²⁸⁵ strongly contribute to binding to the microtubules along with clusters of positively charged residues upstream of the PGGG motifs (Mukrasch, Biernat et al. 2005, Mukrasch, Markwick et al. 2007).

The Tau-MT/tubulin interaction was studied for the first time using the thermodynamic point of view by isothermal titration calorimetry (ITC) provided similar isotherms within the temperature range of 10°C and 37°C (Tsvetkov, Makarov et al. 2012). At all temperature conditions two stoichiometric values obtained, 0.8 and 0.2, suggested the possible binding mechanism involved in Tau-tubulin interaction where it does not depend on the type of the polymer formed. The model proposed is in good agreement with the longitudinal binding mode of Tau along the protofilaments outside the MT surface (Al-Bassam, Ozer et al. 2002, Schaap, Hoffmann et al. 2007).

1.6 Binding site of Tau on Microtubules

Considering the Tau-MT interaction and the mechanism involved therein, a number of questions arise such as how Tau interact with MTs, what is the driving force, where do they interact and what are the conformational changes happening during interaction. In terms of the binding site of Tau on MTs different binding sites and binding models have been proposed. Many studies showed that Tau binds to MTs on their outer surface being the negatively charged carboxyl termini of tubulin as the binding site (Chau, Radeke et al. 1998, Ackmann, Wiech et al. 2000, Al-Bassam, Ozer et al. 2002). The interaction between the positively charged microtubule binding domain and the negatively charged c-terminal domain of tubulin was the underlying mechanism behind this model.

The surface decoration model of Tau on MTs (Santarella, Skiniotis et al. 2004) again suggested Tau binds more or less outside the MTs by retaining their unfolded nature. Though it was suggested to be the outer surface another remarkable observation is it is α -tubulin. This further explains the mutual independence in binding between kinesin and Tau, where the former is supposed to bind on β -tubulin and Tau on α -tubulin.

Another model suggests that that Tau binds at the inner surface of MTs near the M-loop of β -tubulin, which is the binding site for taxol (Kar, Fan et al. 2003). In this model the repeats of Tau bind at the inner side near the M-loop and the positively charged proline rich region of Tau binds at the C-terminus of tubulin (Kar, Fan et al. 2003). On the other hand, high-resolution metal-shadowing and cryo-electron microscopy using full-length Tau suggested that Tau is not only largely disordered when bound to microtubules but also it binds exclusively to the outer surface of the microtubules (Marx, Muller et al. 2005). All the proposed models were on the basis of experiments performed in different conditions as well as using different methods. It is therefore still unclear which binding site is biologically relevant in terms of their structure and function. However there are different tubulin targeting drugs with highly specific binding sites like taxane binding site, vinca ligand binding site and colchicine binding site as reported (Amos 2011, Canales, Rodriguez-Salarichs et al. 2011) and the possibility for sharing the binding site between Tau and these compounds need to be considered.

1.7 Protein NMR Spectroscopy

Both liquid- and solid-state NMR have become major techniques in structural biology. Liquid-state NMR is a powerful, robust and noninvasive technique to investigate soluble proteins at atomic resolution (Wüthrich 1990). Compared to X-ray crystallography, solution NMR allows not only to investigate the protein structures in a nearly physiological environment, but is also to determine their dynamic properties. Moreover, solution NMR technique allows the study protein-ligand and protein-protein interactions, protein folding, kinetics, catalysis and moreover structure determination.

1.7.1 Relevance of structure determination using NMR

Many biological activities are regulated by the interaction of proteins with nucleic acids and other biomacromolecules. Therefore it is quite essential to study these interactions both spatially and temporally. On top of that, it is important to investigate the mechanism involved in interactions including the specificity and selectivity. Structural analysis at atomic-resolution will give deep insight in understanding these aspects. X-ray crystallography and NMR are the widely used techniques for structural analysis of biomacromolecules. X-ray crystallography is most suitable for high molecular weight systems where crystallization is possible. Whereas NMR is highly flexible and robust in terms of sample conditions and handling although there is a certain degree of size limitation.

It is becoming more relevant to study the protein-protein interactions that form even macromolecular complexes as many biological processes are mediated by interactions between proteins. The involvement of protein interactions with its partner proteins, peptides and drugs makes it important to study them at a molecular level which thereby helps in understanding the molecular basis of diseases.

1.7.2 Application of NMR to structure determination of biomacromolecules

Structure determination of protein complexes using NMR has certain size limitations and is generally upto ~ 40kDa. The implementation of Transverse Relaxation Optimized Spectroscopy (TROSY) (Pervushin, Riek et al. 1997) in the traditional NMR methods and other NMR methodologies brought the size limitation near 100kDa (Pervushin, Riek et al. 1997, Riek, Wider et al. 1999, Riek, Fiaux et al. 2002). Isotope labeling and other methodological developments are the accelerating factors in NMR based structural calculations. NMR based 3D structure determination of biomolecules is usually performed by distance geometry calculations or simulated annealing (Güntert, Mumenthaler et al. 1997, GÜNTERT 1998, Schwieters, Kuszewski et al. 2003). Structural constraints can be derived from NOE, J-coupling, Residual Dipolar Couplings (RDC), Paramagnetic Relaxation Enhancement (PRE) etc. Another feasible approach is to map the binding interface of large complexes if the exchange is in the NMR time scale is suitable for signal detection.

The strategy of structure determination by NMR depends on the timescales of chemical or conformational exchange processes, which may affect line shapes, relaxation rates, and chemical shifts of resonances. Depending on the strength of the interaction of a complex, it can be broadly classified into slow exchange, intermediate exchange and fast exchange. That is strong binding, weak binding and the intermediate exchange case, called coalescence.

1.7.3 Protein-ligand interactions by NMR spectroscopy

NMR spectroscopy is a useful technique in studying protein-protein and protein-ligand interaction. The study of these interactions can be broadly classified into two classes on the basis of the target resonances in-study. (1) Focusing the protein resonances and (2) Ligand resonance studies (Carlomagno 2005). There are several factors that determine this selection. In the case of target resonance detected experiments it relies on the availability of the isotopically labeled target and the size of which is suitable to detect by NMR. Here mapping the binding interface of the target is possible with the help of

two dimensional heteronuclear correlation experiments (eg: HSQC) (Bodenhausen and Ruben 1980). Whereas in the ligand detected methods such as transferred NOE (tr-NOE), saturation transfer difference (STD) (Mayer and Meyer 1999, Viegas, Manso et al. 2011), NOE pumping (Chen and Shapiro 1998), Water LOGSY (Dalvit, Pevarello et al. 2000) and INPHARMA (Sánchez-Pedregal, Reese et al. 2005, Orts, Griesinger et al. 2009), only the resonances of the ligand is observed and is exclusively applicable for the ligands in the low affinity range (millimolar range). Latter approach is highly desirable when the target is either too large to be detected by NMR or not available in the isotopically labeled form. Binding interface information can be obtained by following NMR spectral parameters:

- (a) Line broadening
- (b) Chemical shift perturbation
- (c) Change in NOE
- (d) Intermolecular magnetization transfer

NMR chemical shifts are very sensitive to variations in the local electronic environment, for example, due to binding. Hence it is possible to map the binding interface of weakly binding ligand and protein receptor using the small changes in ^1H and ^{15}N shifts in a calibrated titration. The ligand can either be a protein, peptide or small molecule. No chemical shift changes will be observed for residues that do not participate in the interaction and those resonances that are shifted highlight the residues involved in the binding interface or are affected by minor conformational rearrangements caused by the interaction. Here, the intensity of the resonances will be varying according to the exchange rate and if it is near coalescence condition there will have severe line broadening that will again reflect the involvement of the respective regions of protein involved in binding.

Considering the Tau-tubulin/MT interaction, where tubulin is ~100kDa and MTs is in the range of several megadaltons it is beyond the limit of NMR detection. The application of sophisticated NMR methods is very much limited in the case of tubulin as it cannot be obtained in the isotopically labelled form. Till now the recombinant expression of tubulin in significant amount is unsuccessful because of their complexity in the folding (Clement, Savarin et al. 2010). However there are several studies involving

tubulin and its binding partners as smaller drug molecules, peptides where the exchange transferred methods (Carlomagno 2005, Sánchez-Pedregal, Reese et al. 2005, Orts, Griesinger et al. 2009) have been employed. These include tr-NOE, STD-NMR, tr-CCR and INPHARMA and are detailed in the section methods.

1.8 Aim of the study

The majority of the functions of MTs are regulated by the interaction with its partners. To gain insights into the different aspects of physiological processes and mechanisms involved in the interaction between MTs and its binding partners several biophysical techniques have been used. In particular, detailed information regarding the role of MT and associated proteins and drugs is possible via structural investigation. Among the available techniques to derive structural information, NMR is the only method that allows a structural description in near physiological conditions and at atomic resolution.

As Tau is an intrinsically disordered protein (Dyson and Wright 2005) X-ray crystallography cannot be applied and NMR spectroscopy is the method that allows the description of its conformations. Although the function of Tau and Microtubules has been studied for many years, it is still unclear how Tau binds to microtubules. The intrinsically disordered Tau protein binds and stabilizes MTs. Though the ensemble of conformations that Tau populates in solution was described (Mukrasch, Bibow et al. 2009), the high resolution structure of microtubule-bound Tau is still unknown. The aim of the project was therefore to perform an in depth study of the Tau-MT interaction and to determine the MT-bound conformation of the Tau protein. Furthermore, the identification of the binding sites of Tau on MTs will help to provide a three-dimensional view of the MT-bound Tau protein. To achieve these goals, I combined a “divide and conquer approach” with exchange-transferred NMR methods. Understanding the Tau-MT interaction and the mechanism involved in the stabilization of MTs will shed new insights into the molecular mechanism of Tau-mediated neurodegeneration and also foster new ideas to increase the therapeutic efficiency of MT-targeting drugs, especially in the treatment of neurodegenerative diseases such as AD.

2 Materials and Methods

2.1 Chemical compounds

Taxol, Baccatin, Thalidomide, Vinblastine, Colchicine and GTP were purchased from Sigma Aldrich.

2.2 Protein preparation and purification

Cloning, expression and purification of wt and mutant hTau40, hTau23, K18 and F4 proteins were performed by Dr. Jacek Biernat in collaboration with Prof. Mandelkow group, DZNE, Bonn.

2.2.1 Tau constructs used in this study

1. hTau40 (441 residues, I2R4) the largest human Tau isoform in the central nervous system, contains 2 amino terminal inserts (I2) and four C-terminal repeats (R4).
2. hTau23 (352 residues, I0R3) the shortest human Tau isoform, doesn't contain any amino terminal insert (I0) and contains three C-terminal repeats (R3).
3. The human Tau constructs K18, representing the 4-repeat C-terminal assembly domain contains the amino acids: Q244-E372 with amino terminal methionine.
4. F4, construct published by Fauquant/Knossow et al. (2011) comprises the amino acids S208 – S324 with amino terminal methionine.

All residue numbers refer to hTau40.

Tau constructs K18 and F4 were generated using PCR method on the template of hTau40 DNA sequence and provided with NdeI and BamHI restriction enzyme recognition sites.

hTau40, hTau23, K18 and F4 were introduced into pNG2 vector, a derivative of commercial plasmid pET-3a (Merck-Novagen, Darmstadt) using the NdeI and BamHI restriction sites.

2.2.2 Protein expression in E.coli

pNG2 plasmids with inserted hTau40, hTau23, K18 and F4 coding sequences were transformed into E.coli strain BL21(DE3) (Merck-Novagen, Darmstadt). These bacterial strains were used for protein expression. The expressed proteins were purified from bacterial extract by making use of the heat stability of the Tau protein and by FPLC SP-Sepharose ion exchange chromatography (GE Healthcare, Freiburg).

The bacterial pellet was resuspended in the boiling-extraction buffer (50 mM MES, 500 mM NaCl, 1 mM MgCl₂, 1 mM EGTA, 5 mM DTT, pH 6.8) complemented with protease inhibitor cocktail. The cells were disrupted with a French pressure cell and subsequently boiled for 20 min. The soluble extract was isolated by centrifugation, the supernatant was dialyzed against two changes of cation exchange chromatography buffer A (20 mM MES, 50 mM NaCl, 1 mM EGTA, 1 mM MgCl₂, 2 mM DTT, 0.1 mM PMSF, pH 6.8) and loaded on FPLC SP-Sepharose column. The proteins were eluted by a linear gradient of cation exchange chromatography buffer B (20 mM MES, 1 M NaCl, 1 mM EGTA, 1 mM MgCl₂, 2 mM DTT, 0.1 mM PMSF, pH 6.8).

In the case of hTau isoforms hTau23 and hTau40, Tau breakdown products were separated in the second chromatography step using gel filtration method on Superdex G200 column (GE Healthcare, Freiburg). PBS buffer was used for gel filtration column (137 mM NaCl, 3 mM KCl, 10 mM Na₂HPO₄, 2 mM KH₂PO₄, pH 7.4) with 1 mM DTT (freshly added).

2.2.3 Protein expression in E.coli with isotope labeling

To label the Tau proteins with ¹⁵N and ¹³C isotopes, the E.coli cultures were grown in a M9 minimal medium with ¹⁵NH₄Cl (1g/liter) and ¹³C glucose (4g/liter) (Eurisotop, Saarbrücken).

Protein samples uniformly enriched in ¹⁵N were prepared by growing E.coli bacteria in minimal medium containing 1g/liter of ¹⁵NH₄Cl exclusively.

For isotope labeling of Tau proteins for NMR experiments a rapid and efficient approach for preparing isotopically labeled recombinant proteins was used, the general “Marley” protocol based on Marley, J and Bracken, C. *J.Biomolec. NMR* 20, 71(2001).

This production method generates cell mass using unlabeled rich media followed by exchange into a small volume of labeled media at high cell density. Following a short period for growth recovery and unlabeled metabolite clearance, the cells were induced with 0.8 mM IPTG. The expression yields obtained provide reduction in isotope costs.

Example for 1L E.coli culture, bacteria were grown in 1 L LB (Luria broth) at 37°C, upon reaching optical cell density at 600 nm (OD_{600}) ~ 0.7. The cells were pelleted, washed using an M9 salt solution and the pellet was resuspended in 250 ml of isotopically labeled minimal medium. The culture was incubated for one hour to allow the recovery of growth and clearance of unlabeled metabolites. After this 1 h step protein expression was induced by addition IPTG to a concentration of 0.8 mM. The cells were harvested after 4 hours of incubation. The expressed proteins were purified from bacterial extract by method described for non isotopic expression protocol.

2.2.4 Standard 5 x M9 Minimal Media salts without nitrogen source.

For 1L 5xM9 salts:

64g $Na_2HPO_4 \cdot 7H_2O$

15g KH_2PO_4 and 2.5g NaCl

Add H_2O to final volume 1L and autoclave.

2.2.5 Preparation of 500mL M9 minimal medium.

100mL 5xM9 salts

1 mL 1M $MgSO_4$

50 uL 1M $CaCl_2$

5 mL 100x Basal Medium Eagle Vitamin Solution (Gibco)

2.5 mL filter sterilized NH_4Cl (0.2 g/mL) or 0.5g dry

10 mL 20% d-glucose or 2g dry

2.2.6 Adaptation of E.coli bacteria for growing in D_2O /minimal medium (M9) labeled with ^{15}N NH_4Cl

Bacteria from E.coli colony containing pNG2/Tau construct plasmid growing on LB dish were inoculated and grown in 1 ml of M9/33% D_2O medium over night. The

bacteria were spun down and resuspended into M9/66% D₂O medium and grown again over night. After centrifugation the bacteria were resuspended in M9/100% D₂O medium and grown to 0.5-0.6 OD₆₀₀ and induced for the expression with IPTG. After incubation the expressing cells for 3 hrs, the bacteria were harvested and purified from bacterial extract by method described for non-isotopic expression protocol. In the case of difficulties in growing E.coli expressing Tau construct in M9/100% D₂O the content of D₂O was reduced to 85%.

2.3 Microtubule assembly

Porcine brain tubulin was purified as described (Mandelkow, Herrmann et al. 1985, Gustke, Trinczek et al. 1994). Tubulin polymerization was performed in MT assembly buffer 100 mM Na-PIPES, pH 6.9, 1 mM EGTA, 1 mM MgSO₄, 1 mM GTP, 1 mM DTT. Fixed concentration of tubulin (20-50μM) was incubated with equal concentration of taxol (paclitaxel) at 37°C for 20-30 min to induce microtubule formation. The suspensions of the samples were fractionated by ultracentrifugation at 40,000 x g for 20 min. Resuspended the MT pellet to the required buffer. The stabilized microtubule solutions were then diluted to the desired concentration.

2.4 Synthetic peptides

A list of synthetic peptides used in this study is given in **Table 2**. TP2, TR1, TR2, TR3 and TP2_pT231 were purchased from EZBiolab, USA. Other Tau, tubulin and I19L peptides were synthesized by Kerstin Overkamp in Department of NMR-based Structural Biology, Max Planck Institute for Biophysical Chemistry in Göttingen. Synthesis was based on standard Fmoc-solid-phase peptide synthesis method using an ABI 433A synthesizer (Applied Biosystems). Peptides were synthesized with acetyl- and amide protection groups at the N- and C-termini, respectively. Peptides were further purified by reversed-phase HPLC and the pure product was lyophilized. All the peptides in **Table 2** are unlabeled.

Table 2: Synthetic peptides used are listed with the sequence and nomenclature followed during the study.

Peptide	Sequence	Name
Tau162-188	QKGQA NATRI PAKTPPAPKTPPSSGEP	TP1
Tau211-242	RTPSLPTPPTREPKKVAVVRTPPKSPSSAKSR	TP2
Tau239-267	AKSRLQTAPVPMPLKKNVKSIGSTENLK	TR1
Tau265-290	NLKHQPGGGKVQIINKKLDLSNVQSK	TR2
Tau296-321	NIKHVPGGGSVQIVYKPVLDLSKVTSK	TR3
Tau267-312	KHQPGGGKVQIINKKLDLSNVQSKCGSKDNIK HVPGGGSVQIVYKP	TR23
Tau327-353	NIHHKPGGGQVEVKSEKLDKDRVQSK	TR4
Tau368-402	NKKIETHKLTFRNAAKAKTDHGAEIVYKSPVV SGD	TR'
Tau52-69	TEDGSEEPGSETSDAKST	TN1
Tau1-26	MAEP RQEFVEMEDHAGTYGLGDRKDQ	TN2
Tau403-422	TSPRHLSNVSTGSIDMVDSP	TC1
α -Tubulin433-451	EEVGVDSVEGEGEEEGEEY	aTubC
β -Tubulin424-445	QYQDATADEQGEFEEEGEEDEA	bTubC
Stathmin N-terminal domain	IQVKELEKRASGQAFELIL	I19L

In addition to these, single residue mutated and phosphorylated samples of selected Tau peptides were synthesized which include TR3_P301L, TR3_P301S, TR23_ΔK280 and TP2_pT231.

2.5 NMR Spectroscopy

2.5.1 Interaction studies

The different NMR interaction experiments performed are listed in **Table 3**.

Table 3: Interaction studies performed using Tau and Tau constructs

Protein	Protein Receptor	Interacting molecule
HTau40	MT	
HTau40	Tubulin	
HTau23	MT	
HTau40	MT	NaCl
HTau40_Y310N	MT	
Hatu40_Emutant	MT	
Hatu40	MT	Taxol
Hatu40	MT	Baccatin
Hatu40	MT	Thalidomide
Hatu40	MT	Vinblastine
Hatu40	MT	Colchicine
Hatu40	MT	TP2
Hatu40	MT	TR3
Hatu40	MT	TN1
K18	Tubulin	
F4	Tubulin	
F4	MT	
F4	MT	NaCl

2.5.2 2-D NMR experiments

2.5.2.1 Heteronuclear Single Quantum Coherence (HSQC)

The Heteronuclear Single Quantum Coherence (HSQC) is one of the frequently used experiments in the protein NMR. This method gives one peak per pair of coupled

nuclei, whose two coordinates are the chemical shifts of the two coupled atoms (Keeler). HSQC detects correlations between nuclei of two different types which are separated by one bond. Each residue of the protein except proline has an amide proton attached to a nitrogen in the peptide bond and the HSQC provides the correlation between the nitrogen and amide proton and each amide yields a peak in the HSQC spectrum.

The protein-protein or protein ligand interactions can be well studied using the 2D ^1H - ^{15}N HSQC experiments, where one can probe the interaction with the help of change in chemical shifts (δ) of the resonances and line broadening. The HSQC spectrum of the ^{15}N labeled protein will be recorded with and without the unlabeled receptor or ligand at stoichiometric or sub stoichiometric conditions. The modifications such as chemical shift perturbation, line broadening or signal disappearance of the cross peaks of specific residues involved in binding indicates the interaction between partners. These modifications depend on the size of the complex formed. In the case of Tau-MT/tubulin complex as the receptor is very large the binding residues experience extensive dipolar interaction as well as large correlation time, leading to severe line broadening.

2.5.2.1.1 Chemical shift difference

To compare the 2D ^1H - ^{15}N HSQC chemical shifts from different samples, the differences in the resonance position was calculated using the formula:

$$\Delta\delta = ((\Delta\delta_{\text{N}}/5)^2 + (\Delta\delta_{\text{H}})^2)^{1/2}$$

2.5.2.1.2 Intensity ratio

Peak intensities from the 2D ^1H - ^{15}N HSQC experiments were collected and the line broadening was evaluated by calculating the intensity ratio of the NMR signals originating from the bound and free protein as $I_{\text{bound}}/I_{\text{free}}$ and was averaged over a 3 residue window.

2.5.2.1.3 Experimental procedure

All 2D ^1H - ^{15}N -HSQC experiments were recorded on a Bruker spectrometer (Bruker Karlsruhe, Germany) with 700, 800 or 900 MHz proton frequency. The spectrometers are equipped with a TCI cryo probe (Z-gradient). The HSQC pulse sequence contained a 3-9-19 watergate block for water suppression. The experiments

were recorded with 600 increments in the indirect dimension and 2k points (cryo probe) in the direct dimension, zero filled to 4k and 1k points in the direct and indirect dimension, respectively and processed with a sine-squared bell window function shifted either by 90 degree (SSB=2 in TopSpin), or by 60 degree (SSB=3 in TopSpin). The nitrogen carrier frequency was set to 118 ppm and the spectral width was 24 ppm. For protons, the carrier was set to the water resonance frequency. The data were processed using TopSpin 3.0 (Bruker).

2.5.2.2 TROSY and CRINEPT-HMQC-TROSY

CRINEPT (cross-correlated relaxation-enhanced polarization transfer) provide more polarization transfer than INEPT. CRINEPT-HMQC-TROSY enables the detection of very high molecular weight proteins greater than 500kDa. Similar to the TROSY it detects the ^1H - ^{15}N moieties but with CRINEPT (cross-correlated relaxation-enhanced polarization transfer) as the element for polarization transfer. Deuteration and TROSY element reduce transverse relaxation and CRINEPT further increase the sensitivity compared to INEPT transfer. Since decoupling is applied during t_1 evolution but not during acquisition there will be two multiplet peaks per ^1H - ^{15}N moiety. Unlike TROSY, where it enables to detect residues which are in the flexible region, CRINEPT-HMQC-TROSY give peaks from both flexible and rigidly structured regions. For flexible parts one observes both multiple components whereas for the rigidly structured region of the protein the rapid transverse relaxation suppresses the fine structure component in the lower field. Thus it enables to detect and distinguish both the highly flexible and more rigidly structured region of the protein. If imperfect deuteration or size limitation suppress detection of any residues it indicates the presence of the highly rigid and structured region of the protein or protein complex.

2.5.2.2.1 Experimental procedure

All the CRINEPT-HMQC-TROSY experiments were done on 900 MHz spectrometer with a cryo probe at 30°C. ^2H , ^{15}N labeled F4 was used for the experiments. Samples were prepared with a concentration of 40 μM F4 and 120 μM tubulin and 25 μM F4 and 75 μM MTs. The buffer contained 50 mM $\text{NaH}_2\text{PO}_4/\text{Na}_2\text{HPO}_4$, pH 6.8, 10% (v/v) D_2O and was filled in a 3mm shigemi tube. The 2D ^1H - ^{15}N - CRINEPT-HMQC-TROSY

and TROSY experiments were recorded on a Bruker 900 MHz spectrometer equipped with a TCI cryoprobe (Z-gradient). The experiments were recorded with 128 increments in the indirect dimension and 2k points (cryo probe) in the direct dimension; zero filled to 4k and 1k points in the direct and indirect dimension, respectively.

2.6 Structure determination of MT-bound Tau peptides

Considering the Tau-tubulin/MT interaction and structural investigation, NMR has got size limitations where tubulin is ~100kDa and MTs in many MDa, it is beyond the limit of NMR detection. Together with the NMR size limitation and unavailability of the isotopically labeled tubulin, the structural investigation of MT-bound Tau can be done using shorter Tau peptides. The peptides which bind with low affinity act as a promising ligands with tubulin/MT and allow the structural investigation of the bound peptides with the aid of the exchange transferred NMR methods. The methods which are implemented in Tau peptide-MT/tubulin complex include tr-NOE, STD-NMR and INPHARMA.

2.6.1 NMR structure determination of peptides

The overall process involved in structure determination of peptides includes;

- 1) Sequential resonance assignment of peptides
- 2) Determination of distance restraints using tr-NOE
- 3) 3D structure calculation of peptides using the specific algorithms

The first step in NMR structure determination involves optimizing the sample conditions followed by collecting experimental data such as COSY, TOCSY and NOESY spectra of the peptide. It is necessary to fulfill the assignment of the resonances in the spectra beforehand which will be used to provide distance restraints between protons and finally to determine the three dimensional structure of the peptide.

2.6.1.1 Assignment procedure

NMR structural characterization of peptides and proteins requires resonance assignment of all the residues. In the case of shorter unlabeled peptides which are having

the size of ~3 kDa, the proton (^1H) assignments can be used for the structural characterization. To that end it is possible to use the through bond and through space correlation spectroscopy. A short description of the basic 2D experiments used for the assignment in the present study is given below.

2.6.1.1.1 COSY (Correlation spectroscopy)

Assignment of the peptide starts with the analysis of proton through bond connectivities with the help of COSY and TOCSY spectra and thereby achieves identification of the spin systems. This allows to separate different amino acid types present in the peptide sequence. The COSY displays ^1H - ^1H -correlations due to through-bond scalar couplings. Different amino acids possess characteristic positions of cross peaks in the spectrum. COSY is used to identify spins which are coupled to each other.

2.6.1.1.2 TOCSY (Total correlation spectroscopy)

The TOCSY experiment is similar to the COSY experiment, in that cross peaks of coupled protons are observed. However, cross peaks are observed not only for nuclei which are directly coupled, but also between nuclei which are connected by a chain of couplings. This makes it useful for identifying the larger interconnected networks of spin couplings. This ability is achieved by inserting a repetitive series of pulses which cause *isotropic mixing* during the mixing period. Longer isotropic mixing times cause the polarization to spread out through an increasing number of bonds (Keeler). A TOCSY experiment results in all cross peaks due to protons of the same spin system. Since no scalar coupling across the amide bond protons from different amino acids always belong to different spin systems. Thus it is possible to decide to which type of amino acids the spin system belongs.

2.6.1.1.3 NOESY (Nuclear Overhauser Effect spectroscopy)

NOESY cross peaks are originating from the dipolar couplings resulting from interactions of spins through space and hence only depend on the distance but not on the number of intervening bonds. Dipolar couplings are averaged to zero in solution but give rise to one of the very important relaxation phenomena called NOE (nuclear Overhauser effect). Thus the strong dependence of the cross peak intensity on the distance separation

between the protons makes it an ultimate tool for the 3D structure determination of peptides and proteins.

Sequential resonance assignment means connecting spin systems in their sequential order. In the next step it involves the sequential assignment where different spin systems identified are connected with the help of NOESY spectra. The sequential connectivity from i^{th} residue to $i+1^{\text{th}}$ residue should be continued until the complete sequential resonance assignment of individual amino acids in the NOESY spectrum is achieved unambiguously.

2.6.1.1.4 NMR spectroscopy for assignment of peptides

All unlabeled Tau peptides in **Table 2** were assigned using two-dimensional ^1H , ^1H -DQF-COSY, ^1H , ^1H -TOCSY and ^1H , ^1H -NOESY spectra recorded at 5 °C, either on Bruker 700 MHz spectrometer equipped with a cryo probe or 700 MHz oxford spectrometer with a room temperature probe. Samples were prepared with a concentration of 1 mM and the buffer contained 50 mM $\text{NaH}_2\text{PO}_4/\text{Na}_2\text{HPO}_4$, pH 6.8, 10% (v/v) D_2O . Acquisition parameters were commonly set to 40 transients, sweep widths of 12 x 12 ppm (F2 x F1), 2048 x 512 total points (F2 x F1), and mixing times of 60 ms(DQF-COSY), 60 ms (TOCSY) or 150 ms (NOESY). The side chain proton assignments were confirmed by using the natural abundance ^1H , ^{13}C -HSQC and ^1H , ^{15}N -HSQC spectra acquired. Spectra were processed using Topspin 3.0 or NMRPipe and analyzed using Sparky 3.

2.6.1.2 Transferred-NOE (tr-NOE)

The basic principle of the transferred detection methods depends on the transfer of relaxation properties from the bound state to the free state of the ligand that allows the detection of intra-ligand NOEs generated in the bound state which are transferred to the free ligands by means of chemical exchange and are finally observed. For tr-NOE detection the binding affinity should be relatively weak and there should be fast exchange between bound and free forms of ligands (Balaram, Bothnerb.Aa et al. 1972,

Clore and Gronenborn 1982). It is a necessary condition to be fulfilled for the transferred techniques that there should be fast exchange between ligands in the bound and free states, with the dissociation constant (K_D) is of the order of μM to mM range. Ligand is usually taken in large excess with varying ratios with receptor like 10:1 to 100:1. The resultant NOEs are expected to be relatively larger than those generated in the free ligand as a consequence of the slow molecular tumbling of the protein-ligand complex. The concept of tr-NOE is represented as a cartoon as shown in Figure 11.

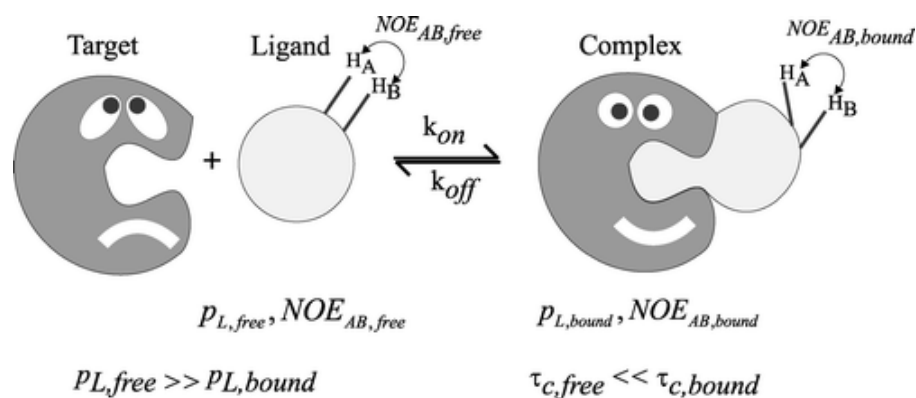


Figure 11: Pictorial representation of the ligand-receptor interaction and reversible binding of the ligand. The possible change in conformation upon binding will be observed as the population weighted averaging of the NMR observable NOE. The average of the NOE observed depends on the rotational correlation time of the ligand and complex. (figure reproduced from (Carlomagno 2005))

If a ligand having very short rotational correlation time (τ_c) is bound to a large receptor with long τ_c , the τ_c of the ligand becomes equivalent to that of the receptor. The NOE developed in the bound state will be transferred back to free state as a result of the fast exchange. The observed NOE will be the population weighted average of the bound and free ligands and the information from the bound state will be dominant with all the information about the receptor bound conformation of the ligand. The tr-NOE cross peaks are finally treated as the normal NOEs to derive distance restraints to be used for structure determination. A detailed description of the NMR methods applicable for the weakly binding ligands and tr-NOE method is reviewed in (Carlomagno 2005, Clement, Savarin et al. 2010). Tr-NOE method is being used in a variety of systems like small molecules to peptides which are bound to macromolecules (Gizachew and Dratz, Adams, Dratz et al. 1997, Jiménez-Barbero, Canales et al. 2006, Canales, Rodriguez-

Salarichs et al. 2011, De Bona, Deshmukh et al. 2012). Finally tr-NOE allows determination of the 3D structure of MT-bound Tau peptides which are in fast exchange with the free peptides.

2.6.1.3 Introduction to INPHARMA

The basic principle of tr-NOESY experiment, where the magnetization from one ligand is transferred to protein and back to the same ligand, is applied to map the binding site of more than one ligand provided the binding orientation of one ligand is known (Sánchez-Pedregal, Reese et al. 2005, Orts, Griesinger et al. 2009). If both ligands are competing for a common binding site the magnetization transfer from one ligand is transferred to the protein and transferred back to the second ligand so that additional cross peaks can be observed between the two ligands as a result of the overall magnetization transfer between the two ligands. This method is particularly useful to determine the orientation of one ligand if the complex structure of another ligand bound to the protein is known from prior studies. This method works well with a low concentration of receptor protein and comparatively very high concentration of the ligands. This was demonstrated by Carlomagno to determine the tubulin bound conformation of taxoids (Carlomagno 2005, Orts, Griesinger et al. 2009). A simple schematic diagram is shown in **Figure 12**.

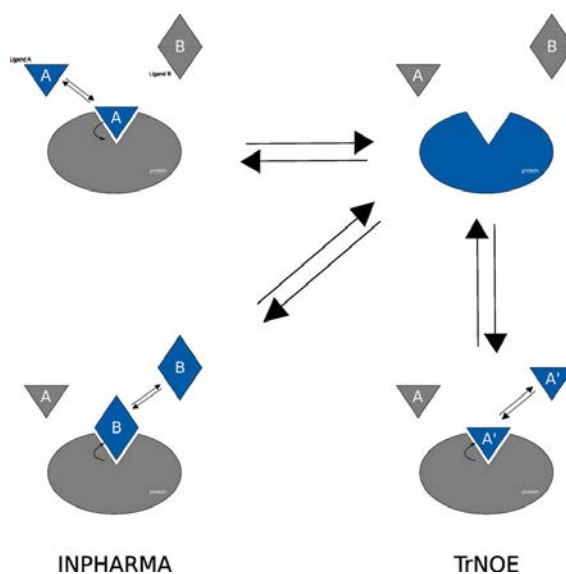


Figure 12: Basic principle of the Tr-NOE and INPHARMA experiment. Transferred NOE involves the transfer of magnetization from ligand A back to itself through the protein and back to another competitively binding ligand B in INPHARMA. Figure taken from (Frontiers in Bioscience 14, 4565-4574, January 1, 2009)

2.6.1.3.1 Experimental details

The tr-NOESY spectra of all the Tau peptides in the presence of MTs were performed at 5 °C, on a Bruker 900 MHz spectrometer equipped with a cryo probe. Samples were prepared with a concentration of 0.7 mM peptide and 35 μ M MTs in the 20:1 ratio. The buffer contained 50 mM $\text{NaH}_2\text{PO}_4/\text{Na}_2\text{HPO}_4$, pH 6.8, 10% D_2O . All the 2D tr-NOESY experiments were carried out with 2048 data points x 512 increments x 40-64 transients per FID. The sweep width of 12 x 12 ppm was used in both dimensions. The NOE mixing times of 30, 50, 80, 100, 150 and 250 ms were used for different peptides. The data were zero filled to 4096 x 1024 data matrix prior to Fourier transformation. All the spectra were processed using Topspin 3.1 or NMRPipe and analyzed using Sparky 3.114.

2.6.2 Structure calculation

Transferred-NOESY data acquired with shorter mixing time were used to extract distance restraints for quantitative structure calculations. The manually assigned cross peak intensities were calibrated using the automated calibration method ‘calibrate’ available in CYANA (Güntert, Mumenthaler et al. 1997, GÜNTERT 1998). NOE calibration converts NOESY cross-peak intensities into upper distance limits (UPL). A certain functional relationship is assumed between peak intensities and UPLs for a given group of peaks. The most common is NOE peak volume proportional to interproton distance to the minus six:

$$V = A/d^6$$

where V is the peak volume (or intensity), d is the upper distance limit, and A is the calibration constant. Initial structure calculations were performed using CYANA 3.0 and 200 conformers were calculated using the standard simulated annealing schedule with 10000 torsion angle dynamics steps per conformer. Finally, the 20 conformers with the lowest final target function values were analyzed.

All the structures derived from CYANA were refined using XPLOR-NIH using the restrained simulated annealing protocol (Schwieters, Kuszewski et al. 2003). The distance restraints generated from CYANA were converted to the XPLOR format. The default values were used for all the force constants and molecular parameters that were involved. 200 conformers were calculated and 20 lowest energy conformers were selected for analysis. Structures were visualized using MOLMOL and PYMOL programs and images were produced using PYMOL.

2.6.3 Saturation Transfer Difference (STD)

The saturation transfer difference (STD) technique (26-28) allows the detection of small molecules which are binding transiently to the target and was initially designed to distinguish those ligands from a mixture of molecules that binds to a receptor protein (Mayer and Meyer 1999). The method is based on the selective saturation of macromolecule such as tubulin/MT, following which magnetization is transferred to the bound ligand, whose signals can be detected in a difference spectrum resulting from an

on- and off resonance setup. The selective saturation of the receptor protons are done by applying a series of selective pulses and the receptor saturation frequency is applied at a frequency window where there is no ligand resonances are observed (eg: -0.5 or -2 ppm). The saturation is spread rapidly through spin diffusion throughout the receptor which is then transferred to the protons of the ligand in the binding interface with the aid of intermolecular ^1H - ^1H cross relaxation. The schematic representation of the STD NMR principle is shown in **Figure 13**.

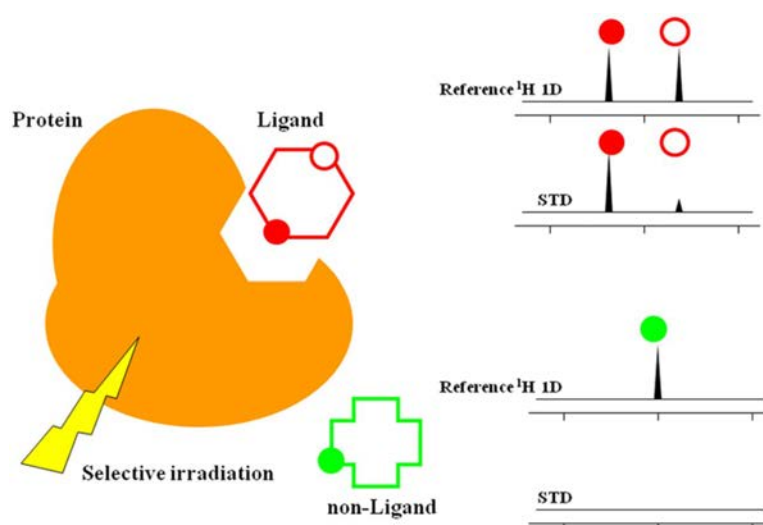


Figure 13: Schematic representation of STD NMR spectroscopy. Selective saturation transfer of the magnetization from a protein to the binding region of the ligand. Ligands which are in the close proximity and binds to the protein will show STD NMR signal (brown triangle). STD signals from non-ligand (shown in the oval-shape) do not appear in the spectrum. For the binding ligand, the STD signal intensities of the proton closer to the protein (black circle) is higher than that from the proton far from the receptor (red circle). (Figure taken from Hiraishi N et.al, 2013 (Hiraishi, Tochio et al. 2013))

It is of great advantage that ligands in mixture can be screened on the basis of binding. Ligand's binding epitope can be identified easily as the ligand protons or residues in peptides which are in close proximity to the receptor binding site show stronger STD signal. STD is a very powerful technique as small molecules or peptide ligands when the interaction of these with proteins is reversible and exhibit characteristic differences in the relaxation properties and molecular mobilities. These properties are much different from those of the other molecules which are having low or even no affinity. STD technique is applied in a wide range of applications (Mayer and Meyer 2001, Streiff, Juranic et al. 2004, Martin-Pastor, Vega-Vazquez et al. 2006, Xia, Zhu et al. 2010, Canales, Rodriguez-Salarichs et al. 2011, Viegas, Manso et al. 2011, Fiege, Rademacher et al. 2012, Hiraishi, Tochio et al. 2013).

2.6.3.1 Experimental set up

All the samples contained Tau peptide/MT drugs in 1mM concentration and tubulin/MT in 25 μ M in 40:1 ratio. The samples were dissolved in 50 mM NaH₂PO₄/Na₂HPO₄, pH 6.8, 10% D₂O. The table lists the ligands used for STD experiments. In all cases the STD NMR spectra of ligand (L1) were recorded with and without tubulin to characterize the binding. In competition experiments the second ligand (L2) was added to the solution and variation in the STD signal intensities of the first ligand were observed.

All the STD spectra were recorded on 700 MHz spectrometer equipped with cryo probe. Prior to binding tests and screening, the parameters were carefully optimized. Spectra were acquired at 25°C by using a series of 40 equally spaced 50 ms Gaussian-shaped pulses for saturation of the protein, with a total saturation time of 1.5 s. Different on-resonance irradiation frequencies were tested as -0.5, -2.0 and 10.0 ppm. The frequency of the on-resonance irradiation was chosen to achieve effective and selective saturation of the protein and for the competition experiments the protein saturation was applied at -0.5 ppm. In all cases, the off-resonance saturation frequency was set at 60.0 ppm. A total of 1024 scans were collected for each experiment with recycle delay of 1.5s.

2.6.4 1D HRMAS experiment

The 1D experiment for MTs under static and MAS conditions were recorded on the 900 MHz spectrometer, equipped with a 4mm TXI high-resolution MAS (HRMAS) probe head (Z-gradient). The spectra were recorded at 5°C and a spinning speed of 8 kHz was used for MAS conditions.

2.6.5 Turbidity assays

The turbidity assays were performed for hTau40, F4, TP1, TP2, TP2_pT231, TR1, TR2, TR3, TR23, TR' and I19L. Tau/Tau fragment-induced microtubule assembly was monitored by light scattering in a FluoroMax spectrophotometer (HORIBA) by absorption at 350nm. 10 μ M PC-purified and cycled Tubulin were mixed with 5 μ M Tau

protein in RB-Buffer (100 mM PIPES pH 6.9, 1 mM DTT, 1mM MgSO₄, 1mM EGTA, 1 mM GTP). The polymerization was started by transferring the ice-cold Tubulin-Tau solution to the 37°C warm cuvette-holder at time point 0 minutes. The turbidity assay was monitored for 30 minutes.

2.6.6 Electron Microscopy

The Electron Microscopy was performed at the Facility for Transmission Electron Microscopy and the images were scanned by Heim Gudrun and Dr. Dietmar Riedel. The microtubules assembled were diluted to 10 µM in MT assembly buffer (PIPES buffer) at pH 6.9 and was placed on copper 600mesh grids covered with carbon film. The sample was stained with 2% uranyl acetate and examined on a CM12 transmission electron microscope.

2.6.7 Chemical cross-linking and Mass spectrometry.

Protein cross linking and mass spectrometry was performed in collaboration with R. Hofele and Prof. Henning Urlaub, Bioanalytical Mass Spectrometry group, MPIBPC.

2.6.7.1 Tau-Tubulin cross-linking.

In all experiments, the optimal cross-linker to protein complex ratio was determined with a titration. Preincubated Tubulin-Tau complexes (TauF4-Tubulin dimer/hTau40-Tubulin dimer/hTau40-microtubules) were mixed with freshly prepared cross-linker bis(sulfosuccinimidyl) suberate (BS3) at different cross-linker to protein ratios of 5, 10, 25, 50, 100 and 200 as well as a control. The cross-linking reaction was carried out for 30 mins at room temperature and quenched with 2uL of 2M Tris pH 7.2. Cross-linked samples were visualized by coomasie stained SDS-PAGE and the ratio that exhibited maximum cross-linking yield and minimum formation of higher order aggregates was selected.

For the identification of cross-linked peptides, the reaction was repeated at the determined optimal cross-linker to complex ratio. Pre-weighed vials of BS3 were freshly dissolved in DMSO and taken to final concentration with 50mM sodium phosphate

buffer, pH 7.2. Reactions were performed in the same buffer. After quenching, samples were analyzed by SDS-PAGE in a 4-12% Bis-Tris gradient gel. Several lanes were pooled to increase sample amount. In gel digestion was performed as elsewhere (Shevchenko, Tomas et al. 2006). After extraction from the gel samples were immediately analyzed on the mass spectrometer.

2.6.7.2 Nano-liquid chromatography separation and MS analysis.

For LC-MS/MS analyses, samples were dissolved in 30 μ L sample solvent (5% v/v acetonitrile, 1% v/v FA). 5 μ L were injected onto a nano-liquid chromatography system (Agilent 1100 series, Agilent Technologies) including a ~2 cm long, 150 μ m inner diameter C18 trapping column in-line with a ~15 cm long, 75 μ m inner diameter C18 analytical column (both packed in-house, C18 AQ 120 Å 5 μ m, Dr. Maisch GmbH, Ammerbuch, Germany). Peptides were loaded on the trapping column at a flow rate of 10 μ L/min in buffer A (0.1% FA in H₂O, v/v) and subsequently eluted and separated on the analytical column with a gradient of 7.5–37.5% buffer B (95% acetonitrile, 0.1% FA in H₂O, v/v) with an elution time of 97 min and a flow rate of 300 nL/min.

Online ESI-MS was performed with an LTQ-Orbitrap Velos instrument (Thermo Scientific), operated in data-dependant mode using a TOP8 method. MS scans were recorded in the m/z range of 300-1800 and a resolution of 100000. The 8 most intense ions were selected for subsequent MS/MS, and only charge state 3 and above were selected for fragmentation. Dynamic exclusion was enabled (30 second repeat duration, repeat count 1). Both Precursor ions as well as fragment ions were scanned in the Orbitrap. Fragment ions were generated by CID activation (normalized collision energy=37.5). As precursor ions as well as fragment ions were scanned in the Orbitrap, the resulting spectra were measured with high accuracy (< 5 ppm) both in the MS and MS/MS level.

2.6.7.3 Identification of cross-linked peptides.

Data analysis was performed with MassMatrix as described in their publications and manuals (Xu, Zhang et al. 2008, Xu and Freitas 2009, Xu, Hsu et al. 2010). Thermo Scientific Raw files were converted to the mzxml data format with MMConverter and submitted to database search with the following parameters: peptide length between 6-40 amino acid long, 10 ppm MS1 tolerance, and 0.02 Da MS2 tolerance, tryptic fragments with a maximum of 2 missed cleavages. Oxidation in methionine was set as a variable modification, whereas carbamidomethylation of cysteine was set as a fixed modification. Spectra were searched against a FASTA file composed of the sequences of Tau and Tubulin and a reversed decoy database. The resulting matches were manually checked.

3 Results

3.1 Interaction of Tau and Tau fragments with tubulin and Microtubule

To study the structural properties of MT-bound Tau, it is important to map the binding region of Tau on MTs. Here we investigated the features of Tau protein and Tau fragments either in the MT-bound or tubulin bound state. Two different isoforms of human Tau protein, hTau40 and hTau23, were used to study their interaction with MTs. We further used different Tau fragments like K18 and F4 having different binding affinities as well as mutated and pseudophosphorylated full length Tau to describe the properties of MT-bound Tau.

3.2 Identification of the binding hot spots of the Tau-MT interaction

3.2.1 Interaction of hTau40 with MT

The Tau-MT interaction was probed by using NMR spectroscopy to get insight into the regions of Tau that interact with MTs. The binding of hTau40 to taxol-stabilized MTs was characterized using the 2D ^1H - ^{15}N HSQC spectra measured at 278K. The spectra of free and MT-bound Tau were compared as shown in Figure 14, where the spectra showed poor proton chemical shift dispersion, a characteristic feature of unfolded proteins. The previously assigned resonance assignment of hTau40 was used for the analysis (Mukrasch, Bibow et al. 2009, Narayanan, Dürr et al. 2010). The line broadening and chemical shift perturbations of the resonances in the 2D ^1H - ^{15}N HSQC

spectra were analyzed and it is found that a number of resonances were either disappeared or diminished in intensity. The ratio of the resonance intensities of the MT-bound and unbound Tau was plotted against the residue number as shown in **Figure 15** and is similar to that reported before in the case of Tau-MT interaction at 298K (Mukrasch, Bibow et al. 2009). The non-uniform reduction in signal intensities in the spectra of hTau40 bound to MTs is caused by an exchange of Tau molecules between the free and MT-bound states. It revealed the interacting regions of Tau bound to microtubules and

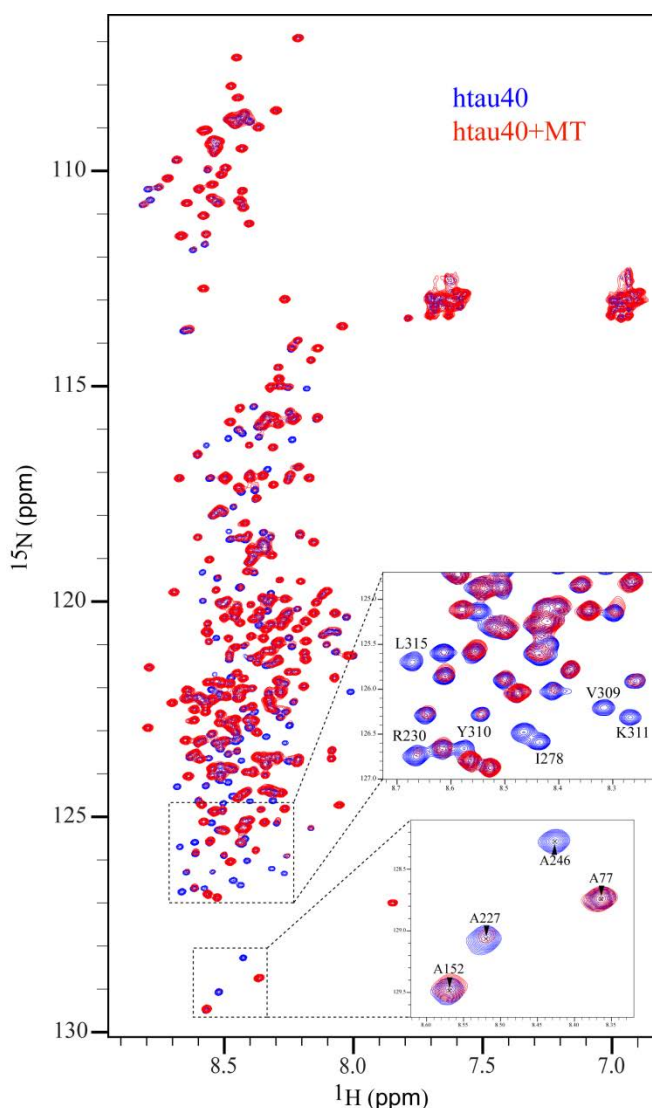


Figure 14: Overlay of the 2D ^1H - ^{15}N HSQC spectra of hTau40 without (blue) and with MTs (red) at 2:1 ratio of Tau:MT and at 5°C. A few selected resolved peaks are labeled with their assignments and shown in the insets.

Results

the binding domain include both the proline rich and the repeat domain in the full length Tau, especially the linear motifs $^{168}\text{ATRIPAKTPPA}^{178}$, $^{225}\text{KVAVVRTPPKSPSS}^{238}$, $^{245}\text{TAPVPMPDL}^{253}$, $^{275}\text{VQIINKKLDLSNV}^{287}$, $^{306}\text{VQIVYKPVDSLKV}^{318}$ and $^{375}\text{KLTFRNAKAK}^{385}$. In addition a considerable change in chemical shifts for the

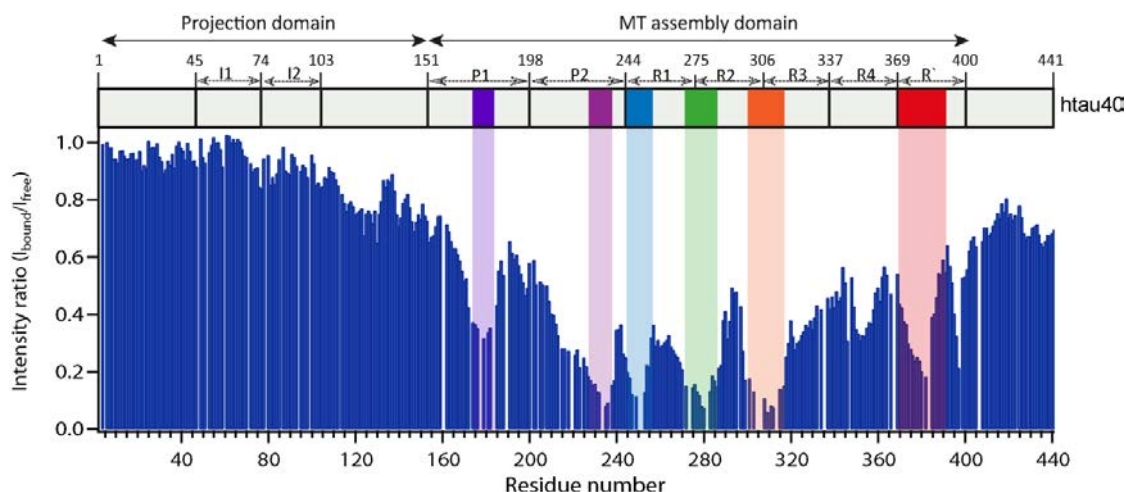


Figure 15: Tau-microtubule interaction. NMR signal intensity ratios between signals observed in the ^1H - ^{15}N HSQC spectra for MT-bound and free states of hTau40 acquired at 5 °C with 2:1 stoichiometry of Tau:MT. The domain organization diagram is shown on top of the intensity ratio plot and distinct colour coding is used to highlight the binding hot spots involved in Tau-MT interaction. The ratio of Tau:MT is calculated on the basis of the initial concentration of tubulin chose for MT assembly.

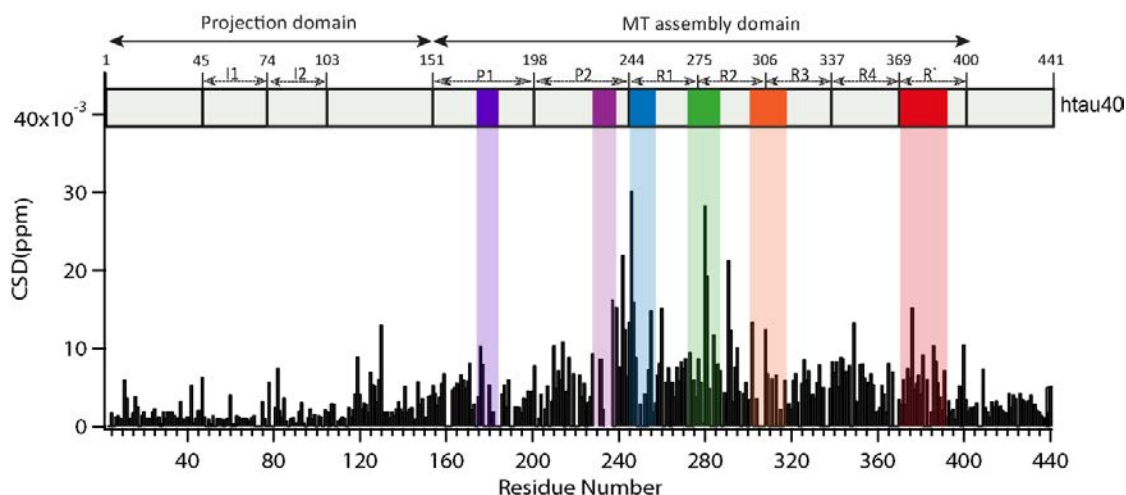


Figure 16: ^1H - ^{15}N combined chemical shift difference observed for the NMR signals in the MT-bound state of Tau compared to free Tau at 5 °C.

identified residues is observed as represented in **Figure 16**. The binding hot spots identified here are highly localized and are separated by highly flexible linkers. It was shown before that the Tau-MT binding involves both hydrophobic and charged residues (Mukrasch, Bibow et al. 2009). Whereas the intensities and chemical shift of the amino acid residues at the N-terminus remained unaffected, indicating that this region is not involved in binding. In short the binding interaction between Tau and MTs is mediated through residues from the proline rich region (PRR) to the pseudo repeat R` near the C-terminal end of hTau40. The broadening observed for the residues in between the binding hot spots and at the C-terminus is due to the transient interaction of this region to the MTs and thereby having smaller transverse relaxation rate than that of the residues at the N-terminus in the Tau-MT complex.

3.2.2 Isoform specific binding of Tau to MTs

We investigated the isoform specific features in the binding of Tau to microtubules by comparing the binding profiles of hTau23 and hTau40 which are the shortest and longest isoforms of Tau in the human brain respectively. The 2D ^1H - ^{15}N HSQC experiments were performed in the case of hTau23 at 278K at multiple hTau23:MT ratios. Analysis of the NMR spectra revealed that the interaction profile was in line with that of htau40 as similar binding regions and residues were involved in binding. The comparison of the intensity ratio profiles of hTau23 and hTau40 at 1:2 ratio of Tau:MT is shown in **Figure 17**. At the same time, comparison of the NMR broadening profiles of hTau40 and hTau23 reveals a reduced signal intensity broadening in case of hTau23, pointing to a lower binding affinity of hTau23, in accord with the absence of the repeat R2 in hTau23 (Drechsel, Hyman et al. 1992, Goode, Chau et al. 2000).

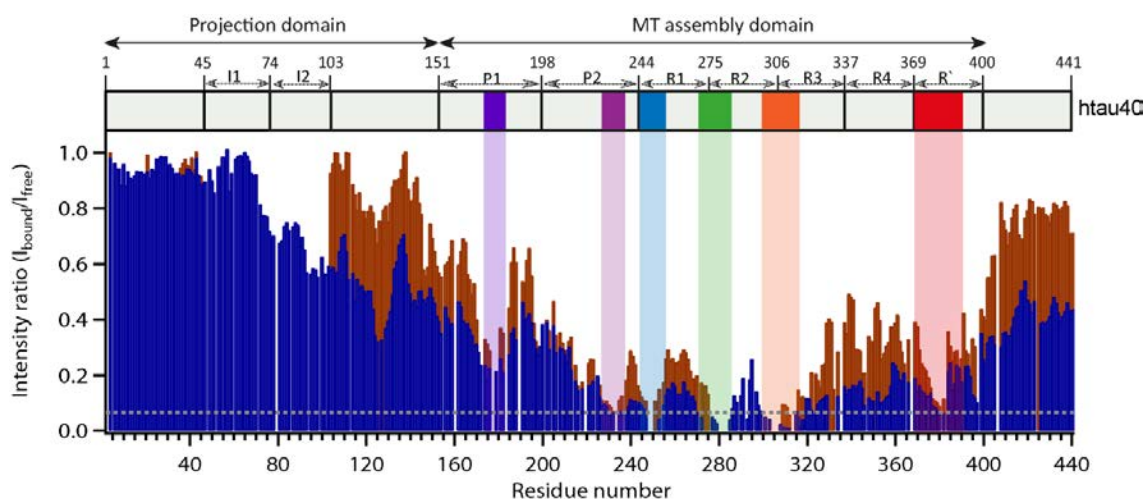


Figure 17: Similarities in the interaction of different isoforms of Tau and MTs. Comparison of Tau-MT interaction in two different isoforms hTau23 and hTau40 of human Tau. NMR signal intensity ratios between signals observed in the ^1H - ^{15}N HSQC spectra for MT-bound and free state of hTau23 (brown bars) and hTau40 (blue bars) with 1:2 stoichiometry of Tau:MT. The domain organization diagram is shown on top of the intensity ratio plot and distinct colour coding is used to highlight the binding hot spots involved in Tau-MT interaction. The grey line indicates the peak intensities in the noise level.

The chemical shift perturbation observed for the amino acid resonances of both hTau40 and hTau23 upon interaction with MTs is compared in **Figure 18**. Similar residue stretches involved in MT binding are perturbed in both isoforms.

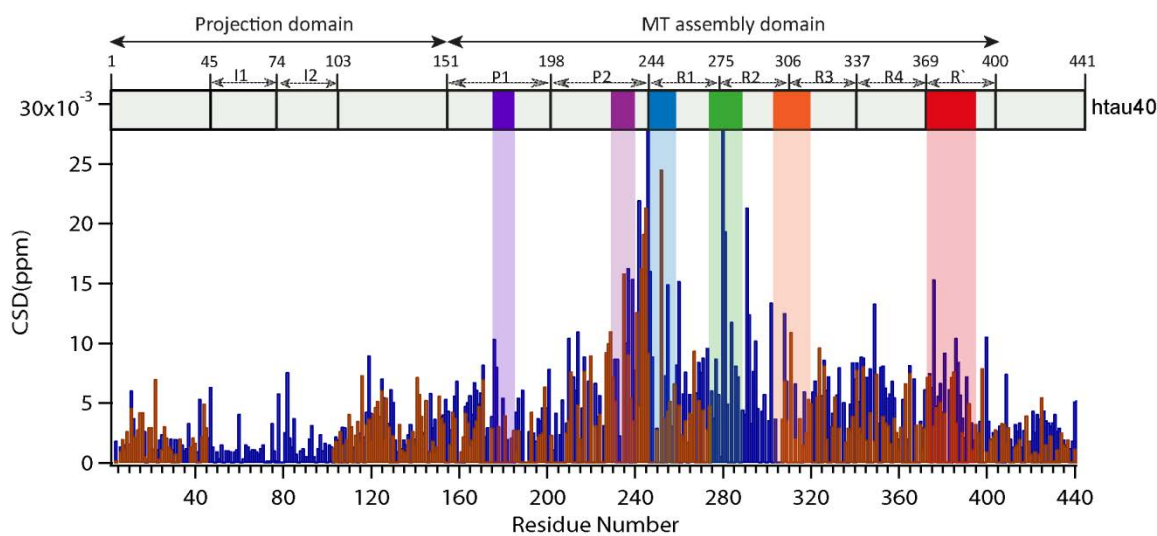


Figure 18: Comparison of the ^1H - ^{15}N combined chemical shift differences observed for hTau40 (blue) and hTau23 (brown) in the MT-bound state and free state. The amino acids are numbered with respect to hTau40 in both isoforms.

3.2.3 Effect of overloading of MTs

It was previously reported that at elevated Tau concentrations, Tau molecules might aggregate on top of each other similar to paired helical filament formation. It was proposed that the accumulation of Tau occur on top of each other in a non-saturable binding mode (Ackmann, Wiech et al. 2000). This kind of overloading of MTs was investigated by varying the stoichiometry from 2:1 to 1:2 and 1:3. Repeating the NMR titrations in different ratios, with excess of MTs has been shown that overloading of MTs does not lead to different interaction sites. The line broadening in the ^1H - ^{15}N HSQC spectra of Tau with MTs at 2:1 and 1:3 ratios are compared in **Figure 19**. It is clear from the figure that similar region of the spectra are affected by the interaction with MTs, though a few residues beyond the MT binding region shows additional broadening at higher MT concentration. This is attributed to the fast relaxation associated with the large size of the Tau-MT complex and is pronounced at higher MT concentration. The resonances of residues at the N-terminal projection domain remained largely unaffected without strong broadening. These experiments were performed in the shortest isoform hTau23 as well and it is noticed that similar binding sites are involved in two different isoforms (**Figure 20**).

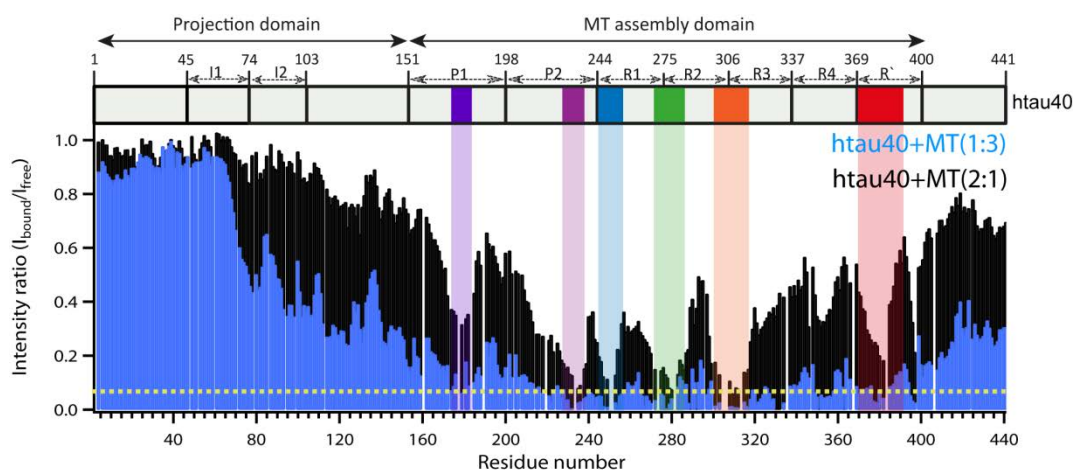


Figure 19: Effect of overloading of MTs. NMR signal intensity ratios of hTau40 resonances in the presence and absence of MTs obtained from the ^1H - ^{15}N HSQC spectra is plotted against residue number, with hTau40:MT stoichiometry of 2:1 (black bars) and 1:3 (blue bars) acquired at 5°C .

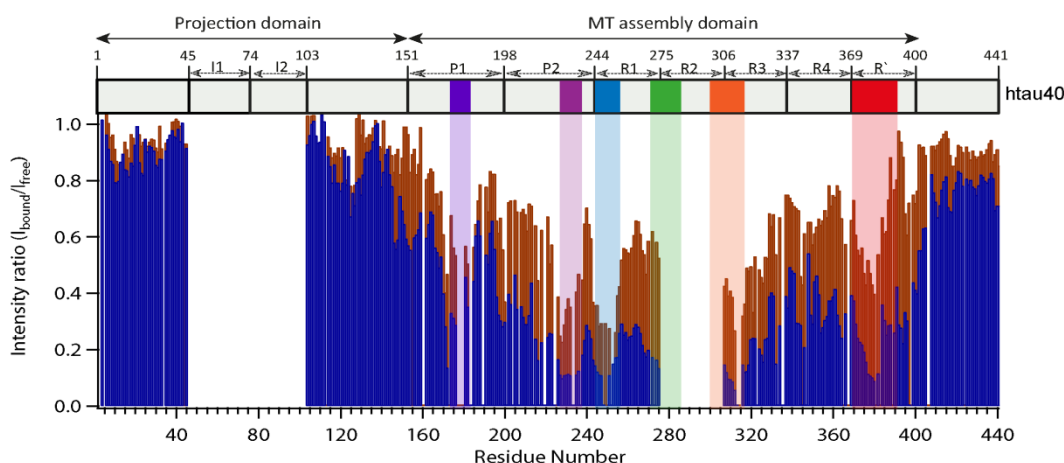


Figure 20: hTau23-MT interaction at different relative concentrations. Line broadening profiles of hTau23 obtained from the ^1H - ^{15}N HSQC spectra with hTau23: MT ratio of 2:1 (brown) and 1:2 (blue). Amino acid residues are numbered with respect to hTau40. The regions without any bars indicate the absence of two N-terminal inserts I1 and I2 and repeat R2.

3.2.4 Influence of ionic strength on Tau-MT binding

The importance of electrostatic interactions in Tau-MT binding was investigated by performing the NMR interaction experiment at increasing ionic strength (**Figure 21**). In the presence of sodium chloride, the MT-binding strength of Tau was reduced in a salt concentration dependent manner: at salt concentration of ~150 mM NaCl in the Tau-MT solution the average ratio of Tau signal intensities was increased from 25% in the at lower salt concentration in 50mM sodium phosphate buffer to about 50%, while further increase to 300mM NaCl recovered the average ratio of signal intensities of MT-bound Tau to more than 90%. It is to be noticed that even at elevated ionic strength the hydrophobic residues in the second hexapeptide in repeat R3 showed partial broadening. These data indicate the important contribution of electrostatic interactions to MT-Tau binding, together with the hydrophobic residues in the binding hot spots previously identified.

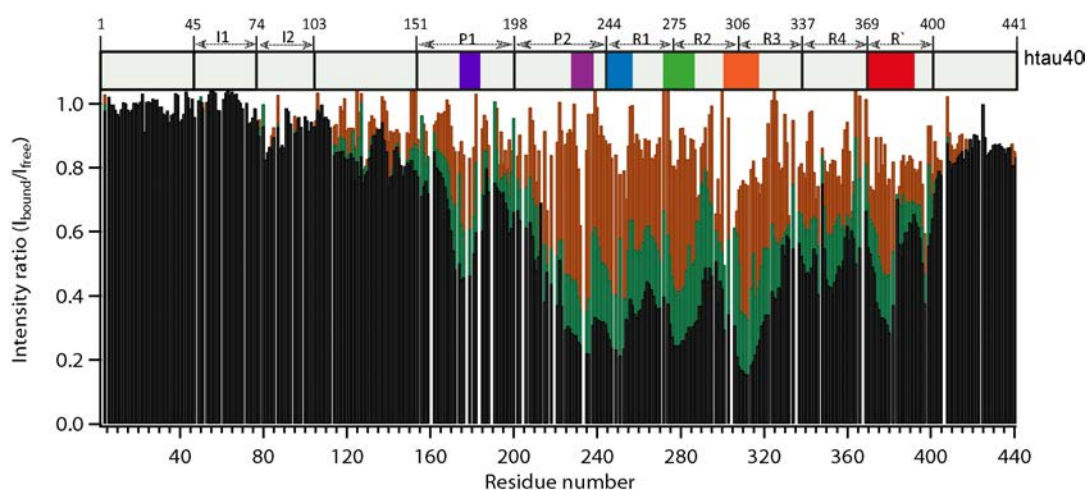


Figure 21: Effect of ionic strength on Tau-MT interaction. Comparison of intensity ratio profiles of hTau40 with MTs by varying the ionic strength without NaCl (black), with 150mM NaCl (green) and with 300mM NaCl (brown) 2:1 ratio of hTau40 and MTs.

3.2.5 Interaction of hTau40 with tubulin

The function of Tau to promote tubulin assembly and stabilize microtubules raises the question whether the mode of interaction is the same in both Tau-tubulin and Tau-MT interaction or not. The binding of hTau40 with unpolymerized tubulin was investigated using the 2D ^1H - ^{15}N HSQC experiments as in the case of MTs. The ratio of the intensities (**Figure 22**) in the tubulin-bound and free Tau give the strong evidence that the binding features are the same, as the same set of residues as in the case of MT binding are affected. The titrations were done at different stoichiometric ratios and the intensity profiles at 1:2 ratio is compared to that of the interaction with MTs. The residues near the projection domain and the C-terminal domain of Tau are found to be less broadened by binding to tubulin than MT. This is either due to slight differences in the binding affinities in these regions or due to the smaller transverse relaxation rate of the Tau-tubulin complex when compared to that of the Tau-MT complex, which leads to less broadening in the regions that are next to the binding hot spots. The comparable binding profiles of Tau for MT and Tubulin suggest that the Tau binding site is largely localized on the individual $\alpha\beta$ -dimer.

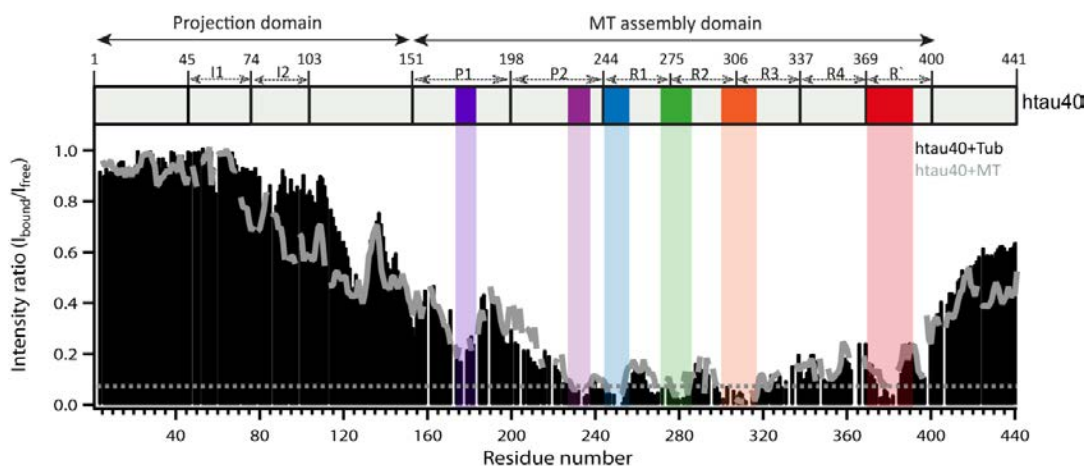


Figure 22: Interaction of hTau40 with tubulin and MTs. Comparison of intensity ratio profiles of hTau40 with MTs (grey line) and unpolymerized tubulin (black bars) at 1:2 ratio of hTau40:MT/tubulin.

3.2.6 Characterization of MTs using NMR

The microtubules assembly, performed as described in the methods section, was confirmed with electron microscopy showing nice array of protofilaments (**Figure 23a**). The absence of unpolymerized tubulin in the sample during NMR experiments at low temperature was verified by employing High Resolution Magic Angle Spinning (HRMAS) NMR experiments. HR-MAS is an established technique for analyzing intact biological tissue samples. By spinning at the magic angle, susceptibility differences within the sample are removed resulting in high resolution quality spectra. The 1D ^1H spectrum of $100\mu\text{M}$ MTs filled in the rotor in the static conditions showed only very broad lines characteristic of mega Dalton MTs. No sharp signals, in particular in the methyl region, that could originate from $\alpha\beta$ -tubulin dimers of 100kDa molecular mass were observed. By spinning the sample at 8 kHz under MAS conditions averages out the stronger proton-proton and weaker proton-carbon/nitrogen dipolar interactions and the narrow signals are observed from the microtubules. The 1D ^1H spectra of MTs obtained under static and MAS conditions are shown in **Figure 23b**.

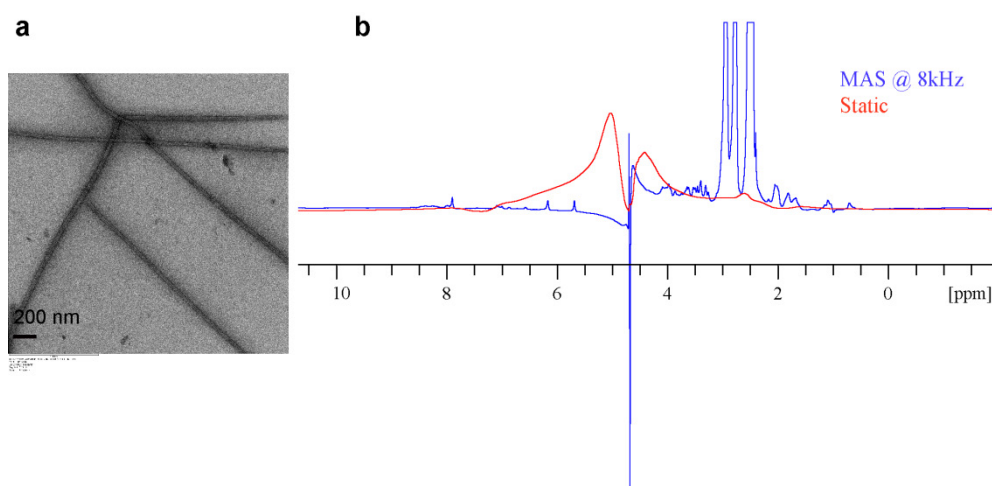


Figure 23: Characterization of MT assembly. (a) EM image of the microtubules assembled from PC tubulin (The EM image was recorded in the facility for Transmission Electron Microscopy, MPIBPC). (b) The 1D ¹H NMR spectra of MTs both under static (red) and MAS conditions of 8 kHz (blue).

3.3 Influence of mutation and phosphorylation

3.3.1 Effect of mutation (Y310N) of Tau on MT binding

It has been shown that Tau-MT interaction is mediated through highly localized binding hot spots separated by flexible linkers. To understand the mechanism involved in Tau-MT binding, which is a combination of both electrostatic and hydrophobic interaction Tau protein with Y310N mutation was used. Y310 is one of the binding residues involved in the binding hot spot in repeat R3. Comparison of the intensity ratios derived from the wild type and Y310N mutated hTau40 in the MT bound state is shown in **Figure 24**.

The data show that a single residue mutation doesn't affect the overall binding. Although residues close to the site of Y310 mutation are slightly affected as evidenced from their intensities, no considerable long-range effect in the other binding hot spots was observed. The data suggest the independent nature of different linear motifs of Tau which are involved in Tau-MT interaction.

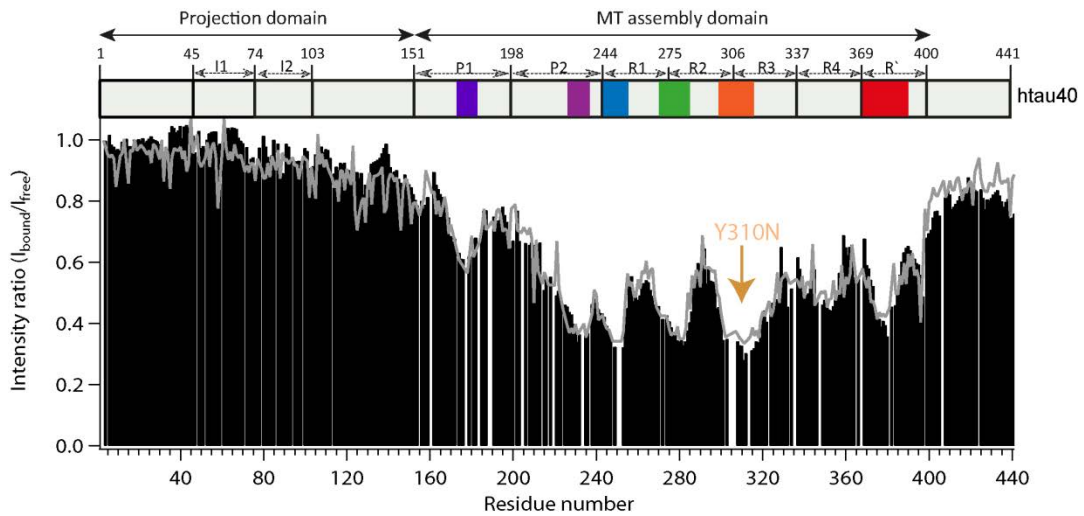


Figure 24: Influence of single residue mutation (Y310N) on MT binding. The NMR line broadening profiles of wt hTau40 (black bars) and Y310N mutated hTau40 (grey line) upon interaction with MTs is compared. The position of mutation is indicated by an arrow.

3.3.2 Effect of pseudophosphorylation of Tau on MT binding

It is known that hyperphosphorylation of Tau leads to detachment of Tau from the MT surface causing MT destabilization and thereby the formation of NFTs composed by Tau (Stoothoff and Johnson 2005, Mi and Johnson 2006). To probe the phosphorylation-dependent Tau-MT interaction we used hTau40 for which residues S199, S202, T205, T212, S214, S396 and S404 were mutated to glutamic acid. Mutation of serine to negatively charged aspartate or glutamate residue is widely used as a mimic of phosphorylation (Jeganathan, Hascher et al. 2008). The 7E mutation sites mentioned above form epitopes for the Alzheimer's diagnostic antibodies AT8, AT100 and PHF1 (Jeganathan, Hascher et al. 2008). The effect of phosphorylation was investigated by comparing the MT-induced line broadening in the case of wild-type hTau40 to that of 7E mutant of hTau40 as shown in **Figure 25**.

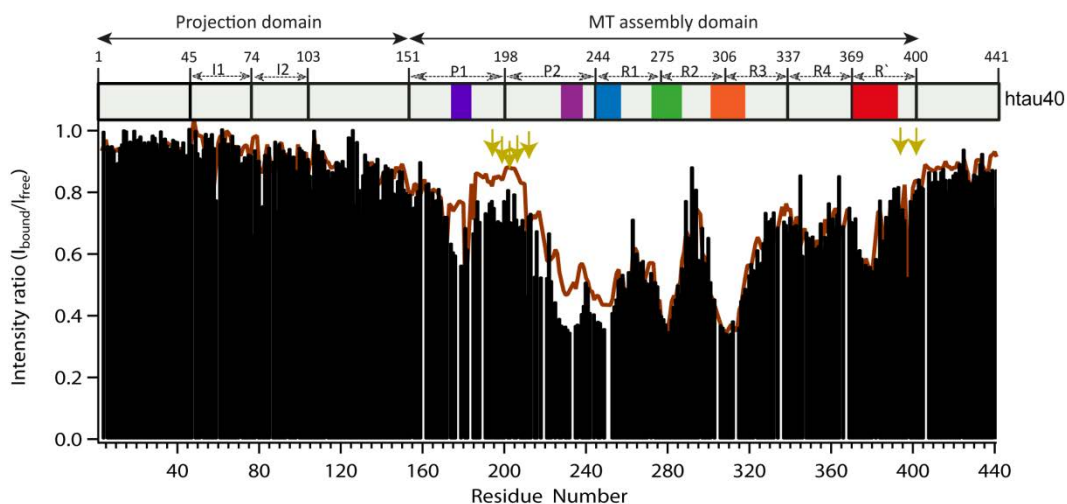


Figure 25: Effect of phosphorylation on MT-binding. Intensity ratios for the hTau40-7E variant (brown line), which was pseudo-phosphorylated at the AT8, AT100 and PHF1 epitopes (indicated by yellow arrows), between the MT-bound and unbound state. MT-induced resonance broadening of non-phosphorylated wild-type hTau40 is shown for comparison (black bars).

The results showed that the pseudo-phosphorylation at the AT8, AT100 and PHF1 epitopes enhances the signal intensities of the nearby residues indicating that MT binding is weakened especially in the proline rich region and to a less extent in the R` around mutation sites S396 and S404. The repeat domains with other binding hot spots remain unaffected and the data underline one of the important features of Tau, possessing highly independent binding sites for MTs.

3.4 Interaction of Tau fragments with tubulin/MT

3.4.1 Interaction of K18 with tubulin

To get further insights into the exact amino acid residues involved in binding and to extract detailed information regarding the mechanism involved in binding we used ^2H , ^{15}N labeled K18. NMR investigation of ^2H , ^{15}N labeled K18 in complex with tubulin was performed using TROSY and CRINEPT-TROSY experiments that facilitate detection of signals from the large molecular weight systems. The analysis of TROSY spectra of tubulin-bound and unbound K18 shows the overall reduction in the intensities as well as

additional line broadening as shown in **Figure 26** consistent to the previously identified binding hot spots (**Figure 15**). Still the CRINEPT-TROSY couldn't reveal information only from the completely bound state as the similar residues are found to be broad both in the TROSY and CRINEPT-TROSY spectra. Yet another observation is that the residues in the repeats R1, R2 and R3 showed severe line broadening, whereas repeat R4 was less affected consistent to the observation as in the case of hTau40. R4 remained highly flexible without involving in binding.

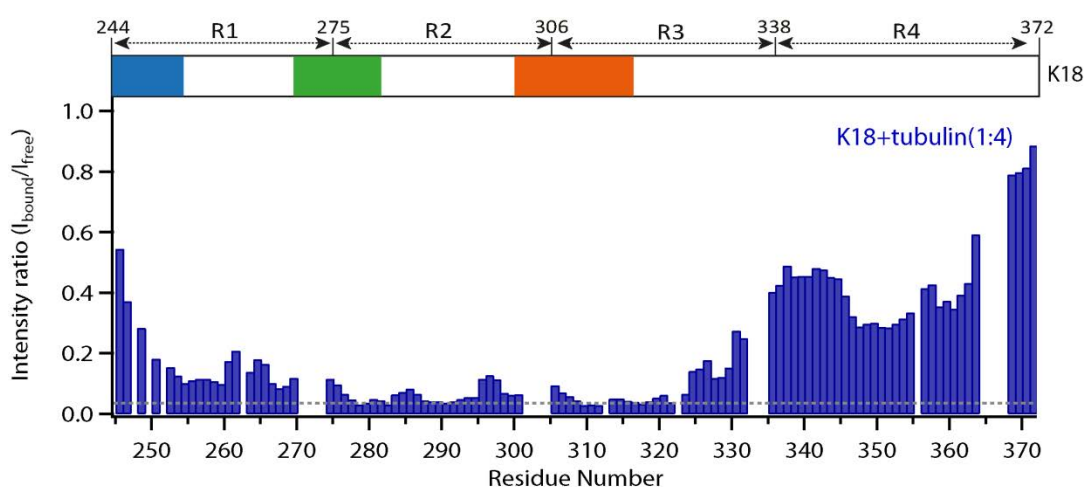


Figure 26: K18-Tubulin interaction. Intensity ratio of 2H, 15N labeled K18 calculated from the TROSY spectra recorded in the tubulin-bound and free state of K18 at 5°C. The horizontal dashed line indicates the severe line broadening of residues in the NMR spectrum.

3.4.2 Characterization of interaction of TauF4 with Tubulin/MT

A new Tau fragment, TauF4 [S208-S324] that comprises the MTBR and the proline rich domain closest to the MTBR in Tau sequence was used for further investigation in the MT-bound state. The F4 fragment binds tightly to MTs and promotes MT assembly (Fauquant, Redeker et al. 2011). 2D ^1H - ^{15}N HSQC spectra of F4 showed poor proton chemical shift dispersion as observed in the case of hTau40. Assignment of the resonances in the F4 fragment was done with the help of the previously assigned K18, hTau23 and hTau40 and was confirmed with the assignment of F4 reported before (Sibille, Huvent et al. 2011). The interaction of F4 with MTs leads to overall reduction in signal intensity **Figure 27** in the 2-D ^1H - ^{15}N HSQC spectra as a result of the tight

binding. The experiments were performed with varying F4:MT stoichiometric conditions of 10:1, 5:1 and 1:2 with MTs. The residual intensity of the protein is found to be attenuated on increasing the concentration of tubulin/MT. The results indicate very high affinity of F4 to MTs thereby having very slow or even negligible exchange between the bound and free forms of F4 in solution. It can therefore be concluded that the signal disappearance is due to the immobilization of the F4 fragment on MTs. The complete signal attenuation is at the ratio of 1:2 which is the known stoichiometry of Tau:tubulin.

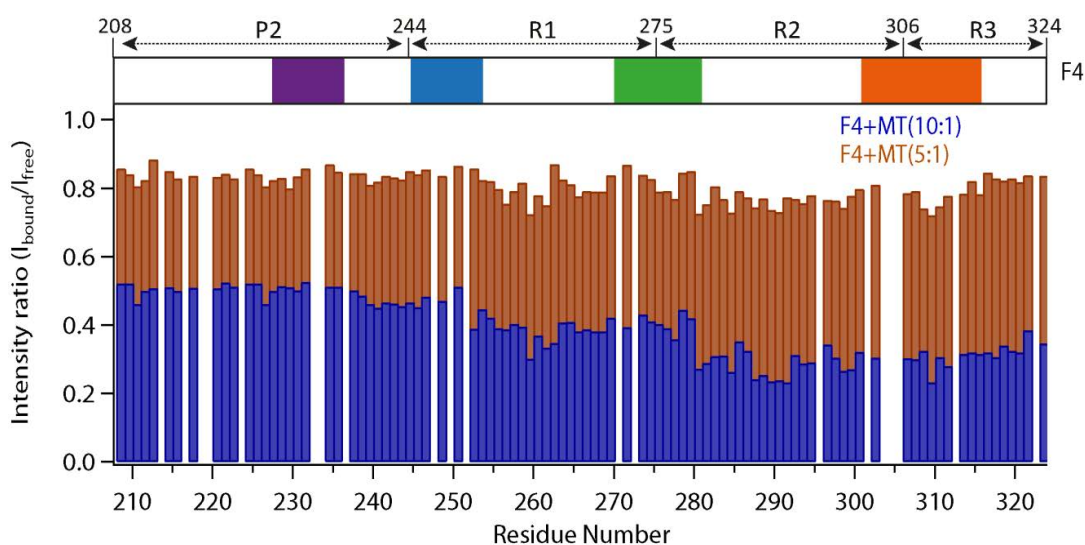


Figure 27: Interaction of F4 with MTs. NMR signal intensity ratios of F4 resonances in the presence and absence of MTs obtained from the ^1H - ^{15}N HSQC spectra is plotted against residue number, with F4:MT stoichiometry of 10:1 (blue) and 2:1 (brown) acquired at 5°C .

3.4.2.1 Effect of ionic strength on binding of F4 with tubulin/MTs

It is known that solution NMR spectroscopy cannot detect the signals of proteins in the complex with large molecular weight receptors since the NMR signals would be broadened beyond the detection limit of experiment. To further verify the influence of ionic strength in Tau-MT interaction (**Figure 21**), the effect of increasing ionic strength on F4-MT interaction was monitored through sodium chloride titration experiments. At 120 mM NaCl most of the signals from the proline rich region and the signals of the other positively charged residues were found to be recovered as shown in **Figure 28a**. Further increase in the salt concentration to 500mM increased the overall signal intensities of all the residues including hydrophobic residues as shown in **Figure 28b**. Although the signals of all charged residues in NMR spectra were retained at higher salt concentration of $\sim 500\text{mM}$, the hydrophobic residues in the binding hot spots of repeats

Results

R2 and R3 were found to be partially broadened indicating the contribution from hydrophobic residues. All the titrations were performed by varying the temperature and it has been found that there is no temperature dependence in the binding mode and binding affinity of F4 with MTs as the mode of interaction is similar at 278, 288 and 298K.

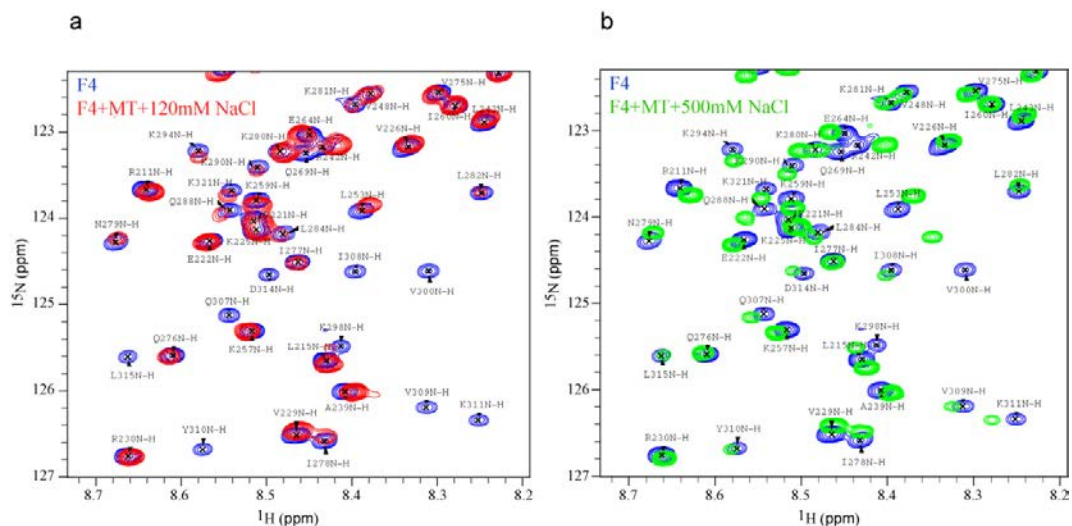


Figure 28: Influence of ionic strength on F4-MT interaction. Superposition of the well resolved region of the hsqc spectra of F4 alone (blue) and in the presence of MTs with 120 mM NaCl (red) and 500 mM NaCl (green).

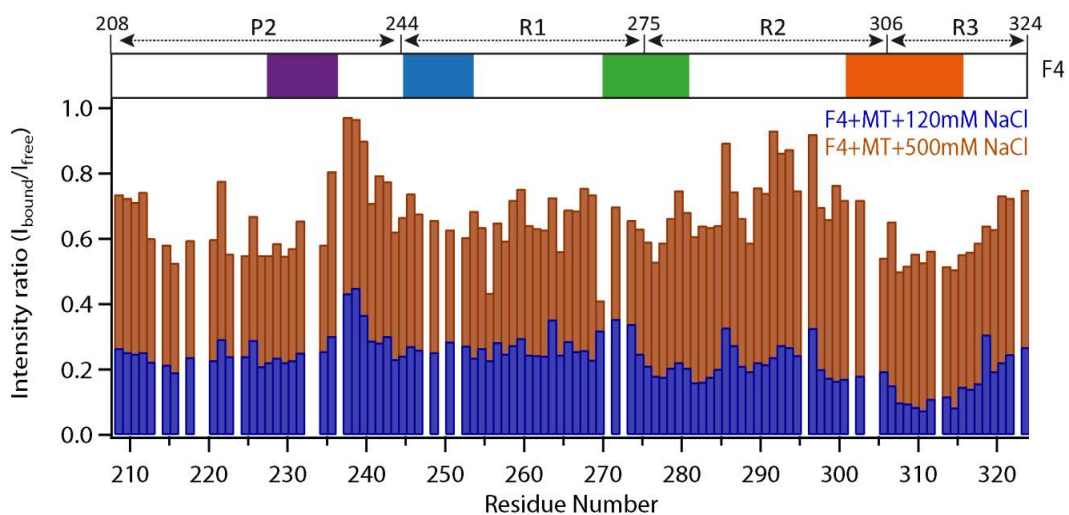


Figure 29: Influence of ionic strength on F4-MT interaction. Comparison of intensity ratio profiles of F4 with MTs at 1:2 ratio and 5°C by varying the ionic strength with 120mM NaCl (blue) and with 500mM NaCl (brown).

The gain in the resonance intensities by changing the ionic strength is represented as the ratio of their intensities **Figure 29**. It is quite evident from these experiments that TauF4 interact with tubulin/MT with higher affinity than full length Tau protein.

3.4.2.2 MT assembly properties of F4 and hTau40

It is clear from the interaction of both F4 and hTau40 with MTs that the binding affinity is relatively higher for F4. To further investigate their MT assembly capabilities, the polymerization assay of tubulin induced by F4 and hTau40 were measured turbidimetrically. The MT assembly properties of F4 were investigated by varying the concentrations of F4 from 5 μ M to 25 μ M and compared with that of 5 μ M hTau40. A fixed tubulin concentration of 10 μ M, below its critical concentration for MT assembly if it is alone (Mitchison and Kirschner 1984), was used in all cases. In comparison to the wild type hTau40, F4 has less effect on MT assembly. The comparison is shown in **Figure 30a**. Tubulin with a concentration of 10 μ M was used as control and was unable to assemble to MTs by itself as it is below the critical concentration for the tubulin self-assembly. The EM images of the MTs formed by 5 μ M of hTau40 and 25 μ M of F4 are shown in **Figure 30b** and **Figure 30c**. F4 shows strong bundling effect on MTs.

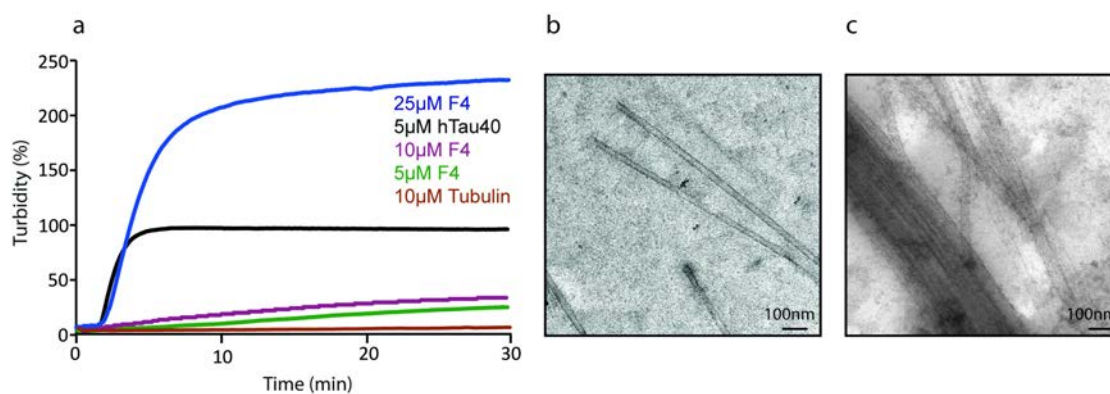


Figure 30: Comparison of the MT assembly efficiency of hTau40 and F4. (a) Turbidity at 350nm was recorded over time to monitor the microtubule assembly in the presence of hTau40 and F4. Assembly experiments were performed in the presence of 1 mM GTP at 37°C with a fixed tubulin concentration of 10 μ M. Intensities were normalized to the assembly in the presence of hTau40 (set to 100% in the plateau phase). 5 μ M of hTau40 and 5, 10 and 25 μ M of F4 were used. (b) EM image of MTs formed by 5 μ M of hTau40 and (c) MTs formed by 25 μ M of F4. (The experiments were performed by Dr. Satish Kumar, DZNE, Bonn, Germany.)

3.4.3 Information from the bound state

3.4.3.1 CRINEPT-HMQC of ^2H - ^{15}N F4 bound to tubulin

The very tight binding of F4 fragment to MTs/tubulin allowed us for further structural investigation of high molecular weight complex using CRINEPT (cross-correlated relaxation-enhanced polarization transfer) based experiments. We used ^2H , ^{15}N labeled F4 in the tubulin bound state to see the bound form of the protein, where the complex formed has very high molecular weight of ~115 kDa. At 303K we could observe the signals arising only from the flexible linkers in the bound state. This observation provided further insights how Tau interacts with tubulin. The HSQC, TROSY and CRINEPT-HMQC provided consistent result that while the binding residues in the binding hot spots remained rigid on tubulin and invisible by solution NMR, the linkers remained highly flexible. Almost all the signals observed in the CRINEPT HMQC spectrum were visible in the 2D ^1H - ^{15}N HSQC and ^1H - ^{15}N TROSY spectra. The intensities of observed resonances in the tubulin bound and free states of F4 were analysed and the broadening profile **Figure 31b** largely resemble that observed in the case of hTau40 bound to tubulin/MT. The complete loss of flexibility of the residues from the binding region is reflected by the disappearance of the signals only from the binding hot spots.

3.4.3.2 CRINEPT-HMQC of ^2H - ^{15}N F4 bound to MTs

The interaction of F4 bound to MTs was investigated by employing the CRINEPT-HMQC-TROSY on ^2H , ^{15}N -labeled F4. It was found that the signals observed for F4 in the MT-bound state is much weaker than that observed in F4-tubulin complex. Further it is noticed that all the visible, albeit weaker, signals are originating from the highly flexible residues lying in between the binding hot spots. Overlay of the CRINEPT-HMQC-TROSY spectra of MT-bound and free F4 acquired using the ^2H , ^{15}N labeled F4 is shown in the **Figure 31a** with selected residues in the binding hot spots labeled. Unlike the tubulin-bound F4, MT-bound F4 is less sensitive for HSQC and TROSY-HSQC experiments and none of the resonances are clearly visible. This shows the influence of the size of the complex formed in the deterioration of the signal intensities as a result of faster relaxation and clear evidence for the advantage of

CRINEPT based polarization transfer compared to INEPT. It is much more clear from the analysis of the intensities derived from the CRINEPT-HMQC-TROSY spectra as shown in **Figure 31c**. In short the line broadening observed in the case of F4-MT complex is more prominent than that of F4-tubulin complex.

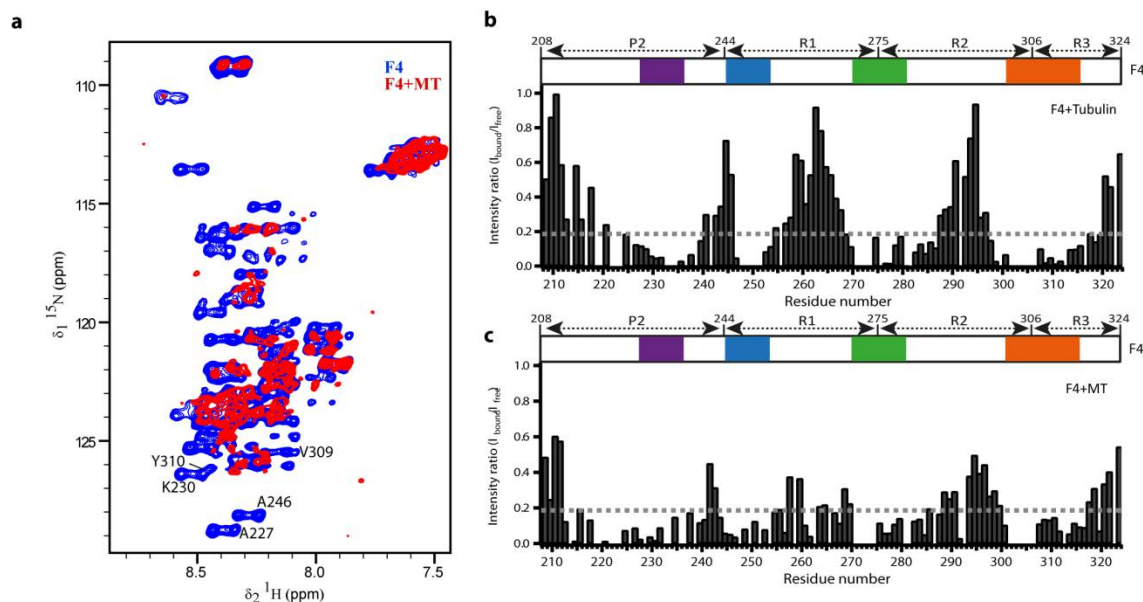


Figure 31: (a) Superposition of the ^1H - ^{15}N CRINEPT-HMQC-TROSY spectra of F4 in the free (blue) and MT-bound (red) state acquired at 30°C . (b) Interaction of TauF4 fragment with unpolymerized tubulin. Intensity ratio from the ^1H - ^{15}N HSQC spectra of tubulin bound TauF4 at 1:4 ratio at 30°C . (c) Intensity ratio obtained for F4 from the ^1H - ^{15}N CRINEPT-HMQC-TROSY spectra in the presence and absence of MTs at 30°C . The dashed grey line indicates the noise level of the spectra obtained.

3.5 Structure determination of the MT-bound Tau

One of the major functions of Tau is to bind and stabilize MTs and promote tubulin assembly. The results described in the previous sections (3.2 and 3.4) provide evidence for the active participation of Tau in binding and stabilization of MTs or promoting tubulin polymerization. Being intrinsically disordered in the free form in solution, it is important to understand the mechanism involved in MT stabilization. However the high resolution structural information of MT-bound Tau is missing. Extracting structural information from Tau-MT complex with size of the order of 1MDa is challenging with the help of NMR, although NMR is the only tool that allows the

structural description of systems like MT-bound Tau. If the size of the receptor is too large it is difficult to extract structural parameter from their NMR spectra.

If the ligand is weakly bound and there exists fast exchange between free and bound forms of the ligands, detailed structural and dynamic information can be obtained by employing transferred NOEs and CCR rate measurements (Balaram, Bothnerb.Aa et al. 1972, Post 2003, Carlomagno 2005, Williamson 2006) (section 2.6). Application of these techniques to get the structure of MT-bound Tau is possible via the “divide and conquer strategy”.

3.5.1 Selection of Tau peptides

On the basis of the findings based on the interaction studies of Tau isoforms and other Tau constructs with MTs, it is exclusively evident that Tau possess highly localized linear motifs which independently bind to MTs and are separated by highly flexible linkers. This allowed us to use the “divide and conquer strategy” that is by using shorter Tau peptides to derive the MT-bound structure of Tau. A list of the Tau peptides used is schematically represented in **Figure 32**.

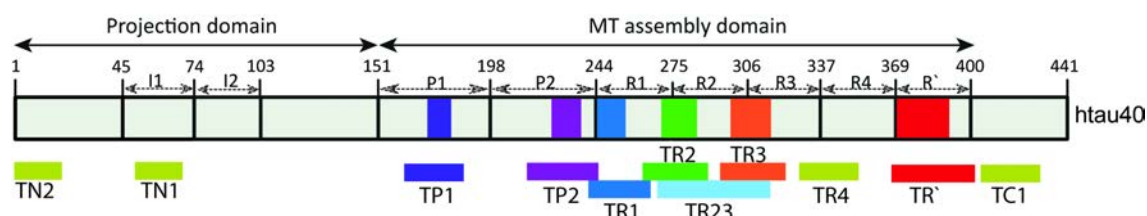


Figure 32: Divide and conquer strategy. Pictorial representation of the selected peptide regions to determine the structure in the MT-bound state. The binding hot spots identified are extended to both N and C-terminus by a few residues to select the sequence. The yellow color coding is for the control peptides which are not expected to bind to MTs.

The dissociation constant of Tau peptides used in this study are expected to be of the order of μM to mM range that enables fast exchange between the MT-bound and free peptides. This allowed us to implement tr-NOESY experiments to derive structural restraints from the bound peptides.

3.5.2 Assignment of the peptides

To implement the divide and conquer strategy for the structure determination of MT-bound Tau, different Tau peptides were synthesized with reference to the binding hot spots identified. These peptides include TP1, TP2, TR1, TR2, TR3, TR23 and TR'. The primary requirement for the NMR based structure determination is the complete resonance assignment of the spectra. The sequential resonance assignment of all the residues was done using the standard Wuethrich method (section 2.6.1.1). The spin systems were identified using the TOCSY spectra at different mixing times together with the DQF-COSY spectra. TOCSY spectra at two different mixing times of 60 and 80 ms helped to identify the spin systems unambiguously. All the residues were sequentially connected by combining TOCSY and NOESY spectra. The natural abundance ^{13}C and ^{15}N HSQC spectra acquired with these peptides provided the proton chemical shifts identical to those of full length Tau. These chemical shift information together with the sequential assignment from TOCSY and NOESY spectra provided highly reliable resonance assignment.

3.5.3 Assignment of TR3

The identification of different spin systems in TR3 was achieved unambiguously using TOCSY spectrum and a selected region of the spectrum is shown in **Figure 33a**. The sequential connectivity from i^{th} residue to $i+1^{\text{th}}$ residue is shown in **Figure 33b** where the finger print region of the spectrum is displayed. Thus the complete resonance assignment of individual amino acids in the NOESY spectrum of TR3 was achieved unambiguously.

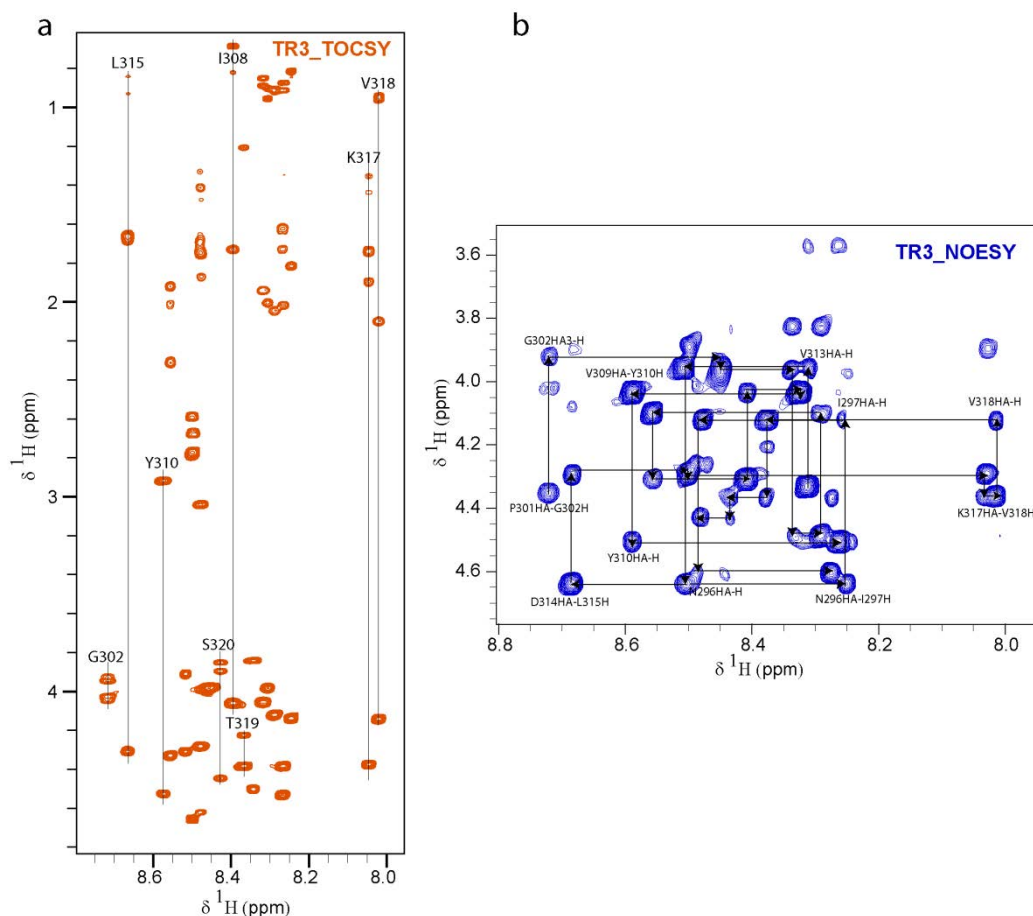


Figure 33: Sequential resonance assignment of TR3 peptide. (a) Spin system identification. The fingerprint region of the TOCSY spectrum with selected spin systems labeled. The vertical lines indicate the complete spin system of a specific residue type. (b) Fingerprint region of NOESY spectrum of TR3 with HA-HN correlation peaks. The spin systems identified from the TOCSY spectrum are connected sequentially by arrows and selected peaks are assigned to show the connectivity.

3.5.4 Tau peptides bind effectively to tubulin/MT: STD NMR

STD NMR method yields the spectra if and only if there is binding and the binding should be relatively weak resulting in fast exchange regime between bound and free states of the ligands (Mayer and Meyer 1999). The 1D STD NMR spectrum of MT-bound TR3 is shown in **Figure 34** and it clearly shows binding and gives indication about the exchange is fast enough to detect NMR observable developed in the bound state to be detected in the free ligands.

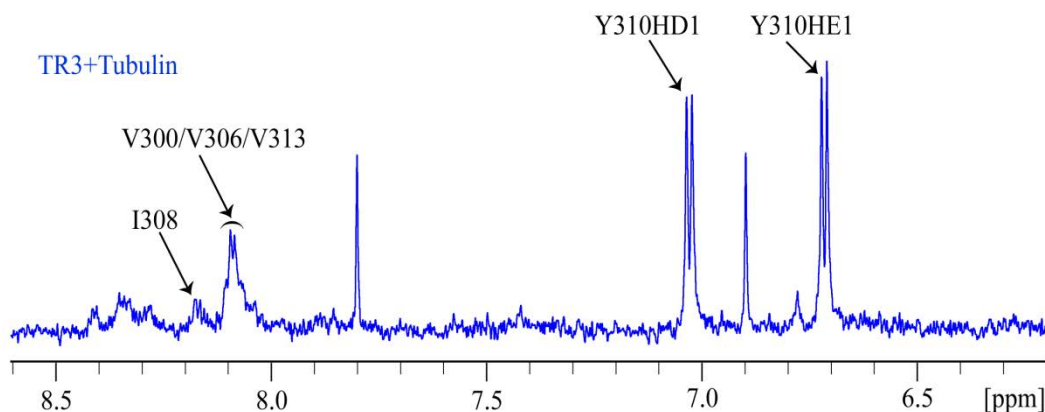


Figure 34: TR3 binds to tubulin. Selected region of 1D ^1H STD NMR spectrum of TR3 in the presence of tubulin with selective saturation of tubulin at -0.5 ppm. The most affected protons in TR3 upon selective saturation of tubulin are labeled.

3.6 Structure of MT-bound Tau peptides

To accomplish the central goal of the study, deriving the MT-bound structure, the tr-NOESY experiments were performed in the MT-bound state. The necessary and sufficient condition for the detection of transferred NOE such as the dissociation constant of the peptide-MT complex of the order of 10^{-6} to 10^{-3} M, peptide: MT ratio were satisfied. That is the chemical exchange of Tau peptides in the MT-bound and free state should be fast. One of the complimentary NMR methods that support detection of tr-NOEs is STD effect. STD NMR method yields the spectra if there exists weak binding and thereby fast exchange between bound and free states of the ligands. The 1D STD NMR spectrum of MT-bound TR3 **Figure 34** clearly shows binding and the exchange is fast enough to extract structural information from the bound state. The tr-NOESY spectra of the peptides were recorded with the NOE mixing time of 80 ms to avoid errors generating from spin diffusion and were used for the structure determination.

The manually assigned NOEs were used for generating the distance restraints and further structure calculation. The initial NOE peak calibration, conversion of the NOEs to distances and structure calculation were done using CYANA 3.0 with the standard simulated annealing protocol and torsion angle dynamics. The structures obtained were

refined using the program Xplor-NIH using the restrained simulated annealing protocol. Twenty lowest energy structures were taken for the analysis and validation of the structures using PROCHECK and rmsd values were calculated for the back bone and heavy atoms using MOLMOL. Finally ten best fitting structures are displayed.

3.6.1 Structure of MT-bound TR3

3.6.1.1 Tr-NOESY NMR spectrum of TR3-MT complex

The conformation of MT-bound TR3 was investigated using homonuclear ^1H - ^1H tr-NOESY experiments. The tr-NOESY spectrum of TR3 peptide was acquired in the presence of MTs in 20:1 ratio of TR3:MT with 80 ms mixing time. The spectrum showed a number of intense cross peaks in comparison to the spectrum acquired in the absence of MTs. This indicates that the additional peaks in the MT-bound state of TR3 are originating as a result of change in conformation induced by interaction. **Figure 35a** shows the overlay of the selected region of the tr-NOESY spectra of MT-bound and free TR3 and this region shows significant difference between the free and MT-bound TR3.

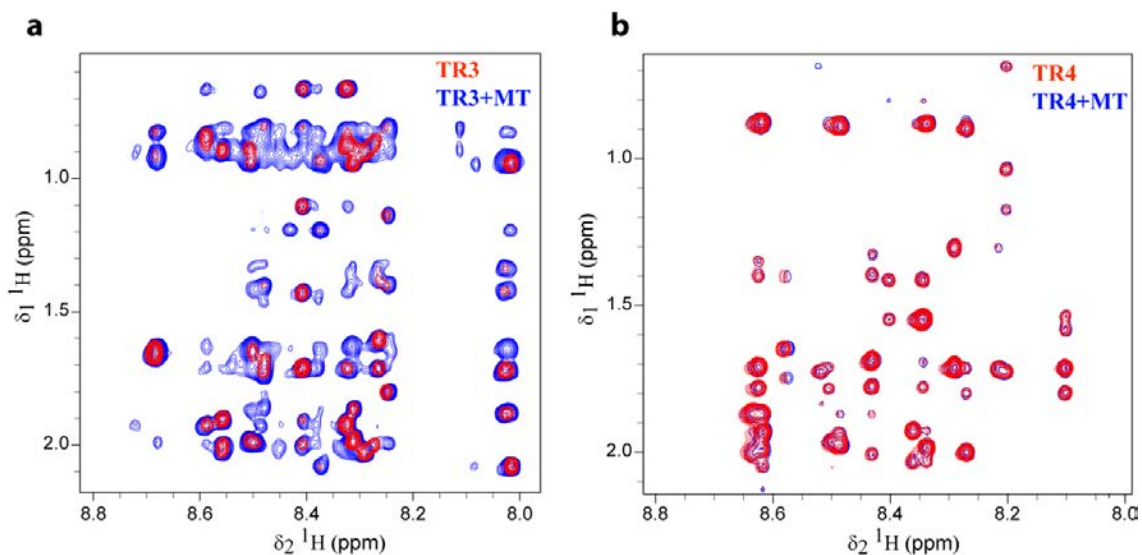


Figure 35: a) Region of the NOESY spectrum of 1mM TR3 peptide alone (red) overlaid with the tr-NOESY spectrum of 1mM TR3 peptide with 50uM MTs (blue) with a peptide to MT ratio of 20:1 in 50mM sodium phosphate buffer, pH 6.8. (b) Overlay of the NOESY (red) and tr-NOESY (blue) spectra of 1mM TR4 peptide. Spectra were recorded at 900 MHz and 278K.

3.6.1.2 Tr-NOESY spectrum of TR4 (Tau327-353)

In order to verify the tr-NOEs observed in the case of TR3, a control peptide TR4 (Tau327-353) encompassing the region of hTau40, which is immediately after the TR3 sequence, is selected. The residues in this region are less affected by signal broadening in the 2D ^1H - ^{15}N HSQC experiments of hTau40 due to the interaction with MTs. Hence it is believed to be the flexible linker between two binding domains. The NOESY spectra of TR4 acquired in the MT-bound state doesn't show tr-NOEs as shown in **Figure 35b**.

3.6.1.3 Structure calculation

Analysis of the tr-NOEs indicates the presence of a number of medium and even long range NOEs between the residues which belong to the amino acid stretch identified as the binding hot spot in repeat R3 as explained in section 3.2. The interaction of TR3 with MTs is reflected by the detection of transferred NOEs. In the absence of MTs TR3 only showed a small number of medium-range cross peaks in NOESY spectrum. Upon interaction with MTs significant number of NOE cross peaks were visible because of the rigidity in the conformation of TR3. As a result of the tr-NOESY experiment, it was possible to collect 319 distance restraints with 98 intra residue and 221 inter residue NOEs. These NOEs were further classified into 246 short-range, 60 medium-range and 13 long-range NOEs. The NOE connectivity that are the hallmark for the secondary structure element and the number of NOEs per each residue are shown in **Figure 36** with short range NOEs in white, medium in grey and long range NOEs in black color coding.

The most striking observation is the presence of many medium- and long-range tr-NOE cross peaks, especially within the residues which are identified as the binding epitope. The long-range contacts are predominantly from P301 to V306, V309, V313, K311 and D314. In addition other long-range contacts identified are also highly specific in the MT-bound state.

The initial structure calculations of MT-bound TR3 were performed with CYANA 3.0 using the distance restraints derived from tr-NOESY experiment. The structures were refined using XPLOR-NIH using the standard simulated annealing

Results

protocol and 20 lowest energy structures were selected for analysis, the structural statistics of which are summarized in **Table 4**. There were no violations larger than 0.5Å observed in these structures. The 10 best structures are displayed in figure 22. The mean structure is displayed to show the side chain orientation of the structured region of the peptide.

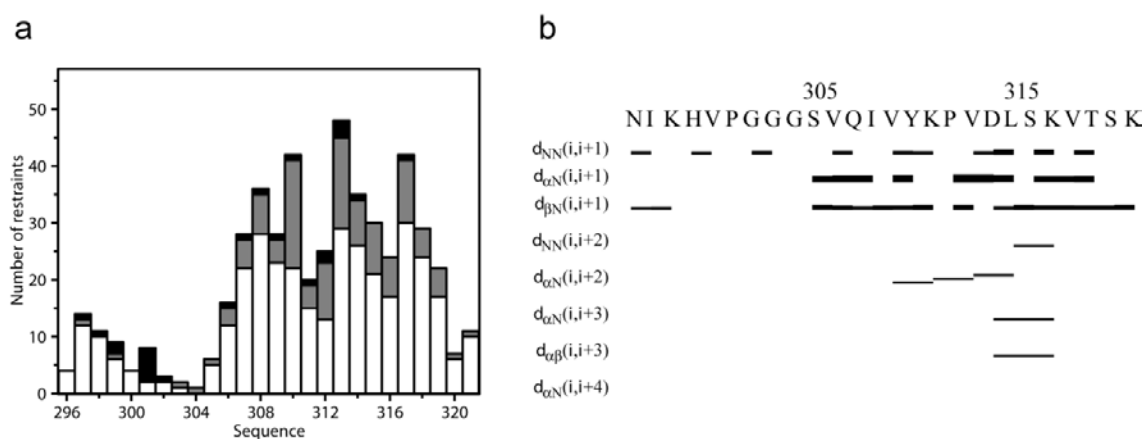


Figure 36: (a) The distribution of NOE interactions. Plots of the distribution of distance constraints as a function of their residue numbers for MT-bound TR3 peptide used for structure calculation. In the plot against the sequence upper distance limits are classified according to their range as intra and sequential constraints (white), medium range (grey) and long range (black) respectively. (b) Overview over sequential and medium-range 1H-1H NOEs in various secondary structural elements. Short distances are indicated by horizontal lines connecting the corresponding proton positions and the thickness of the bars is proportional to the intensity of the observed NOE.

It is to be noticed that most of the medium and long range NOEs observed are within the Val-300-Thr319 residues stretch of TR3. It is highly reflected from the convergence of the conformers displayed in **Figure 37a** and **Figure 37b** with an rmsd of 1.09Å for the backbone atoms and 1.58Å for heavy atoms. One of the key features observed is that the presence of long range NOEs from P-301 to I-308, V-309, and V313. The side chains of these residues stabilize the turn conformation adopted by TR3 in the presence of MTs. A few residues involved in long range contacts are indicated in one of the conformers of TR3 in **Figure 37c**.

Table 4: Structural statistics of the MT-bound TR3

Structural statistics for the 20 final conformers of MT-bound TR3 (26 residues)	
Number of restraints	319
Intra residue NOE ($ i-j = 0$)	98
Sequential NOE ($ i-j = 1$)	148
Medium range NOE ($1 < i-j < 5$)	60
Long range NOE ($ i-j \geq 5$)	13
NOE violations $> 0.5 \text{ \AA}$ /structure	0
Ramachandran plot statistics	
Residues in most favored regions	56.1%
Residues in additionally allowed regions	22.1%
Residues in generously allowed regions	15.8%
Residues in disallowed regions	6.0%
RMS deviations from the average structure	
Backbone atoms	
(Residues 300-301, 305-312)	1.09 \AA
Heavy atoms	1.58 \AA

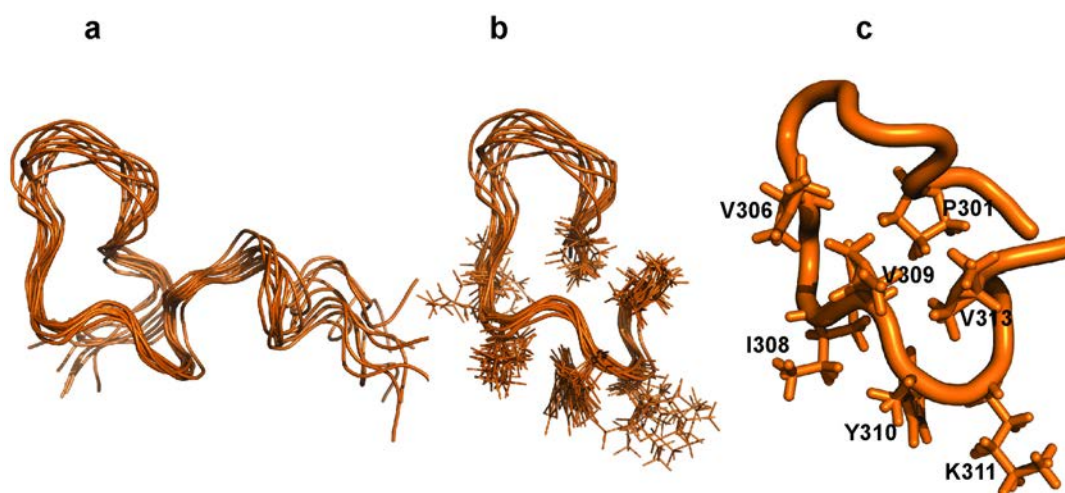


Figure 37: Structure of TR3 in the MT-bound state. (a) Backbone superposition of the ten best structures of the MT-bound TR3 as calculated from the tr-NOESY experiments. (b) Structured region of the MT-bound TR3 with side chains identified as binding epitopes. (c) The mean structure of the TR3 in the MT-bound state. The side chains of the residues involved in the long and medium range interactions within the structured region are highlighted.

3.6.2 Structure of MT-bound TR2

The sequential assignment of NOESY spectra of TR2 was done as in the case of TR3. The tr-NOESY spectrum of TR2 in the MT-bound state was acquired with different mixing times and compared with the NOESY spectrum of TR2 in the free state. Albeit the fewer number of tr-NOE cross peaks, we could collect 131 intraresidue and 80 interresidue NOE restraints in the presence of MTs. 10 medium and 11 long range NOEs were identified which defined the MT bound structure with a reasonable convergence of the backbone atoms.

The remarkable NOEs in the tr-NOESY spectrum include the long range NOEs from Q269 and P270 to I278, K280, K281 and D283 etc. The residues in the structured part of the peptide are characterized by the medium range and long range tr-NOEs compared to other residues and it underlines the observation from the interaction studies where the amino acid residues in the structured region being the binding epitope. The structure calculations were done as in the case of TR3 and the final 20 lowest energy structures were selected for analysis.

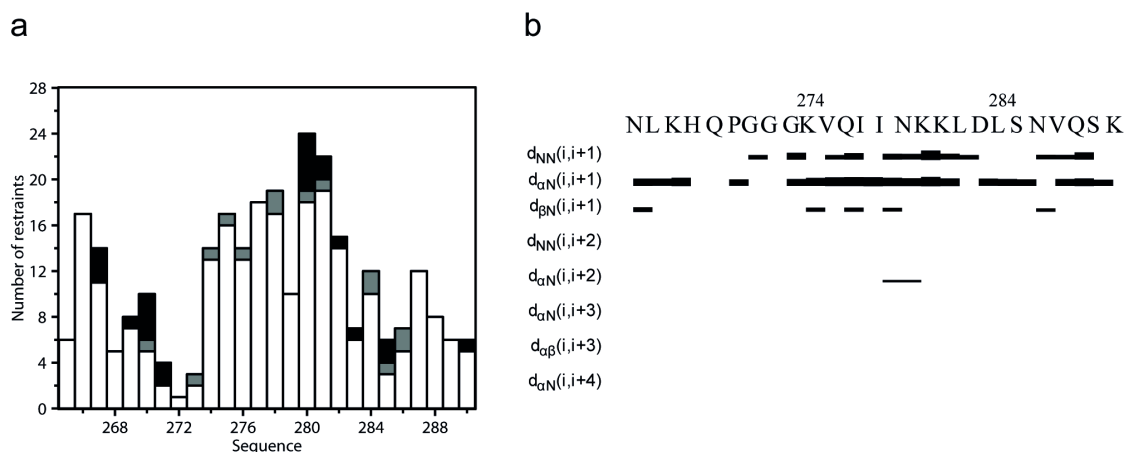


Figure 38: (a) The distribution of NOE interactions. Plots of the distribution of distance constraints as a function of their residue numbers for MT-bound TR2 peptide used for structure calculation. In the plot against the sequence upper distance limits are classified according to their range as intra and sequential constraints (white), medium range (grey) and long range (black) respectively. (b) Overview over sequential and medium-range ^1H - ^1H NOEs in various secondary structural elements. Short distances are indicated by horizontal lines connecting the corresponding proton positions and the thickness of the bars is proportional to the intensity of the observed NOE.

Results

Table 5: Structural statistics of the MT-bound TR2

Structural statistics for the 20 final conformers of MT-bound TR2 (26 residues)	
Number of restraints	211
Intra residue NOE ($ i-j = 0$)	131
Sequential NOE ($ i-j = 1$)	59
Medium range NOE ($1 < i-j < 5$)	10
Long range NOE ($ i-j \geq 5$)	11
NOE violations $> 0.5 \text{ \AA}/\text{structure}$	0
Ramachandran plot statistics	
Residues in most favored regions	55.0%
Residues in additionally allowed regions	25.8%
Residues in generously allowed regions	13.3%
Residues in disallowed regions	6.0%
RMS deviations from the average structure	
Backbone atoms (Residues 269-270, 274-280)	1.14 \AA
Heavy atoms	2.02 \AA

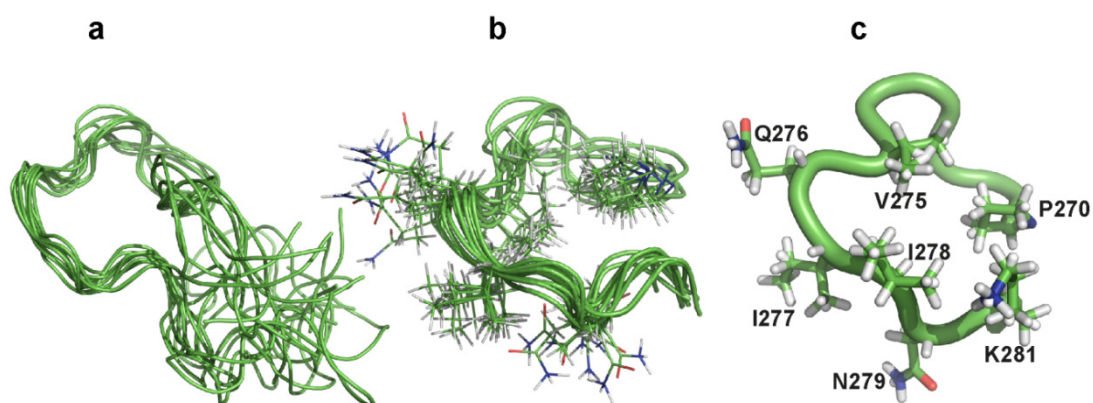


Figure 39: Structure of TR2 in the MT-bound state. (a) Main chain superposition of the ten best structures of the MT-bound TR2 as calculated from the tr-NOESY experiments. (b) Structured region of the MT-bound TR2 with side chains identified as binding epitopes. (c) The mean structure of the TR2 in the MT-bound state. The side chains of the residues involved in the long and medium range interactions within the structured region are highlighted.

3.6.3 Structure of MT-bound TR1

The tr-NOESY spectrum of MT-bound TR1 was acquired in the presence of MTs in 20:1 ratio of TR1:MT and it showed a number of additional cross peaks in comparison to the spectrum acquired in the absence of MTs. The additional peaks in the MT-bound state of TR1 reflect its binding to MTs according to the principle of tr-NOE and thereby possess a conformation other than the free TR1. The complete resonance assignment of the peptide was done as explained in the case of TR3. As a result of the tr-NOESY experiment, it was possible to collect 253 distance restraints with 118 intra residue and 135 interresidue NOEs. The effective binding of this peptide is shown by the presence of 36 medium range and 8 long range NOEs.

Structure of MT-bound TR1 was determined following the strategy used in the TR3 structure determination. The distance restraints were calibrated using CYANA automated calibration method and classified into 209 short, 36 medium and 8 long range NOEs. The NOE connectivities and the number of NOEs observed per each residue are shown in **Figure 40**. The initial structure calculation was done using CYANA and refined in XPLOR-NIH.

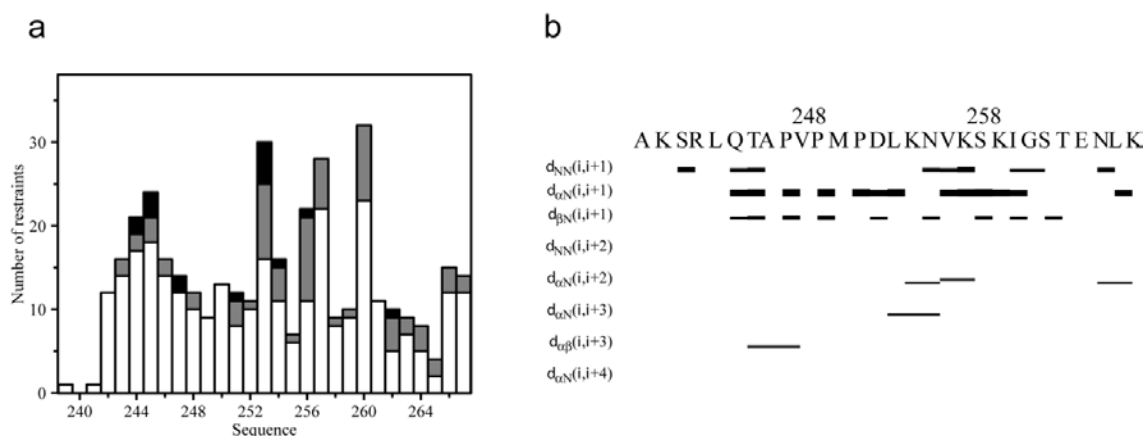


Figure 40: (a) The distribution of NOE interactions. Plots of the distribution of distance constraints as a function of their residue numbers for MT-bound TR1 peptide used for structure calculation. In the plot against the sequence upper distance limits are classified according to their range as intra and sequential constraints (white), medium range (grey) and long range (black) respectively. (b) Overview over sequential and medium-range ^1H - ^1H NOEs in various secondary structural elements. Short distances are indicated by horizontal lines connecting the corresponding proton positions and the thickness of the bars is proportional to the intensity of the observed NOE.

The structural statistics of the 20 lowest energy structures is given in **Table 6** and 10 best converged structures are displayed as an ensemble in **Figure 41** together with the

Results

mean structure showing the side chain orientation. The structured region of the peptide T245-K253 shows better convergence with an rmsd of 0.76 Å for the back bone atoms and 1.32 Å for the heavy atoms.

Table 6: Structural statistics of the MT-bound TR1

Structural statistics for the 20 final conformers of MT-bound TR1 (29 residues)	
Number of restraints	253
Intra residue NOE ($ i-j = 0$)	118
Sequential NOE ($ i-j = 1$)	91
Medium range NOE ($1 < i-j < 5$)	36
Long range NOE ($ i-j \geq 5$)	8
NOE violations > 0.5 Å/structure	0
Ramachandran plot statistics	
Residues in most favored regions	80.0%
Residues in additionally allowed regions	13.9%
Residues in generously allowed regions	4.3%
Residues in disallowed regions	1.7%
RMS deviations from the average structure	
Backbone atoms (Residues 245-253)	0.76 Å
Heavy atoms	1.32 Å

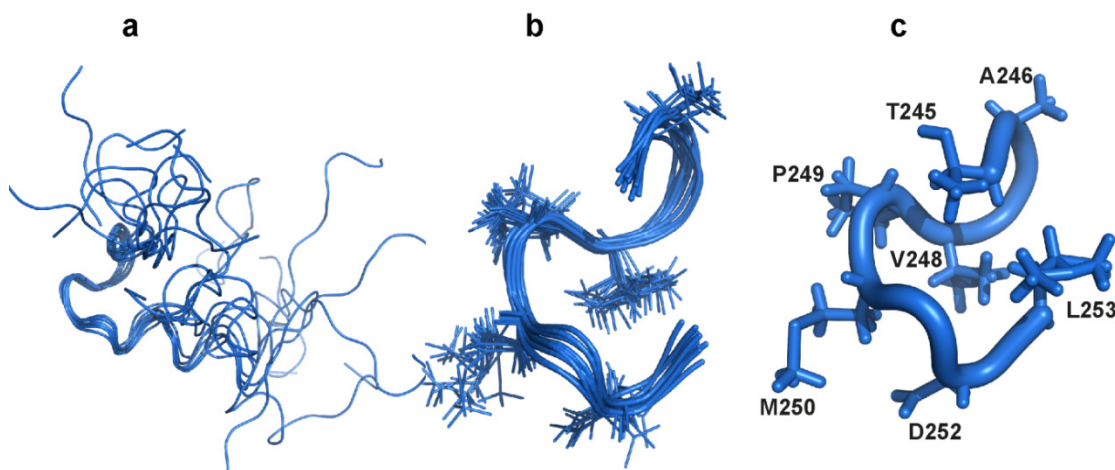


Figure 41: Structure of TR1 in the MT-bound state. (a) Main chain superposition of the ten best structures of the MT-bound TR1 as calculated from the tr-NOESY experiments. (b) Structured region of the MT-bound TR1 with sidechains identified as binding epitopes. (c) The mean structure of the TR1 in the MT-bound state. The sidechains of the residues involved in the long and medium range interactions within the structured region are highlighted.

3.6.4 Structure of MT-bound TP2

The peptide TP2 from the proline rich region of Tau is shown to be one of the important regions involved in MT binding. The relatively high positive charge of the peptide region was shown to be the driving force involved in binding. The structure of MT-bound TP2 was calculated by collecting 321 tr-NOE cross peaks with 134 intra residue and 187 inter residue NOEs. The distance restraints generated were classified into 270 short, 45 medium and 6 long range NOEs and were used in the structure calculation of MT-bound TP2 using the same protocol followed in the previous cases. The NOE connectivities and number of NOEs used per residue are shown in **Figure 42**. The structural statistics of the lowest 20 structures is given in **Table 7** and the best 10 structures are displayed in **Figure 43**.

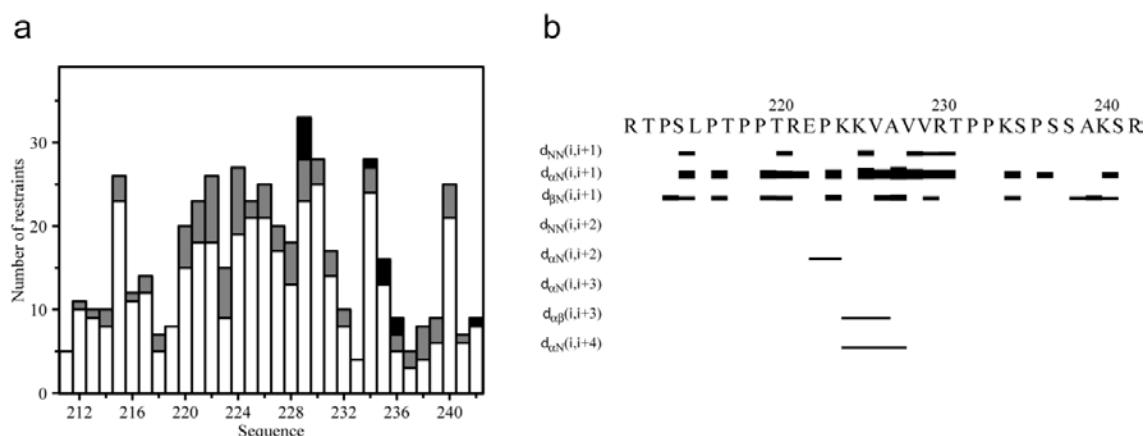


Figure 42: (a) The distribution of NOE interactions. Plots of the distribution of distance constraints as a function of their residue numbers for MT-bound TP2 peptide used for structure calculation. In the plot against the sequence upper distance limits are classified according to their range as intra and sequential constraints (white), medium range (grey) and long range (black) respectively. (b) Overview over sequential and medium-range ^1H - ^1H NOEs in various secondary structural elements. Short distances are indicated by horizontal lines connecting the corresponding proton positions and the thickness of the bars is proportional to the intensity of the observed NOE.

The rmsd of the structured part of the peptide is analysed and showed high degree of convergence within the regions K224-V228 and V228-P236. The back bone rmsd of 0.68 Å is calculated in the V228-P236 region of the TP2 peptide. A number of medium range NOEs were observed in these structured regions of TP2.

Table 7: Structural statistics of the MT-bound TP2

Structural statistics for the 20 final conformers of MT-bound TP2 (32 residues)	
Number of restraints	321
Intra residue NOE ($ i-j = 0$)	134
Sequential NOE ($ i-j = 1$)	136
Medium range NOE ($1 < i-j < 5$)	45
Long range NOE ($ i-j \geq 5$)	6
NOE violations $> 0.5 \text{ \AA}/\text{structure}$	0
Ramachandran plot statistics	
Residues in most favored regions	60.0%
Residues in additionally allowed regions	27.0%
Residues in generously allowed regions	9.6%
Residues in disallowed regions	3.4%
RMS deviations from the average structure	
Backbone atoms (Residues 224-228)	0.84 \AA
Heavy atoms	1.90 \AA
Backbone atoms (Residues 228-236)	0.68 \AA
Heavy atoms	1.49 \AA
Backbone atoms (Residues 224-236)	1.35 \AA
Heavy atoms	2.30 \AA

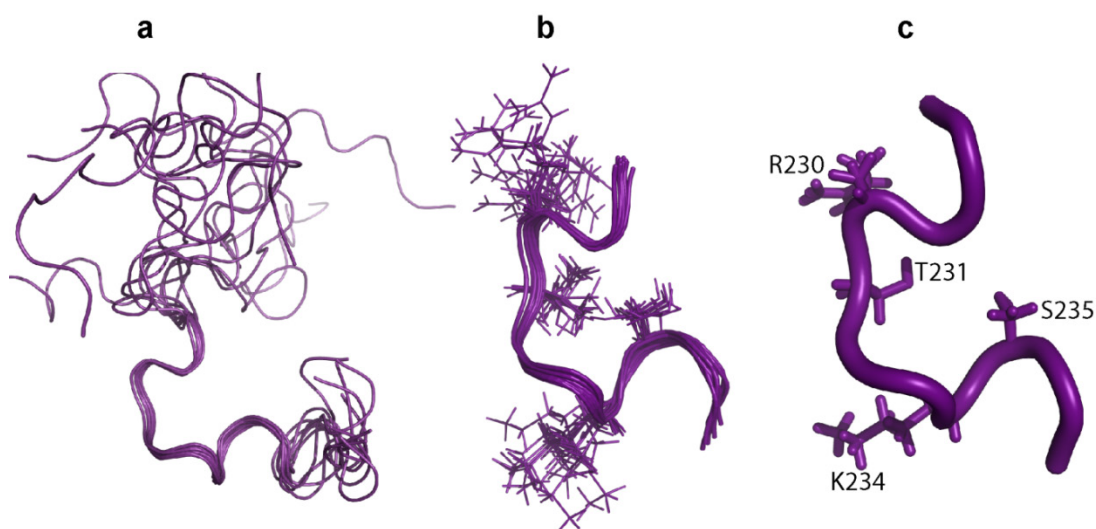


Figure 43: Structure of TP2 in the MT-bound state. (a) Mainchain superposition of the ten best structures of the MT-bound TP2 as calculated from the tr-NOESY experiments. (b) Structured region of the MT-bound TP2 with sidechains identified as binding epitopes. (c) The mean structure of the TP2 in the MT-bound state. The sidechains of the residues involved in the long and medium range interactions within the structured region are highlighted.

3.6.5 Structure of MT-bound TP1

The structure of TP1 in the MT-bound state was calculated using the tr-NOE method. The comparison of the NOESY and tr-NOESY spectra shows that there are not many new NOE cross peaks in the MT-bound state, leaving a significant portion of the peptide unstructured. Out of the 210 tr-NOEs observed in the MT-bound state, 78 cross peaks were identified as intra residue and 132 inter residue NOEs. These NOE restraints were used for the structure determination by classifying them into 194 short range and 16 medium range NOEs, without having any long range contact within the peptide residues. The structural statistics of the 20 low energy structures is shown in **Table 8**. There were no NOE violations larger than 0.5\AA per structure.

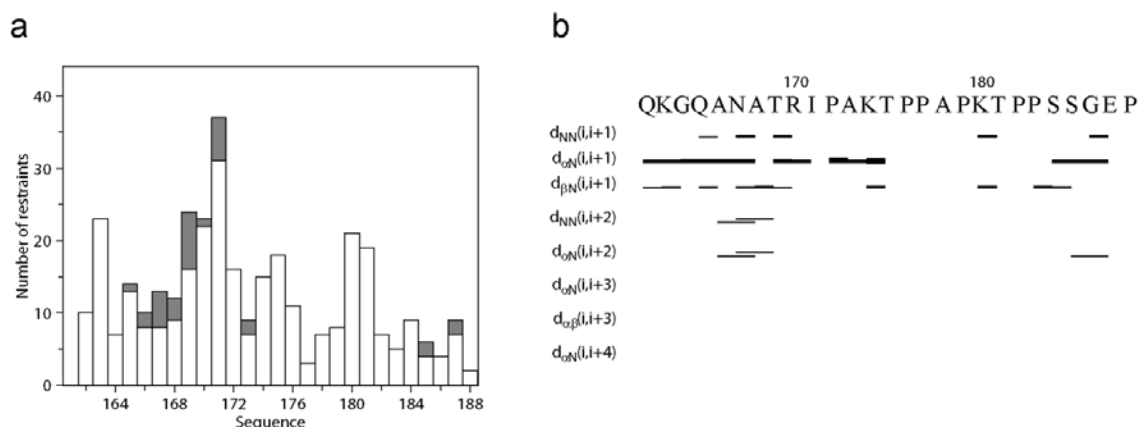


Figure 44: (a) The distribution of NOE interactions. Plots of the distribution of distance constraints as a function of their residue numbers for MT-bound TP1 peptide used for structure calculation. In the plot against the sequence upper distance limits are classified according to their range as intra and sequential constraints (white), medium range (grey) and long range (black) respectively. (b) Overview over sequential and medium-range ^1H - ^1H NOEs in various secondary structural elements. Short distances are indicated by horizontal lines connecting the corresponding proton positions and the thickness of the bars is proportional to the intensity of the observed NOE.

An ensemble structure of 10 best fitting conformers is shown in **Figure 45**. It was found that shorter amino acid stretches are structured in different regions after interaction with MTs. The back bone rmsd of 0.9\AA and heavy atom rmsd of 1.9\AA was calculated between the residues 171 and 176.

Results

Table 8: Structural statistics of the MT-bound TP1

(Structure of this TP1 was calculated by Dr. Mariusz Jaremko and Dr.Lukasz Jaremko).

Structural statistics for the 20 final conformers of MT-bound TP1 (27 residues)	
Number of restraints	210
Intra residue NOE ($ i-j = 0$)	78
Sequential NOE ($ i-j = 1$)	116
Medium range NOE ($1 < i-j < 5$)	16
Long range NOE ($ i-j \geq 5$)	0
NOE violations $> 0.5 \text{ \AA}$ /structure	0
Ramachandran plot statistics	
Residues in most favored regions	85.6%
Residues in additionally allowed regions	12.2%
Residues in generously allowed regions	1.4%
Residues in disallowed regions	0.8%
RMS deviations from the average structure	
Backbone atoms (Residues 171-176)	0.90 \AA
Heavy atoms	1.90 \AA

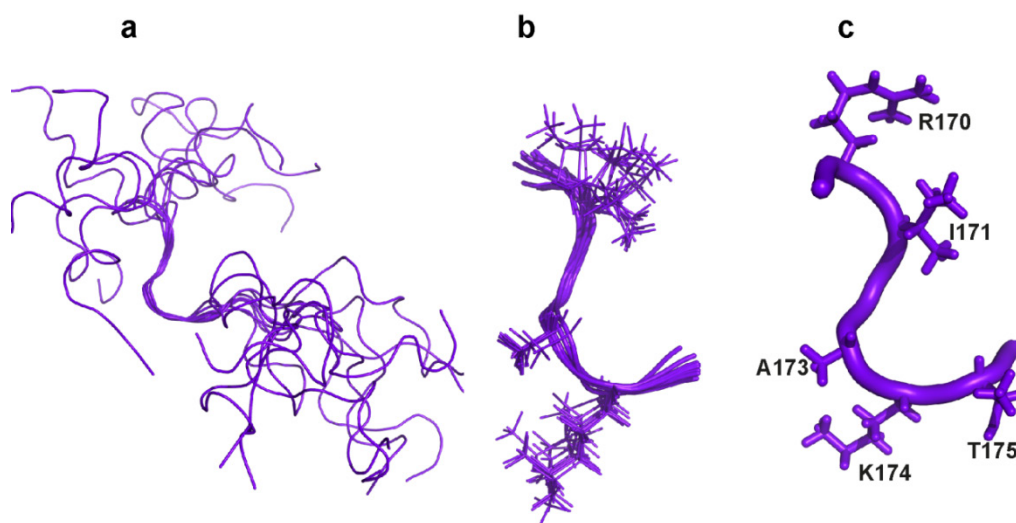


Figure 45: Structure of TP1 in the MT-bound state. (a) Mainchain superposition of the ten best structures of the MT-bound TP1 as calculated from the tr-NOESY experiments. (b) Structured region of the MT-bound TP1 with sidechains identified as binding epitopes. (c) The mean structure of the TP1 in the MT-bound state. The sidechains of the residues involved in the long and medium range interactions within the structured region are highlighted.

3.6.6 Structure of MT-bound TR'

The peptide TR' from the pseudo repeat region of Tau was shown as one of the important regions involved in MT binding. The comparison of tr-NOESY spectrum of TR' with MTs and NOESY spectrum of free TR' showed significant number of NOE cross peaks appeared in the MT-bound state, indicating the effective binding as well as a specific conformation in the MT-bound state. The structure of MT-bound TR' was calculated by collecting 434 tr-NOE cross peaks with 107 intra residue and 327 inter residue NOEs. The distance restraints generated were classified into 278 short, 108 medium and 48 long range NOEs and were used in the structure determination of MT-bound TR' using the same protocol followed in the previous cases. The NOE connectivities and number of NOEs used per residue are shown in **Figure 46**. The structural statistics of the lowest 20 structures is given in **Table 9** and the best 10 structures are displayed in **Figure 47**.

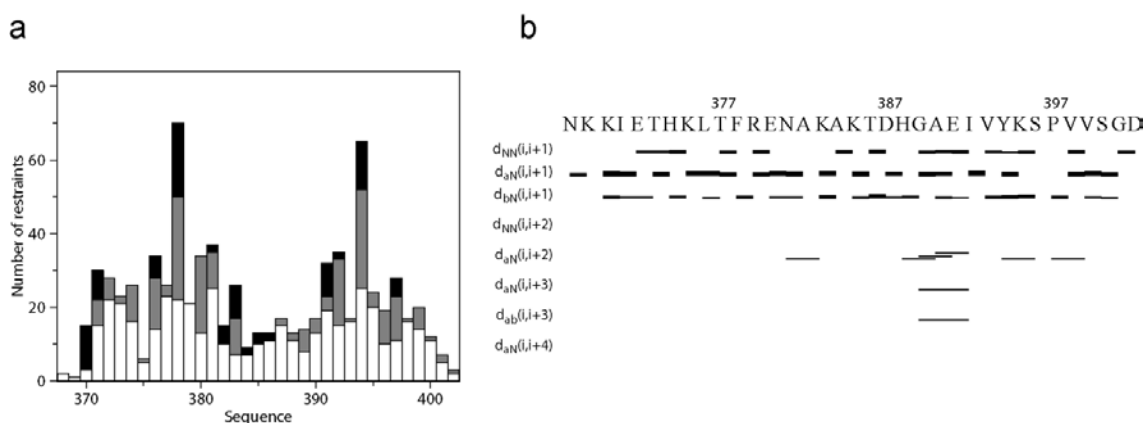


Figure 46: (a) The distribution of NOE interactions. Plots of the distribution of distance constraints as a function of their residue numbers for MT-bound TR' peptide used for structure calculation. In the plot against the sequence upper distance limits are classified according to their range as intra and sequential constraints (white), medium range (grey) and long range (black) respectively. (b) Overview over sequential and medium-range ^1H - ^1H NOEs in various secondary structural elements. Short distances are indicated by horizontal lines connecting the corresponding proton positions and the thickness of the bars is proportional to the intensity of the observed NOE.

Results

Table 9: Structural statistics of the MT-bound TR'

(Structure of this TP1 was calculated by Dr. Mariusz Jaremko and Dr. Lukasz Jaremko).

Structural statistics for the 20 final conformers of MT-bound TR' (35 residues)	
Number of restraints	434
Intra residue NOE ($ i-j = 0$)	107
Sequential NOE ($ i-j = 1$)	171
Medium range NOE ($1 < i-j < 5$)	108
Long range NOE ($ i-j \geq 5$)	48
NOE violations $> 0.5 \text{ \AA}/\text{structure}$	0
Ramachandran plot statistics	
Residues in most favored regions	79.8%
Residues in additionally allowed regions	12.3%
Residues in generously allowed regions	7.2%
Residues in disallowed regions	0.7%
RMS deviations from the average structure	
Backbone atoms	1.35 \AA
Heavy atoms	1.83 \AA

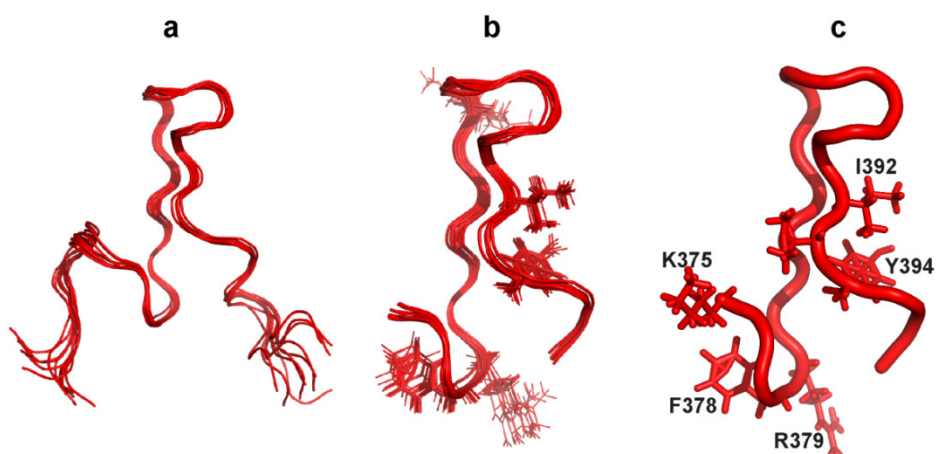


Figure 47 : Structure of TR' in the MT-bound state. (a) Main chain superposition of the ten best structures of the MT-bound TR' as calculated from the tr-NOESY experiments. (b) Structured region of the MT-bound TR' with side chains identified as binding epitopes. (c) The mean structure of the TR' in the MT-bound state. The side chains of the residues involved in the long and medium range interactions within the structured region are highlighted.

3.6.7 Structure of MT-bound TR23

As explained before TR23 is the peptide that comprise of the binding regions of both TR2 and TR3 which are two nearest independent binding domains in hTau40. The tr-NOESY spectrum of TR23 peptide was acquired in the presence of MTs in 20:1 ratio of TR23:MT and it showed a number of intense cross peaks in comparison to the spectrum acquired in the absence of MTs. This indicates that the additional peaks in the MT-bound state of TR23 are originating as a result of effective binding and change in conformation in the MT-bound state. The combined effect of two interacting region is reflected from the number of tr-NOEs observed in comparison to the number of cross peaks observed in the free state of the peptide. It clearly indicates the net effect of two interacting fragments being together.

A total of 652 tr-NOEs were used in the structure calculation which were assigned to 208 intra residue and 444 inter residue NOEs. The distance restraints generated from these tr-NOEs were classified into 460 short, 141 medium and 41 long range NOEs. The NOE connectivities and number of NOEs used per residue are shown in **Figure 48**.

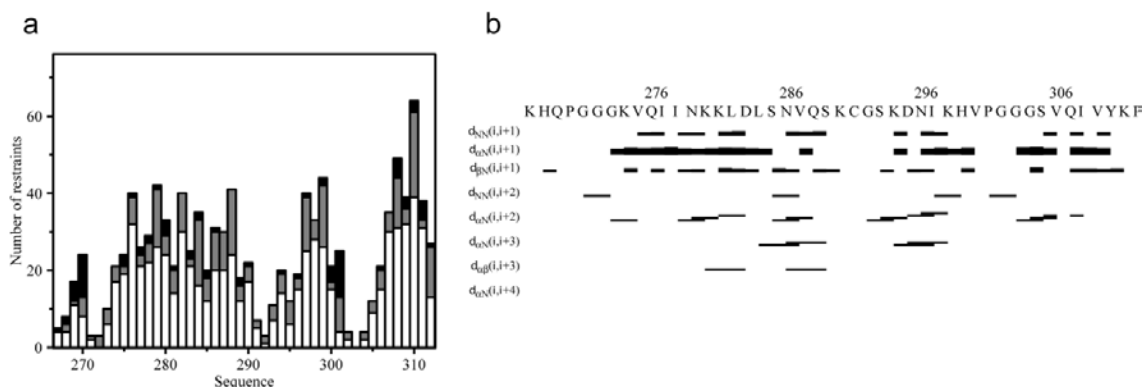


Figure 48: (a) The distribution of NOE interactions. Plots of the distribution of distance constraints as a function of their residue numbers for MT-bound TR23 peptide used for structure calculation. In the plot against the sequence upper distance limits are classified according to their range as intra and sequential constraints (white), medium range (grey) and long range (black) respectively. (b) Overview over sequential and medium-range ^1H - ^1H NOEs in various secondary structural elements. Short distances are indicated by horizontal lines connecting the corresponding proton positions and the thickness of the bars is proportional to the intensity of the observed NOE.

Results

The structure of MT-bound TR23 was determined using the similar protocol as explained in the previous cases and the structural statistics of 20 lowest energy structures are given in

Table 10 and there were no violations larger than 0.5 Å per structure. The structured regions of the TR23 peptide are identical to the structured regions of TR2 and TR3 and are shown separately as an ensemble of 10 best fitting structures in **Figure 49a** and **Figure 49b** respectively.

Table 10: Structural statistics of the MT-bound TR23

Structural statistics for the 20 final conformers of MT-bound TR23 (46 residues)	
Number of restraints	652
Intra residue NOE ($ i-j = 0$)	208
Sequential NOE ($ i-j = 1$)	262
Medium range NOE ($1 < i-j < 5$)	141
Long range NOE ($ i-j \geq 5$)	41
NOE violations > 0.5 Å/structure	0
Ramachandran plot statistics	
Residues in most favored regions	46.7%
Residues in additionally allowed regions	26.6%
Residues in generously allowed regions	19.0%
Residues in disallowed regions	7.7%
RMS deviations from the average structure	
Backbone atoms (Residues 269-281)	1.43 Å
Heavy atoms	2.53 Å
Backbone atoms (Residues 299-311)	1.1 Å
Heavy atoms	1.90 Å

The two structured regions of the combined peptide TR23 were compared with the short individual peptides TR2 and TR3 as shown in **Figure 49c** and **Figure 49d** respectively, where it is evident that the structure of TR2 and TR3 are conserved in TR23.

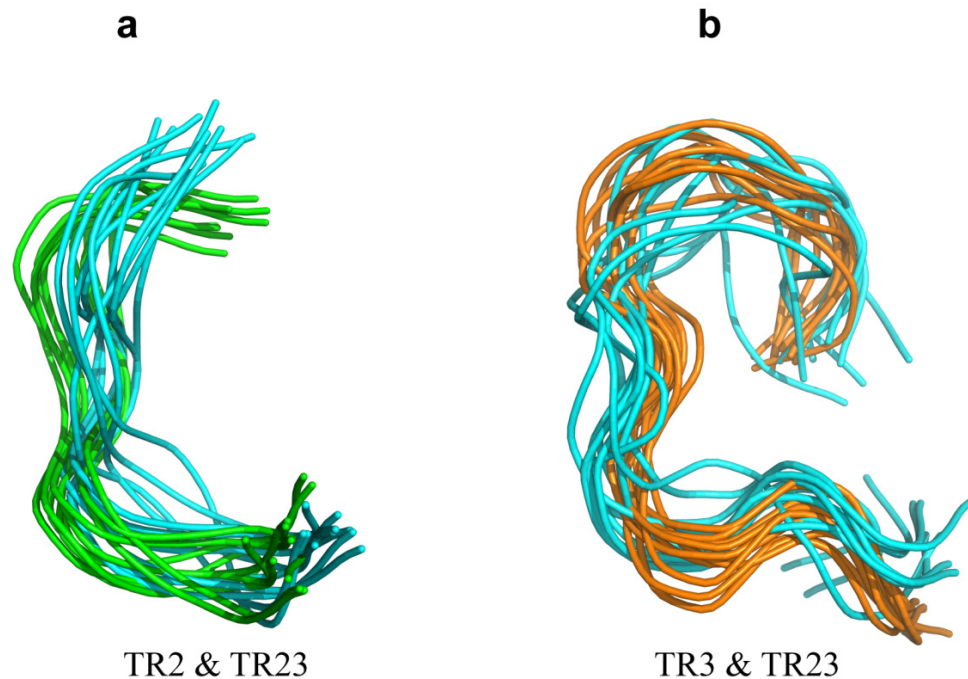


Figure 49: The structure of MT-bound Tau peptides is conserved in the longer Tau constructs. Structure of TR23 in the MT-bound state. (a and b) Structure of TR23 in the MT-bound state with superposition of the structured regions of 10 low energy conformers of TR23 peptide (cyan) with structured region of TR2 (green) and with TR3 (orange) respectively.

3.7 Properties of Tau peptides

3.7.1 Competition between Tau and Tau peptides for MT binding

The observation that the binding regions of Tau on MT are independent of each other allowed to use shorter Tau fragments to perform competition experiments with full length Tau for MT binding. Shorter Tau fragments from the microtubule binding domains can bind, stabilize and/or promote MT assembly (Joly, Flynn et al. 1989). The previous study using different fragments showed that although all the peptides from the microtubule binding domain are able to bind to tubulin or MT not all of them promoted MT assembly (Joly, Flynn et al. 1989). The Tau fragments TP2 and TR3 are two important binding hot spots of Tau for MT binding and adopt well defined structure in the MT bound state (**section 3.2**). These peptides were chosen to compete with full length Tau protein for MT binding.

3.7.1.1 Competition between TP2 and hTau40 for MT binding

Titration of TP2 into the solution containing hTau40 and MTs in different ratios varying from 5, 10 and 15 times excess than hTau40 was done at a Tau concentration of 50 μ M. The line broadening observed in the hTau40-MT complex was taken as the reference to specify the relative influence of TP2 and is shown in **Figure 50a**. Subsequent addition of TP2 reduces the overall line broadening observed in the Tau-MT complex indicates both hTau40 and TP2 are competitively targeting MTs for the same binding site. The reduction in line broadening indicates the presence of relatively high number of free Tau molecules in solution after the addition of TP2. An almost 60% reduction in the initial line broadening after 15 fold excess addition of TP2 indicates competition between Tau and TP2 highlighting the importance of proline rich region in MT binding. Most specific observation to be noticed is that a shorter peptide from P2 is competing with all other independent binding domains of Tau protein.

3.7.1.2 Competition between TR3 and hTau40 for MT binding

The ability of independent binding features of Tau domains in the repeat region was further tested with the help of TR3 peptide. We could see the similar behaviour as found in the case of TP2 when it was allowed to compete with hTau40 for MT binding. The peptide was added in the successive amounts of 250 μ M, 500 μ M and 750 μ M concentrations. At 15 fold excess concentration of TR3 in the hTau40-MT complex reduces the line broadening in the hsqc spectra upto ~40% with a relatively less effect near R'. It is clear from the **Figure 50b** that TR3 shows competitive binding with hTau40.

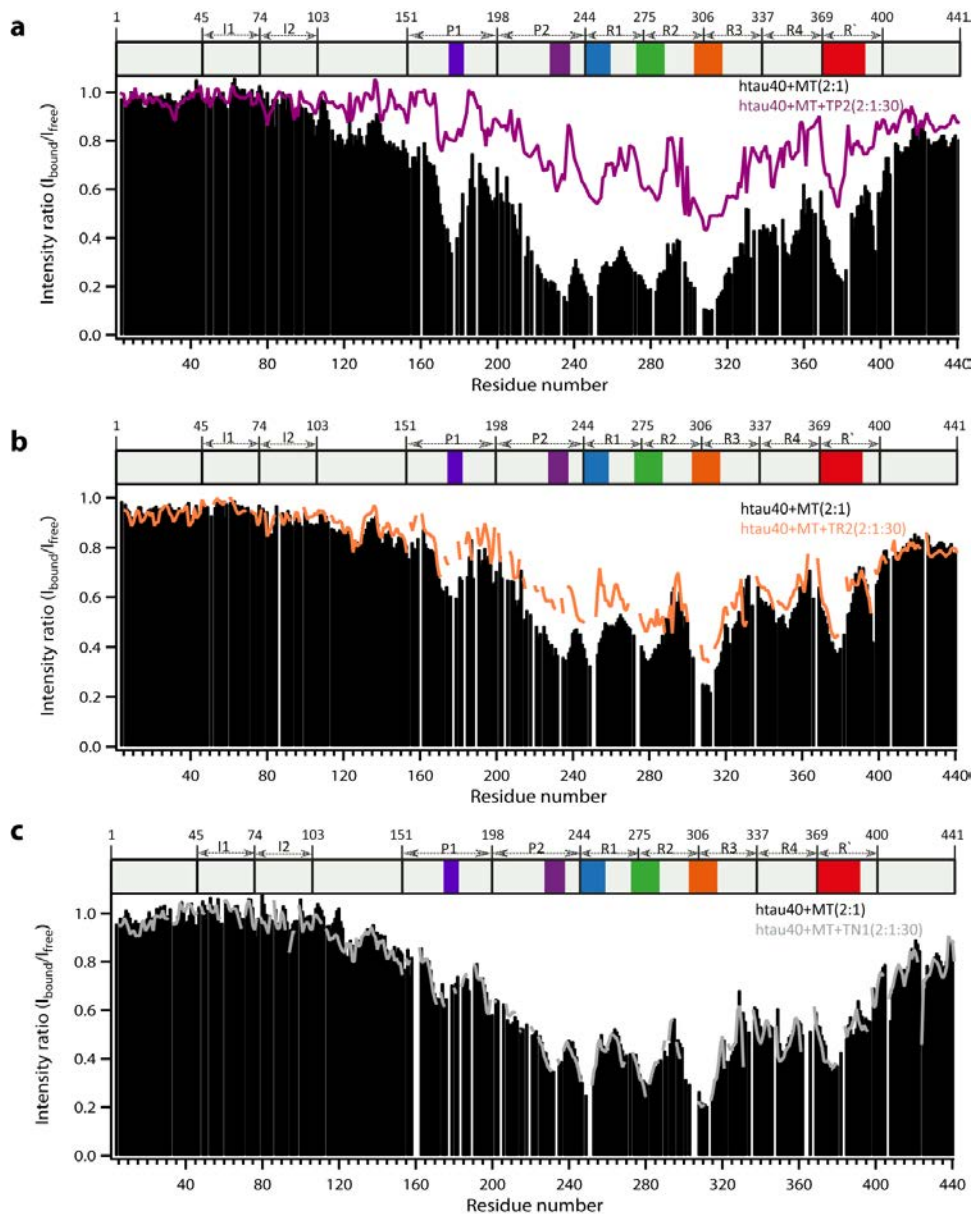


Figure 50: Efficiency of Tau peptides for microtubule binding. (a) Residue specific NMR signal intensity ratios of hTau40 between the MT-bound and unbound state with a stoichiometry of 2:1 (black bars). TP2 peptide shows competition for MT binding against hTau40 and the decrease in line broadening is reflected in the intensity ratio plot between the ternary complex of hTau40, TP2 and MT and unbound hTau40 (purple line). (b) Competition of TR3 peptide and hTau40 for MT binding is depicted in the intensity ratio plot of hTau40 alone bound to MTs (black bars) and hTau40 and TR3 peptide together bind to MTs (orange line). The colouring code in the domain organization diagram and the intensity plots represent the structured regions of corresponding peptides. (c) Addition of the control peptide TN1 from the N-terminal insert of the hTau40 to the Tau-MT complex has no effect on MT binding. The intensity of resonances of full length Tau bound to MTs (black bars) remains unaffected after the addition of TN1 peptide (grey line). The Tau peptides were taken 15 times in excess of hTau40 in all three cases.

3.7.1.3 N-terminal TN1 peptide does not compete for MT binding

To address whether these observations and results are specific or not, we performed the control experiment using the TN1 peptide (Tau52-69) from the N-terminal projection domain. The addition of TN1 to the hTau40-MT complex didn't exhibit any competition for MT binding (**Figure 50c**). To summarize, the competition experiments described here between short Tau peptides and hTau40 for MT binding clearly indicate the independent binding of the Tau domains.

3.7.2 Effect of phosphorylation and mutations in MT-binding

3.7.2.1 Effect of phosphorylation (T231 phosphorylation)

Phosphorylation of Tau protein is an integral part of its function in regulation of many cellular processes. Phosphorylation at specific sites (e.g. T231 phosphorylation) leads to detachment of Tau from MT, MT disassembly and formation of neurofibrillary tangles (NFTs). The effect of site-specific phosphorylation on MT binding was tested by acquiring the tr-NOESY spectrum of TP2_pT231 with MT. The overlay of the spectra in the presence and absence of MTs is compared with the tr-NOESY spectra of wild type TP2 as shown in **Figure 51**.

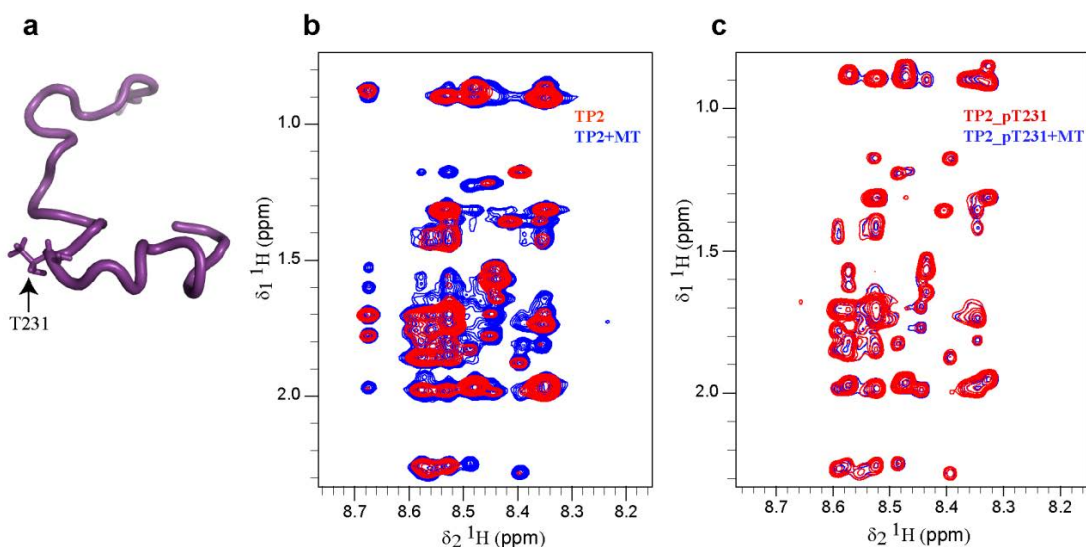


Figure 51: Effect of Phosphorylation of Tau peptides on MT binding and assembly. (a) The lowest energy conformer of TP2 peptide for which the structure is determined in the presence of MTs, with side chain of T231 highlighted. (b) Overlay of NOESY spectra of 1mM TP2 alone and TP2 in the presence of 50μM MTs. (c) NOESY spectra of TP2 with T231 phosphorylated in the presence and absence of MTs. Phosphorylation of T231 significantly reduces the interaction with MTs and is reflected in the tr-NOESY spectrum without showing newer tr-NOE peaks or enhancement in the signal intensities.

It is clear that there are no transferred NOE peaks resulting from interaction of TP2_pT231 with MTs. Phosphorylation of T231 significantly reduces the interaction with MTs and is reflected in the tr-NOESY spectrum without showing newer tr-NOESY peaks or enhancement in the signal intensities.

3.7.2.2 Effect of genetic mutation on MT binding

Genetic mutations in Tau lead to a series of neurodegenerative disorders known as Tauopathies. Here, we are interested to understand how these effects are related to the structure and function of Tau, especially in terms of its binding to MTs. Among different regions of Tau sequence, mutations in exon 10 of the Tau gene have been widely investigated, which is further studied here. P301S mutation is known to be linked to the development of frontotemporal dementia (FTD) (Bugiani, Murrell et al. 1999). There are many missense mutations and deletion mutations like G272V, Δ K280 and G389R that lead to Tau dysfunction and lead to neurodegeneration (Bunker, Kamath et al. 2006).

3.7.2.2.1 P301S

To address how P301S mutations alter Tau binding to MTs, we prepared the P301S variants of TR3 peptide and studied through tr-NOESY experiments. In comparison with *wt*-TR3, very weak cross peaks were found in the spectra of TR3_P301S (**Figure 52**). It is evident from the spectra that the binding is relatively weak and is reflected in the whole tr-NOESY spectrum, where all the cross peaks are too weak to be observed.

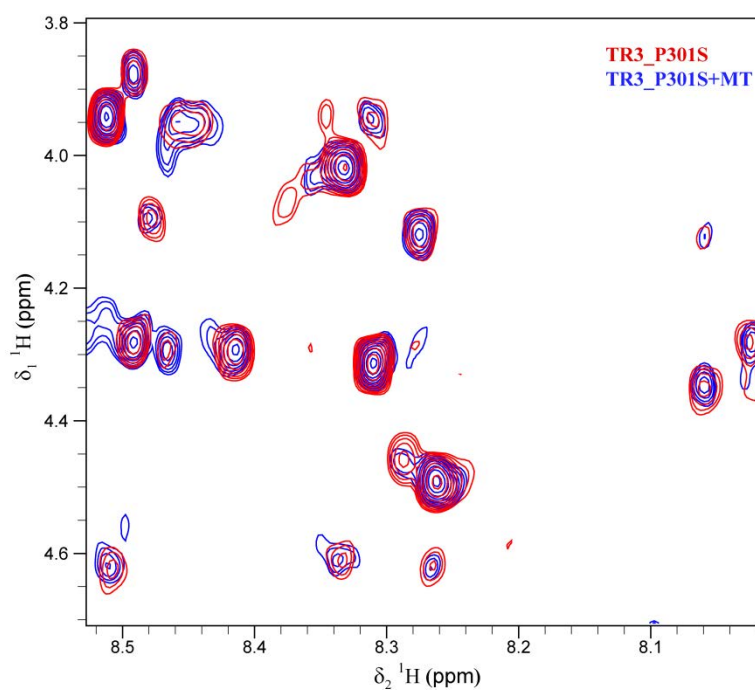


Figure 52: Superposition of region of the NOESY spectrum of 1mM TR3_P301S peptide alone (red) with the tr-NOESY spectrum of 1mM TR3_P301S with 50μM MTs (blue) with a peptide to MT ratio of 20:1 in 50mM sodium phosphate buffer, pH 6.8. . Similar results were obtained for TR3_P301L variant (not shown).

3.7.2.2.2 ΔK280 mutation

Deletion mutation of the residue K280 from the Tau sequence is found to be one of the hallmarks in certain neurodegenerative diseases. The MT binding properties of Tau is independent of this deletion mutation as it is evident from the tr-NOESY spectrum (Appendix Figure 1) of TR23_ΔK280. The comparison of NOESY spectra of MT-bound and unbound TR23_ΔK280 clearly showed that there is no significant effect of this single residue mutation.

3.7.3 MT assembly properties of Tau peptides

Having the structure of Tau peptides in the MT-bound state it is possible to integrate these structures into the structure of MT-bound Tau which is supported by our findings that the Tau-MT interaction is highly localized and independent of different binding domains. In this context it has high relevance to investigate how these Tau peptides behave independently in MT assembly and binding. The ability of the individual Tau peptides to bind and promote MT assembly is a key question in comparison with full length Tau protein. It was reported before that some of the Tau fragments and short peptides bind and nucleate MT assembly (Ennulat, Liem et al. 1989, Joly, Flynn et al. 1989, Gustke, Trinczek et al. 1994) and it should be considered that all the peptides which are binding with MTs may not necessarily promote tubulin polymerization. The experiments with shorter Tau fragments provided further evidence to bind, stabilize and promote MT assembly. These experiments were done by Dr. Satish Kumar and Dr. Katharina Tepper (Prof. E. Mandelkow group, DZNE, Bonn).

3.7.3.1 MT assembly of Tau peptides

The tubulin polymerization assay with Tau peptides was performed using the turbidity measurement in combination with electron microscopy. The systematic tubulin polymerization assay was done using 10 μ M of tubulin which is below the critical concentration, above which the tubulin itself can polymerize in the presence of polymerizing agents. The polymerization capacity of hTau40 and TauF4 was taken as the reference and the light scattering of these proteins in the presence of tubulin showed polymerization at low protein concentrations of 5 and 25 μ M respectively (**section 3.4.2.2**). The polymerization assay of tubulin was further tested using each Tau peptide by increasing the concentrations. TP2 promoted tubulin assembly at higher concentration of peptide and the optimum concentration was found to be 500 μ M although polymerization was visible already at 250 μ M. The temporal development of turbidity in the solution was followed at 37°C as shown in **Figure 53a** and the EM image of the MTs formed by TP2 induced tubulin assembly is shown in **Figure 53d**. The role of repeat domain of Tau to promote MT assembly was investigated in the similar manner by using the TR2, TR3 and TR23 peptides. 250 μ M of TR2 (green curve) and 250 μ M TR23 did not support the microtubule assembly. Monitoring the microtubule assembly in

the presence of TR3 (Tau296-321) was not reliable due to the high scattering intensity of 250 μ M TR3 peptide

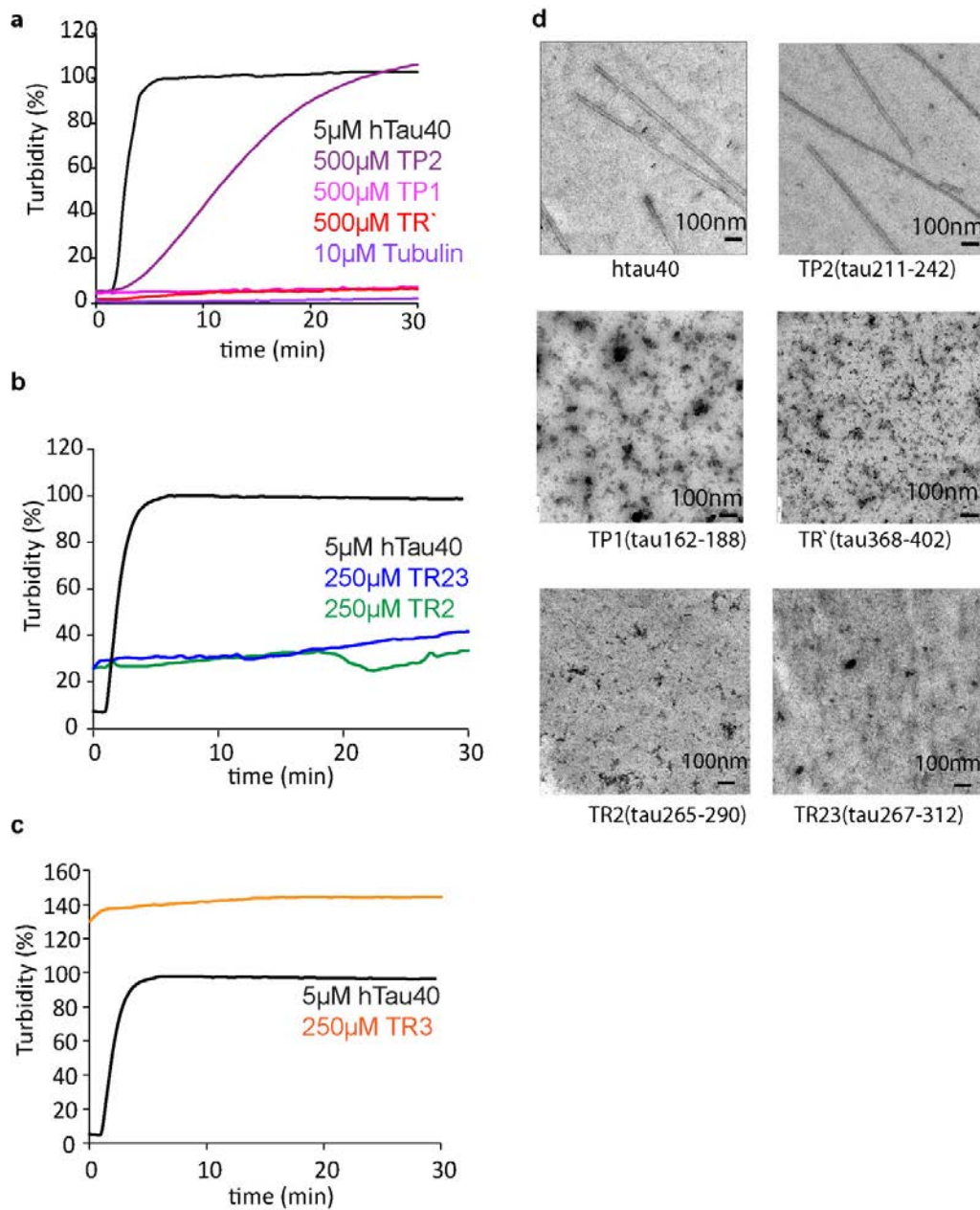


Figure 53: Effect of Tau peptides on microtubule assembly. Light scattering at 350nm was recorded over time to monitor the microtubule assembly in the presence of different Tau peptides. Assembly experiments were performed in the presence of 1 mM GTP at 37°C with a fixed tubulin concentration of 10 μ M. Intensities were normalized to the assembly in the presence of hTau40 (set to 100% in the plateau phase). (a) Tubulin polymerization assay using hTau40, TP1, TP2 and TR' with concentration 5 μ M for hTau40 and 500 μ M each for Tau peptides. (b) 5 μ M hTau40 and 250 μ M each of TR2 and TR23. (c) Monitoring a microtubule assembly in presence of 250 μ M TR3. The high scattering intensity of TR3 in absence of Tubulin causes interference. (d) The EM images of the respective MT assembly assay experiments.

In the absence of tubulin (orange curve), that caused interference in the measurements. 500 μ M Tau peptide TP1 (magenta curve) and 500 μ M TR'(red curve) did not support MT-Assembly. The binding-deficient peptide TR4 (Tau327-353) was used as negative control that didn't support the MT assembly as shown in **Figure 54**(grey curve). Tubulin by itself didn't polymerize (violet curve, **Figure 53a**) since the concentration is below the critical tubulin concentration.

3.7.3.2 Effect of phosphorylation in MT assembly

The polymerization capacity of TP2 with phosphorylation of the residue T231 which is one of the potential biomarkers in AD was checked by using turbidity measurement. The turbidity measurement showed complete abolishment of the MT assembly. The **Figure 54** shows the comparison of the turbidity measurements of both wild type and phosphorylated TP2.

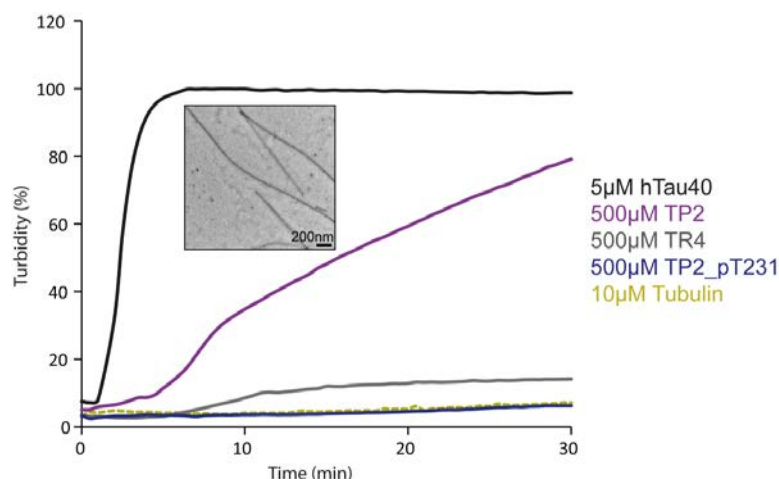


Figure 54: Tubulin polymerization assay using hTau40, Tau peptides TP2, TP2_pT231, TR4 and tubulin itself. Light scattering at 350nm was recorded over time to monitor the microtubule assembly in the presence of different Tau peptides. Tubulin concentration was 10 μ M, Tau concentrations were 5 μ M (hTau40, black) and 500 μ M for the Tau peptides TP2 (Tau211-242, purple), TP2_pT231 (brown) and TR4(Tau327-353, grey). Assembly experiments were performed in the presence of 1 mM GTP at 37°C. Intensities were normalized to the assembly in the presence of hTau40 (set to 100% in the plateau phase). Tubulin alone (dotted lines, yellow), TP2_pT231 and TR4 did not support the microtubule assembly. The EM image of MT assembly by TP2 is shown in the inset.

3.7.4 Independent binding of Tau fragments to the same binding site

The findings on the basis of interaction studies as explained in **section 3.2** with hTau40 and F4 provided the interesting information that the binding of Tau to MTs is mediated by highly localized linear motifs of Tau which are separated by highly flexible linkers. These isolated linear motifs can bind independent of the other binding domains of Tau. In addition to these the competition of hTau40 and Tau peptides for MT binding as reflected from the HSQC spectra (**section 3.7.1**) give further information that TP2 and TR3 have the tendency to bind at one of the potential binding sites of Tau.

3.7.4.1 Inter peptide competition for MT binding

Tr-NOESY based competition experiment was performed using TR2 and TR3 peptides. The NOESY spectrum of 1mM TR3 was acquired at 278K in 50mM sodium phosphate buffer, pH 6.8. The spectrum obtained is shown in **Figure 55 b** in red contours.

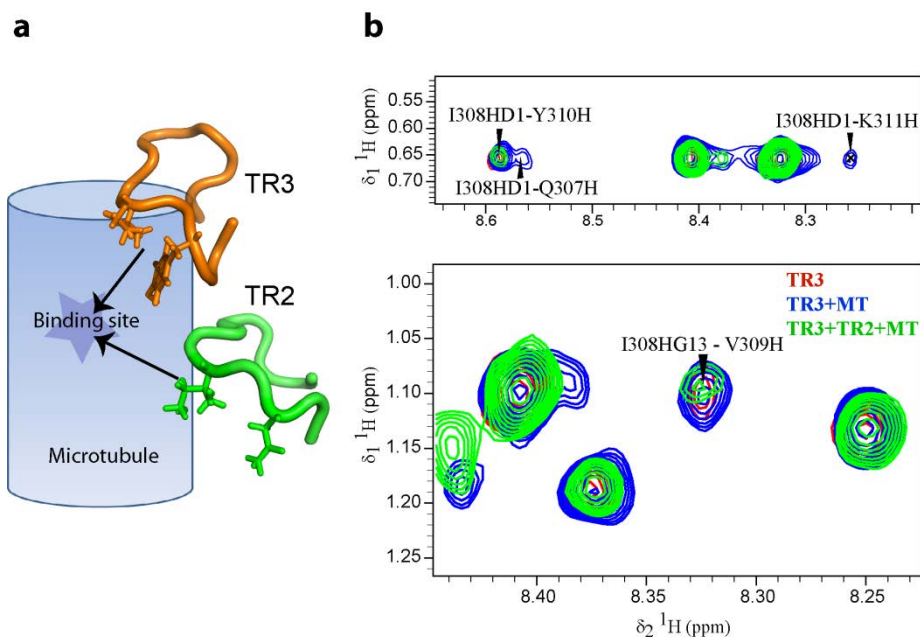


Figure 55: The binding motifs in the repeat region of Tau interact with MTs independently and compete for the same binding site. (a) Cartoon representation of competition between TR2 (green) and TR3 (orange) peptides for MT binding which are targeting the same binding site on MT. (b) Overlay of the regions of tr-NOESY spectra of TR3 peptide alone (red), TR3 with MTs (blue) and TR3 and TR2 together with MTs (green) measured with a mixing time of 150ms at 5°C. The tr-NOESY peaks in the spectra upon interaction of TR3 with MT (blue contours) is diminished after competition with TR2 and selected resonances are labeled.

The addition of MTs into this solution allowed to detect tr-NOESY resonances in the MT-bound state of TR3 as reflected from the appearance of new signals corresponding to the change in conformation after binding as well as enhancement of the signals because of the large rotational correlation time of the complex. The spectrum is shown in blue contours. Upon further addition of TR2 into the same solution reduces the tr-NOESY signal intensities of TR3 as a result of the competition of TR2 and TR3 for a common binding site on MT. The overlay of the three spectra clearly shows the three states of TR3 peptide. The schematic representation of this competition between TR2 and TR3 for MT binding is shown as a cartoon representation in **Figure 55a**.

3.7.4.2 Intrapeptide competition: INPHARMA NOEs

It is also possible to get additional information regarding the competition between the binding domains within the same ligand in a similar approach as described in the previous section (3.7.4.1) using tr-NOESY experiments. If a ligand possesses two domains binding to the same binding site, the intra-ligand protein-mediated NOEs can provide information regarding their spatial configuration. This is the extended concept of INPHARMA approach, where protein-mediated interligand NOEs were detected for pharmacophore mapping.

An attempt to determine the relative spatial arrangement of the linear binding motifs of Tau identified was done using MT-binding peptide TR23. The TR23 peptide that comprises both the binding regions from TR2 and TR3 peptide was allowed to bind to MTs and the tr-NOESY spectrum was measured. The resulting cross peaks after binding with MTs include cross peaks between residues in the two separate binding domains of TR2 and TR3 peptide indicates that these binding domains come closer during binding and indicates the possibility for competitive binding. The cross peaks assigned as intra ligand INPHARMA NOEs are listed in **Table 11**.

Results

Table 11: List of INPHARMA NOEs identified within the tr-NOESY spectrum of MT-bound TR23. R2 and R3 denote the two binding regions in the TR23 peptide, that belongs to the second and third repeats in hTau40.

R2	R3
K267HD2	H299HE2
K267HG3	I297HA
Q269HG2	I308HD1
Q276HB3	Q307HE22
I277HA	Q307HE22
I278HG12	Q307H
I278HG2	Q307H
N279HD22	Q307HB3

R2	R3
N279HB2	Y310HD1
K280HG2	Y310HD1
K281HG3	Y310HE1
Q276HG3	I308HD1
N279HD22	I308HG12
K280HD2	Q307H
K281HD3	Q307HE22

These NOEs were not observed in the absence of MTs and the NOEs primarily involve the two hexapeptides, indicating that they are important for binding to MTs in line with the 3D structures of TR2 and TR3. This way the intraligand transferred NOEs described here provides the experimental basis for the relative orientation of the two binding domains in TR23 peptide during binding with MTs and provide strong experimental evidence that they are in close spatial proximity at a certain time point. These data indicates the presence of a common binding site located on MT/tubulin which is occupied by the Tau binding motifs in an interchangeable manner.

3.8 Identification of binding site of Tau on tubulin/MT

The nature of the binding site of Tau on MTs is still a matter of debate. It has been proposed for example that Tau binds on the outer surface of MTs or it shares the binding site of MT targeting drugs like taxol (Kar, Fan et al. 2003). Different approaches were used to identify the binding site of Tau on MTs. First, on the basis of the hypothesis that Tau-MT binding is mediated by the C-terminus of tubulin (Santarella, Skiniotis et al. 2004, Lefevre, Chernov et al. 2011), we synthesized C-terminal peptides of both α - and β -tubulin and performed NMR titration experiments with full length Tau protein. A significant number of amino acid residues at the C-terminus of tubulin are completely unstructured in the tubulin subunit.

Second, with the availability of different MT binding drugs and information regarding their binding sites, we performed competition experiments between hTau40 and tubulin-targeting drugs using ^1H - ^{15}N HSQC experiments. Later on STD-NMR and tr-NOESY-based competition experiments were performed to verify the findings. Third, and as a complementary method, chemical cross-linking in combination with mass spectrometry was employed to further validate the competition results.

3.8.1 Interaction of Tau with C-terminal peptides of tubulin

The tubulin C-terminal peptides were designed as, α -Tub433-451 and β -Tub424-445. The 2-D ^1H - ^{15}N HSQC spectra were acquired with the C-terminal peptides of tubulin and compared with that of Tau-MT complex. The data show that the C-terminus of tubulin can bind to Tau, when present as an isolated peptide. The chemical shift perturbation profiles from the 2-D ^1H - ^{15}N HSQC spectra were found to be similar to that of the Tau-MT interaction as shown in **Figure 56**. Hence it shows that, similar interaction is present both in the Tau-MT and Tau-aTubC/bTubC binding. It is evident from these results that C-terminal end of tubulin can bind to Tau.

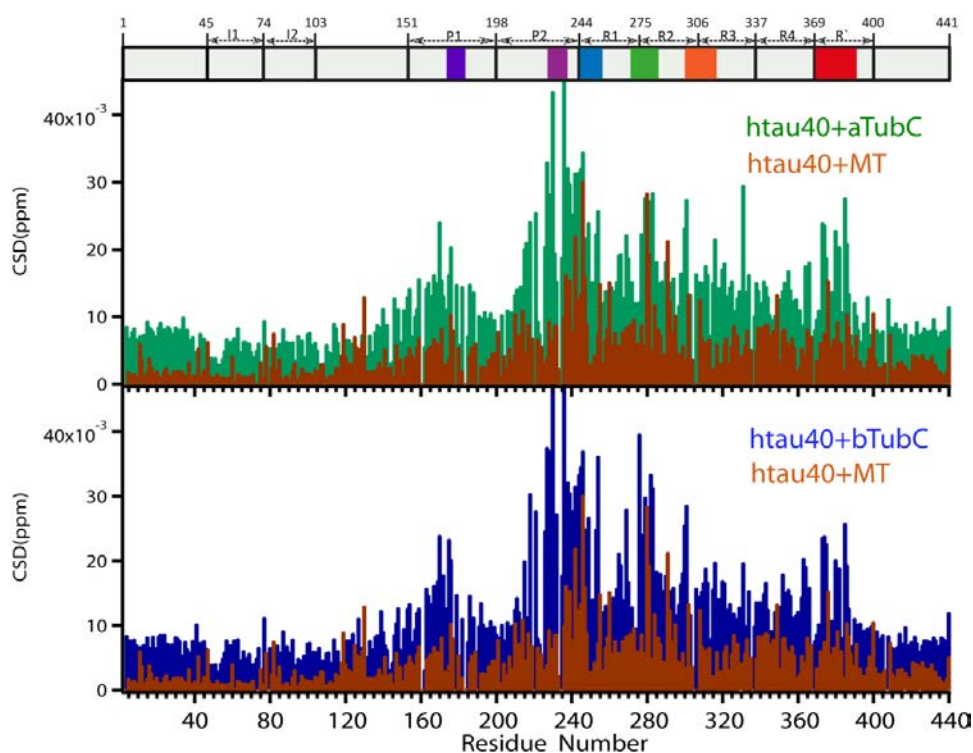


Figure 56: ^1H - ^{15}N combined chemical shift difference observed for the NMR signals in the MT-bound state of Tau (brown) is compared to the profiles of C-terminal peptide of alpha (green) and beta (blue) tubulin.

3.8.2 Competition of Tau with MT drugs for binding

Interpretation of the titration with the C-terminal tubulin peptides is difficult as these are isolated peptides. More solid approach is the use of the MT drugs. The well characterized MT drugs are classified into four different classes on the basis of their stabilizing/destabilizing properties as well as their binding sites. The MT drugs used in our study include Taxol (Paclitaxel), Baccatin, (-)-Thalidomide, Colchicine and Vinblastine. The binding regions of these compounds are highlighted in **Figure 57**. Competition experiments were done by adding the MT drugs into the Tau-MT or Tau-tubulin complex and variation in the signal intensities of 2-D ^1H - ^{15}N HSQC spectra was analysed.

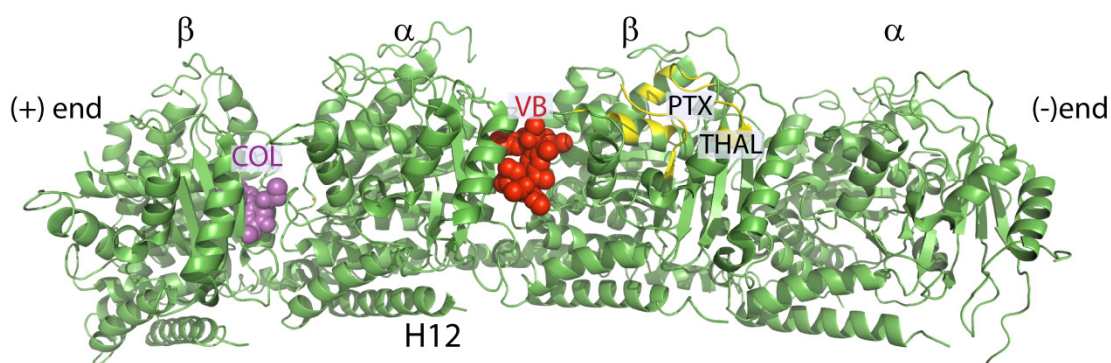


Figure 57: Binding sites of MT drugs. The binding sites of vinblastine (VB), colchicine (COL), taxol (PTX) and thalidomide (THAL) are indicated in the crystallographic structure of T₂R complex consisting of two tubulin heterodimers, vinblastine, colchicine and RB3 protein-stathmin like domain. The bound colchicine and vinblastine are shown using the stick model and a few residues involved in taxol binding are highlighted in pink color near the M-loop. (Figure modified from PDB 1Z2B) (Gigant, Wang et al. 2005).

3.8.2.1 Competition experiment with Vinblastine and hTau40

Vinblastine binds on α -tubulin, in between two tubulin heterodimers and inhibits MT assembly, instead it promotes the tubulin dimers to form curved protofilaments (Gigant, Wang et al. 2005). The possibility for vinblastine and Tau to share the same binding site was explored through competition experiments monitored by 2-D ¹H-¹⁵N HSQC spectra. Vinblastine (VB) was allowed to interfere with Tau for MT binding by titrating it against the Tau-MT complex up to a concentration 20 times higher than Tau. It was observed that the line broadening in the HSQC spectrum of Tau-MT complex is reduced upon addition of VB. The successive addition of vinblastine separated Tau from MTs and led to an ~80% gain in the intensity (**Figure 58a**). Repeating these experiments with unpolymerized tubulin results in the similar observation (section 3.8.2.6). Hence the result supports the possibility for Tau and vinblastine to bind at the same or nearby binding site as the binding is influenced by each other.

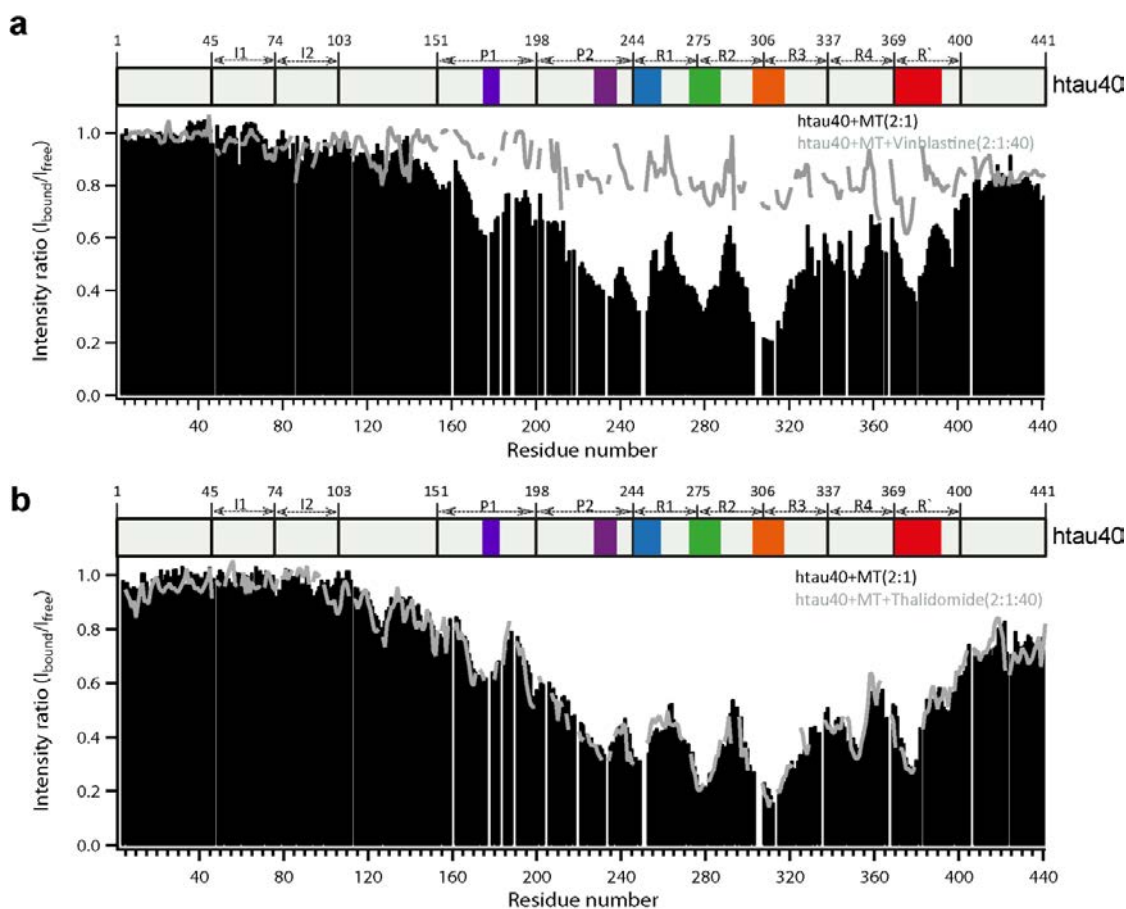


Figure 58: The competition of htau40 and MT drugs vinblastine (a) and Thalidomide (b) are shown as the variation in the intensity ratios observed in the 2-D ^1H - ^{15}N HSQC spectra of MT-bound state. Black bars represent the line broadening of specific residues in hTau40 in the MT-bound state and grey lines shows the residual signal intensity of MT-bound hTau40 in the presence of compounds. The elevation in the intensity after the addition of vinblastine shows competition with hTau40 for MT binding as a result of impairing of hTau40 from MT.

3.8.2.2 Competition experiment with Thalidomide and hTau40

(-)-Thalidomide promotes MT assembly by binding to the side pocket on β -tubulin (Amos 2011), which is accessible from the outer surface of MTs. Addition of thalidomide in to the Tau-MT complex has no influence on the line broadening of hTau40 resonances in the ^1H - ^{15}N HSQC spectra (Figure 58b) and it was concluded that there is no competition between hTau40 and thalidomide for tubulin binding.

3.8.2.3 Competition experiment with Baccatin and hTau40

Baccatin is another taxoid, an alternative for taxol and has higher solubility than taxol in water. Addition of baccatin in variable concentrations upto 20 times excess of hTau40 to the Tau-MT complex has no influence on the line broadening of hTau40 resonances in the ^1H - ^{15}N HSQC spectra as shown in **Figure 59a**. The result again ruled out the possibility of Tau to bind near the M-loop and taken together competition experiments with taxol and baccatin rules out the possibility of Tau to bind at the luminal binding site

3.8.2.4 Competition experiment with Colchicine and hTau40

Colchicine is responsible for the inhibition of MT assembly binding within the heterodimer between α and β -tubulin in a pocket near the non-exchangeable GTP(Nogales, Wolf et al. 1998). Addition of colchicine in variable concentrations upto 20 times excess of hTau40 to the Tau-MT complex has no influence on the line broadening of hTau40 resonances in the ^1H - ^{15}N HSQC spectra (**Figure 59b**). It indicates that Tau-MT interaction is not mediated by colchicine binding site.

3.8.2.5 Competition experiment with Taxol and hTau40 for MT binding

Taxol is one of the MT stabilizing drugs that bind in the luminal pocket (Nogales, Wolf et al. 1998). It has been believed that Tau and other MAPs stabilize MTs by binding at the taxol binding site near the M-loop of β -tubulin(Amos 2004). To verify the previous findings we performed the competition experiment using 2-D ^1H - ^{15}N HSQC experiments where taxol was allowed to interfere with Tau for MT binding. Titrating different fractions of taxol to the Tau-MT complex didn't affect the Tau-MT binding as it was observed in the line broadening profile shown in **Figure 59c**. By increasing the concentration of Taxol, there is no competition with hTau40 as the signal intensities of hTau40 remain unchanged. The experiments using Tau-tubulin complex also provided the same result excluding the possibility of Tau to bind in the M-loop on β -tubulin.

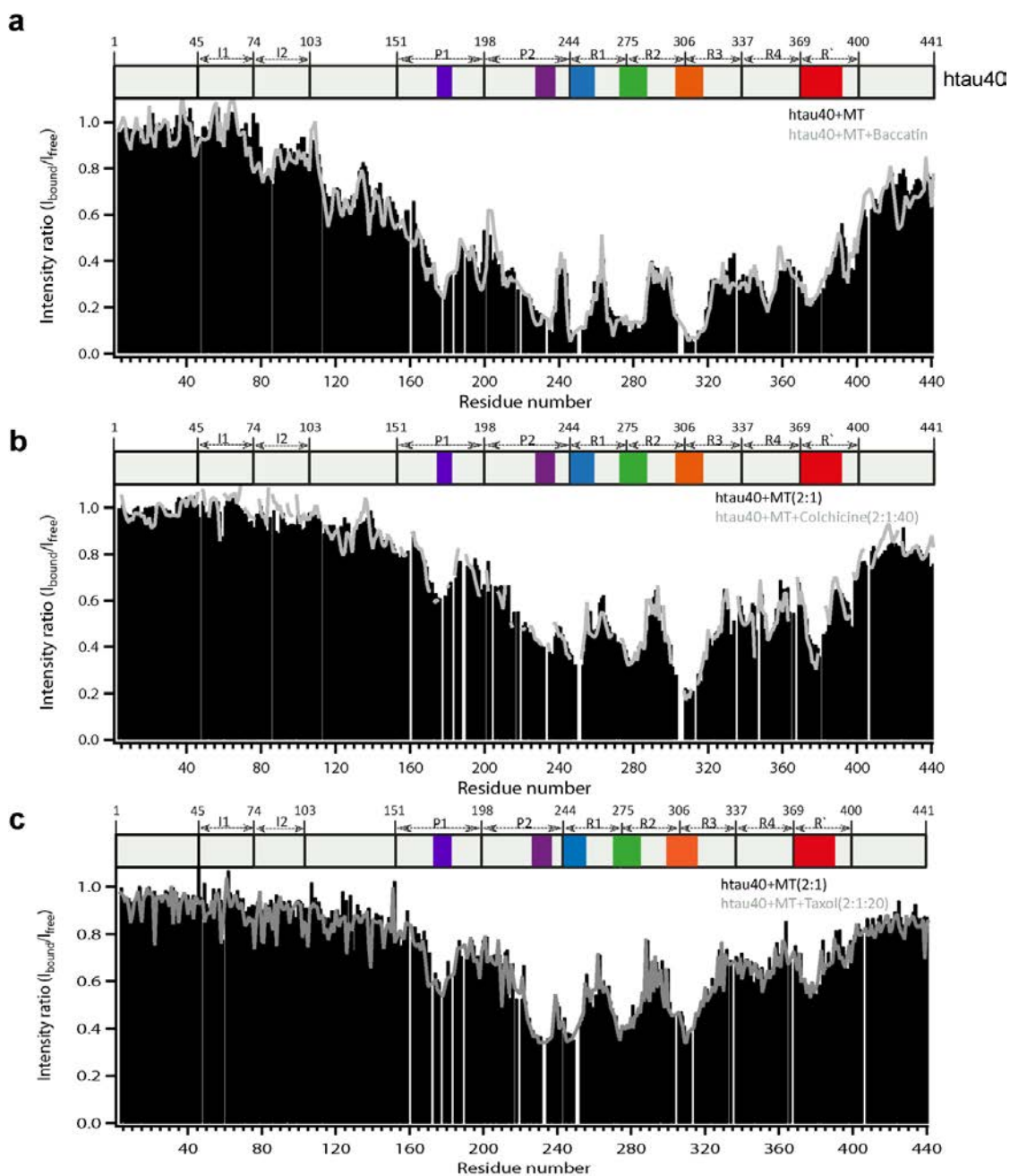


Figure 59: Inertness of Tau to compete with Baccatin, Colchicine and Taxol. No competition is observed as evident from the 2-D ^1H - ^{15}N HSQC spectra of MT-bound hTau40 with Baccatin (a), Colchicine (b) and Taxol (c) for MT-binding. The intensity ratio of MT-bound hTau40 is shown as black bars and grey line shows the residual signal intensity of MT-bound hTau40 in the presence of compounds.

It is evident from the competition experiments using hTau40 and MT drugs that only vinblastine shows clear competition for tubulin/MT binding.

3.8.2.6 Vinblastine compete with hTau40 to bind to tubulin

Repeating the competition experiments between Vinblastine and hTau40 to bind to unpolymerized tubulin resulted in the similar observation found in the presence of MTs (section 3.8.2.1). Hence the result (**Figure 60**) supports the possibility for Tau and vinblastine to bind at the same or nearby binding site as the binding is influenced by each other.

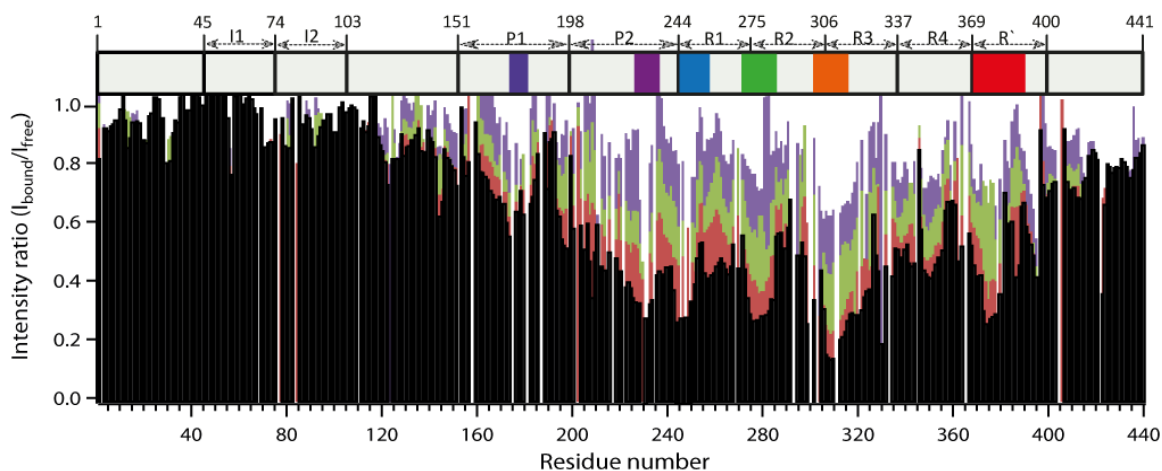


Figure 60: Vinblastine competes with hTau40 for tubulin binding. Variation in the intensity ratios observed in the 2-D ^1H - ^{15}N HSQC spectra of hTau40 in the tubulin-bound state. Black bars represent the line broadening of specific residues in hTau40 in the tubulin-bound state and red, green and purple bars represent the residual signal intensity of tubulin-bound hTau40 in the presence of 5, 10 and 20 fold excess of vinblastine. The elevation in the intensity after the addition of vinblastine shows competition with hTau40 for tubulin binding.

All these data are in line with the presence of a single major binding site for Tau on MTs. At this point the question is where all these Tau domains bind. Initial competitions showed vinblastine compete and showed significant effect. To further investigate the presence of a common binding site for Tau and vinblastine we combined the results from competition experiments and final confirmation by NMR was done with the help of STD NMR experiments.

3.8.3 Competition experiments using STD NMR spectroscopy

In the next step, we used STD-NMR spectroscopy to further characterize the binding properties of peptides. The 1D STD-NMR method was used by saturating the resonances of tubulin at -0.5 ppm corresponding to the methyl protons in tubulin and 60 ppm, far from any proton resonance in the sample, for reference. The saturation of methyl protons in tubulin is first spread via a network of proton-proton dipolar couplings to all the protons of tubulin, then transferred to ligand protons which transiently come spatially close to tubulin through binding. In this way, weak tubulin-ligand binding is detected and ligand protons involved in binding are identified.

3.8.3.1 Competition between Tau peptides and MT drugs: binding to tubulin

The strategy involved in identifying the binding site utilizes the availability of the MT/tubulin targeting drugs and the crystallographic structure of their complex. The peptides used in structure determination of MT-bound Tau were allowed to compete with different compounds for binding. One compound each was selected from the classification of compounds as described before (Amos 2011) for which the binding sites are already known. The prior information obtained from the competition experiments of these compounds against hTau40 for MT/tubulin binding using ^1H - ^{15}N HSQC experiments (section 3.8.2) were expected to be complementary to the STD experiments.

3.8.3.1.1 Competition between Vinblastine (VB) and Tau peptides

The 1D STD NMR experiments were performed for all peptides used for structure determination and were compared with their 1D proton NMR spectra. It was noticed that the spectra clearly indicated the binding and specific residues involved in binding that constituted the structured region of the peptide showed highest STD effects. STD spectra of 1mM solution of TP1, TP2, TR1, TR2, TR3 and TR' in presence of 20 μM tubulin were measured at 298K. The spectra showed clear evidence that each peptide binds to tubulin as expected. The control experiment was done using a non-binding peptide (TN1), the sequence of which constitute the N-terminal region of hTau40. No saturation transfer was observed.

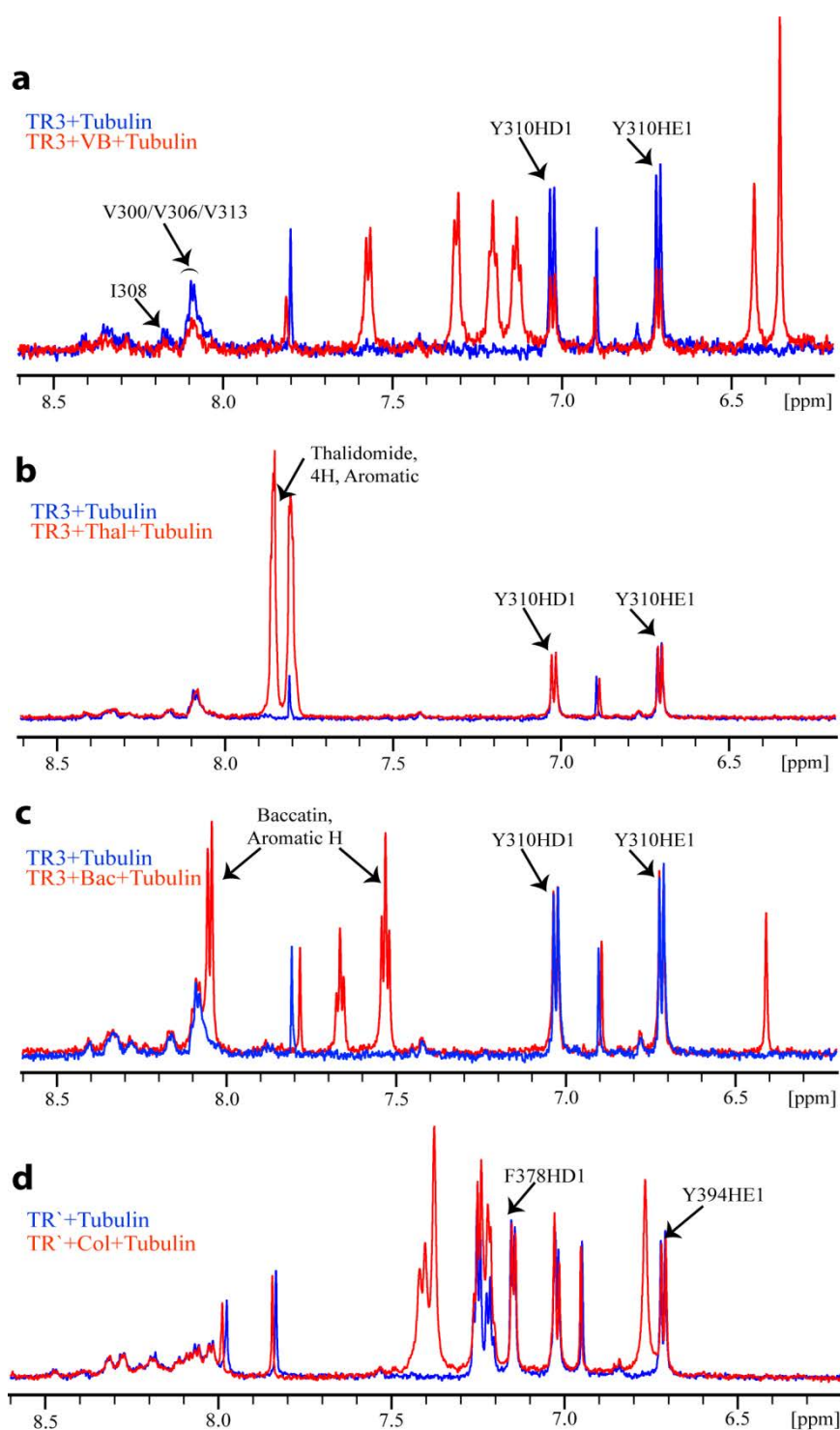


Figure 61: (a-d) Competition between Tau peptides and MT drugs for same binding site tested using STD NMR experiments. All the STD experiments were done with 1mM each of peptide and compound and 20uM of tubulin with selective saturation of the protein resonances at -0.5ppm and at 60 ppm for reference spectra. (a) The one-dimensional STD NMR spectra of the TR3 peptide in the presence of tubulin (blue) and after the addition of vinblastine (red). (b) STD NMR spectra of TR3 with tubulin (blue) and after the addition of thalidomide (red). Aromatic protons of thalidomide affected by the selective saturation of tubulin are labeled. (c) STD NMR spectra of TR3 with tubulin (blue) and after the addition of baccatin (red). (d) 1D-STD NMR spectra of TR' peptide in the presence of tubulin (blue) and after the addition of colchicine (red). The addition of the equal concentration of the competing ligand (VB) to a sample

containing TR3 reduced the signals of TR3 which are characteristic of the tubulin binding as shown in **Figure 61a**. The peaks corresponding to the side chain protons in Y310 residue at 6.7 ppm and 7.05 ppm were analyzed consistently. The resonance intensity reduced by 60% indicating strong competition between TR3 and vinblastine for the same binding site. The result is consistent with the competition of hTau40 and vinblastine for tubulin/MT binding (**Figure 58a** and **Figure 60**).

The STD based competition experiments were performed with all the peptides. Addition of vinblastine reduced the STD intensities of TP1, TP2, TR1, TR2 and TR' by 20, 50, 30, 40 and 40% , respectively. In contrast, the control peptide TN1 did not modulate binding of vinblastine to MTs, as the STD intensity of vinblastine remained unchanged by the addition of TN1 peptide.

3.8.3.1.2 Competition between Thalidomide (Thal) and Tau peptides

To give further evidence that Tau doesn't share the binding site of thalidomide, as observed in the ^1H - ^{15}N HSQC based competition, STD experiments were performed with all the peptides bound to tubulin followed by thalidomide. The data acquired with all the peptides in the tubulin bound state underline that the binding site of Tau is different compared to that of thalidomide. The overlay of the STD spectra of thalidomide and TR3 together with tubulin and of TR3 alone with tubulin is shown in **Figure 61b**.

3.8.3.1.3 Competition between Baccatin (Bac) and Tau peptides

The addition of the equal concentration of the ligand baccatin to a sample containing TR3 with tubulin didn't affect any characteristic tubulin binding resonances of TR3. The peaks corresponding to the side chain protons in Y310 residue at 6.7 ppm and 7.05 ppm were analyzed as shown in **Figure 61c**. The data clearly indicate the independent binding of TR3 and baccatin. Hence the data clearly show both are targeting two entirely different binding site. The result is consistent with the competition experiment of hTau40 and baccatin for MT binding (**Figure 59**).

3.8.3.1.4 Competition between Colchicine (Col) and Tau peptides

The STD experiments were performed with each of the binding peptides and colchicine as it was done in the case of vinblastine. There was no competition observed

as the resonance intensities of peptides remain largely unaffected. The STD NMR spectra of tubulin-bound TR' and TR' and colchicine together with tubulin are overlaid and is shown in **Figure 61d**. The resonances of Y394HE1 at 6.7 ppm and F378HD1 at 7.15 ppm, which is one of the residues in the binding epitope, are labeled and comparison of both spectra clearly shows that there is no competition for tubulin binding.

The STD NMR based competition experiments performed are listed in the **Table 12**. The complete analysis of the STD spectra of all the combinations of peptides and MT drugs can be summarized as shown in the histogram **Figure 62**. It is evident from the graph that only vinblastine is competing with all the Tau binding peptides. Thalidomide and baccatin didn't show competition with any of the Tau peptides at all for tubulin binding.

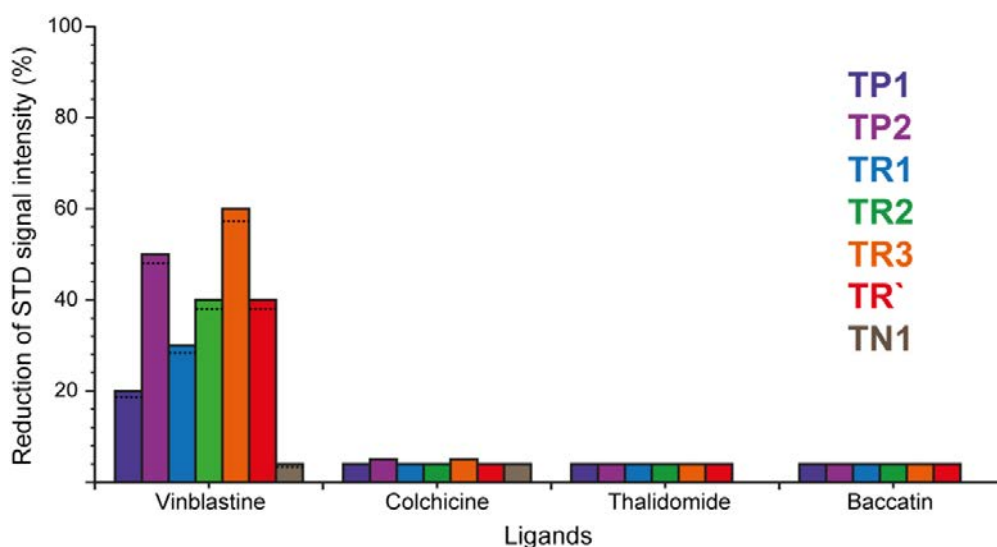


Figure 62: Relative effect of STD signals intensities of different Tau peptides and MT drugs. The reduction in STD NMR signal intensities after competition between peptides and compounds is plotted. - The variation in the 1D STD signal intensities of peptides in the presence of tubulin after the addition of different compounds is presented. The horizontal dotted lines on the bars show the error in comparison of signal intensities. All the STD experiments were performed at 298 K and ligand:tubulin ratio of 40:1. The relative effect of STD signals were determined by taking the intensity reduction of the signal of a residue that forms the binding epitope.

The different degrees of reduction in STD NMR signal intensities suggest different affinities for the peptides, as TR3 and TP2 bind most strongly, followed by TR2 and TR' and relatively weaker affinities for TR1 and TP1.

3.8.3.2 Competition between Tau peptides and MT drugs: binding to MTs

All the above mentioned STD based competition experiments were performed with unpolymerized tubulin. To further validate whether this observation is consistent with MTs, competition experiments were performed using TP2, TR3 and TR' against

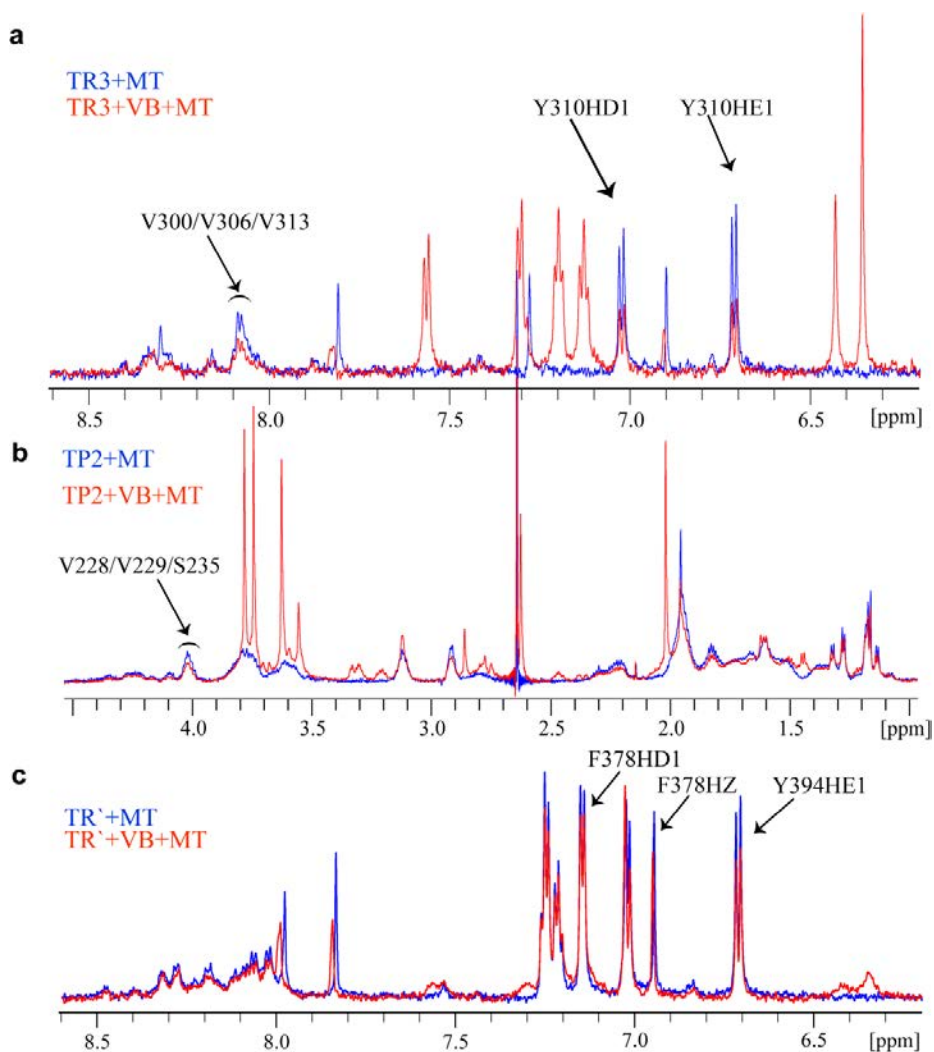


Figure 63: STD NMR spectra of VB and Tau peptides in the presence of MTs. The one-dimensional STD NMR spectra of the Tau peptide in the presence of MT (blue) and after the addition of vinblastine (red) (a-c). Competition between TR3, TP2 and TR' against VB as in a, b and c respectively. Selected protons of peptides affected by the selective saturation of MT and reflect competition with vinblastine are labeled.

vinblastine. It has been found that the data are consistent with that observed in the case of unpolymerized tubulin dimer. The extent of competition was different for each peptide

in comparison to that of tubulin. The STD NMR spectra of TP2, TR3 and TR' are shown in **Figure 63**.

3.8.3.3 Influence of stathmin like peptide I19L

It has been found that the tubulin/MT binding of Tau and Tau fragments are interfered by the presence of vinblastine, one of the inhibitors of MT assembly. To further support for this finding the N-terminal stathmin peptide, I19L, (Clément, Jourdain et al. 2005) was used. The peptide I19L reduces the tubulin polymerization rate to MT protofilaments, instead it leads to a curved conformation of tubulin subunits. The sequence of the Tau peptides from the repeats R2, R3 and R' are aligned with that of the N-terminal sequence of stathmin like domain peptide, which is otherwise called I19L peptide. The sequence alignment is shown in **Figure 64**. The similarities in the sequences suggest the presence of a common binding site for these peptides while binding to tubulin.

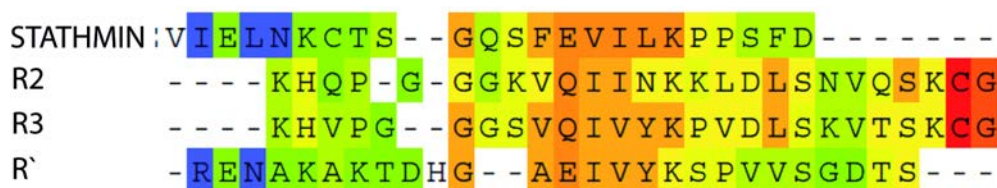


Figure 64: Sequence conservations and divergences of stathmin peptide and Tau repeats. Sequence of stathmin peptide is aligned with the repeats R2, R3 and R' of human Tau.

Stathmin binding site and its binding mode in tubulin was characterized by employing STD and tr-NOESY NMR experiments (Clément, Jourdain et al. 2005). The STD spectrum of I19L in the tubulin bound state revealed the residues which form the binding epitope. The binding site was mapped to be near the helix 10 (H10) of α -tubulin and is in close proximity to the vinblastine binding site. This vinblastine binding site was revealed at high resolution using X-ray crystallography.

We assumed that Tau peptides having the similar sequence to that of I19L may exhibit the similar binding features of stathmin peptide. We performed the competition experiments with Tau fragments and vinblastine against I19L using STD NMR method as explained in the previous sections. It is found that TP2, TR3 and VB compete with I19L for tubulin binding, indicating that they share the same binding site or bind in the

close proximity that the other ligand is affected. The comparison of the STD NMR spectra is shown in **Figure 65**(a-c). Another exciting observation is that the residues in TR2 and TR3 that are most conserved with I19L showed strong STD effects as well as the INPHARMA NOE contacts (**Table 11**).

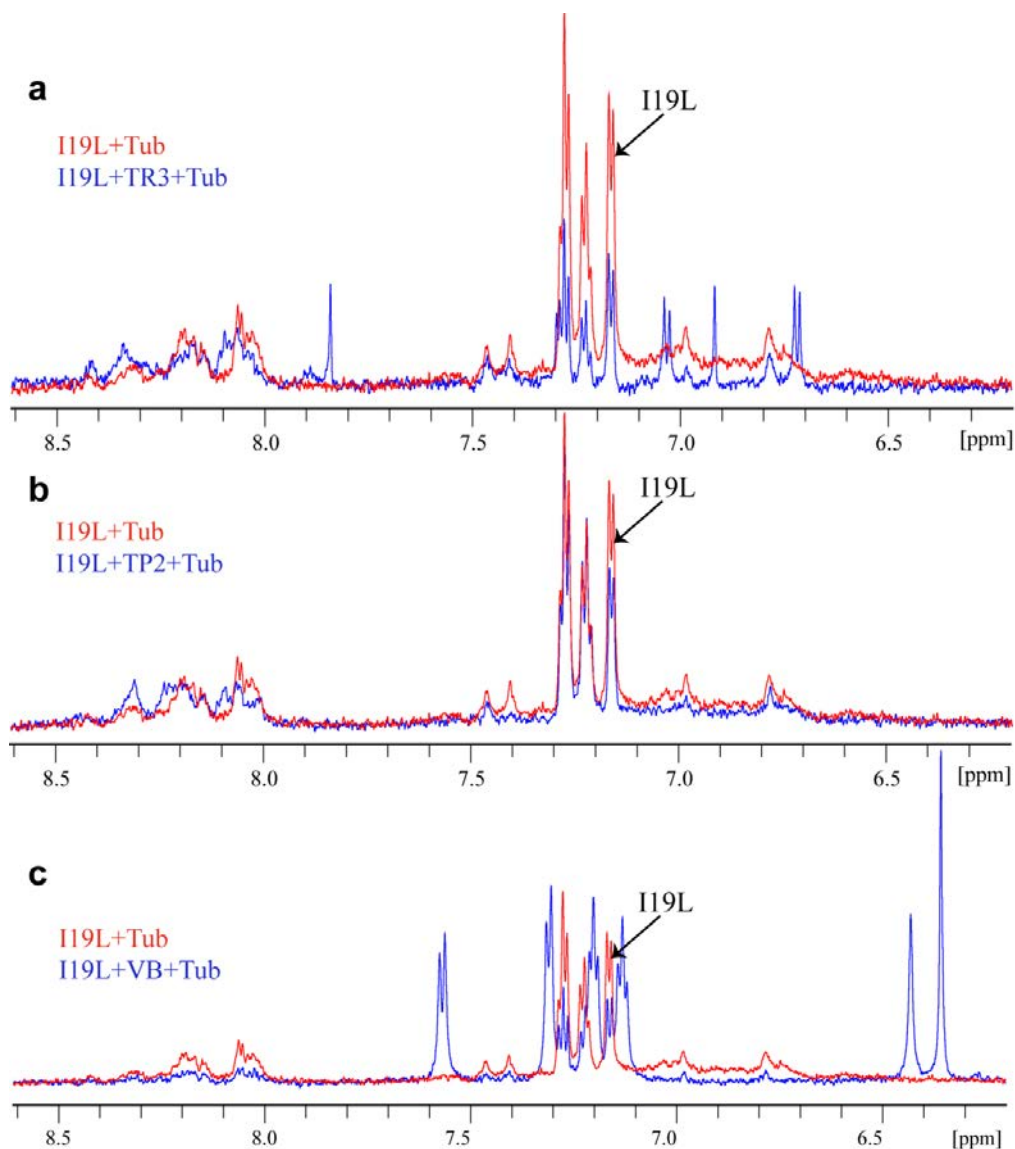


Figure 65: STD NMR competition of TR3, TP2 and VB against I19L. The one-dimensional STD NMR spectra of the I19L in the presence of Tubulin (red) and after the addition of TR3, TP2 and VB (blue) are shown in a, b and c respectively. The Phenylalanine side chain protons are highlighted to show the competition.

Taken together, the competition observed between Tau peptides and I19L indicates all these peptides bind near the vinblastine binding site, which is verified by the competition between I19L and vinblastine. The addition of vinblastine to the I19L-

tubulin complex reduced the STD effect of I19L to 50% (**Figure 65c**). The addition of TR3 and TP2 reduced the I19L STD signal intensity by 60% (**Figure 65a**) and 40% (**Figure 65b**) respectively.

Table 12: Summary of the STD experiments performed between Tau peptides, MT drugs and I19L peptide. Here “nd” refers to the combination is not performed. Tick marks represent the competitive binding between ligands.

Ligands	Vinblastine	Colchicine	Thalidomide	Baccatin	I19L
TP1	✓	X	X	X	✓
TP2	✓	X	X	X	✓
TR1	✓	X	X	X	nd
TR2	✓	X	X	X	✓
TR3	✓	X	X	X	✓
TR'	✓	X	X	X	✓
TN1	X	X	nd	nd	X
Colchicine	X	nd	nd	nd	nd
I19L	✓	nd	nd	nd	nd

3.9 Mass spectrometry

Mass spectrometry based investigation of protein structure and binding interfaces constitutes an increasingly utilized approach in structural biology. The NMR studies with the aid of HSQC and STD-NMR based competition experiments revealed the potentially possible binding site of Tau on MTs. In order to validate the NMR studies we used mass spectrometry as a complementary method to characterize the binding site. Chemical cross linking in combination with mass spectrometry was employed to validate the determined binding sites in collaboration with Prof. Dr. Henning Urlaub (Bioanalytical

Mass Spectrometry, MPIBPC) group and the experiments were performed by Romina Hofele.

3.9.1 Cross linking TauF4/hTau40 to tubulin

TauF4 was cross linked to tubulin which has strong affinity for tubulin/MT binding, with the lysine specific cross linker bis(sulfosuccinimidyl) suberate (BS3). The titration of BS3 with preincubated TauF4-tubulin complex allowed the selection of optimal cross linking conditions, 1:25 ratio of complex:BS3. The cross-linking reaction was performed with increasing molar excesses of BS3, 0, 5, 10, 25, 50, 100, and 200. A 25-fold molar excess showed maximum cross linking yield while avoiding the formation of larger aggregates or extensive band smearing on the gels (**Figure 66**).

The cross linking was performed at room temperature and as revealed by SDS-PAGE, the bands were visible at around 60KDa and 115 KDa represent the desired cross linked F4-tubulin complex in the monomeric and dimeric state respectively. The bands at approximately 60KDa were excised and pooled before in-gel digestion.

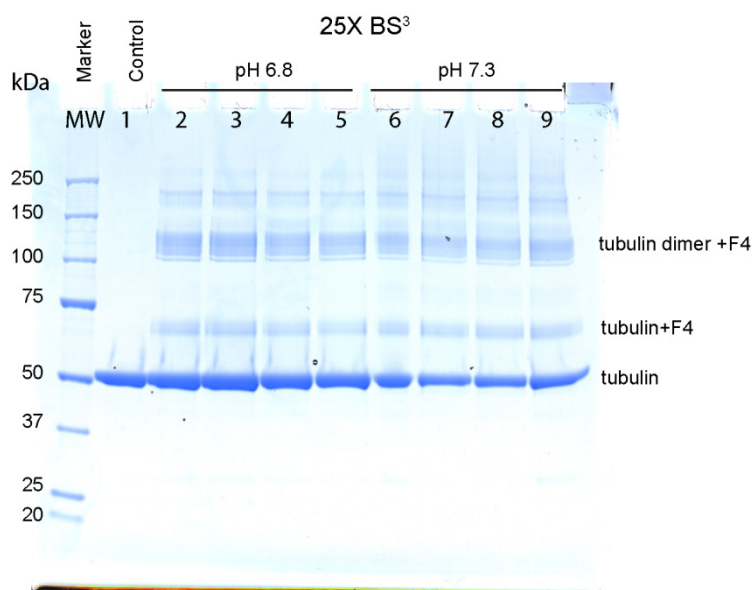


Figure 66: Separation of cross-linked Tau-Tubulin complexes by SDS-PAGE. Samples were preincubated, cross linked and loaded to SDS-PAGE. MW, molecular weight marker; lane 1, non cross linked F4+tubulin; lane 2-5, samples cross-linked using BS3 at pH 6.8; lane 6-9, cross linked F4+tubulin at pH 7.3.

3.9.2 Mass spectrometric analysis of cross linked F4 and tubulin

Cross linked peptide pairs were identified by mass spectrometry. These reflected regions of Tau and tubulin in spatial proximity, as defined by the spacer arm of the cross linking reagent.

Five cross-links were identified between TauF4 and alpha-tubulin and no cross links were identified to beta-tubulin. In addition, one cross link was found between alpha and beta-tubulin. Even if BS3 is highly reactive toward amino groups and lysine residues are abundant in tubulin (19 in α -tubulin and 15 in β -tubulin) the cross linked lysine residues are highly localized and the frequency of the particular cross linked lysine is high. The cross linked residues as identified between F4 and tubulin include K336, K338 and K401 in α -tubulin and K240, K257 and K311 in TauF4 as shown in **Table 13**.

Table 13: Interprotein cross-links identified between TauF4 and tubulin (1:1)

Protein 1	Protein 2	Peptide 1	Peptide 2	Residue 1	Residue 2
α -tubulin	TauF4	DVNAAIATIKTK	SPSSAKSR	K336	K240
α -tubulin	TauF4	DVNAAIATIKTK	NVKSK	K336	K257
α -tubulin	TauF4	LDHKFDLMYAKR	SPSSAKSR	K401	K240
α -tubulin	TauF4	TKR	HVPGGGSVQIVYKPV DLSK	K338	K311
α -tubulin	TauF4	TKR	SPSSAKSR	K338	K240

The cross linking of TauF4 with tubulin was repeated by varying the stoichiometry of the complex. At an excess concentration of tubulin in the ratio 1:3 an additional cross link was identified between K336 in α -tubulin to K225 in TauF4. The cross links identified are listed in **Table 14**.

Table 14: Interprotein cross-links identified between TauF4 and tubulin (1:3)

Protein 1	Protein 2	Peptide 1	Peptide 2	Residue 1	Residue 2
α -tubulin	TauF4	DVNAAIATIKTK	SPSSAKSR	K336	K240
α -tubulin	TauF4	DVNAAIATIKTK	KVAVVR	K336	K225
α -tubulin	TauF4	TKR	HVPGGGSVQIVYKPV DLSK	K338	K311
α -tubulin	TauF4	TKR	SPSSAKSR	K338	K240

Next, the interaction of full length Tau (hTau40) and tubulin was investigated with cross linking and mass spectrometry. The cross linked residues identified were K336 and K338 in α -tubulin and K225, K240, K257 and K383 in hTau40. K383 is present only in hTau40 as the TauF4 construct is comprised of residues Tau208-324. It is

Results

an important observation that the additional cross link identified in hTau40, K383, falls in the pseudo repeat of Tau, which constitutes another important cross linking hot spot identified. **Table 15** shows the cross linked peptides and residues identified between α -tubulin and hTau40.

Table 15: Interprotein cross-links identified between hTau40 and tubulin (1:1)

Protein 1	Protein 2	Peptide 1	Peptide 2	Residue 1	Residue 2
α -tubulin	HTau40	DVNAAIATIKTK	SPSSAKSR	K336	K240
α -tubulin	HTau40	DVNAAIATIKTK	KVAVVR	K336	K225
α -tubulin	HTau40	DVNAAIATIKTK	NVKSK	K336	K257
α -tubulin	HTau40	TKR	SPSSAKSR	K338	K240
α -tubulin	HTau40	DVNAAIATIKTK	ENAKAK	K336	K383

Finally hTau40 was allowed to cross link with MTs. Pre-assembled MTs and hTau40 were incubated to form the complex and was cross linked as in the case of hTau40 and tubulin. The cross linked Tau-MT complex was further heated at 90°C for 20 minutes to depolymerize MTs. The cross linked Tau-MT complex was analyzed by mass the identified cross links reflected a similar cross linking pattern to the previous experiments of Tau-tubulin cross linking, where residues within the P2 and R1 region of Tau cross link to the K336 and K338 residues in alpha tubulin. The cross links identified between Tau and MTs are summarized in **Table 16**.

Table 16: Interprotein cross-links identified between hTau40 and microtubules (1:1)

Protein 1	Protein 2	Peptide 1	Peptide 2	Residue 1	Residue 2
α -tubulin	HTau40	DVNAAIATIKTK	KVAVVR	K336	K225
α -tubulin	HTau40	DVNAAIATIKTK	NVKSK	K336	K257
α -tubulin	HTau40	TKR	SPSSAKSR	K338	K240

It is noteworthy that only a few residues in Tau and tubulin are consistently involved in inter protein Tau-tubulin/MT cross linking even if there are numerous lysine residues in both Tau and tubulin. Among the 34 lysine residues present altogether in the α - and β -tubulin dimer, the cross linked residues are K336, K338 and K401. K401 was identified only once in the case of F4 and hence predominantly K336 and K338 of α -tubulin were cross linked. Combining the results from F4 and hTau40, it can be concluded that only a few lysine residues within the MT binding domain of Tau are involved in the cross links identified. In addition to these inter protein cross links, there

Results

were intra protein cross links identified between the lysine residues within Tau and tubulin.

The cross links identified between Tau and tubulin/MT can be summarized as a cross linking map (**Figure 67**).

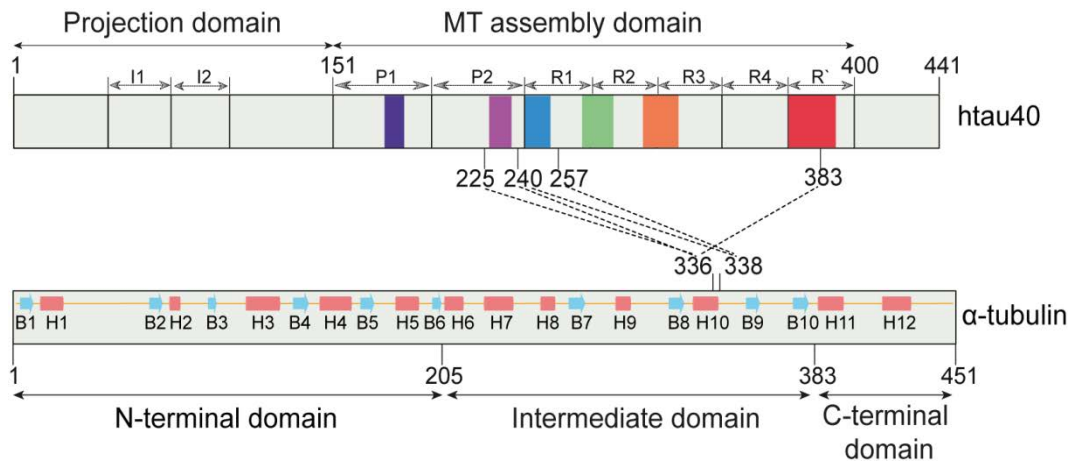


Figure 67: Protein-Protein cross linking map of the Tau-Tubulin/MT complex. Chemical Cross-linking between Tau and tubulin/MT is represented in the domain organization diagram of Tau and tubulin. The residues involved in cross linking of Tau and tubulin/MT are connected by dotted lines. The colour code in the Tau domain corresponds to the structured region of the Tau peptides. The secondary structure elements in tubulin are indicated by arrows and cylinders and labelled.

4 Discussion

4.1 Towards the structure of MT-bound Tau

The current study addresses three biological questions on MT-bound Tau, employing NMR as the major investigation method and supporting the findings with complementary biophysical studies. 1) Initially the Tau-microtubule interaction was characterized; extending the attempt to identify the binding hot spots involved in interaction. Though the Tau-MT interaction has been studied for a long time, the detailed mechanism involved in interaction and the structure of MT-bound Tau was not yet established. 2) The identification of the amino acid residues involved in binding and the characteristic features of the binding hot spots allowed the structure determination of MT-bound Tau. This shed insights into the correlation between structure of MT-bound Tau and neurodegenerative Tauopathies. 3) Finally NMR-based competition experiments provided insight into the binding region of Tau on MTs and the obtained information was complemented by chemical cross-linking and mass spectrometry studies.

4.2 Interaction of Tau with microtubules

Microtubules play a crucial role in a number of cellular processes such as cell division, intracellular transport and axonal stability (Weisenberg 1972, Hirokawa and Takemura 2005). MTs are highly dynamic in nature and the dynamic structure is regulated by a number of factors where microtubule-associated proteins (MAPs) play significant roles (Hirokawa 1994). These MAPs include both stabilizing and

destabilizing proteins. Tau has been given significant attention due to the large dependence of MT regulation in the human brain on Tau and other MAPs. The dysregulations of the Tau-MT interaction such as hyperphosphorylation lead to several neurodegenerative diseases (Gong, Liu et al. 2005, Gong, Liu et al. 2006). Different techniques and approaches have been employed in the investigation of Tau-MT interaction. NMR has been recently used to gain new insights into the mechanism of Tau-MT binding, especially as NMR is capable of providing information at atomic resolution (Mukrasch, von Bergen et al. 2007, Mukrasch, Bibow et al. 2009, Landrieu, Leroy et al. 2010, Bibow, Mukrasch et al. 2011, Fauquant, Redeker et al. 2011). As the structure and function of proteins are related to each other, it is important to understand in detail the mechanism of interaction involved. Identifying the interacting region of those proteins and their binding interface is of primary importance. Therefore, studies on this interaction provide highly-detailed structural information which can reveal the structure-function relationship acting in Tauopathies and other Tau-related neurodegenerative diseases.

In previous studies, the Tau-MT/tubulin complex formation and interaction were characterized using different biophysical techniques such as analytical ultracentrifugation (AUC), isothermal titration calorimetry (ITC) (Tsvetkov, Makarov et al. 2012) or fluorescence resonance energy transfer (FRET) (Jeganathan, Hascher et al. 2008). ITC provided insights into the mode of interaction of Tau and tubulin at different temperature and it proposed that the mode of interaction is independent of the type of the polymer formed (Tsvetkov, Makarov et al. 2012). FRET was used to quantify the Tau-tubulin interaction and to calculate the stoichiometry. AUC was used to characterize the oligomerization state of tubulin. Still, structural information at the atomic level was missing. For example, X-ray crystallography which is traditionally employed in protein structure determination could not give structural information of disordered proteins as those proteins do not crystallize easily. Previous NMR studies using tubulin and other MAPs (Kotani, Kawai et al. 1990, Reed, Hull et al. 1992) showed that it is possible to utilize the strength of NMR to extend the investigation from short fragments to full-length protein. The interaction mechanism involved in tubulin binding was characterized using transferred NOE and identified the involvement of hydrophobic residues critical for binding (Kotani, Kawai et al. 1990). This strategy was followed in different Tau

fragments to achieve the complete backbone assignment of full-length Tau protein (Smet, Leroy et al. 2004, Mukrasch, Biernat et al. 2005, Mukrasch, von Bergen et al. 2007, Sillen, Barbier et al. 2007, Mukrasch, Bibow et al. 2009, Narayanan, Dürr et al. 2010). Here we performed a detailed investigation to establish the complex structure of MT-bound Tau.

4.2.1 Tau-MT interaction studies revealed the highly localized binding hot spots of Tau

In spite of the very high molecular weight of the Tau-MT complex, it was possible to demonstrate the mode of interaction between Tau and MTs. The initial studies shows the feasibility to work with such high molecular weight systems like Tau-MT complex and gather information regarding the binding residues involved (Mukrasch, Bibow et al. 2009). The binding of hTau40 to taxol-stabilized MTs was characterized in different conditions using the 2D ^1H - ^{15}N HSQC experiments (section 3.2.1) and provided results consistent with previous results where the data was acquired at 20°C (Mukrasch, Bibow et al. 2009). The line broadening observed in the spectrum of MT-bound hTau40 (**Figure 14**) due to the chemical exchange between the bound and free Tau molecules shows the region of Tau involved in direct binding. A highly remarkable observation is that a few continuous stretches of amino acids showed line broadening and are separated by highly flexible linkers (**Figure 15**).

4.2.1.1 Similar binding mode is present in both 3R and 4R Tau isoforms

The differential regulation of both 3R and 4R Tau isoforms were investigated with respect to different aspects (section 1.4). Among the isoforms of Tau, both 3R and 4R Tau bind directly to microtubules, stimulate microtubule polymerization, and regulate microtubule dynamics (Trinczek, Biernat et al. 1995). Several studies compared the efficiency of different isoforms to regulate MT dynamics and assembly by varying the relative concentration of Tau and tubulin. Those studies found that at low Tau: tubulin ratio 4R Tau is more potent than 3R Tau (Drechsel, Hyman et al. 1992, Panda, Goode et al. 1995, Trinczek, Biernat et al. 1995, Goode, Chau et al. 2000) whereas at high Tau:tubulin ratio both 3R and 4R Tau show nearly similar activity (Levy, LeBoeuf et al.

2005). To investigate the isoform specific nature of binding of both 3R and 4R Tau isoforms, the interaction of hTau23 and hTau40 with MTs was compared (section 3.2.2) and the line broadening profiles of both isoforms (**Figure 17**) revealed that similar residues are involved in binding. The experiments performed by varying the Tau: MT ratios showed a similar effect. This suggests that a similar binding mode is involved in both isoforms. The discrepancy in the binding efficiency between isoforms could be due to the difference in the number of repeats in the isoforms as the binding affinity is largely dependent on the number of binding domains (Butner and Kirschner 1991). The broadening in repeat 3 of both isoforms is highly similar (**Figure 17**) indicating the relevance of the residues between P306-D314 for MT binding. The highly similar binding profile of hTau40 and htau23 shows the feature of Tau to possess highly localized binding domains.

4.2.1.2 Tau:MT interaction is monophasic

It was previously reported that at very high concentrations, Tau molecules might aggregate on top of each other similar to paired helical filament formation. It was proposed that the interaction is biphasic: 1) the initial phase involves strong interaction binding of Tau on the MT surface; 2) in the second phase, excess Tau molecules are accumulating on top of each other in a non-saturable binding mode (Ackmann, Wiech et al. 2000). On the basis of this hypothesis, the authors proposed a model where the paired helical filament aggregation of Tau is initiated on the microtubule surface by inducing an early conformational change.

To study the effect of overloading of MTs at elevated Tau concentration, the Tau-MT interaction was investigated in different Tau:MT ratios (**Figure 19**). The NMR measurements showed that similar regions of the spectra are affected by the interaction with MTs, though a few residues beyond the MT binding region show additional broadening at higher MT concentration. This is attributed to the fast relaxation (short T_2) associated with the large size of the Tau-MT complex as more Tau molecules are in the bound state at higher MT concentration. The resonances of residues in the N-terminal projection domain remained largely unaffected. The previous biphasic binding mode and accumulation of Tau on the MT surface with different binding mode is not supported by

our findings. Hence it is expected to have similar interaction mode at all Tau:MT concentration ratios suggesting that the interaction is monophasic.

4.2.1.3 Tau interacts with tubulin and MTs in the similar manner

Tau binds to tubulin and promotes MT assembly. In order to address whether the potential binding modes of Tau with tubulin during MT assembly and with stabilized MTs are different or not, the interaction of hTau40 with unpolymerized tubulin was probed. The results showed that similar residue stretches of Tau are involved in binding with tubulin and MTs (**Figure 22**). Hence it can be generalized that binding of Tau to tubulin/MT involves similar interaction mechanisms for the two situations. We highlight here that there are different opinions on using taxol-stabilized microtubules and Tau assembled microtubules to study the interaction (Kar, Fan et al. 2003). Particularly, the experimental evidence is being questioned depending on the type of MTs used in a particular study. Here we claim that when using taxol-stabilized MTs and Tau assembled MTs, Tau and MTs will interact in the similar manner as the Tau-tubulin interaction is identical to that with taxol-stabilized MTs.

In contrast, the type of sample employed is relevant when comparing the MT binding properties of other microtubule associated proteins (MAP) like doublecortin (DCX), which is a microtubule stabilizing MAP. It was shown before that purified DCX has no effect on the growth rate of microtubules although it is a potent microtubule stabilizing agent which binds in between protofilaments and counteracts their outward bending in depolymerizing microtubules (Moores, Perderiset et al. 2006). Probably DCX is highly selective to stabilize MTs without interacting with tubulin to promote MT assembly.

4.2.1.4 Tau-MT interaction is mediated by both charged and hydrophobic residues

The role of both electrostatic and hydrophobic interactions that together contribute to MT binding has been previously discussed. The hypothesis is similar in the case of other MAPs as reported for MAP-tubulin interaction (Kotani, Kawai et al. 1990). The information obtained from the large dependence on the ionic strength of Tau-MT interaction (**Figure 21**) is consistent with the observation reported before for the K32-MT interaction (Mukrasch, von Bergen et al. 2007). The residues affected by MT

binding were found to be broad at low salt concentration, which further confirmed the specific residues identified as part of the binding region.

The assumptions and arguments behind this electrostatic interaction model (Serrano, Avila et al. 1984, Serrano, Delatorre et al. 1984) propose charge neutralization during the binding event. The acidic C-terminal tail of tubulin should be neutralized by the basic residues of Tau or other MAPs. In the current context, the positively charged residues of Tau are believed to fulfill this requirement. This kind of charge neutralization followed by tubulin polymerization can be considered as the first stage in MT assembly. Still, the role of the hydrophobic interaction can be considered important in the second phase of the binding that stabilizes the MT interaction. It is to be noticed that the tightest binding is observed for the amino acids Val, Ile, and Tyr in the active binding sites. Hence, specific mechanisms involving both the electrostatic and hydrophobic interactions are proposed. It was proposed that the hydrophobic part in the side chains of Lys and Arg can also play the roles of Val, Leu and Ile (Kotani, Kawai et al. 1990).

With these results, it can be concluded that the Tau-MT interaction is mediated through the binding of highly localized linear motifs which are separated by highly flexible amino acid linkers. This observation is consistent in all the experiments described under the section 3.2 as indicated by the colour codes in the domain organization diagrams. Thus we could identify the potential binding hot spots of Tau involved in MT binding. It was broadly divided into an acidic N-terminal 'Projection domain' (M1-Y197) and a C-terminal 'assembly domain' (S198- L441) based on limited proteolysis and microtubule binding ability (Gustke et al., 1994). Together with the identification of the binding hot spots, the Tau domains can be reorganized as N-terminal projection domain (1-160), MT binding and assembly domain (161-400) and C-terminal domain (400-441).

4.2.1.5 Site specific mutation and pseudophosphorylation lead to local alteration in MT binding

To understand the features of the Tau-MT interaction where the localized amino acid stretches contribute to binding as a combination of both electrostatic and hydrophobic interaction, the single residue mutant (Y310N) in repeat 3 of hTau40 was used. Although Y310 sits in the core region of the binding hot spot in R3, this specific

residue mutation only slightly affected the binding of hTau40 (**Figure 24**). The line broadening of only the nearby residues decreased slightly showing that this effect is highly localized in that particular binding domain.

Furthermore, this specific binding feature was investigated using phosphorylation, as it is known that the site specific phosphorylation affects microtubule binding (Stoothoff and Johnson 2005, Mi and Johnson 2006). Pseudophosphorylation of Tau was used as it decreases its affinity for microtubules, and pseudohyperphosphorylated forms of Tau do not have significantly decreased levels of microtubule binding as compared to single and double sites (Sun and Gamblin 2009, Sibille, Huvent et al. 2011). The pseudophosphorylation of hTau40 at the sites which form epitopes for the Alzheimer's diagnostic antibodies AT8, AT100 and PHF1 (Jeganathan, Hascher et al. 2008) also revealed that the Tau-MT binding is highly localized in different binding domains (**Figure 25**). Only the residues near the E-mutation sites impaired binding from MTs, without having any effect on other binding regions of Tau. In summary, no considerable long-range effect in the other binding hot spots was observed, showing the independent nature of the different linear motifs of Tau which are involved in Tau-MT interaction. This result is published recently as a part of the phosphorylation study of Tau using MARK-2 kinase (Schwalbe, Biernat et al. 2013).

4.2.1.6 Confirmation of the binding hot spots using Tau constructs

The use of [²H, ¹⁵N]-labeled K18 Tau in complex with tubulin gave further insight in terms of the core binding region of Tau. The amino acid residues in the repeats R1, R2 and R3 were broadened significantly even though a deuterated protein was used. However, the repeat R4 was largely flexible as reflected from the intensity of the resonances (**Figure 26**).

A new fragment of Tau, F4, comprising residues S208-S324 of the Tau sequence was designed by Fauquant et al. F4 has a very high affinity for MT binding (Fauquant, Redeker et al. 2011). The MT assembly assay of hTau40 and F4 was compared using turbidity measurements (**Figure 23**). The comparatively lower efficiency of F4 for MT assembly may be due to the lack of pseudo repeat R' and the part of proline rich region P1. In the present study, it has been found that F4 shows very high affinity for MT binding as evidenced from the overall reduction in the signal intensities at low Tau:MT

ratios and disappearance of all resonances at high F4:MT/tubulin ratios (section 3.4.2). The F4-MT interaction was further probed by varying the ionic strength. The residues which showed broadening in the NMR spectra were visible after the addition of salt. Although most of the residues regained their initial intensities, those which fall in the binding hot spots (section 3.2) experienced line broadening. This indicates very strong binding of F4 to MTs. Additionally, there was no temperature dependence in the binding mode.

This strong binding affinity of F4 with MTs and tubulin raised the question whether detection of MT-bound F4 is possible or not. An attempt to get information from the bound residues prompted us to perform the CRINEPT-HMQC-TROSY (Riek, Wider et al. 1999, Riek, Pervushin et al. 2000, Riek, Fiaux et al. 2002) experiments, which allow the NMR detection of high molecular weight systems above 150 kDa. To minimize the relaxation-induced line broadening, deuterated ^{15}N labeled F4 was used. The spectra of tubulin-bound F4 showed only a part of the resonances which lie in the flexible linkers of Tau after binding (**Figure 31a**). The similar observation found in the case of MT-bound F4 confirmed the highly localized and independent nature of the linear motifs of Tau in MT binding. In the case of MT-bound F4, these flexible residues in-between the binding hot spots were visible only in the CRINEPT-HMQC-TROSY spectrum (**Figure 31c**) but not in the TROSY experiments. This is due to the large number of protons in tubulin that makes the relaxation faster, resulting in broadening of resonances from the bound residues. This again supported the large size of the complex formed between F4 and MTs as well as the advantage of using CRINEPT-based polarization transfer for NMR experiments of large systems. The bound residues were beyond detection even after employing the CRINEPT element is associated with the sample conditions where the deuteration of the protein was about 60% as well as fully protonated tubulin. Perdeuterated protein might give better results together with the deuterated receptors, which is not possible in the case of tubulin until now. With these findings, it is concluded that Tau possesses highly localized binding regions which are separated by highly flexible linkers.

4.3 Insights into the structure of MT-bound Tau

One of the major functions of Tau is to bind and stabilize MTs and promote tubulin assembly (Weingarten, Lockwood et al. 1975). The results described in sections 3.2 and 3.4 provide evidence for the active participation of Tau in binding with MTs. As Tau is intrinsically disordered in its free form in solution, an important research aim is to understand the mechanism involved in MT stabilization. However, structural information is necessary for a detailed understanding of this mechanism. For instance, we are interested to know how Tau favours MT assembly, and what its physiological roles are during phosphorylation. Extracting structural information directly from the Tau-MT complex, which has a size on the order of MDa, is challenging due to the size limitation of NMR. Whether NMR will be able to provide structural information on how Tau binds on MTs is a key question. It was shown before that even using protein deuteration, spectra are beyond detection (Fauquant, Redeker et al. 2011). Alternatively, for systems having different and distinct binding domains where a dynamic complex is formed and the binding sites are independent, a divide and conquer approach may be applied.

The data discussed under sections (3.2 and 3.4) allowed us to identify highly localized binding hot spots of Tau which are important for binding and promoting tubulin assembly. It is known from previous studies that the individual Tau repeats and shorter Tau domains can bind, stabilize and promote MT assembly (Lee, Cowan et al. 1988, Aizawa and Murofushi 1989, Ennulat, Liem et al. 1989, Himmler, Drechsel et al. 1989, Joly, Flynn et al. 1989, Joly and Purich 1990). Together with other biophysical data, our experiments with different isoforms of Tau and other Tau fragments F4 and K18 indicates that the binding hot spots identified are highly independent in nature. Based on these findings, it is possible to apply a “divide and conquer strategy” to determine the structure of MT-bound Tau. We used short synthetic Tau peptides and determined their structure in the MT-bound state. The obtained structures were finally integrated into the complex structure of full length Tau bound to MTs.

If the ligand is weakly bound and there exists fast exchange between free and bound forms of the ligands, detailed structural and dynamic information can be obtained by employing transferred NOEs and STD measurements (section 2.6). As the binding affinity of shorter Tau peptides are found to be in the micromolar to millimolar range

(Butner and Kirschner 1991, Gustke, Trinczek et al. 1994), the exchange between free and MT-bound peptides is expected to be fast enough on the NMR time scale to use the transferred NOE method

Tau peptides selected for structure determination (section 3.5.1) were able to bind to tubulin/MT as evidenced from the STD NMR spectra (section 3.6). STD stands as a complementary method to identify the binding events of ligands to its receptor. Further confirmation of the specificity in the binding of Tau peptides clearly appears when comparing the tr-NOESY spectra of TR3 and TR4, where TR4 is not expected to bind to MTs. The tr-NOESY spectrum of TR3 peptide acquired in the presence of MTs showed a number of intense cross-peaks in comparison to the spectrum acquired in the absence of MTs. This indicates that the additional peaks in the MT-bound state of TR3 are originating as a result of binding and that the interaction induces a change in conformation (**Figure 35a**). On the contrary, tr-NOE cross-peaks were not visible for TR4 in the presence of MTs (**Figure 35b**). The basic principle of the tr-NOESY experiment relies on the fast dissociation rate of the ligand between its bound and free forms. The cross relaxation between the protons in the peptide in the MT-bound state is governed by the large rotational correlation time of the complex and is transferred back to the peptide in the free state during chemical exchange. As a consequence, additional NOE cross peaks are observed in the bound state reflecting the change in conformation of the peptide. Prior to the structure calculation of all the peptides, the assignment of all the resonances in the NOESY spectrum of all the peptides was done as described (section 3.5.2).

4.3.1 Characteristic structural features of the MT-bound Tau peptides

Although Tau is unstructured in the free form in solution, with the NOESY peaks consisting of mostly intra-residue or sequential NOEs, interaction with MTs brings additional medium range or long range NOEs that define the structure that is involved in the change in conformation needed for MT-binding. It is noticed that most of the additional tr-NOE cross-peaks are observed between the residues which belongs to the linear motif identified from interaction studies. This reveals the limited side chain

motions of these residues as a result of binding with MTs. The most striking observation is the presence of many medium and long-range tr-NOE cross-peaks within the residues which are identified as the binding epitope. The STD NMR spectrum obtained in the presence of tubulin and MT further proved the involvement of the residues belonging to the structured region, as STD is a measure of the interaction of a ligand with its receptor.

There is no regular secondary structure such as an α -helix or a β -sheet in the overall fold. Instead, there is a well-defined turn/hairpin conformation which is defined by the binding residues. In addition, the DLSK turn near the C-terminus of TR3, which is transiently populated in monomeric Tau in solution (Mukrasch, Markwick et al. 2007), was found to be stabilized in the MT bound state. It is to be noticed that most of the medium and long range NOEs observed are within the Val-300-Asp314 residues stretch of TR3. One of the key features observed is the presence of long range NOEs from P-301 to I-308, V-309, and V313. The side chains of these residues stabilize the turn conformation adopted by TR3 in the presence of MTs (**Figure 37c**). Notably, the side chains of several hydrophobic residues are pointing outwards, supporting the importance of these residues for binding to MTs.

For, TR2 a smaller number of medium and long range NOEs compared to TR3 were detected, probably due to the difference in their binding affinities. Remarkable NOEs in the tr-NOESY spectrum include the long range NOEs from Q269 and P270 to I278, K280, K281 and D283 which defines the structure of TR2.

The comparison of the structures of TR2 and TR3 shows the involvement of the two hexapeptides (VQIVYK in TR3 and VQIINK in TR2) in the MT binding. These hexapeptides are the core regions involved in the paired helical filament (PHF) formation of Tau that leads to Tau aggregation and intracellular deposits (Eckermann, Mocanu et al. 2007). These regions adopt a beta-sheet structure in the PHFs (von Bergen, Barghorn et al. 2005, Mukrasch, Bibow et al. 2009, Daebel, Chinnathambi et al. 2012). In contrast, there is no beta-sheet content in the MT-bound state other than the well-defined turn conformation of TR2 and TR3. It can be hypothesized that the disruption of the Tau binding from the MT surface leads to the loss of the identified structure of TR2 and TR3 in the pathological conditions.

To demonstrate that the structure obtained for the MT-bound linear motifs is retained in a longer Tau construct, the structure of the TR23 peptide, which covers both TR2 and TR3, was studied. The two structured regions in TR23 were compared to the structure of the short individual peptides TR2 and TR3 (**Figure 49**). From this comparison, it is evident that the structures of TR2 and TR3 are conserved in TR23. Thus, the results validate the hypothesis that the structure obtained for shorter Tau fragment peptides is the same as for MT-bound Tau.

The effective binding of TR1 is evident from the presence of 36 medium range and 8 long range NOEs. The obtained structure (**Figure 41**) highlights the important residues involved in MT binding. The residues T245, V248, M250 and D252 holds their side chains in such a spatial configuration that effective binding with MTs is possible while keeping the medium and long range contacts defining the structure. The three proline residues within this structured part play a significant role in the stabilization of the identified structure.

The TR' peptide possesses a well-defined structure in the MT-bound state (**Figure 47**), which is an integral part of MT binding forming one of the 'jaws' for MT binding. The structure is defined by a significant number of medium and long-range NOEs with L376, F378, I392 and Y394 as key residues involved in binding. Notably, the region of TR' that is well-structured in the MT-bound state has already an increased rigidity according to ^{15}N $R_{1\rho}$ measurements in monomeric Tau prior to binding to MTs (Mukrasch, Bibow et al. 2009). The structure of TP1 is moderately defined in specific regions with a well-defined turn between residues T169-T175. The consecutive proline residues in the sequence increase the flexibility of the structure.

The structure of MT-bound TP2 is defined by 45 medium-range and 6 long-range NOEs and showed high degree of convergence within the regions K224-V228 and V228-P236. The structured part of the peptide (**Figure 43**) constitutes a turn from V228 up to P236. Figure 27 shows the number of NOEs present in the well-structured region. Within This structured part attracted significant attention since the phosphorylation of residues T231 and S235 was found to reduce the MT binding and polymerization abilities of Tau. The relevance of this turn conformation can be explained on the basis of the MT binding and assembly observed for TP2. MT-bound TP2 showed significant number of tr-NOEs

whereas TP2 with phosphorylated T231 showed a strong decrease in binding as reflected from the tr-NOESY data (section 3.17). In addition, the phosphorylated peptide showed complete abolishment of MT assembly (section 4.4), providing a mechanistic explanation for the pathogenic consequences of T231 phosphorylation.

The transferred NOE intensities are a measure of the extent of interaction with the receptor. In this context, the intensities of side chain cross-peaks are higher for residues in the structured region compared to terminal residues. Taken together, the structures of all peptides in the MT-bound state possess a similar turn conformation which is especially remarkable in the highly-structured region. The sequences of TR2, TR3 and TR' share many identical and homologous residues as well. Although the superposition of all the structures exhibit slightly different backbone conformations, a high degree of similarities in the side chain orientations that might enhance the interaction is observed. This indicates that all the Tau peptides possess a similar binding pattern in line with a common binding site.

4.4 Tau peptides resemble full-length Tau in their function

The investigation of structure of MT-bound Tau is performed using shorter Tau fragments. This was supported by the previous findings that short Tau repeats and synthetic Tau peptides can promote MT assembly (Aizawa, Kawasaki et al. 1988, Aizawa, Kawasaki et al. 1989, Aizawa and Murofushi 1989, Ennulat, Liem et al. 1989). As the Tau-MT complex is highly dynamic and depends on well-defined linear motifs connected by flexible linkers, the 3D structures of MT-bound Tau peptides form the basis for the structure of full length Tau in complex with MTs.

4.4.1 Tau peptides compete with hTau40 for MT binding

In the current scenario the question is whether these short peptides used here behave in the same way as a full length Tau protein interacts with MTs? To address this question we investigated the MT binding ability of Tau peptides by allowing them to compete with hTau40. The competition experiments described in section 3.16

demonstrated the ability of short peptides to compete with hTau40 for Mt binding. Both TP2 and TR3 compete for binding as observed in the line broadening profiles of HSQC spectrum of MT-bound hTau40 (**Figure 50**). The reduction in line broadening is due to the interaction of TP2 and TR3 with MTs that attenuates binding of full length Tau to MTs. As a control TN1 from the N-terminus of Tau didn't compete with htau40.

It is to be highlighted here that a short peptide, either from proline rich region (PRR) or from the repeat region, from the Tau sequence can compete with full length Tau protein impair it from MTs independent of the binding domain. This is evident from the overall gain in intensity across the Tau sequence. This suggests the possibility for the independent binding domains to bind at a single binding site.

4.4.2 Linear motifs in Tau cooperate in tubulin binding and polymerization

It has been shown that Tau peptides bind to MTs as full length Tau protein and compete for binding. The ability of the individual Tau peptides to bind and promote MT assembly is therefore a key question. The tubulin polymerization assay of all Tau peptides were compared to that of hTau40 and only TP2 was found to be active in polymerization at concentrations of 250 μ M and above (**Figure 54**). In contrast, TR2, TP1, TR' and TR23 were found to be inactive in the concentration range up to 750 μ M. TR3 due to the high scattering intensity – likely due to partial aggregation – caused interference in the measurement in the absence of tubulin itself and hence the experiment with it was not reliable. The data demonstrate that the linear motifs in the repeat region, in particular the hexapeptide motif in repeat R2, strongly bind to MTs, but are not sufficient for MT assembly. MT polymerization requires the linear motif in the proline-rich region P2.

The polymerization assay of these peptides was compared with that of hTau40 and F4, where hTau40 was more potent for MT assembly (**Figure 23**). The high concentration of TP2 needed can be correlated to the absence of other repeat domains. In short in spite of the inactivity of repeat domains in MT assembly they cooperatively coordinate MT assembly. These results are consistent with the polymerization assay

observed in the peptides from the sequence of mouse Tau (Ennulat, Liem et al. 1989) where only the proline rich region showed MT assembly properties and a random analog of the same peptide as well as peptide from the repeat domain didn't promote tubulin assembly even at 800 μ M concentration.

4.4.2.1 Influence of T231 phosphorylation on TP2 in MT assembly

Being a potent tubulin polymerizing peptide the effect of phosphorylation of T231 residue on TP2 was investigated and the turbidity measurement of TP2_pT231 clearly indicates the complete abolishment of MT assembly. The results of tubulin polymerization assay is consistent with that of phosphorylated TauF4 reported (Sibille, Huvent et al. 2011) where the residues T231, S235, T212 and T217 were phosphorylated. The phosphorylation in the PRR was found to be stabilizing a short α -helix starting from pS235 upto T245 (Sibille, Huvent et al. 2011). The loss of MT polymerizing ability of T231 phosphorylated TP2_pT231 can be due to the deficiency in the positive charge of this peptide as a result of the introduction of a phosphate group and thereby having less interaction with tubulin.

4.4.3 Phosphorylation and mutation of specific residues reduces MT binding

4.4.3.1 Influence of T231 phosphorylation on TP2 reduced its MT affinity

The effect of site specific phosphorylation and mutation of these peptides in the MT binding was tested using the tr-NOESY experiments. The wild type TP2 and TR3 interacts with MTs showing a number of tr-NOE cross peaks (**section 3.7**). Phosphorylation of T231 residue, which is a biomarker in Alzheimer disease (Hoffmann, Lee et al. 1997), significantly reduced their MT binding affinity. It is clear from **Figure 51** that there are no transferred NOE peaks resulting from interaction of TP2_pT231 with MTs.

This is consistent with the abolishment of this peptide to promote MT assembly. The absence of tr-NOE peaks compared to the wt TP2 can be attributed to the specific conformation of MT-bound TP2. Irrespective of the highly flexible nature of free TP2, it adopts a defined structure upon binding to MTs (**section 3.11**). The turn conformation

between V228-P236 is disrupted by the phosphorylation of T231 and the MT binding is disrupted. Another possibility is the possible salt bridge formation between the side chain of R230 and the phosphate group. The two consecutive proline residues after T231 might undergo cis-trans isomerization and thereby losing the NOE contacts within the structured region of TP2. This leads to reduced microtubule polymerization and binding thereby cause Alzheimer's symptoms. A similar cis-trans isomerization model of proline residues and impact on AD was proposed in a study using phosphorylated Tau peptide (Daly, Hoffmann et al. 2000). Hence it is to be concluded that the phosphorylation not only bring negative charge near the Tau binding domain but also it induces conformational changes that cannot support MT binding.

4.4.3.2 P301S mutation in TR3 disrupts MT binding

The effect of mutations linked to neurodegenerative diseases were studied using P301S variant of TR3 peptide through tr-NOESY experiments. In comparison with *wt*-TR3, very weak cross peaks were found in the spectra of TR3_ P301S (**Figure 52**). This observation can be linked to the specific conformation of MT-bound TR3. The structure of MT-bound TR3 is defined by many medium and long range NOEs involving P301 and has many long range contacts with the residues labeled (**Figure 68**). Due to the mutation of P301 to Serine these NOE contacts are disrupted that leads to the loss of defined structure impairing from MT surface. This might be the reason for their reduced rate of MT assembly and binding. In fact different clinical phenotypes are found to be originated from a single mutation of P301S (Bugiani, Murrell et al. 1999).

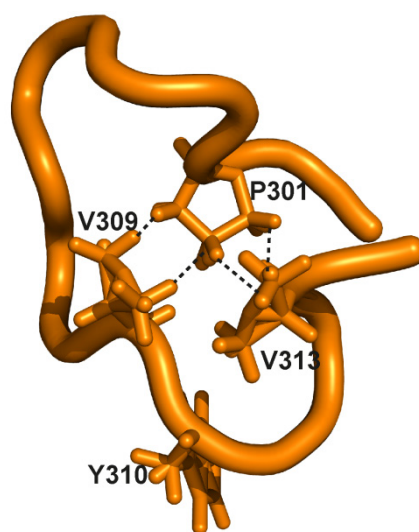


Figure 68: Representation of the structured region of TR3 peptide that shows the long-range contacts of P301 to the V309 and V313. Side chains of selected residues which stabilize the structure are highlighted.

Together, the data corresponding to the T231 phosphorylation and P301S and P301L amino acid substitutions proposes a loss-of-function model in which the peptides shows diminished ability to properly regulate microtubule dynamics.

Deletion mutation of the residue K280 from the Tau sequence is found to be one of the hallmarks in certain neurodegenerative diseases. The mechanism involved in binding is highly dependent on the specific conformation adopted by Tau in the MT-bound state. It has been shown previously that the PHF formation of wild type hTau40 and hTau40_ΔK280 are influenced by this single residue deletion mutation. Unlike this observation the MT binding properties of Tau is not strongly affected by this deletion mutation as it is evident from the tr-NOESY spectrum of TR23_ΔK280 (**Supplementary figure 1**). This could be due to the presence of the R3 region that can bind together with the R2 region of TR23. Or even the K281 plays the role of K280 to keep the long range contact within the structured region. This observation again supports the independent binding feature of Tau.

4.4.4 Independent Tau domains target the same binding site on MT

The Tau peptides compete with hTau40 for MT binding and relatively overall effect over the broadening profile indicate one binding peptide can deplete off all the independent binding domains of hTau40 suggesting the presence of a common binding site (section 4.4.1). To further verify this observation the tr-NOESY based competition was performed using TR3 and TR2 peptides. Addition of TR2 into the same solution reduces the tr-NOESY signal intensities of TR3 as a result of the competition of TR2 and TR3 for a common binding site on MT (**Figure 55**). The tr-NOE competition between peptides TR2 and TR3 shows the diminishing effect of NOE cross peak intensity of the initially bound peptide.

These evidences that an individual Tau peptide can compete with another one as well as hTau40 were further supported by intra ligand competition, where the two binding domains within the same peptide ligand were found to be competing for the identical or nearest binding sites. We have seen Tau possess distinct binding domains separated by flexible linkers. To verify the competition between these domains within the same protein, the tr-NOESY spectrum of TR23 was analyzed. There are intra ligand INPHARMA NOE (**section 2.6.1.3**) cross peaks between residues in the two separate binding domains of TR2 and TR3 peptides indicating that these domains come closer during binding. These two binding domains within the same peptide act as two distinct ligands targeting MT receptor. It can be visualized as at a certain time point TR2 binds at the preferred binding region and later TR3 approaches MT for binding. This can be attributed to the presence of a common binding site for these two binding domains TR2 and TR3 or they are approaching for the two nearby binding sites on MT.

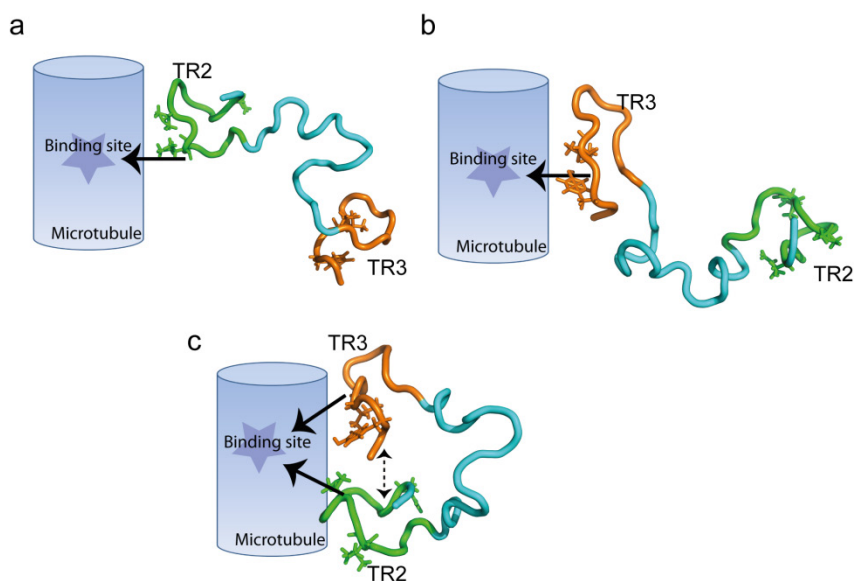


Figure 69: Intraligand competition of Tau domains for MT binding. Representation of the observation of INPHARMA NOEs. Individual Tau domains are binding with MTs (a) only TR2 and (b) only TR3. (c) At a certain time point both the domains are close to each other targeting the same binding site. This results in the observation of intraligand INPHARMA NOEs.

Thus consistent with all the competition experiments described in the previous section our findings give strong evidence for the highly independent binding domains which target to a single binding site on MTs.

4.5 Variety of competition experiments revealed the binding site of Tau on MTs

Till now we were able to describe the binding residues of Tau involved in MT binding and the structure adopted by MT-bound Tau. It is highly important to identify the binding interface that will shed further insights to the mechanism involved in Tau-MT interaction and thereby open new approaches for the treatment of neurodegenerative Tauopathies. Previous studies concluded that Tau binds either to the outer surface of MTs directly at the negatively charged C-terminus of tubulin (Ackmann, Wiech et al. 2000, Al-Bassam, Ozer et al. 2002, Santarella, Skiniotis et al. 2004, Clement, Savarin et al. 2010). Another widely discussed binding site is the taxol binding site on beta tubulin near the M-loop (Amos 2004) or positively charged proline rich region binds at the negatively charged C-terminus. There are further models proposing the presence of two

distinct binding sites, where Tau binds both inside and outside of MTs (Chau, Radeke et al. 1998, Makrides, Massie et al. 2004). High resolution metal shadowing and cryo electron microscopy provided information regarding the binding region of Tau on MTs, which is largely localized on the outer surface of MTs (Santarella, Skiniotis et al. 2004). Using gold nanolabelling strategy Kar *et al.* demonstrated that Tau binds on β -tubulin near the taxol binding site (Kar, Fan et al. 2003).

Different binding regions and binding models proposed till now raises the question, which of the models can be biologically relevant? Different biophysical methods employed in the previous investigations and controversial findings make it rather difficult to assign a specific binding site for Tau on tubulin/MT.

4.5.1 NMR approaches identified the potential binding site

Our Tau-MT/tubulin interaction studies showed clear evidence that the different binding domains bind independent of each other. To confirm whether all these binding hot spots or active sites bind at a single binding pocket or not and also to see where does it bind different competition experiments were performed. The attempt to obtain further insight into the tubulin binding site of the Tau binding domains a combination of methods were used.

4.5.1.1 Tau-MT interaction involves interaction with C-terminal domain of tubulin

The titration of hTau40 with the C-terminal peptides of tubulin (**section 3.20.1**) suggests that the positively charged MT binding region of Tau can transiently interact with the negatively charged C-terminus of tubulin. The similarities in the chemical shift profiles with that of hTau40 in presence of MTs (**Figure 16, Figure 56**) underline the affected regions with this interaction. By using recombinant alpha and beta-tubulin C-terminal fragments, the involvement of both of these tubulin regions in Tau binding had been suggested previously (Devred, Barbier et al. 2004, Lefevre, Chernov et al. 2011). The data suggest that neutralization of the electrostatic field generated by the negatively charged C-terminus of tubulin is required for MT-assembly, in line with the observation

that removal of the C-terminus of tubulin by subtilisin promotes MT-assembly (Serrano, Avila et al. 1984).

4.5.1.2 MT targeting drug Vinblastine and hTau40 compete for binding

We further used different tubulin drugs with known binding sites (**Figure 57**), which are classified into different categories based on their activities and functions (**section 1.3.6**). These compounds were allowed to compete with hTau40 or Tau peptides for binding with MT/Tubulin. Initially we performed the competition experiments of full length Tau with MT targeting drugs such as Taxol, Baccatin, Thalidomide, Colchicine and Vinblastine (**section 3.20.2**).

Titration of each MT drug was carried out in increasing amounts of concentrations to a solution of ^{15}N -labeled hTau40 bound to MTs and the variation in the NMR signal line broadening caused by MT interaction in specific regions of Tau was observed. None of the compounds other than Vinblastine was found to be competing with Tau for MT binding (**Figure 58 and Figure 59**). The decrease in NMR line broadening is as a result of the impairing of Tau-MT complex as Vinblastine depletes Tau off from tubulin/MT binding pocket and more Tau becomes free in solution. Hence line broadening is less compared to the isolated Tau-MT complex. The competition experiments were performed with unpolymerized tubulin in the similar manner using Vinblastine, Taxol and Thalidomide, where only Vinblastine showed tendency to compete with Tau (**Figure 60**).

Taxol, Baccatin, Colchicine and Thalidomide were found to be inert to compete with Tau for tubulin/MT binding. The fact that Vinblastine competes with Tau bound to MT as well as tubulin shows the mutual dependence of Tau and Vinblastine for binding at a single binding site on MT.

4.5.1.3 STD NMR method revealed the potential binding site of Tau on MTs

To further verify the competition observed between Tau and vinblastine 1D STD NMR based competition experiments were performed with all the peptides used in the structural investigation. The STD spectra of each peptide bound to tubulin indicated the specific residues involved in binding, which are part of the structured region of these peptides in the MT-bound state (**section 3.6**). Moreover the residues that constituted the structured region of the peptide showed highest STD effects showing their contact with

tubulin. All the peptides were allowed to compete with the compounds and the STD NMR based competition experiments performed are listed in the **Table 9**. The complete analysis of the STD spectra of all the combinations of peptides and MT drugs shows that only vinblastine is competing with the Tau binding peptides (**Figure 61**) and the relative effect is different for different peptides (**Figure 62**) and this suggests that TR3 and TP2 are having highest affinity for MT/tubulin binding. The similar observation was found when vinblastine was competing with MT-bound Tau peptides. The variation in intensities of different resonances in the spectrum is different depending on the residues which are nearby tubulin. This is possible only if the ligands are coming in the close proximity to share the same binding site. The extent of competition is found to be prominent between TR3 peptide and vinblastine where the STD signal intensities of TR3 is reduced by 60%, where the Y310 aromatic side chain proton intensities were compared in the presence and absence of MT drugs. This strongly supports the competition between hTau40 and Vinblastine for MT/tubulin binding (**Figure 61 and Figure 63**). Till now it is evident that Tau and vinblastine target the same binding site or their binding is mutually dependent.

4.5.1.4 I19L peptide from the N-terminal stathmin like domain compete with Tau peptides

The conflict in these findings is the competition between MT stabilizing and destabilizing agents. Tau as a MT stabilizing agent is found to be competing with vinblastine for binding either to tubulin or MTs. The characteristic feature of vinblastine as a MT destabilizing agent is it induces the formation of spiral tubulin aggregates (Weisenberg and Timasheff 1970, Himes 1991) whereas Tau promotes the formation of straight protofilaments. To further support the possibility for Tau to share the vinblastine binding site, the I19L peptide belongs to the N-terminal part of the stathmin like domain (Clément, Jourdain et al. 2005) was allowed to compete with Tau peptides. The reason behind this is that I19L was shown to be binding on α -tubulin at the longitudinal tubulin interdimer interface between the helix 10 (H10) and β -strand S9 of the crystal structure determined for tubulin-colchicine/RB3-SLD crystal (Clément, Jourdain et al. 2005). This is very close to the vinblastine binding site which also binds on α -tubulin at the tubulin interdimer interface. The STD based competition experiments revealed that Tau peptides compete with I19L as observed in the case of Vinblastine (**Figure 65a** and

b). Finally Vinblastine showed competitive binding with I19L (**Figure 65c**). It is to be noticed that the repeat domains of hTau40 have sequence identities and similarities (**Figure 64**) and hence the competition observed between I19L and Tau fragments is in line with the sequence similarity.

It is highly important that Vinblastine being a MT destabilizing agent compete with MT stabilizing protein Tau. It was shown that the negative regulator of MT dynamics shows competition with the stabilizing agents. A similar observation was found while characterizing the binding site of antimetabolic drug Tubulysin, a microtubule destabilizing agent, it shared the binding site of Etoposide, which is a microtubule stabilizing agent (Kubicek, Grimm et al.).

4.5.2 Chemical cross-linking and Mass spectrometry validated the binding site

Chemical cross linking in combination with mass spectrometry was employed to validate the identified binding site (section 3.22). The NMR competition experiments showed that the Tau interaction motifs bind to the vinblastine-binding domain on α -tubulin in between two heterodimers. Our mass spectrometric studies further showed that the amine directed cross-linking of Tau to tubulin/MT is highly specific to the side chains of K336 and K338 of α -tubulin. These residues are in the close proximity to the vinblastine binding site (Gigant, Wang et al. 2005) where the residues P325, V328, I332, F351, V353 and I 355 are important for vinblastine binding.

It is noteworthy that only a few residues in Tau and tubulin are consistently involved in inter protein Tau-tubulin/MT cross linking though there are numerous lysine residues in both Tau and tubulin. Among the 34 lysine residues present altogether in the α - and β -tubulin dimer, the cross linked residues are K336, K338 and K401. K401 was identified only once in the case of F4-tubulin cross linking and hence predominantly K336 and K338 of α -tubulin were cross linked. Combining the results from F4 and hTau40, it can be concluded that only lysine residues of tubulin in close proximity to where Tau binds were involved in the cross links (**Figure 67**). In addition to these inter protein cross links, there were intra protein cross links identified between the lysine

residues within Tau and tubulin, which is expected as BS3 is a highly reactive and amine directed cross linker. Thus chemical cross-linking of Tau and tubulin/MT strongly supported the NMR revealed binding site of Tau on MTs.

4.5.3 Tau binds to α -tubulin at the inter-dimer interface

The previous studies where the taxol binding site is proposed for Tau considered the possibility of having two nearby binding site, one near the M-loop and another luminal pocket on β -tubulin which is close to the tubulin heterodimer interface. The authors considered the possibilities of having errors that can occur during the averaging of the image analysis (Kar, Fan et al. 2003). The proposed binding site could also be the similar binding site we have identified.

Al-Bassam *et al.* proposed that Tau binds on outer surface either on α or β -tubulin as the resolution of the image analysis was not sufficient enough to distinguish the subunits. Still only one of the units is targeted by Tau repeats and Tau binds longitudinally along the protofilaments (Al-Bassam, Ozer et al. 2002). Our current finding with Tau binding to α -tubulin at the interface of tubulin dimers is consistent with these previous studies. Notably, the binding site of Tau to tubulin/MT identified here does not overlap with that of the motor proteins kinesin and dynein, which binds on β -tubulin (Sosa, Dias et al. 1997).

The Tau binding site identified here serves as a bridging point of different tubulin heterodimers. The characteristic property of vinblastine is to promote the formation of curved tubulin rings instead of favouring straight protofilaments which is necessary for MT formation. This can be attributed to entirely different mechanism involved in the activities of Tau and Vinblastine. Although they are sharing the similar tubulin interface, vinblastine induces an orientation to impede MT assembly whereas the linear motifs of Tau take bind in such a way to α -tubulin that promotes a straightening of the protofilaments and thereby favours formation of stable microtubules.

Taken together the studies showed that localized interaction motifs of Tau, which are separated by highly flexible linkers, assume a well-defined structure upon binding to MTs. These binding domains compete each other for binding on α -tubulin subunit of MT at the interdimer interface near the binding site of Vinblastine. The binding occurs in a cooperative manner together with the charge neutralization at the C-terminus of tubulin. The dynamic structure of MT-bound Tau can therefore be represented as shown in **Figure 70**.

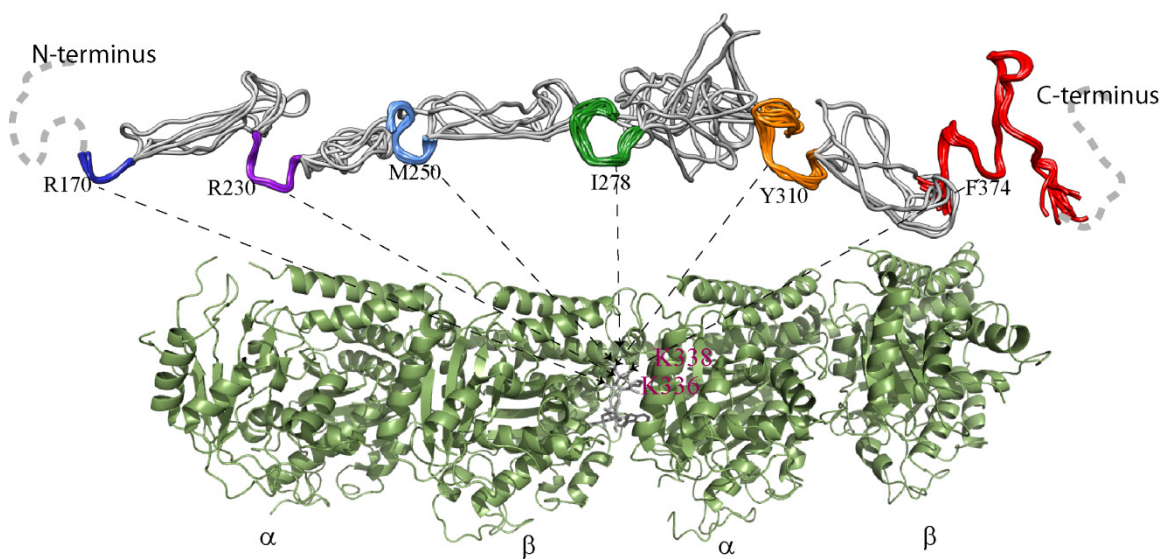


Figure 70: The dynamic structure of MT-bound Tau. The structure of independent binding domains of MT-bound Tau are presented as an ensemble of 10 conformers and are connected by flexible linkers generated using ModLoop web server (Fiser, Do et al. 2000, Fiser and Sali 2003). The binding site identified, where Vinblastine binds, at the inter dimer interface of tubulin heterodimers is highlighted with the structure of Vinblastine (grey) on $(Tc)_2R$ complex (PDB 1Z2B). The arrows indicate the preferred destination of each structured region of Tau.

References

- Abraha, A., N. Ghoshal, T. C. Gamblin, V. Cryns, R. W. Berry, J. Kuret and L. I. Binder (2000). "C-terminal inhibition of tau assembly in vitro and in Alzheimer's disease." J. Cell Sci. **113 Pt 21**: 3737-3745.
- Ackmann, M., H. Wiech and E. Mandelkow (2000). "Nonsaturable Binding Indicates Clustering of Tau on the Microtubule Surface in a Paired Helical Filament-like Conformation." J. Biol. Chem. **275**(39): 30335-30343.
- Adams, E. R., E. A. Dratz, D. Gizachew, F. R. Deleo, L. Yu, B. D. Volpp, M. Vlases, A. J. Jesaitis and M. T. Quinn (1997). "Interaction of human neutrophil flavocytochrome b with cytosolic proteins: transferred-NOESY NMR studies of a gp91phox C-terminal peptide bound to p47phox." Biochem. J. **325**(1): 249-257.
- Ahmad, F. J., T. P. Pienkowski and P. W. Baas (1993). "Regional Differences in Microtubule Dynamics in the Axon." J. Neurosci. **13**(2): 856-866.
- Aizawa, H., H. Kawasaki, H. Murofushi, S. Kotani, K. Suzuki and H. Sakai (1988). "Microtubule-binding domain of tau proteins." J. Biol. Chem. **263**(16): 7703-7707.
- Aizawa, H., H. Kawasaki, H. Murofushi, S. Kotani, K. Suzuki and H. Sakai (1989). "A common amino acid sequence in 190-kDa microtubule-associated protein and tau for the promotion of microtubule assembly." J. Biol. Chem. **264**(10): 5885-5890.
- Aizawa, H. and H. Murofushi (1989). "[Consensus sequence of microtubule-associated proteins for the stimulation of microtubule assembly]." Tanpakushitsu Kakusan Koso **34**(12 Suppl): 1447-1454.
- Akhmanova, A. and M. O. Steinmetz (2008). "Tracking the ends: a dynamic protein network controls the fate of microtubule tips." Nat. Rev. Mol. Cell Biol. **9**(4): 309-322.
- Al-Bassam, J., R. S. Ozer, D. Safer, S. Halpain and R. A. Milligan (2002). "MAP2 and tau bind longitudinally along the outer ridges of microtubule protofilaments." J. Cell Biol. **157**(7): 1187-1196.
- Alonso, A., T. Zaidi, M. Novak, I. Grundke-Iqbal and K. Iqbal (2001). "Hyperphosphorylation induces self-assembly of tau into tangles of paired helical filaments/straight filaments." Proc. Natl. Acad. Sci. USA **98**(12): 6923-6928.
- Alzheimer, A. (1907). "Über eine eigenartige Erkrankung der Hirnrinde." Allg. Z. Psychiatrie **64**: 146-148.

References

- Amos, L. A. (2004). "Microtubule structure and its stabilisation." Org. Biomol. Chem. **2**(15): 2153-2160.
- Amos, L. A. (2011). "What tubulin drugs tell us about microtubule structure and dynamics." Semin. Cell Dev. Biol.(0).
- Andreadis, A. (2005). "Tau gene alternative splicing: expression patterns, regulation and modulation of function in normal brain and neurodegenerative diseases." BBA-Mol. Basis Dis. **1739**(2-3): 91-103.
- Baas, P. W., T. P. Pienkowski and K. S. Kosik (1991). "Processes induced by tau expression in Sf9 cells have an axon-like microtubule organization." J. Cell Biol. **115**(5): 1333-1344.
- Balaram, P., Bothnerb.Aa and J. Dadok (1972). "Negative Nuclear Overhauser Effects as Probes of Macromolecular Structure." J. Am. Chem. Soc. **94**(11): 4015-4017.
- Ballatore, C., V. M. Lee and J. Q. Trojanowski (2007). "Tau-mediated neurodegeneration in Alzheimer's disease and related disorders." Nat. Rev. Neurosci. **8**(9): 663-672.
- Bibow, S., M. D. Mukrasch, S. Chinnathambi, J. Biernat, C. Griesinger, E. Mandelkow and M. Zweckstetter (2011). "The dynamic structure of filamentous tau." Angew. Chem., Int. Ed. **50**(48): 11520-11524.
- Bielska, A. A. and N. J. Zondlo (2006). "Hyperphosphorylation of tau induces local polyproline II helix." Biochemistry **45**(17): 5527-5537.
- Biernat, J. and E. M. Mandelkow (1999). "The development of cell processes induced by tau protein requires phosphorylation of serine 262 and 356 in the repeat domain and is inhibited by phosphorylation in the proline-rich domains." Mol. Biol. Cell **10**(3): 727-740.
- Biernat, J., Y. Z. Wu, T. Timm, Q. Zheng-Fischhofer, E. Mandelkow, L. Meijer and E. M. Mandelkow (2002). "Protein kinase MARK/PAR-1 is required for neurite outgrowth and establishment of neuronal polarity." Mol. Biol. Cell **13**(11): 4013-4028.
- Bodenhausen, G. and D. J. Ruben (1980). "Natural abundance nitrogen-15 NMR by enhanced heteronuclear spectroscopy." Chem. Phys. Lett. **69**(1): 185-189.
- Brandt, R., G. Lee, D. B. Teplow, D. Shalloway and M. Abdel-Ghany (1994). "Differential effect of phosphorylation and substrate modulation on tau's ability to promote microtubule growth and nucleation." J. Biol. Chem. **269**(16): 11776-11782.
- Bre, M. H. and E. Karsenti (1990). "Effects of brain microtubule-associated proteins on microtubule dynamics and the nucleating activity of centrosomes." Cytoskeleton **15**(2): 88-98.

References

- Buee, L., T. Bussiere, V. Buee-Scherrer, A. Delacourte and P. R. Hof (2000). "Tau protein isoforms, phosphorylation and role in neurodegenerative disorders." Brain. Res. Rev. **33**(1): 95-130.
- Bugiani, O., J. R. Murrell, G. Giaccone, M. Hasegawa, G. Ghigo, M. Tabaton, M. Morbin, A. Primavera, F. Carella, C. Solaro, M. Grisoli, M. Savoirdo, M. G. Spillantini, F. Tagliavini, M. Goedert and B. Ghetti (1999). "Frontotemporal dementia and corticobasal degeneration in a family with a P301S mutation in tau." J. Neuropath. Exp. Neur. **58**(6): 667-677.
- Bunker, J. M., K. Kamath, L. Wilson, M. A. Jordan and S. C. Feinstein (2006). "FTDP-17 mutations compromise the ability of tau to regulate microtubule dynamics in cells." J. Biol. Chem. **281**(17): 11856-11863.
- Bunker, J. M., L. Wilson, M. A. Jordan and S. C. Feinstein (2004). "Modulation of microtubule dynamics by tau in living cells: implications for development and neurodegeneration." Mol. Biol. Cell **15**(6): 2720-2728.
- Butner, K. A. and M. W. Kirschner (1991). "Tau-Protein Binds to Microtubules through a Flexible Array of Distributed Weak Sites." J. Cell Biol. **115**(3): 717-730.
- Caceres, A. and K. S. Kosik (1990). "Inhibition of neurite polarity by tau antisense oligonucleotides in primary cerebellar neurons." Nature **343**(6257): 461-463.
- Caceres, A., J. Mautino and K. S. Kosik (1992). "Suppression of Map2 in Cultured Cerebellar Macroneurons Inhibits Minor Neurite Formation." Neuron **9**(4): 607-618.
- Caceres, A., S. Potrebic and K. S. Kosik (1991). "The effect of tau antisense oligonucleotides on neurite formation of cultured cerebellar macroneurons." J. Neurosci. **11**(6): 1515-1523.
- Canales, A., J. Rodriguez-Salarichs, C. Trigili, L. Nieto, C. Coderch, J. M. Andreu, I. Paterson, J. Jimenez-Barbero and J. F. Diaz (2011). "Insights into the interaction of Discodermolide and Docetaxel with Tubulin. Mapping the Binding Sites of Microtubule-Stabilizing Agents by Using an Integrated NMR and Computational Approach." ACS Chem. Biol. **6**(8): 789-799.
- Carlomagno, T. (2005). "LIGAND-TARGET INTERACTIONS: What Can We Learn from NMR?" Annual Review of Biophysics and Biomolecular Structure **34**(1): 245-266.
- Chau, M. F., M. J. Radeke, C. de Ines, I. Barasoain, L. A. Kohlstaedt and S. C. Feinstein (1998). "The microtubule-associated protein tau cross-links to two distinct sites on each alpha and beta tubulin monomer via separate domains." Biochemistry **37**(51): 17692-17703.
- Chen, A. and M. J. Shapiro (1998). "NOE pumping: A novel NMR technique for identification of compounds with binding affinity to macromolecules." J. Am. Chem. Soc. **120**(39): 10258-10259.

- Clément, M.-J., I. Jourdain, S. Lachkar, P. Savarin, B. Gigant, M. Knossow, F. Toma, A. Sobel and P. A. Curmi (2005). "N-Terminal Stathmin-like Peptides Bind Tubulin and Impede Microtubule Assembly†." Biochemistry **44**(44): 14616-14625.
- Clement, M. J., P. Savarin, E. Adjadj, A. Sobel, F. Toma and P. A. Curmi (2010). "Probing Interactions of Tubulin with Small Molecules, Peptides, and Protein Fragments by Solution Nuclear Magnetic Resonance." Methods Cell Biol. **95**: 407-447.
- Cleveland, D. W., S.-Y. Hwo and M. W. Kirschner (1977). "Physical and chemical properties of purified tau factor and the role of tau in microtubule assembly." J. Mol. Biol. **116**(2): 227-247.
- Clore, G. M. and A. M. Gronenborn (1982). "Theory and applications of the transferred nuclear overhauser effect to the study of the conformations of small ligands bound to proteins." J. Magn. Reson. **48**(3): 402-417.
- Cocca, C., J. Dorado, E. Calvo, J. A. Lopez, A. Santos and A. Perez-Castillo (2009). "15-Deoxy-Delta(12,14)-prostaglandin J(2) is a tubulin-binding agent that destabilizes microtubules and induces mitotic arrest." Biochem. Pharmacol. **78**(10): 1330-1339.
- Daebel, V., S. Chinnathambi, J. Biernat, M. Schwalbe, B. Habenstein, A. Loquet, E. Akoury, K. Tepper, H. Muller, M. Baldus, C. Griesinger, M. Zweckstetter, E. Mandelkow, V. Vijayan and A. Lange (2012). "beta-Sheet Core of Tau Paired Helical Filaments Revealed by Solid-State NMR." J. Am. Chem. Soc. **134**(34): 13982-13989.
- Dalvit, C., P. Pevarello, M. Tato, M. Veronesi, A. Vulpetti and M. Sundstrom (2000). "Identification of compounds with binding affinity to proteins via magnetization transfer from bulk water." J. Biomol. NMR **18**(1): 65-68.
- Daly, N. L., R. Hoffmann, L. Otvos and D. J. Craik (2000). "Role of phosphorylation in the conformation of tau peptides implicated in Alzheimer's disease." Biochemistry **39**(30): 9039-9046.
- De Bona, P., L. Deshmukh, V. Gorbatyuk, O. Vinogradova and D. A. Kendall (2012). "Structural studies of a signal peptide in complex with signal peptidase I cytoplasmic domain: The stabilizing effect of membrane-mimetics on the acquired fold." Proteins: Struct., Funct., Bioinf. **80**(3): 807-817.
- Desai, A. and T. J. Mitchison (1997). "Microtubule polymerization dynamics." Annu. Rev. Cell Dev. Biol. **13**: 83-117.
- Devred, F., P. Barbier, S. Douillard, O. Monasterio, J. M. Andreu and V. Peyrot (2004). "Tau induces ring and microtubule formation from alpha beta-tubulin dimers under nonassembly conditions." Biochemistry **43**(32): 10520-10531.
- Dixit, R., J. L. Ross, Y. E. Goldman and E. L. Holzbaur (2008). "Differential regulation of dynein and kinesin motor proteins by tau." Science **319**(5866): 1086-1089.

References

- Drechsel, D. N., A. A. Hyman, M. H. Cobb and M. W. Kirschner (1992). "Modulation of the Dynamic Instability of Tubulin Assembly by the Microtubule-Associated Protein Tau." Mol. Biol. Cell **3**(10): 1141-1154.
- Drewes, G., A. Ebnet, U. Preuss, E. M. Mandelkow and E. Mandelkow (1997). "MARK, a novel family of protein kinases that phosphorylate microtubule-associated proteins and trigger microtubule disruption." Cell **89**(2): 297-308.
- Drubin, D. and M. Kirschner (1986). "Tau protein function in living cells." J. Cell Biol. **103**: 2739-2746.
- Drubin, D., S. Kobayashi and M. Kirschner (1986). "Association of tau protein with microtubules in living cells." Ann. N. Y. Acad. Sci. **466**: 257-268.
- Duan, A. R. and H. V. Goodson (2012). "Taxol-stabilized microtubules promote the formation of filaments from unmodified full-length Tau in vitro." Mol. Biol. Cell **23**(24): 4796-4806.
- Dunker, A. K., J. D. Lawson, C. J. Brown, R. M. Williams, P. Romero, J. S. Oh, C. J. Oldfield, A. M. Campen, C. M. Ratliff, K. W. Hipps, J. Ausio, M. S. Nissen, R. Reeves, C. Kang, C. R. Kissinger, R. W. Bailey, M. D. Griswold, W. Chiu, E. C. Garner and Z. Obradovic (2001). "Intrinsically disordered protein." J. Mol. Graph. Model. **19**(1): 26-59.
- Dyson, H. J. and P. E. Wright (2005). "Intrinsically unstructured proteins and their functions." Nat. Rev. Mol. Cell Biol. **6**(3): 197-208.
- Ebnet, A., G. Drewes, E. M. Mandelkow and E. Mandelkow (1999). "Phosphorylation of MAP2c and MAP4 by MARK kinases leads to the destabilization of microtubules in cells." Cytoskeleton **44**(3): 209-224.
- Ebnet, A., R. Godemann, K. Stamer, S. Illenberger, B. Trinczek and E. Mandelkow (1998). "Overexpression of tau protein inhibits kinesin-dependent trafficking of vesicles, mitochondria, and endoplasmic reticulum: implications for Alzheimer's disease." J. Cell Biol. **143**(3): 777-794.
- Eckermann, K., M. M. Mocanu, I. Khlistunova, J. Biernat, A. Nissen, A. Hofmann, K. Schonig, H. Bujard, A. Haemisch, E. Mandelkow, L. Zhou, G. Rune and E. M. Mandelkow (2007). "The beta-propensity of Tau determines aggregation and synaptic loss in inducible mouse models of tauopathy." J. Biol. Chem. **282**(43): 31755-31765.
- Ennulat, D. J., R. K. Liem, G. A. Hashim and M. L. Shelanski (1989). "Two separate 18-amino acid domains of tau promote the polymerization of tubulin." J. Biol. Chem. **264**(10): 5327-5330.
- Esmaeliazad, B., J. H. Mccarty and S. C. Feinstein (1994). "Sense and Antisense Transfection Analysis of Tau-Function - Tau-Influences Net Microtubule Assembly, Neurite Outgrowth and Neuritic Stability." J. Cell Sci. **107**: 869-879.

- Fath, T., J. Eidenmuller and R. Brandt (2002). "Tau-mediated cytotoxicity in a pseudohyperphosphorylation model of Alzheimer's disease." J. Neurosci. **22**(22): 9733-9741.
- Fauquant, C., V. Redeker, I. Landrieu, J.-M. Wieruzseski, D. Verdegem, O. Laprevote, G. Lippens, B. Gigant and M. Knossow (2011). "Systematic identification of tubulin interacting fragments of the microtubule-associated protein TAU leads to a highly efficient promoter of microtubule assembly." J. Biol. Chem.
- Feinstein, S. C. and L. Wilson (2005). "Inability of tau to properly regulate neuronal microtubule dynamics: a loss-of-function mechanism by which tau might mediate neuronal cell death." BBA-Mol. Basis Dis. **1739**(2-3): 268-279.
- Fiege, B., C. Rademacher, J. Cartmell, P. I. Kitov, F. Parra and T. Peters (2012). "Molecular Details of the Recognition of Blood Group Antigens by a Human Norovirus as Determined by STD NMR Spectroscopy." Angew. Chem., Int. Ed. **51**(4): 928-932.
- Fischer, D., M. D. Mukrasch, J. Biernat, S. Bibow, M. Blackledge, C. Griesinger, E. Mandelkow and M. Zweckstetter (2009). "Conformational Changes Specific for Pseudophosphorylation at Serine 262 Selectively Impair Binding of Tau to Microtubules." Biochemistry **48**(42): 10047-10055.
- Fiser, A., R. K. G. Do and A. Šali (2000). "Modeling of loops in protein structures." Protein Science **9**(9): 1753-1773.
- Fiser, A. and A. Sali (2003). "ModLoop: automated modeling of loops in protein structures." Bioinformatics **19**(18): 2500-2501.
- Fleming, L. M., K. H. Weisgraber, W. J. Strittmatter, J. C. Troncoso and G. V. W. Johnson (1996). "Differential binding of apolipoprotein E isoforms to tau and other cytoskeletal proteins." Exp. Neurol. **138**(2): 252-260.
- Fratiglioni, L., D. De Ronchi and H. Aguero-Torres (1999). "Worldwide prevalence and incidence of dementia." Drug & Aging **15**(5): 365-375.
- Fulga, T. A., I. Elson-Schwab, V. Khurana, M. L. Steinhilb, T. L. Spires, B. T. Hyman and M. B. Feany (2007). "Abnormal bundling and accumulation of F-actin mediates tau-induced neuronal degeneration in vivo." Nat. Cell Biol. **9**(2): 139-U117.
- Gaskin, F., C. R. Cantor and M. L. Shelanski (1974). "Turbidimetric studies of the in vitro assembly and disassembly of porcine neurotubules." J. Mol. Biol. **89**(4): 737-755.
- Gigant, B., C. Wang, R. B. G. Ravelli, F. Roussi, M. O. Steinmetz, P. A. Curmi, A. Sobel and M. Knossow (2005). "Structural basis for the regulation of tubulin by vinblastine." Nature **435**(7041): 519-522.
- Gizachew, D. and E. Dratz "Transferred NOESY NMR Studies of Biotin Mimetic Peptide (FSHPQNT) Bound to Streptavidin: A Structural Model for Studies of Peptide-Protein Interactions." Chem. Biol. Drug. Des. **78**(1): 14-24.

References

- Goedert, M. (1996). "Tau protein and the neurofibrillary pathology of Alzheimer's disease." Ann. NY. Acad. Sci. **777**: 121-131.
- Goedert, M. and M. G. Spillantini (2006). "A century of Alzheimer's disease." Science **314**(5800): 777-781.
- Goedert, M., C. M. Wischik, R. A. Crowther, J. E. Walker and A. Klug (1988). "Cloning and Sequencing of the Cdna-Encoding a Core Protein of the Paired Helical Filament of Alzheimer-Disease - Identification as the Microtubule-Associated Protein Tau." Proc. Natl. Acad. Sci. USA **85**(11): 4051-4055.
- Gong, C. X., F. Liu, I. Grundke-Iqbal and K. Iqbal (2005). "Post-translational modifications of tau protein in Alzheimer's disease." J. Neural Transm. **112**(6): 813-838.
- Gong, C. X., F. Liu, I. Grundke-Iqbal and K. Iqbal (2006). "Dysregulation of protein phosphorylation/dephosphorylation in Alzheimer's disease: A therapeutic target." J. Biomed. Biotechnol.
- Goode, B. L., M. Chau, P. E. Denis and S. C. Feinstein (2000). "Structural and functional differences between 3-repeat and 4-repeat tau isoforms. Implications for normal tau function and the onset of neurodegenerative disease." J. Biol. Chem. **275**(49): 38182-38189.
- Goode, B. L., P. E. Denis, D. Panda, M. J. Radeke, H. P. Miller, L. Wilson and S. C. Feinstein (1997). "Functional interactions between the proline-rich and repeat regions of tau enhance microtubule binding and assembly." Mol. Biol. Cell **8**(2): 353-365.
- Gordonweeks, P. R. (1993). "Organization of Microtubules in Axonal Growth Cones - a Role for Microtubule-Associated Protein Map 1b." J Neurocytol **22**(9): 717-725.
- Grundke-Iqbal, I. and K. Iqbal (1989). "Neuronal cytoskeleton in the biology of Alzheimer disease." Prog. Clin. Biol. Res. **317**: 745-753.
- Grundke-Iqbal, I., K. Iqbal, L. George, Y. C. Tung, K. S. Kim and H. M. Wisniewski (1989). "Amyloid protein and neurofibrillary tangles coexist in the same neuron in Alzheimer disease." Proc. Natl. Acad. Sci. USA **86**(8): 2853-2857.
- Grundke-Iqbal, I., K. Iqbal, M. Quinlan, Y. C. Tung, M. S. Zaidi and H. M. Wisniewski (1986). "Microtubule-associated protein tau. A component of Alzheimer paired helical filaments." J. Biol. Chem. **261**(13): 6084-6089.
- GÜNTERT, P. (1998). "Structure calculation of biological macromolecules from NMR data." Q. Rev. Biophys. **31**(02): 145-237.
- Güntert, P., C. Mumenthaler and K. Wüthrich (1997). "Torsion angle dynamics for NMR structure calculation with the new program Dyana." J. Mol. Biol. **273**(1): 283-298.
- Gustke, N., B. Steiner, E. M. Mandelkow, J. Biernat, H. E. Meyer, M. Goedert and E. Mandelkow (1992). "The Alzheimer-like phosphorylation of tau protein reduces

References

- microtubule binding and involves Ser-Pro and Thr-Pro motifs." *FEBS Lett.* **307**(2): 199-205.
- Gustke, N., B. Trinczek, J. Biernat, E. M. Mandelkow and E. Mandelkow (1994). "Domains of Tau-Protein and Interactions with Microtubules." *Biochemistry* **33**(32): 9511-9522.
- Hanger, D. P., J. C. Betts, T. L. F. Loviny, W. P. Blackstock and B. H. Anderton (1998). "New phosphorylation sites identified in hyperphosphorylated tau (paired helical filament-tau) from Alzheimer's disease brain using nanoelectrospray mass spectrometry." *J Neurochem* **71**(6): 2465-2476.
- Harbison, N. W., S. Bhattacharya and D. Eliezer (2012). "Assigning Backbone NMR Resonances for Full Length Tau Isoforms: Efficient Compromise between Manual Assignments and Reduced Dimensionality." *PLOS ONE* **7**(4).
- Himes, R. H. (1991). "Interactions of the Catharanthus (Vinca) Alkaloids with Tubulin and Microtubules." *Pharmacol. Therapeut.* **51**(2): 257-267.
- Himmler, A., D. Drechsel, M. W. Kirschner and D. W. Martin (1989). "Tau Consists of a Set of Proteins with Repeated C-Terminal Microtubule-Binding Domains and Variable N-Terminal Domains." *Mol Cell Biol* **9**(4): 1381-1388.
- Hiraishi, N., N. Tochio, T. Kigawa, M. Otsuki and J. Tagami (2013). "Monomer-Collagen Interactions Studied by Saturation Transfer Difference NMR." *J. Dent. Res.*
- Hirokawa, N. (1994). "Microtubule organization and dynamics dependent on microtubule-associated proteins." *Curr. Opin. Cell. Biol.* **6**(1): 74-81.
- Hirokawa, N., Y. Shiomura and S. Okabe (1988). "Tau proteins: the molecular structure and mode of binding on microtubules." *J. Cell Biol.* **107**(4): 1449-1459.
- Hirokawa, N. and R. Takemura (2005). "Molecular motors and mechanisms of directional transport in neurons." *Nat Rev Neurosci* **6**(3): 201-214.
- Hoffmann, R., V. M. Y. Lee, S. Leight, I. Varga and L. Otvos (1997). "Unique Alzheimer's disease paired helical filament specific epitopes involve double phosphorylation at specific sites." *Biochemistry-U.S.* **36**(26): 8114-8124.
- Hutton, M., C. L. Lendon, P. Rizzu, M. Baker, S. Froelich, H. Houlden, S. Pickering-Brown, S. Chakraverty, A. Isaacs, A. Grover, J. Hackett, J. Adamson, S. Lincoln, D. Dickson, P. Davies, R. C. Petersen, M. Stevens, E. de Graaff, E. Wauters, J. van Baren, M. Hillebrand, M. Joosse, J. M. Kwon, P. Nowotny, P. Heutink and et al. (1998). "Association of missense and 5'-splice-site mutations in tau with the inherited dementia FTDP-17." *Nature* **393**(6686): 702-705.
- Hyman, A. and E. Karsenti (1998). "The role of nucleation in patterning microtubule networks." *J. Cell Sci.* **111**: 2077-2083.

References

- Hyman, A. A., S. Salser, D. N. Drechsel, N. Unwin and T. J. Mitchison (1992). "Role of Gtp Hydrolysis in Microtubule Dynamics - Information from a Slowly Hydrolyzable Analog, Gmpcpp." Mol. Biol. Cell **3**(10): 1155-1167.
- Illenberger, S., G. Drewes, B. Trinczek, J. Biernat, H. E. Meyer, J. B. Olmsted, E. M. Mandelkow and E. Mandelkow (1996). "Phosphorylation of microtubule-associated proteins MAP2 and MAP4 by the protein kinase p110mark. Phosphorylation sites and regulation of microtubule dynamics." J. Biol. Chem. **271**(18): 10834-10843.
- Jeganathan, S., A. Hascher, S. Chinnathambi, J. Biernat, E.-M. Mandelkow and E. Mandelkow (2008). "Proline-directed Pseudo-phosphorylation at AT8 and PHF1 Epitopes Induces a Compaction of the Paperclip Folding of Tau and Generates a Pathological (MC-1) Conformation." J. Biol. Chem. **283**(46): 32066-32076.
- Jeganathan, S., M. von Bergen, H. Brutlach, H. J. Steinhoff and E. Mandelkow (2006). "Global hairpin folding of tau in solution." Biochemistry **45**(7): 2283-2293.
- Jiménez-Barbero, J., A. Canales, P. T. Northcote, R. M. Buey, J. M. Andreu and J. F. Díaz (2006). "NMR Determination of the Bioactive Conformation of Peloruside A Bound To Microtubules." J. Am. Chem. Soc. **128**(27): 8757-8765.
- Johnson, G. V. W. and W. H. Stoothoff (2004). "Tau phosphorylation in neuronal cell function and dysfunction." J. Cell Sci. **117**(24): 5721-5729.
- Joly, J. C., G. Flynn and D. L. Purich (1989). "The microtubule-binding fragment of microtubule-associated protein-2: location of the protease-accessible site and identification of an assembly-promoting peptide." J. Cell Biol. **109**(5): 2289-2294.
- Joly, J. C. and D. L. Purich (1990). "Peptides corresponding to the second repeated sequence in MAP-2 inhibit binding of microtubule-associated proteins to microtubules." Biochemistry **29**(38): 8916-8920.
- Jordan, M. A., D. Walker, M. de Arruda, T. Barlozzari and D. Panda (1998). "Suppression of microtubule dynamics by binding of cemadotin to tubulin: Possible mechanism for its antitumor action." Biochemistry **37**(50): 17571-17578.
- Jordan, M. A. and L. Wilson (2004). "Microtubules as a target for anticancer drugs." Nat. Rev. Cancer **4**(4): 253-265.
- Kar, S., J. Fan, M. J. Smith, M. Goedert and L. A. Amos (2003). "Repeat motifs of tau bind to the insides of microtubules in the absence of taxol." EMBO J. **22**(1): 70-77.
- Kirschner, M. W. and T. Mitchison (1986). "Microtubule Dynamics." Nature **324**(6098): 621-621.
- Knops, J., K. S. Kosik, G. Lee, J. D. Pardee, L. Cohen-Gould and L. McConlogue (1991). "Overexpression of tau in a nonneuronal cell induces long cellular processes." J. Cell Biol. **114**(4): 725-733.

References

- Konzack, S., E. Thies, A. Marx, E. M. Mandelkow and E. Mandelkow (2007). "Swimming against the tide: Mobility of the microtubule-associated protein tau in neurons." J. Neurosci. **27**(37): 9916-9927.
- Kosik, K. S., C. L. Joachim and D. J. Selkoe (1986). "Microtubule-Associated Protein Tau (Tau) Is a Major Antigenic Component of Paired Helical Filaments in Alzheimer-Disease." Proc. Natl. Acad. Sci. USA **83**(11): 4044-4048.
- Kotani, S., G. Kawai, S. Yokoyama and H. Murofushi (1990). "Interaction mechanism between microtubule-associated proteins and microtubules. A proton nuclear magnetic resonance analysis on the binding of synthetic peptide to tubulin." Biochemistry **29**(43): 10049-10054.
- Kubicek, K., S. Grimm, J. Orts, F. Sasse and T. Carlomagno "The Tubulin-Bound Structure of the Antimitotic Drug Tubulysin." Angew. Chem., Int. Ed. **49**(28): 4809-4812.
- Landrieu, I., A. Leroy, C. Smet-nocca, I. Huvent, L. Amniai, M. Hamdane, N. Sibille, L. Buee, J.-M. Wieruszeski and G. Lippens (2010). "NMR spectroscopy of the neuronal tau protein: normal function and implication in Alzheimer's disease." Biochem. Soc. Trans. **038**(4): 1006-1011.
- LeBoeuf, A. C., S. F. Levy, M. Gaylord, A. Bhattacharya, A. K. Singh, M. A. Jordan, L. Wilson and S. C. Feinstein (2008). "FTDP-17 Mutations in Tau Alter the Regulation of Microtubule Dynamics." J. Biol. Chem. **283**(52): 36406-36415.
- Lee, G., N. Cowan and M. Kirschner (1988). "The primary structure and heterogeneity of tau protein from mouse brain." Science **239**(4837): 285-288.
- Lee, V. M. Y., M. Goedert and J. Q. Trojanowski (2001). "Neurodegenerative tauopathies." Annu. Rev. Neurosci. **24**: 1121-1159.
- Lefevre, J., K. G. Chernov, V. Joshi, S. Delga, F. Toma, D. Pastre, P. A. Curmi and P. Savarin (2011). "The C Terminus of Tubulin, a Versatile Partner for Cationic Molecules BINDING OF TAU, POLYAMINES, AND CALCIUM." J. Biol. Chem. **286**(4): 3065-3078.
- Levy, S. F., A. C. LeBoeuf, M. R. Massie, M. A. Jordan, L. Wilson and S. C. Feinstein (2005). "Three- and Four-repeat Tau Regulate the Dynamic Instability of Two Distinct Microtubule Subpopulations in Qualitatively Different Manners." J. Biol. Chem. **280**(14): 13520-13528.
- Makrides, V., M. R. Massie, S. C. Feinstein and J. Lew (2004). "Evidence for two distinct binding sites for tau on microtubules." Proc. Natl. Acad. Sci. USA **101**(17): 6746-6751.
- Mandelkow, E. and E.-M. Mandelkow (1995). "Microtubules and microtubule-associated proteins." Current Opinion in Cell Biology **7**(1): 72-81.

References

- Mandelkow, E. M., M. Herrmann and U. Ruhl (1985). "Tubulin domains probed by limited proteolysis and subunit-specific antibodies." J. Mol. Biol. **185**(2): 311-327.
- Mandelkow, E. M., G. Lange, A. Jagla, U. Spann and E. Mandelkow (1988). "Dynamics of the Microtubule Oscillator - Role of Nucleotides and Tubulin Map Interactions." Embo J **7**(2): 357-365.
- Mandelkow, E. M. and E. Mandelkow (1998). "Tau in Alzheimer's disease." Trends Cell Biol. **8**(11): 425-427.
- Mandelkow, E. M., E. Mandelkow and R. A. Milligan (1991). "Microtubule dynamics and microtubule caps: a time-resolved cryo-electron microscopy study." J. Cell Biol. **114**(5): 977-991.
- Margolis, R. L. and L. Wilson (1981). "Microtubule Treadmills - Possible Molecular Machinery." Nature **293**(5835): 705-711.
- Margolis, R. L. and L. Wilson (1998). "Microtubule treadmilling: what goes around comes around." Bioessays **20**(10): 830-836.
- Martin-Pastor, M., M. Vega-Vazquez, A. De Capua, A. Canales, S. Andre, H. J. Gabius and J. Jimenez-Barbero (2006). "Enhanced signal dispersion in saturation transfer difference experiments by conversion to a 1D-STD-homodecoupled spectrum." J. Biomol. NMR **36**(2): 103-109.
- Marx, A., J. Muller and E. Mandelkow (2005). "The structure of microtubule motor proteins." Adv Protein Chem **71**: 299-+.
- Mayer, M. and B. Meyer (1999). "Characterization of ligand binding by saturation transfer difference NMR spectroscopy." Angew. Chem., Int. Ed. **38**(12): 1784-1788.
- Mayer, M. and B. Meyer (2001). "Group epitope mapping by saturation transfer difference NMR to identify segments of a ligand in direct contact with a protein receptor." J. Am. Chem. Soc. **123**(25): 6108-6117.
- Mazanetz, M. P. and P. M. Fischer (2007). "Untangling tau hyperphosphorylation in drug design for neurodegenerative diseases." Nat Rev Drug Discov **6**(6): 464-479.
- Mcintosh, J. R., U. P. Roos, B. Neighbors and K. L. McDonald (1985). "Architecture of the Microtubule Component of Mitotic Spindles from Dictyostelium-Discoideum." J Cell Sci **75**(Apr): 93-129.
- Mi, K. and G. V. Johnson (2006). "The role of tau phosphorylation in the pathogenesis of Alzheimer's disease." Curr Alzheimer Res **3**(5): 449-463.
- Mitchison, T. and M. Kirschner (1984). "Dynamic instability of microtubule growth." Nature **312**(5991): 237-242.

References

- Moores, C. A., M. Perderiset, F. Francis, J. Chelly, A. Houdusse and R. A. Milligan (2004). "Mechanism of microtubule stabilization by doublecortin." Molecular Cell **14**(6): 833-839.
- Moores, C. A., M. Perderiset, F. Francis, J. Chelly, S. J. Perkins, A. Houdusse and R. A. Milligan (2004). "The role of doublecortin in neuronal migration and differentiation." Mol. Biol. Cell **15**: 156a-156a.
- Moores, C. A., M. Perderiset, C. Kappeler, S. Kain, D. Drummond, S. J. Perkins, J. Chelly, R. Cross, A. Houdusse and F. Francis (2006). "Distinct roles of doublecortin modulating the microtubule cytoskeleton." EMBO J. **25**(19): 4448-4457.
- Morris, M., S. Maeda, K. Vossel and L. Mucke (2011). "The Many Faces of Tau." Neuron **70**(3): 410-426.
- Mukrasch, M. D., S. Bibow, J. Korukottu, S. Jeganathan, J. Biernat, C. Griesinger, E. Mandelkow and M. Zweckstetter (2009). "Structural polymorphism of 441-residue tau at single residue resolution." PLoS Biol. **7**(2): e34.
- Mukrasch, M. D., J. Biernat, M. von Bergen, C. Griesinger, E. Mandelkow and M. Zweckstetter (2005). "Sites of tau important for aggregation populate beta-structure and bind to microtubules and polyanions." J. Biol. Chem. **280**(26): 24978-24986.
- Mukrasch, M. D., P. Markwick, J. Biernat, M. von Bergen, P. Bernado, C. Griesinger, E. Mandelkow, M. Zweckstetter and M. Blackledge (2007). "Highly Populated Turn Conformations in Natively Unfolded Tau Protein Identified from Residual Dipolar Couplings and Molecular Simulation." J. Am. Chem. Soc. **129**(16): 5235-5243.
- Mukrasch, M. D., M. von Bergen, J. Biernat, D. Fischer, C. Griesinger, E. Mandelkow and M. Zweckstetter (2007). "The "jaws" of the Tau-microtubule interaction." J. Biol. Chem. **282**(16): 12230-12239.
- Mylonas, E., A. Hascher, P. Bernado, M. Blackledge, E. Mandelkow and D. I. Svergun (2008). "Domain conformation of tau protein studied by solution small-angle X-ray scattering." Biochemistry-U.S. **47**(39): 10345-10353.
- Narayanan, R. L., U. H. N. Dürr, S. Bibow, J. Biernat, E. Mandelkow and M. Zweckstetter (2010). "Automatic Assignment of the Intrinsically Disordered Protein Tau with 441-Residues." J. Am. Chem. Soc. **132**(34): 11906-11907.
- Neve, R. L., P. Harris, K. S. Kosik, D. M. Kurnit and T. A. Donlon (1986). "Identification of Cdna Clones for the Human Microtubule-Associated Protein Tau and Chromosomal Localization of the Genes for Tau and Microtubule-Associated Protein-2." Mol. Brain. Res. **1**(3): 271-280.
- Noble, W., V. Olm, K. Takata, E. Casey, O. Mary, J. Meyerson, K. Gaynor, J. LaFrancois, L. Wang, T. Kondo, P. Davies, M. Burns, Veeranna, R. Nixon, D. Dickson, Y. Matsuoka, M. Ahljanian, L. F. Lau and K. Duff (2003). "Cdk5 is a key factor in tau aggregation and tangle formation in vivo." Neuron **38**(4): 555-565.

References

- Nogales, E., S. G. Wolf and K. H. Downing (1998). "Structure of the [alpha][beta] tubulin dimer by electron crystallography." Nature **391**(6663): 199-203.
- Oakley, C. E. and B. R. Oakley (1989). "Identification of Gamma-Tubulin, a New Member of the Tubulin Superfamily Encoded by Mipa Gene of *Aspergillus-Nidulans*." Nature **338**(6217): 662-664.
- Orts, J., C. Griesinger and T. Carlomagno (2009). "The INPHARMA technique for pharmacophore mapping: A theoretical guide to the method." J. Magn. Reson. **200**(1): 64-73.
- Paglini, G., L. Peris, F. Mascotti, S. Quiroga and A. Caceres (2000). "Tau protein function in axonal formation." Neurochem Res **25**(1): 37-42.
- Panda, D., B. L. Goode, S. C. Feinstein and L. Wilson (1995). "Kinetic Stabilization of Microtubule Dynamics at Steady-State by Tau and Microtubule-Binding Domains of Tau." Biochemistry **34**(35): 11117-11127.
- Panda, D., H. P. Miller and L. Wilson (1999). "Rapid treadmilling of brain microtubules free of microtubule-associated proteins in vitro and its suppression by tau." Proc. Natl. Acad. Sci. USA **96**(22): 12459-12464.
- Panda, D., J. C. Samuel, M. Massie, S. C. Feinstein and L. Wilson (2003). "Differential regulation of microtubule dynamics by three- and four-repeat tau: Implications for the onset of neurodegenerative disease." Proc. Natl. Acad. Sci. USA **100**(16): 9548-9553.
- Perez, E. A. (2009). "Impact, mechanisms, and novel chemotherapy strategies for overcoming resistance to anthracyclines and taxanes in metastatic breast cancer." Breast Cancer Res. Tr. **114**(2): 195-201.
- Perez, E. A. (2009). "Microtubule inhibitors: Differentiating tubulin-inhibiting agents based on mechanisms of action, clinical activity, and resistance." Mol. Cancer. Ther. **8**(8): 2086-2095.
- Perez, M., I. Santa-Maria, E. G. de Barreda, X. W. Zhu, R. Cuadros, J. R. Cabrero, F. Sanchez-Madrid, H. N. Dawson, M. P. Vitek, G. Perry, M. A. Smith and J. Avila (2009). "Tau - an inhibitor of deacetylase HDAC6 function." J. Neurochem. **109**(6): 1756-1766.
- Pervushin, K., R. Riek, G. Wider and K. Wuthrich (1997). "Attenuated T-2 relaxation by mutual cancellation of dipole-dipole coupling and chemical shift anisotropy indicates an avenue to NMR structures of very large biological macromolecules in solution." Proc. Natl. Acad. Sci. USA **94**(23): 12366-12371.
- Post, C. B. (2003). "Exchange-transferred NOE spectroscopy and bound ligand structure determination." Curr. Opin. Struct. Biol. **13**(5): 581-588.
- Reed, J., W. E. Hull, H. Ponstingl and R. H. Himes (1992). "Conformational properties of the beta(400-436) and beta(400-445) C-terminal peptides of porcine brain tubulin." Biochemistry **31**(47): 11888-11895.

References

- Reiner, T., A. de las Pozas, L. A. Gomez and C. Perez-Stable (2009). "Low dose combinations of 2-methoxyestradiol and docetaxel block prostate cancer cells in mitosis and increase apoptosis." Cancer Lett. **276**(1): 21-31.
- Riek, R., J. Fiaux, E. B. Bertelsen, A. L. Horwich and K. Wuthrich (2002). "Solution NMR techniques for large molecular and supramolecular structures." J. Am. Chem. Soc. **124**(41): 12144-12153.
- Riek, R., K. Pervushin and K. Wuthrich (2000). "TROSY and CRINEPT: NMR with large molecular and supramolecular structures in solution." Trends Biochem. Sci. **25**(10): 462-468.
- Riek, R., G. Wider, K. Pervushin and K. Wuthrich (1999). "Polarization transfer by cross-correlated relaxation in solution NMR with very large molecules." Proc. Natl. Acad. Sci. USA **96**(9): 4918-4923.
- Sánchez-Pedregal, V. M., M. Reese, J. Meiler, M. J. J. Blommers, C. Griesinger and T. Carlomagno (2005). "The INPHARMA Method: Protein-Mediated Interligand NOEs for Pharmacophore Mapping." Angew. Chem., Int. Ed. **44**(27): 4172-4175.
- Santarella, R. A., G. Skiniotis, K. N. Goldie, P. Tittmann, H. Gross, E. M. Mandelkow, E. Mandelkow and A. Hoenger (2004). "Surface-decoration of microtubules by human tau." J. Mol. Biol. **339**(3): 539-553.
- Schaap, I. A. T., B. Hoffmann, C. Carrasco, R. Merkel and C. F. Schmidt (2007). "Tau protein binding forms a 1 nm thick layer along protofilaments without affecting the radial elasticity of microtubules." J. Struct. Biol. **158**(3): 282-292.
- Schwalbe, M., J. Biernat, S. Bibow, V. Ozenne, M. R. Jensen, H. Kadavath, M. Blackledge, E. Mandelkow and M. Zweckstetter (2013). "Phosphorylation of Human Tau Protein by Microtubule Affinity-Regulating Kinase 2." Biochemistry.
- Schweers, O., E. Schonbrunn-Hanebeck, A. Marx and E. Mandelkow (1994). "Structural studies of tau protein and Alzheimer paired helical filaments show no evidence for beta-structure." J. Biol. Chem. **269**(39): 24290-24297.
- Schwieters, C. D., J. J. Kuszewski, N. Tjandra and G. Marius Clore (2003). "The Xplor-NIH NMR molecular structure determination package." J. Magn. Reson. **160**(1): 65-73.
- Serrano, L., J. Avila and R. B. Maccioni (1984). "Controlled Proteolysis of Tubulin by Subtilisin - Localization of the Site for Map2 Interaction." Biochemistry **23**(20): 4675-4681.
- Serrano, L., J. Delatorre, R. B. Maccioni and J. Avila (1984). "Involvement of the Carboxyl-Terminal Domain of Tubulin in the Regulation of Its Assembly." Proc. Natl. Acad. Sci. USA **81**(19): 5989-5993.

Shevchenko, A., H. Tomas, J. Havlis, J. V. Olsen and M. Mann (2006). "In-gel digestion for mass spectrometric characterization of proteins and proteomes." Nat. Protoc. **1**(6): 2856-2860.

Sibille, N., I. Huvent, C. Fauquant, D. Verdegem, L. Amniai, A. Leroy, J.-M. Wieruszeski, G. Lippens and I. Landrieu (2011). "Structural characterization by nuclear magnetic resonance of the impact of phosphorylation in the proline-rich region of the disordered Tau protein." Proteins: Struct., Funct., Bioinf. **80**(2): 454-462.

Sillen, A., P. Barbier, I. Landrieu, S. Lefebvre, J. M. Wieruszeski, A. Leroy, V. Peyrot and G. Lippens (2007). "NMR investigation of the interaction between the neuronal protein tau and the microtubules." Biochemistry **46**(11): 3055-3064.

Smet, C., A. Leroy, A. Sillen, J. M. Wieruszeski, I. Landrieu and G. Lippens (2004). "Accepting its random coil nature allows a partial NMR assignment of the neuronal Tau protein." Chembiochem **5**(12): 1639-1646.

Sosa, H., D. P. Dias, A. Hoenger, M. Whittaker, E. WilsonKubalek, E. Sablin, R. J. Fletterick, R. D. Vale and R. A. Milligan (1997). "A model for the microtubule-Ncd motor protein complex obtained by cryo-electron microscopy and image analysis." Cell **90**(2): 217-224.

Spillantini, M. G., J. R. Murrell, M. Goedert, M. R. Farlow, A. Klug and B. Ghetti (1998). "Mutation in the tau gene in familial multiple system tauopathy with presenile dementia." Proc. Natl. Acad. Sci. USA **95**(13): 7737-7741.

Spillantini, M. G., M. Tolnay, S. Love and M. Goedert (1999). "Microtubule-associated protein tau, heparan sulphate and alpha-synuclein in several neurodegenerative diseases with dementia." Acta Neuropathol. (Berl) **97**(6): 585-594.

Spillantini, M. G., J. C. Van Swieten and M. Goedert (2000). "Tau gene mutations in frontotemporal dementia and parkinsonism linked to chromosome 17 (FTDP-17)." Neurogenetics **2**(4): 193-205.

Spittaels, K., C. Van den Haute, J. Van Dorpe, H. Geerts, M. Mercken, K. Bruynseels, R. Lasrado, K. Vandezande, I. Laenen, T. Boon, J. Van Lint, J. Vandenheede, D. Moechars, R. Loos and F. Van Leuven (2000). "Glycogen synthase kinase-3 beta phosphorylates protein tau and rescues the axonopathy in the central nervous system of human four-repeat tau transgenic mice." J. Biol. Chem. **275**(52): 41340-41349.

Stoothoff, W. H. and G. V. W. Johnson (2005). "Tau phosphorylation: physiological and pathological consequences." BBA-Mol. Basis Dis. **1739**(2-3): 280-297.

Streiff, J. H., N. O. Juranic, S. I. Macura, D. O. Warner, K. A. Jones and W. J. Perkins (2004). "Saturation Transfer Difference Nuclear Magnetic Resonance Spectroscopy As a Method for Screening Proteins for Anesthetic Binding." Mol. Pharmacol. **66**(4): 929-935.

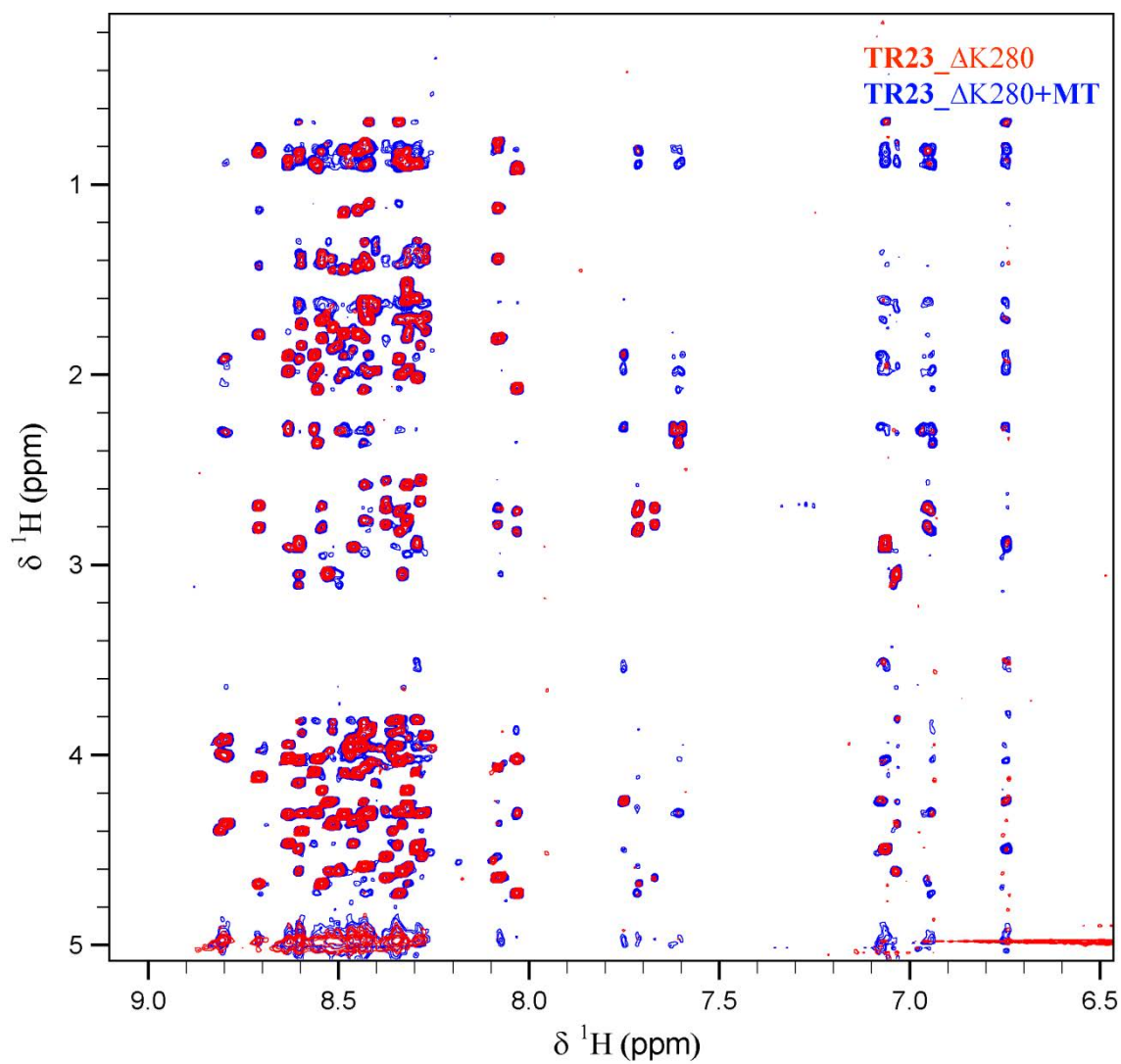
References

- Sun, Q. and T. C. Gambin (2009). "Pseudohyperphosphorylation causing AD-like changes in tau has significant effects on its polymerization." Biochemistry **48**(25): 6002-6011.
- SurrIDGE, C. D. and R. G. Burns (1994). "The difference in the binding of phosphatidylinositol distinguishes MAP2 from MAP2C and Tau." Biochemistry **33**(26): 8051-8057.
- Takemura, R., S. Okabe, T. Umeyama, Y. Kanai, N. J. Cowan and N. Hirokawa (1992). "Increased microtubule stability and alpha tubulin acetylation in cells transfected with microtubule-associated proteins MAP1B, MAP2 or tau." J. Cell Sci. **103** (Pt 4): 953-964.
- Tatebayashi, Y., K. Iqbal and I. Grundke-Iqbal (1999). "Dynamic regulation of expression and phosphorylation of tau by fibroblast growth factor-2 in neural progenitor cells from adult rat hippocampus." J. Neurosci. **19**(13): 5245-5254.
- Tortosa, E., I. Santa-Maria, F. Moreno, F. Lim, M. Perez and J. Avila (2009). "Binding of Hsp90 to Tau Promotes a Conformational Change and Aggregation of Tau Protein." J. Alzheimers Dis. **17**(2): 319-325.
- Trinczek, B., J. Biernat, K. Baumann, E. M. Mandelkow and E. Mandelkow (1995). "Domains of Tau-Protein, Differential Phosphorylation, and Dynamic Instability of Microtubules." Mol. Biol. Cell **6**(12): 1887-1902.
- Tsvetkov, P. O., A. A. Makarov, S. Malesinski, V. Peyrot and F. Devred (2012). "New insights into tau-microtubules interaction revealed by isothermal titration calorimetry." Biochimie **94**(3): 916-919.
- Uversky, V. N., J. R. Gillespie and A. L. Fink (2000). "Why are "natively unfolded" proteins unstructured under physiologic conditions?" Proteins **41**(3): 415-427.
- Vale, R. D. and H. Hotani (1988). "Formation of Membrane Networks In vitro by Kinesin-Driven Microtubule Movement." J. Cell Biol. **107**(6): 2233-2241.
- Viegas, A., J. o. Manso, F. L. Nobrega and E. J. Cabrita (2011). "Saturation-Transfer Difference (STD) NMR: A Simple and Fast Method for Ligand Screening and Characterization of Protein Binding." J. Chem. Educ. **88**(7): 990-994.
- von Bergen, M., S. Barghorn, J. Biernat, E. M. Mandelkow and E. Mandelkow (2005). "Tau aggregation is driven by a transition from random coil to beta sheet structure." Biochim. Biophys. Acta **1739**(2-3): 158-166.
- Weingarten, M. D., A. H. Lockwood, S. Y. Hwo and M. W. Kirschner (1975). "A protein factor essential for microtubule assembly." Proc. Natl. Acad. Sci. USA **72**(5): 1858-1862.
- Weisenberg, R. C. (1972). "Microtubule Formation in vitro in Solutions Containing Low Calcium Concentrations." Science **177**(4054): 1104-1105.

References

- Weisenberg, R. C. and S. N. Timasheff (1970). "Aggregation of Microtubule Subunit Protein - Effects of Divalent Cations, Colchicine and Vinblastine." Biochemistry **9**(21): 4110-4116.
- Williamson, M. P. (2006). The Transferred NOE. Modern Magnetic Resonance: 1357-1362.
- Wilson, L. and M. A. Jordan (2004). "New microtubule/tubulin-targeted anticancer drugs and novel chemotherapeutic strategies." J. Chemother. **16**: 83-85.
- Wilson, L. and R. L. Margolis (1978). "Microtubule Polymerization - Opposite End Assembly and Disassembly of Microtubules at Steady-State In vitro." J. Supramol. Str.: 299-299.
- Witman, G. B., D. W. Cleveland, M. D. Weingarten and M. W. Kirschner (1976). "Tubulin requires tau for growth onto microtubule initiating sites." Proc. Natl. Acad. Sci. USA **73**(11): 4070-4074.
- Wittmann, C. W., M. F. Wszolek, J. M. Shulman, P. M. Salvaterra, J. Lewis, M. Hutton and M. B. Feany (2001). "Tauopathy in Drosophila: neurodegeneration without neurofibrillary tangles." Science **293**(5530): 711-714.
- Wüthrich, K. (1990). "Protein structure determination in solution by NMR spectroscopy." J. Biol. Chem. **265**(36): 22059-22062.
- Xia, Y., Q. Zhu, K.-Y. Jun, J. Wang and X. Gao (2010). "Clean STD-NMR spectrum for improved detection of ligand-protein interactions at low concentration of protein." Magn. Reson. Chem. **48**(12): 918-924.
- Xu, H. and M. A. Freitas (2009). "MassMatrix: a database search program for rapid characterization of proteins and peptides from tandem mass spectrometry data." Proteomics **9**(6): 1548-1555.
- Xu, H., P. H. Hsu, L. Zhang, M. D. Tsai and M. A. Freitas (2010). "Database search algorithm for identification of intact cross-links in proteins and peptides using tandem mass spectrometry." J. Proteome Res. **9**(7): 3384-3393.
- Xu, H., L. Zhang and M. A. Freitas (2008). "Identification and characterization of disulfide bonds in proteins and peptides from tandem MS data by use of the MassMatrix MS/MS search engine." J. Proteome Res. **7**(1): 138-144.
- Zheng, Y. X., M. L. Wong, B. Alberts and T. Mitchison (1995). "Nucleation of Microtubule Assembly by a Gamma-Tubulin-Containing Ring Complex." Nature **378**(6557): 578-583.

Appendix



Appendix Figure1: Overlay of the tr-NOESY spectra of TR23_ΔK280 in the presence (blue) and absence (red) of microtubules.

Curriculum vitae

Personal Data

Name : Harindranath Kadavath
Date of Birth : 30th April 1985
Place of Birth : Malappuram, Kerala
Nationality : India

Educational qualifications

2009-2013 Ph.D student, Max Planck Institute for Biophysical Chemistry, Göttingen,
Graduate School GGNB, University of Göttingen
2005 - 2007 MSc Applied Chemistry, University of Calicut, India
2002 - 2005 BSc Chemistry, University of Calicut, India

Professional Experience

2007 - 2009 Project Assistant, Central NMR Facility, National Chemical Laboratory,
Pune India

Publications

Kadavath, H., Hofele, R.V., Biernat, J., Kumar, S., Tepper, K., Urlaub, H., Mandelkow, E., and Zweckstetter, M. **Tau stabilizes microtubules by binding at the interface between tubulin heterodimers.** *Proc. Natl. Acad. Sci. USA*, **2015**, In Press.

Kadavath, H., Jaremko, M., Jaremko, L., Biernat, J., Mandelkow, E., and Zweckstetter, M. **Folding Of Tau On Microtubules.** *Angew. Chem. Int. Ed. Engl.*, **2015**, In Press.

Schwalbe, M., **Kadavath, H.**, Biernat, J., Ozenne, V., Blackledge, M., Mandelkow, E. and Zweckstetter, M., **Structural Impact of Tau Phosphorylation at Threonine231;** *Structure*, **2015**, In Press.

Schwalbe, M., Biernat, J., Bibow, S., Ozenne, V., Jensen, M. R., **Kadavath, H.**, Blackledge, M., Mandelkow, E. and Zweckstetter, M., **Phosphorylation of Human Tau Protein by Microtubule Affinity-Regulating Kinase 2;** *Biochemistry*, **2013** DOI: 10.1021/bi401266n

Kadavath, H., Kuttatheyl, A. V., Chandran, C. V., Bräuniger, T., Madhu, P. K., Ajithkumar, T. G. and Joy, P. A. **Evidence for the co-existence of distorted tetrahedral and trigonal bipyramidal aluminium sites in SrAl₁₂O₁₉ from ²⁷Al NMR studies;** *Solid State Communications*, **2010**, *150*, 262-266.